

NASA CR-66240

# REPORT ON THE DEVELOPMENT OF THE MANNED ORBITAL RESEARCH LABORATORY (MORL) SYSTEM UTILIZATION POTENTIAL

## TASK AREA IV MORL SYSTEM IMPROVEMENT STUDY

9859

(ACCESSION NUMBER)

(PAGES) 329

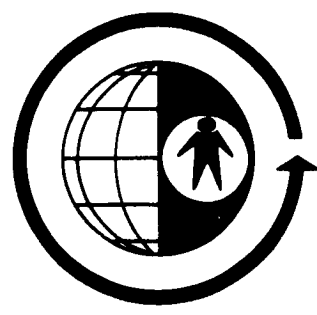
(NASA CR OR TMX OR AD NUMBER) CR-66240

(THRU)

(CODE)

(CATEGORY) 31

FACILITY FORM 502



BOOK 3

(ACCESSION NUMBER)

(PAGES) 329

(NASA CR OR TMX OR AD NUMBER) CR-66240

(THRU)

(CODE)

(CATEGORY)

FACILITY FORM 502

SM-48817  
DECEMBER 1965

MISSILE & SPACE SYSTEMS DIVISION  
DOUGLAS AIRCRAFT COMPANY, INC.  
SANTA MONICA, CALIFORNIA



KAT 4015

REPORT ON THE DEVELOPMENT OF  
THE MANNED ORBITAL RESEARCH LABORATORY (MORL)  
SYSTEM UTILIZATION POTENTIAL

Task Area IV  
MORL System Improvement Study

**BOOK 3**

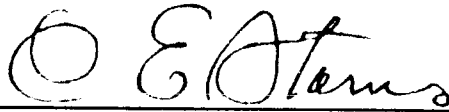
---

SM-48817

DECEMBER 1965

PREPARED BY D. C. WENSLEY AND O. TAYLOR  
BRANCH CHIEF AND STUDY MANAGER  
STABILIZATION ECLIPSE — PIONEER DIVISION  
AND CONTROL BENDIX CORPORATION

APPROVED BY



C. E. STARNES  
PROGRAM MANAGER

SUBMITTED BY  
DOUGLAS AIRCRAFT COMPANY, INC.

PRESENTED TO  
NATIONAL AERONAUTICS AND SPACE ADMINISTRATION  
LANGLEY RESEARCH CENTER  
CONTRACT NO. NAS1-3612

APPROVED BY



R. J. GUNKEI  
DIRECTOR, ADVANCED MANNED SPACECRAFT SYSTEMS

---

**DOUGLAS MISSILE & SPACE SYSTEMS DIVISION**

**The Manned Orbital Research Laboratory (MORL) is a versatile facility for experimental research which provides for:**

- **Simultaneous development of space flight technology and man's capability to function effectively under the combined stresses of the space environment for long periods of time.**
- **Intelligent selectivity in the mode of acquisition, collation, and transmission of data for subsequent detailed scientific analyses.**
- **Continual celestial and terrestrial observations.**

**Future application potential includes use of the MORL as a basic, independent module, which, in combination with the Saturn Launch Vehicles currently planned for the NASA inventory, is responsive to a broad range of advanced mission requirements.**

**The laboratory module includes two independently pressurized compartments connected by an airlock. The larger compartment comprises the following functional spaces:**

- **A Control Deck from which laboratory operations and a major portion of the experiment program will be conducted.**
- **An Internal Centrifuge in which members of the flight crew will perform re-entry simulation, undergo physical condition testing, and which may be useful for therapy, if required.**
- **The Flight Crew Quarters, which include sleeping, eating, recreation, hygiene, and liquids laboratory facilities.**

**The smaller compartment is a Hangar/Test Area which is used for logistics spacecraft maintenance, cargo transfer, experimentation, satellite check-out, and flight crew habitation in a deferred-emergency mode of operation.**

**The logistics vehicle is composed of the following elements:**

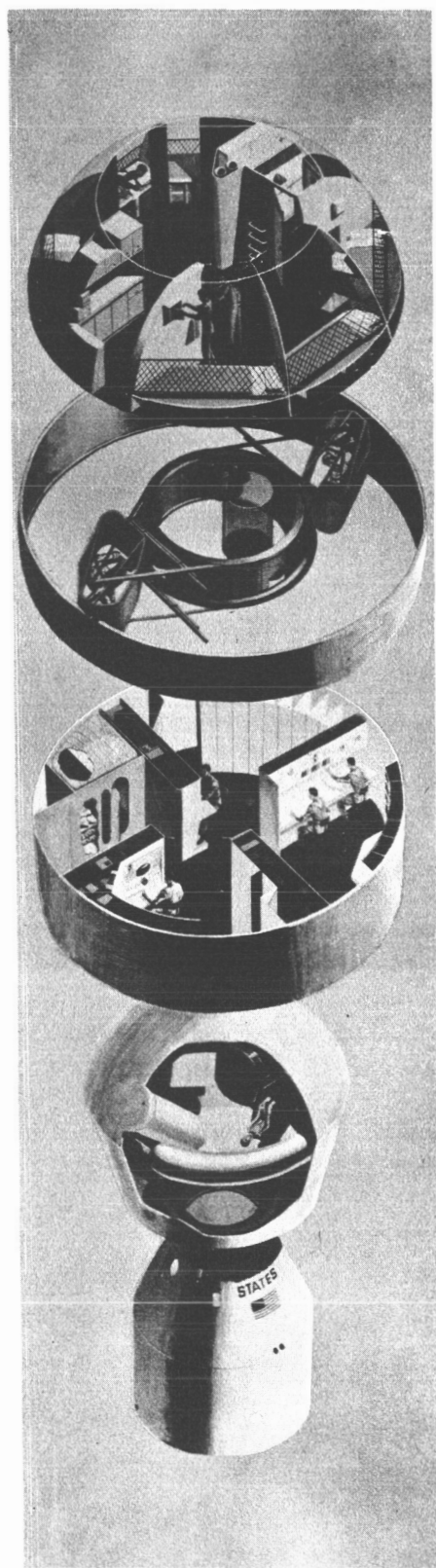
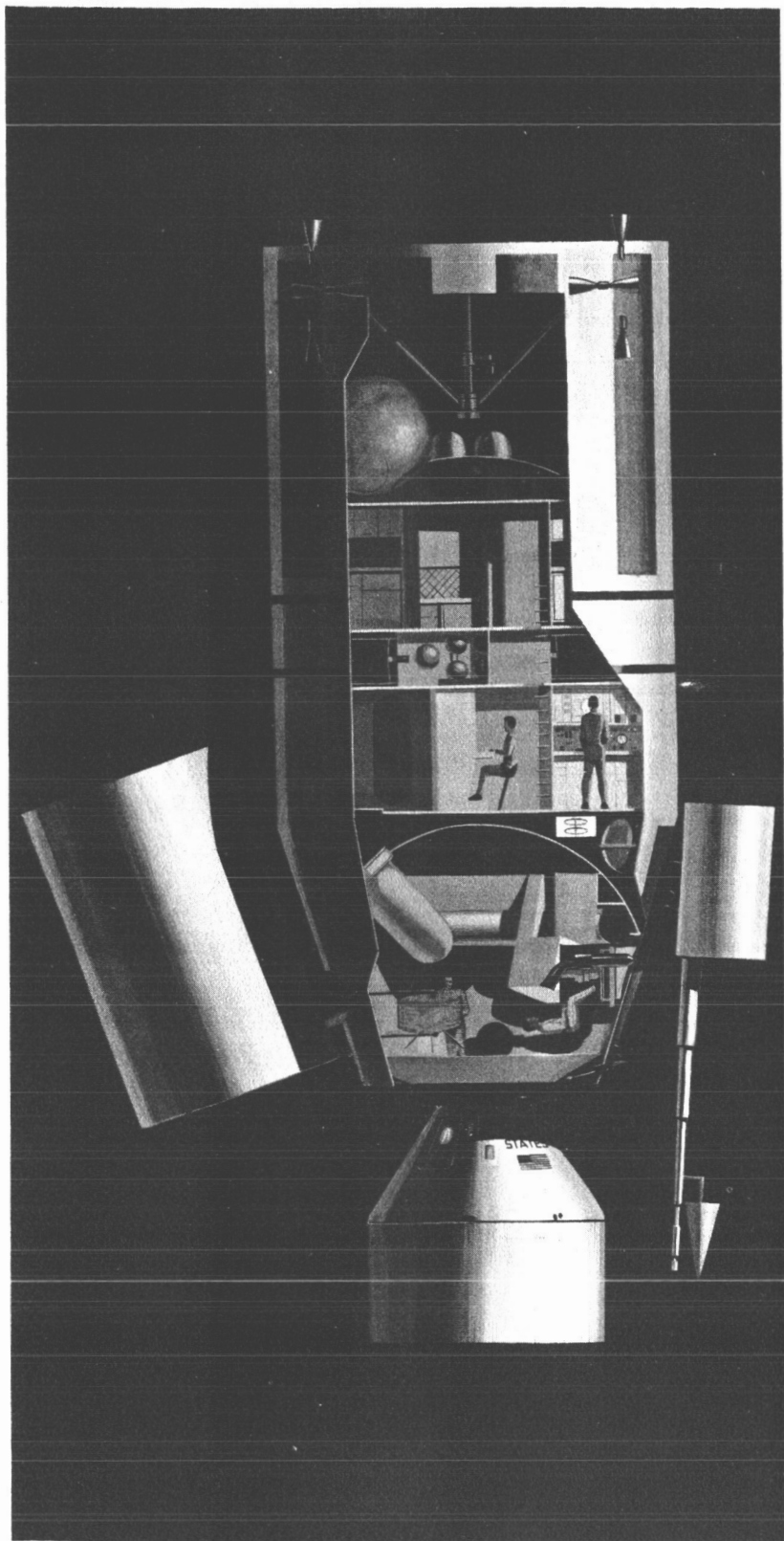
- **A Logistics Spacecraft which generally corresponds to the geometric envelope of the Apollo Command and Service Modules and which includes an Apollo Spacecraft with launch escape system and a service pack for rendezvous and re-entry maneuver propulsion; and a Multi-Mission Module for either cargo, experiments, laboratory facility modifications, or a spacecraft excursion propulsion system.**
- **A Saturn IB Launch Vehicle.**

**Integration of this Logistics System with MORL ensures the flexibility and growth potential required for continued utility of the laboratory during a dynamic experiment program.**

**In addition to the requirements imposed by the experiment program, system design parameters must reflect operational requirements for each phase of the mission to ensure:**

- **Functional adequacy of the laboratory.**
- **Maximum utilization of available facilities.**
- **Identification of important parameters for consideration in future planning of operations support.**

**For this reason, a concept of operations was developed simultaneously with development of the MORL system.**



## PREFACE

This report is submitted by the Douglas Aircraft Company, Inc., to the National Aeronautics and Space Administration's Langley Research Center. It has been prepared under Contract No. NAS1-3612 and describes the analytical and experimental results of a preliminary assessment of the MORL's utilization potential.

Documentation of study results are contained in two types of reports: A final report consisting of a Technical Summary and a 20-page Summary Report, and five Task Area reports, each relating to one of the five major task assignments. The final report will be completed at the end of the study, while the Task Area reports are generated incrementally after each major task assignment is completed.

The five Task Area reports consist of the following: Task Area I, Analysis of Space Related Objectives; Task Area II, Integrated Mission Development Plan; Task Area III, MORL Concept Responsiveness Analysis; Task Area IV, MORL System Improvement Study; and Task Area V, Program Planning and Economic Analysis.

This document contains 1 of the 5 parts of the Task Area IV report, MORL System Improvement Study. The study evaluates potential improvements to the MORL, necessitated by the limitations identified in Task Area III, and evaluates those improvements stemming from investigations aimed at increasing the effectiveness of the MORL through the addition of new system elements.

The contents and identification of the five parts of this report are as follows: Book 1, Douglas Report SM-48815, presents the summary of the Task Area effort and the results of the configuration, structure, electrical power, logistics system and performance analyses; Book 2, Douglas Report SM-48816, presents the results of the analyses performed on the Environmental Control/Life Support subsystem; Book 3, Douglas Report SM-48817, presents the results of the analyses performed on the Stabilization and Control subsystem; Book 4, Douglas Report SM-48818, presents the results of the analyses performed on the Communications and Telemetry subsystem; Book 5, Douglas Report SM-48819, presents the results of the analyses performed on the Propulsion subsystem.

Requests for further information concerning this report will be welcomed by R.J. Gunkel, Director, Advance Manned Spacecraft Systems, Advance Systems and Technology, Missile & Space Systems Division, Douglas Aircraft Company, Inc.

CONTENTS

	LIST OF FIGURES	ix
	LIST OF TABLES	xi
Section 1	INTRODUCTION AND SUMMARY	1
Section 2	STABILITY AND CONTROL SYSTEM REQUIREMENTS	7
	2.1 Nonexperimental	7
	2.2 Experimental	12
Section 3	SYSTEM DEFINITION AND PERFORMANCE	21
	3.1 Attitude Orientations	21
	3.2 Functional Description	23
	3.3 Equipment Summary	28
	3.4 Effect of Disturbances on Torque and Impulse Sizing	31
	3.5 System Performance	40
Section 4	SYSTEM IMPROVEMENT STUDY	43
	4.1 Study Sources	43
	4.2 Improvements in Disturbance and Sizing Analyses	47
	4.3 Gyrocompassing Performance	51
	4.4 Use of Control Moment Gyros for Attitude Maneuvering	59
	4.5 Manual Control	70
	4.6 System Hardware Mechanization Improvements	71
	4.7 Inertial Reference System Selection	78
	4.8 Installation and Alignment of Sensors	79
	4.9 Improvements Made Possible by the Launch Date Extension	81
Section 5	TECHNOLOGICAL REQUIREMENTS	85
	5.1 Summary	85
	5.2 Task Descriptions	90
	5.3 Program Time Phasing	97
Section 6	RECOMMENDATIONS FOR FOLLOW-ON STUDIES	103
	6.1 Experiment Control Interface	103
	6.2 Maneuvering--CMG Compared to RCS	103
	6.3 CMG Configuration Selection	104

6.4	Crew Motion Studies	104
6.5	Attitude Reference Studies	104
6.6	Earth Oblateness Effects	105
6.7	Low-Thrust Reaction Controllers	105
Appendix A	CONTROL SYSTEM ANALYSIS	107
Appendix B	SYSTEM IMPLEMENTATION	231
Appendix C	SENSORS	273
Appendix D	MORL INERTIAL REFERENCE SYSTEM COMPARISON STUDY	297

## FIGURES

2-1	MORL Experiment Requirements --Attitude	17
2-2	MORL Experiment Requirements --Stabilization Rates	18
3-1	MORL Reference Axes	22
3-2	Simplified Block Diagram--Stabilization and Control System	24
3-3	Longitudinal Stowing Configurations	34
3-4	Radial Stowing Configurations	35
3-5	Effect of 11-year Solar Cycle on Propellant Requirements	37
4-1	Roll Solar Drag Impulse History	49
4-2	Roll Solar Accumulated Angular Impulse History	50
4-3	Phase IIa Baseline Belly-Down Mechanization	53
4-4	Phase IIb Baseline Belly-Down Mechanization	59
4-5	CMG Configuration	62
4-6	Resource Usage for CMG Pitch-Yaw Maneuvers	64
4-7	Comparison Between Optimum CMG and Jet Resource Requirements for Maneuvering	65
4-8	CMG Actuator Weight as a Function of Output Torque	68
4-9	CMG Unit Weight as a Function of Angular Momentum	69
4-10	SCS Mechanization	73
4-11	Attitude Reference Base with Sensors	80
5-1	MORL SCS Technology Requirements	86
5-2	Control Moment Gyros	98
5-3	SCS Dynamics Simulator	99
5-4	Alignment System for the Attitude Reference Sensors	100



PRECEDING PAGE BLANK NOT FILMED.

TABLES

2-1	Stabilization and Control Performance Requirements	9
2-2	Experiment Requirements	14
3-1	System Characteristics Summary	29
3-2	Propellant Consumption and Momentum Storage Requirements	35
4-1	Performance Summary of Phase IIa and Phase IIb Baseline SCS Systems Operating in the Belly-Down Mode	55
4-2	CMG Characteristics	70

## Section 1

### INTRODUCTION AND SUMMARY

The MORL Phase IIb study has resulted in an expanded definition of mission requirements and objectives for an orbiting research laboratory, and has yielded increased understanding of the performance and functional requirements which this mission imposes on the laboratory's subsystems. Study of the Stabilization and Control Subsystem (SCS) has continued in parallel with the systems-level progress. The basic objective of this study is to ensure that the recommended SCS concept has a sufficient capability to meet the needs of initial flights, as well as the expanding needs of future missions.

The SCS which has evolved from these studies is designed to satisfy the orientation and attitude control requirements that arise from both the experimental phase of the mission and the operational events associated with placing and maintaining the laboratory facility in space.

For the normal (long-term) operation of the laboratory, an orientation is selected that aligns the longitudinal axis of the laboratory with the velocity vector with one side of the vehicle facing the Earth. This attitude is referred to as the belly-down orientation. For routine operations in this orientation, control signals are provided by a two-axis horizon sensor (used to sense the local vertical) and a roll-rate gyro (used in a gyro-compass mode to sense the yaw attitude error). In addition to this basic mode of operation, the SCS can respond to manually or automatically generated control commands to maneuver the laboratory to any desired inertial orientation.

To accommodate the fine-attitude-hold requirements of some experiments, a precision attitude reference is provided. This system, which can provide attitude reference information in either the belly-down or inertial orientations, consists of a 3-axis platform gyro package, two 2-axis star trackers,

a special purpose computer, and an electro-optical alignment subsystem. The gyro package differs from the conventional gimballed platform in that three separate single-gimbal platforms are used. This configuration improves maintainability by permitting replacement of an individual platform.

Control torques, needed to maneuver the laboratory or stabilize it in a selected orientation, are provided by control-moment gyros (CMG) and the reaction control system's (RCS) gas jets. The CMG's provide primary actuation because of the efficiency resulting from their momentum storage feature. The RCS supplies external torques for desaturating the CMG's, and for other events which require high torque capability.

The present system concept does not differ fundamentally from the baseline SCS developed in the MORL Phase IIa study. The changes incorporated in the current design are more in the nature of refinements which have been found necessary because of a more comprehensive review of requirements. In reaching these conclusions, the mission requirements imposed by operation in both high- and low-inclination, low-altitude orbits, as well as in the synchronous orbit, have been investigated as a part of the MORL Task Area III Concept Responsiveness Analysis study. The study has shown that support of nonexperimental mission events is easily accomplished and that it accounts for a negligible portion of the overall system complexity.

Support of experimental operations presents the most difficult requirements in terms of both functional complexity and performance accuracy. To arrive at this conclusion, the MORL Data Bank of 163 experiments\* was examined as a part of the Task Area III study to determine the total spectrum of requirements that may be imposed on the SCS. Each experiment was examined in detail to determine the requirements for vehicle orientation, pointing accuracy, duty cycle, stabilization and slewing rates, and other pertinent factors. The requirements thus derived from the Data Bank list of experiments

---

\*Subsequent to the SCS accommodation assessment, the Data Bank was further condensed to a total of 157 experiments. However, the overall requirements remain essentially unchanged.

represent a sufficiently diversified set of requirements for evaluating the SCS which are preferable to the use of a more restricted list associated with a specific mission.

Following the identification of this broad range of experimental requirements, the baseline SCS, as defined at the conclusion of the MORL Phase IIa study, was examined to determine the degree of accommodation it afforded. In performing this assessment, it was assumed that the laboratory experiment interface is simplified if a given experiment may use the laboratory as an orientation and stabilization platform and not be required to provide its own control functions. Therefore, the pointing accuracy and rate requirements for a given experiment were first compared with the baseline laboratory's pointing accuracy and rate capabilities. In the simplest mode of operation, which employs horizon sensing and gyrocompassing to define the reference attitude, the baseline SCS can maintain the laboratory's axes aligned to within  $1/2^\circ$  of the belly-down reference orientation. Body rates are largely a function of the transient disturbances induced by crew and equipment motions. While the crew motion disturbance category has not been studied in depth, it is anticipated that vehicle rates of at least as high as  $0.06^\circ/\text{sec}$  will be experienced as the result of crew motions. By restricting crew activity, the vehicle rates may be reduced to  $0.01^\circ/\text{sec}$  or even  $0.005^\circ/\text{sec}$ .

Use of the laboratory's precision inertial reference increases the attitude measurement accuracy to a maximum of approximately  $0.01^\circ$ . Because the same dynamic disturbances exist, the body rates are expected to be the same as in the horizon sensor/gyrocompass mode. Because of the increased measurement accuracy, however, the maximum vehicle attitude errors should not exceed  $0.1^\circ$ .

Of the 163 Data Bank experiments examined in the responsiveness analysis, 102 were found to impose some requirement on the SCS. A total of 101 experiments require pointing, attitude hold, or knowledge of attitude history. A total of 101 experiments require a rate stabilization capability and, of these, 43 also require a slewing capability in excess of  $1.0^\circ/\text{sec}$ . Maneuvering of the laboratory to satisfy the slewing- or tracking-rate profiles demanded by these 43 experiments was determined to be beyond the

capability of the baseline control moment gyros and to require too much propellant if the RCS were used. The preferred alternative is to place these experiments on gimballed mounts. This method reduces the mass to be accelerated to a reasonable amount. An additional requirement for gimbaling experiments arises because crew motions and other transient disturbances limit the degree of attitude-hold and rate-stabilization accuracy attainable on the laboratory. These factors result in the need for 13 additional experiments to be gimbal mounted, bringing the total to 56 experiments.

The result of the responsiveness analysis led to the recommendation that further studies be performed to investigate the problems of experiment integration. This need was further emphasized in the 48-hour study. A task was initiated to develop a concept for accurately aligning gimballed experiment sensors relative to the attitude reference, and to develop a location and installation concept for the laboratory's attitude reference that was better than the concept previously recommended. Successful completion of this task would ensure accurate transfer of pointing command.

Although the accommodation assessment failed to identify any additional major difficulties with the baseline SCS, a comprehensive design review was conducted to determine areas of marginal capability, insufficient definition, or inadequate growth potential. A series of improvement studies was initiated in both analytical and hardware areas. The most significant results from these studies, in addition to the development of an on-board sensor alignment concept, are: (1) increased CMG momentum and torque to provide more attitude maneuvering capability, (2) more detailed definition of the electronic hardware, (3) substantiation of the gyrocompassing and manual-control performance estimates, (4) more accurate estimates of impulse requirements imposed by the external environments, and (5) further substantiation of the inertial reference selection.

To minimize any possible risk in the realization of this subsystem, each element of the concept has been reviewed to identify the need for early research and development activity. Emphasis has been placed on the role of in-orbit testing to support the research and development program.

The main body of this report presents a review of the requirements imposed on the SCS by the MORL mission, describes the functional and equipment aspects of the system, summarizes the results of improvement studies, and presents the recommendations for further study and research. Four Appendixes are included to elaborate on the subjects discussed in the basic report. These Appendixes present the detailed analyses and design data on tradeoff and definition studies performed in the improvement study, which resulted in the recommended system. Seven separate studies are reported on in the Appendixes--four of an analytical nature and three involving the hardware mechanization of the system. The analytical studies investigate: (1) impulse sizing requirements caused by the external environment (namely, the aerodynamic and gravity forces, and torques which act on the vehicle), (2) the problem of maintaining proper orientation using the horizon sensor and gyrocompass technique, (3) attitude maneuvering using momentum storage actuators, and (4) man's role in control of the vehicle. The hardware studies include: (1) definition of the total hardware system, (2) detailed definition of the selected sensors, as well as the sensor inflight alignment and calibration concept, and (3) a tradeoff study which includes three methods of mechanizing the precision inertial reference requirements.

PRECEDING PAGE BLANK NOT FILMED.

## Section 2

### STABILIZATION AND CONTROL SYSTEM REQUIREMENTS

The Stabilization and Control system (SCS) is used to orient and stabilize the MORL attitude during all phases of the mission. The mission activities may be classified into two major categories: (1) those associated with operational (nonexperimental) events such as orbit injection, orbit maintenance, and rendezvous, and (2) those associated with the overall prime mission experimental objectives. Both the nonexperimental and experimental performance requirements must be met in the presence of internal and external dynamic disturbances.

In addition to the SCS performance requirements, there are requirements for overall systems effectiveness in terms of operability, reliability, and maintainability. These requirements are to be met by considering, in the system design, man's presence aboard the zero-g environment laboratory.

These performance and operational requirements apply throughout the entire MORL mission life of 1 to 5 years and, while the requirements are perturbed by launch date changes, laboratory configuration alterations, and orbit parameter variations, consideration must be given in the system design to minimize the effects of these perturbations.

#### 2.1 NONEXPERIMENTAL

The nonexperimental requirements result from the mission events which are concerned primarily with injecting and maintaining the laboratory in its prescribed orbit for the duration of the mission. Specifically, the mission events and functions which must be supported by the SCS are as follows:

1. Orbit injection.
- 2.. Short-term unmanned orientation and stabilization.

3. Orbit-keeping or orbit-altitude maintenance.
4. Long-term manned zero-g stabilization.
5. Rendezvous and docking.
6. Artificial gravity.

Requirements for each of these events and functions, summarized in Table 2-1, are briefly discussed in this section.

#### 2.1.1 Orbit Injection

The SCS is required to maintain an attitude orientation which properly aligns the injection thrusters during orbit injection. Because the booster supplies all but approximately the last 200 fps of orbital velocity, the thrust axis alignment during engine firing is not critical. A value of  $\pm 5^\circ$  is adequate.

Misalignment, thrust eccentricities, and thrust magnitude variations will generate disturbance torques on the laboratory during injection. These torques are not expected to exceed 110 ft-lb, which are easily handled by the Reaction Control system (RCS) engines.

#### 2.1.2 Short-Term Unmanned Orientation and Stabilization

Subsequent to orbit injection, there are no particular orientation requirements imposed (assuming the use of an isotope power system). In the case of a solar panel power source, orientation of the panels toward the sun is required.

For the baseline system, however, it is only necessary to ensure that body rates are not excessive during the rendezvous and docking event. For this purpose, a rate limit of  $0.03^\circ/\text{sec}$  is established.

#### 2.1.3 Orbit Keeping

The SCS provides attitude orientation when the propulsion system is operated to correct orbit decay caused by aerodynamic drag. During periods of thrust by the RCS orbit-keeping engines, the thrust axis must be aligned



Table 2-1  
 STABILIZATION AND CONTROL PERFORMANCE REQUIREMENTS

Mission Event or Function	Orientation	Attitude Accuracy (Steady-State)	Rate Stabilization (Steady-State)
Orbit injection	Belly-down (X-axis along orbit velocity vector, Y-axis perpendicular to orbit plane, Z-axis along local vertical)	All axes $\pm 5^\circ$	0.03°/sec
Short term unmanned orientation	None	None	0.03°/sec
Orbit keeping	Belly-down	All axes $\pm 5^\circ$	0.03°/sec
Long term manned zero-g	Belly-down	All axes $\pm 0.5^\circ$	0.01°/sec nominal 0.06°/sec maximum
Rendezvous and docking (manned)	Belly-down	All axes $\pm 0.5^\circ$ for 1 hour	0.03°/sec maximum
Artificial gravity	Y-axis along spin vector	6° maximum cone angle	+5°/sec X- and Z-axes +3% on spin rate about $\bar{Y}$ -axis
Experiments			
Routine Earth experiments	Belly-down	All axes $\pm 0.5^\circ$	0.01°/sec nominal
Precession Earth experiments	Belly-down	All axes $\pm 0.1^\circ$ measurement accuracy $\pm 0.01$	0.01°/sec nominal
Inertial or celestial oriented	Inertial (arbitrary)	All axes $\pm 0.1^\circ$	0.01°/sec nominal

with the velocity vector in the same manner as in the case of initial orbit injection. Performance requirements for orientation and alignment are the same as those requirements for the orbit-injection mode. Impulse requirements are described briefly in Section 3.4, and in detail in Section A.1.1 of Appendix A.

#### 2.1.4 Long-Term Manned Zero-g Stabilization

Once the laboratory is established in the orbital environment, SCS orientation and performance requirements are determined by the mission event or activity in progress. For the laboratory with solar panels, a solar orientation accurate to approximately  $\pm 10^\circ$  is required. For the baseline laboratory with an Isotope Brayton Cycle power system, no particular orientation is demanded and any body rates are acceptable if they do not interfere with crew comfort. However, selection of an orientation which minimizes drag and other environmental disturbances is desirable. The belly-down orientation, described in detail in Section 3.1, is selected for this purpose because it is easily mechanized, it provides a convenient attitude for most operational and experimental functions, and it results in minimum drag on the vehicle. In this orientation, the longitudinal roll, or X-axis, is aligned in the direction of the orbital velocity vector. The yaw, or Z-axis, is aligned along the local vertical. The pitch, or Y-axis, is aligned perpendicular to the orbit plane.

For routine operations in the belly-down orientation, an attitude hold accuracy of  $\pm 1/2^\circ$  is more than adequate. Body angular rates, within this attitude limit, are essentially determined by the level of crew dynamic activity because crew motions are converted directly into vehicle rates. Volume restrictions within the laboratory will limit crew translation and, therefore, the duration over which an induced body rate can persist. Crew-induced rates are expected to be in the range of 0.001 to 0.1°/sec. A value of 0.06°/sec is assumed to be the nominal value during active periods involving translation of one or more crew members. A value of 0.01°/sec is assumed when crew members are on station.

### 2.1.5 Rendezvous and Docking

The active role in rendezvous operations is performed by the logistic spacecraft. The MORL is required to maintain a fixed attitude in orbit and otherwise act as a cooperative target. Use of the belly-down orientation is compatible with rendezvous requirements. Body rates are limited to  $0.03^\circ/\text{sec}$  to minimize the docking impact.

Rotation of a logistic module from the docking area to a stowage position imposes a severe transient on the control system. As torques of approximately 50 ft-lb are applied, angular momentum of the module may reach 15,000 ft-lb-sec, and inertial properties may change as much as 350,000 slug-ft<sup>2</sup>. There is no specific experimental requirement for orientation during the stowage operation; however, if the belly-down orientation is maintained, most of the zero-g experiments in progress could be continued uninterrupted and the laboratory would remain in position to continue normal operations following completion of the stowage cycle. If the laboratory's attitude is not controlled during this operation, the torques applied to rotate the logistic module will also rotate the laboratory through a large angle and necessitate reorientation following the maneuver.

It is concluded that the SCS must provide positive attitude control during cargo module stowage. The nominal belly-down orientation, with  $\pm 1/2^\circ$  attitude hold and  $0.03^\circ/\text{sec}$  body rates, is adequate. Problems associated with control during stowage are further discussed in Section A.1.1 of Appendix A.

### 2.1.6 Artificial Gravity

The primary method of obtaining artificial gravity on-board MORL is through the use of the internal centrifuge. The SCS is required to counteract the torque and momentum generated by centrifuge operation. For operation in the 0- to 1-g range, momentum storage controllers are selected. Above the 1-g range, the RCS is used to provide control torques. During operation in the 0- to 1-g range, any orientation may be used. However, operation above the 1-g range results in a net change in system angular momentum,

and operation in an inertially fixed orientation is preferred. Use of the belly-down orientation, in which the laboratory is rotated through inertial space at orbit rate, causes large disturbance torques as a result of the cross coupling between the orbital body rate and the angular momentum associated with the uncompensated (above 1-g range) centrifuge rotation. These torques can be counteracted, by the RCS if desired, at the expense of approximately 6 lb of propellant per event.

A second method of supplying artificial gravity is the rotating cable-connected mode. This laboratory configuration, using the S-IVB stage as a counterweight, has been studied extensively in previous phases, and is not investigated further in this report. Elimination of solar panels eliminated the need for a solar orientation in this mode. It is concluded that the rotating system may be spin-stabilized in any inertial orientation desired.

## 2.2 EXPERIMENTAL

In supporting the experimental program, the laboratory acts essentially as an experiment mounting platform, and provides various degrees of attitude accuracy and rate stabilization. The attitude and stabilization depend on the operating mode and requirements of the specific experiment. These requirements are generally more severe than those imposed by any other phase of mission operations.

The current total spectrum of Stabilization and Control system requirements has been determined primarily from an examination of the MORL Data Bank, conducted as a part of the Task III study. In this study, the 700 experiment descriptions were categorized into nine general classes, or types, and grouped into 163 different experiments. Each experiment was examined, in detail, to determine the requirements for laboratory orientation, pointing accuracy, duty cycle, stabilization and slewing rate, and other pertinent factors. It is assumed that the Data Bank list of experiments represents a realistic-to-worst-case set of requirements and, thus, provides a sound base for establishing the SCS requirements.

The following is a summary of the experiment quantities in each of the nine categories examined:

<u>Category</u>		<u>Number of Experiments per Group</u>
I	Biomedical	3
II	Behavioral	9
III	Biological	22
IV	Space measurements and astronomy	8
V	Earth and Earth surface	7
VI	Materials testing and physics	26
VII	Subsystem testing	69
VIII	Logistics/space operations	13
IX	Spacecraft environment	<u>6</u>
	Total	163

In many cases, the reference source descriptions for a particular experiment varied widely in specified SCS requirements (that is, many experiment definitions lacked sufficient detail or contained conflicting rate and attitude hold requirements for the same experiment, and many called for gimbaling of experiment packages without regard to vehicle capability). In general, when the reference source descriptions specified different attitude or rate requirements for the same type of experiment, the most stringent specifications were used.

Table 2-2 is a sample data sheet containing summary SCS requirements extracted from six unclassified experiments in the Data Bank. This sample is included to show the format used to assemble the data and to indicate the quantity of data involved in the accommodation assessment.

In Table 2-2, experiment definition refers to the experiment title and category to which the experiment is assigned in the Data Bank.

Orientation refers to the vehicle or sensor attitude orientation required by the experiment. In most cases where an Earth orientation is specified, it is assumed that the belly-down orientation satisfies the requirement.

Table 2-2  
EXPERIMENT REQUIREMENTS

Experiment	Orientation	Pointing Accuracy (in degrees)	Field of View	Rate	Navigation	Duty Cycle	Integral Gimbals	Manual or Auto Control	Notes
VII-62 (UBL) IIB-4 Sea color distribution	Belly-down	Spacecraft - 0.01 desired (0.1 acceptable)	Telescope to be slewed $\pm 60^\circ$ perpendicular to orbit plane and $\pm 10^\circ$ from L. V. in orbit plane	S/C stability - 1°/sec	Position to 1 nmi. Time reference to 0.1 sec	2 hours per day for 7 days	Yes	Manual and auto pointing of telescopes	High resolution telescope (1 arc sec) with $1^\circ \times 1^\circ$ f. o. v. mounted on gimbals inside MORL
VI-26 IA-4 Auroral survey	Belly-down point sensors to polar regions	Not specified; assume 0.5	10 min. optical window	Not specified assume 0.10°/sec	Not specified	Exp continuous for 1 year 1.5 hour/month crew time required	Yes	Manual	High inclination and synchronous orbits
VII-9 IIB-10 (I-3) Microwave experiments	Belly-down	0.1 all axes		0.01°/sec all axes 0.01° deadband	Time reference 0.02 sec 0.2 nmi	1 hour/day each day for 1 year			See Phase IIa exp Earth radar mapping
VII-59 (UBL) IIB-6 Subsurface oceanographic parameters	Belly-down	Consistent with 2° overall accuracy for up to 3/4 hour per experiment. (0.5 S/C pointing accuracy assumed)	4 ft antenna to be slewed $\pm 72^\circ$ about L. V. (horizon to horizon)	S/C rate stability $\pm 1^\circ$ /sec over 30 sec slewing 1.5°/sec during track and 5°/sec during repositioning	1 kilometer	1 hour per day for 60 days	4 ft parabolic antenna	Manual and auto control of antenna	The attitude of the antenna relative to the buoy must be to within $\pm 2.0^\circ$ . As many as 10 different buoys may have to be acquired and tracked in a 5 min. period
VII-60 (UBL) IIB-3 Two dimension temperature spectrum of ocean surface	Belly-down	0.01 spacecraft pointing accuracy (0.1 acceptable)	Two sets of sensors. (1) $\pm 45^\circ$ gimbal x about L. V. (2) $\pm 72^\circ$ gimbal x about L. V.	Stability $\pm 0.01^\circ$ /sec for 2 min. slewing capability of 5°/sec	Time reference to 0.2 sec or better. Position coordinates 1 nmi or better	1/2 hour per experiment, 4 times per day for 50 days	Yes	Manual and auto control of sensors	Narrow field of view infrared sensor system. (5 heads with coincident $5^\circ \times 5^\circ$ f.o.v.). Also a 0.01 sensor
VII-61 (UBL) IIB-5 Surface salinity spectrum determination	Belly-down	Spacecraft pointing to $\pm 2$	Consistent with gimballed 4 ft antenna $\pm 72^\circ$ (two axes)	0.1°/sec slew up to 5°/sec	Position to 1 mile. Time reference to 0.2 sec	6 hour per day for 10 days while passing over oceans	4 ft antenna mounted on $\pm 72^\circ$ gimbals	Manual control of antenna	Transponder satellite launched from MORL in MORL orbit plane

Pointing accuracy refers to the alignment accuracy required between the sensor and the selected attitude reference. The required accuracy may be obtained by using the laboratory as a pointing platform, or by gimbaling the experiment sensor either relative to the laboratory, or relative to the laboratory's attitude reference.

Field of view refers to the angular coverage required by the experiment sensor. Both instantaneous and total field of view requirements should be specified for each pointing-type experiment.

The rate column includes specifications for the maximum rate, relative to the selected attitude reference, that is permitted during operation of the experiment, and the specifications for slewing or rotating the sensor axis relative to the selected attitude reference.

The navigation requirements, specified in terms of position and time measurement accuracies, are listed in the next column. Although navigation is not an SCS function, it is sometimes useful to know the allowable position error. This is particularly true when pointing accuracy or rate requirements are not specified and must be estimated. In this case, an SCS allowable error, equal to the navigation error, is assumed adequate.

Duty cycle refers to the operating/nonoperating time sequence. This parameter is useful in cases where attitude reference error is a function of time, and the drift during experiment operation must be determined.

Many of the experiment descriptions specify integral gimbals, which means that the experiment sensor package provides for gimbal rotation about one or more axes relative to the laboratory body. Specification of gimbals by the experiment presupposes limitations on the laboratory's pointing capabilities. While this is usually a valid assumption, it is required that the basic experiment requirements be compared with the laboratory's capabilities before specifying the need for a gimballed mount.

The last significant column, manual or auto control, is listed to briefly indicate the role of man in experiment control; for most experiments this division is not clearly defined.

Of this total list of specifications, the ones involving orientation, pointing accuracy, and rate, are the most significant in terms of defining requirements for the SCS.

A total of 102 experiments out of the 163 experiments examined have some attitude orientation requirement. In general, these orientation needs can be classified as either Earth or inertial. In the case of an Earth-orientation requirement, any vehicle attitude that allows one side of the laboratory to face the Earth's surface is assumed adequate. Inertial orientations, usually associated with astronomical observations, require stabilization of the laboratory's axes relative to a fixed inertial reference.

Pointing accuracy and rate requirements are summarized in Figure 2-1 and 2-2, respectively. The pointing requirements in Figure 2-1 are expressed in two categories: (1) those in which the experiment is fixed relative to the laboratory orientation (which is either belly-down or inertial), and (2) those in which the experiment axes must be slewed or rotated relative to the laboratory orientation. The latter category is typified by an Earth-surface-tracking experiment or a satellite-tracking experiment.

In mechanizing these experimental requirements, it is necessary to determine which ones should be gimbal mounted to obtain the necessary accuracy and angular freedom, and which ones should use the laboratory structure as a pointing platform. Further, it is necessary to determine how accurate the attitude reference should be and, in the case of structure-mounted experiments, how accurately the laboratory attitude should be controlled.

The baseline system mechanization, described in detail in Section 3, is compatible with the use of gimbal mounts on the individual experiment packages. These mounts are used both for high accuracy pointing, where it is necessary to isolate the experiment from laboratory angular motion, and for tracking or slewing type experiments. The tracking or slewing experiment must follow a nonlinear rate profile that has high peak values relative to the laboratory's nominal body axis rates. In terms of accuracy, the baseline



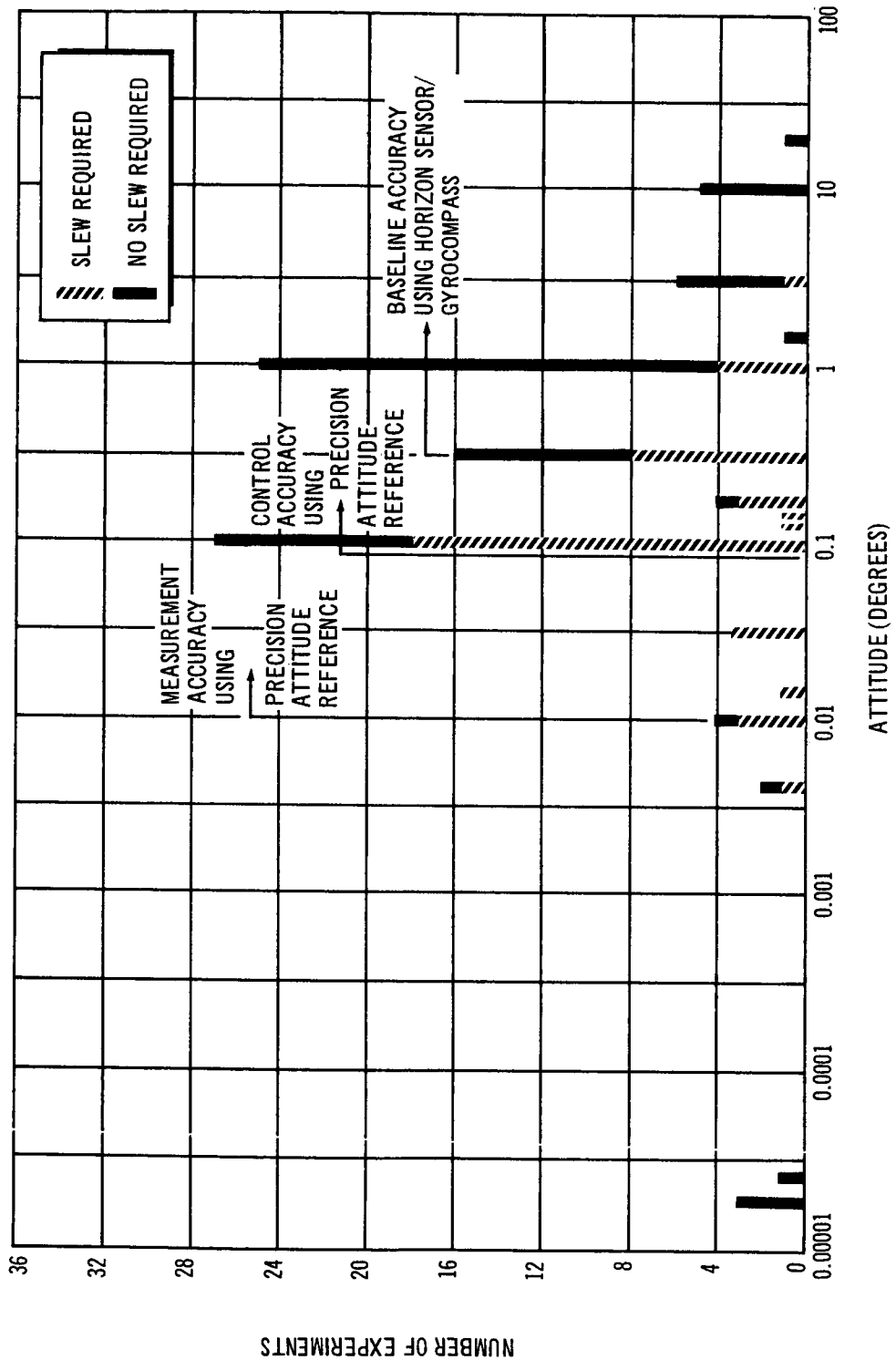


Figure 2-1. MORL Experiment Requirements – Attitude

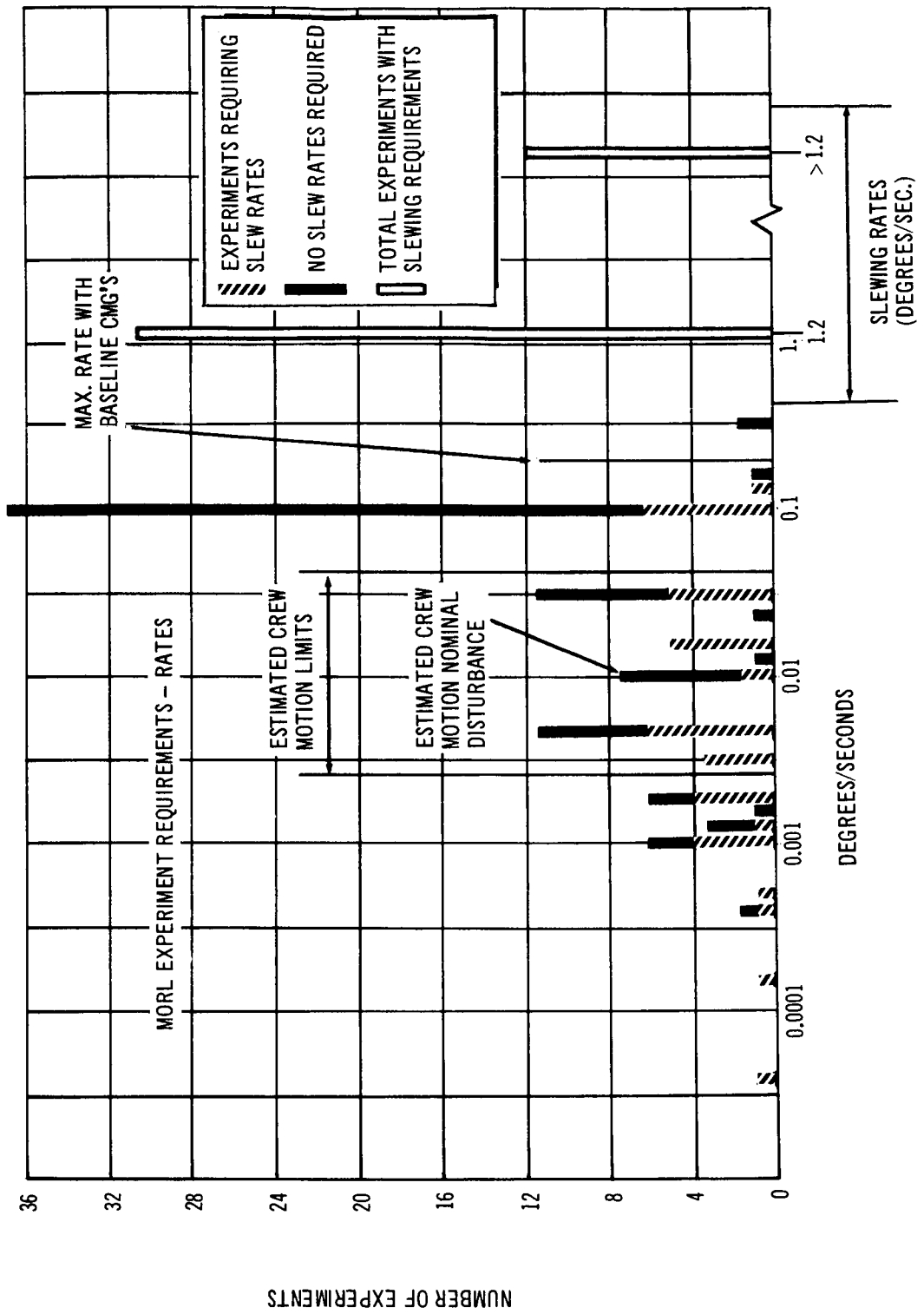


Figure 2-2. MORL Experiment Requirements -- Stabilization Rates

SCS is equipped to provide attitude reference information with a maximum accuracy of  $\pm 0.01^\circ$ ; laboratory attitude can be controlled to approximately  $0.1^\circ$  with nominal disturbances.

As shown in Figure 2-1, these attitude accuracy capabilities permit the SCS to accommodate approximately 94% of the experiments shown; the remainder of the experiments provide their own attitude error sensing and control.

Figure 2-2 shows the rate stabilization and control needs derived from the list of 163 experiments. Again, there are 101 individual experiments that have some form of rate specification. For experiments that do not involve slewing or tracking, the specification applies to the allowable instantaneous rate about the axis which is stabilized relative to the laboratory's reference orientation. As shown in Figure 2-2, many experiments require control of the instantaneous rate relative to a slewing rate (for example,  $1.2^\circ/\text{sec} \pm 0.1^\circ/\text{sec}$ ; where  $1.2^\circ/\text{sec}$  is the slewing rate and  $\pm 0.1^\circ/\text{sec}$  is the stabilization rate or allowable rate error). Figure 2-2 indicates that 31 experiments have a peak slewing rate of approximately  $1.2^\circ/\text{sec}$ , which is the peak value associated with ground tracking. Twelve experiments require slewing rates in excess of this amount.

Figure 2-2 also shows the effects of crew-motion disturbances; these are the most significant dynamic transients imposed on the laboratory. These transients are expected to appear as impulse functions to the laboratory which result in instantaneous body angular rates. These rates are expected to be within the range shown in the figure, with the nominal value being  $0.01^\circ/\text{sec}$  when the crew members are at their control stations.

PRECEDING PAGE BLANK NOT FILMED.

### Section 3 SYSTEM DEFINITION AND PERFORMANCE

The system mechanization, designed to meet the operational and experimental requirements identified in Section 2, is briefly described in this section. This system design, based on the MORL Phase IIa SCS concept, incorporates refinements derived from the subsystem improvement studies which were performed following the Task III recommendations, and which are reported in Section 4 and the attached Appendixes.

To meet the requirements set forth in Section 2, two basically different, but complementary, design philosophies have been applied to the Stabilization and Control system configuration. The first approach is to make the SCS as simple and reliable as possible; the crew is afforded maximum access to control functions and control equipment for the purpose of exercising their extensive human capabilities in ensuring the safe operation of the laboratory. The second approach is to offer the maximum in automatic control and performance for the purpose of efficient use of the laboratory and its most significant resource--crew time. Both of these objectives are adequately met in the selected mechanization scheme.

A brief functional description of the SCS as used in each of its orientation and operating modes is included in this section, as well as a summary of its physical characteristics. The basic performance capabilities of the SCS are summarized along with the effects of disturbances and vehicle mass property changes on propellant consumption rates and momentum storage (CMG) sizing requirements.

#### 3.1 ATTITUDE ORIENTATIONS

The deletion of a solar panel pointing requirement has eliminated the need for the roll solar orientation previously selected (in MORL Phase IIa) for long-term use. The belly-down orientation, illustrated in Figure 3-1, is

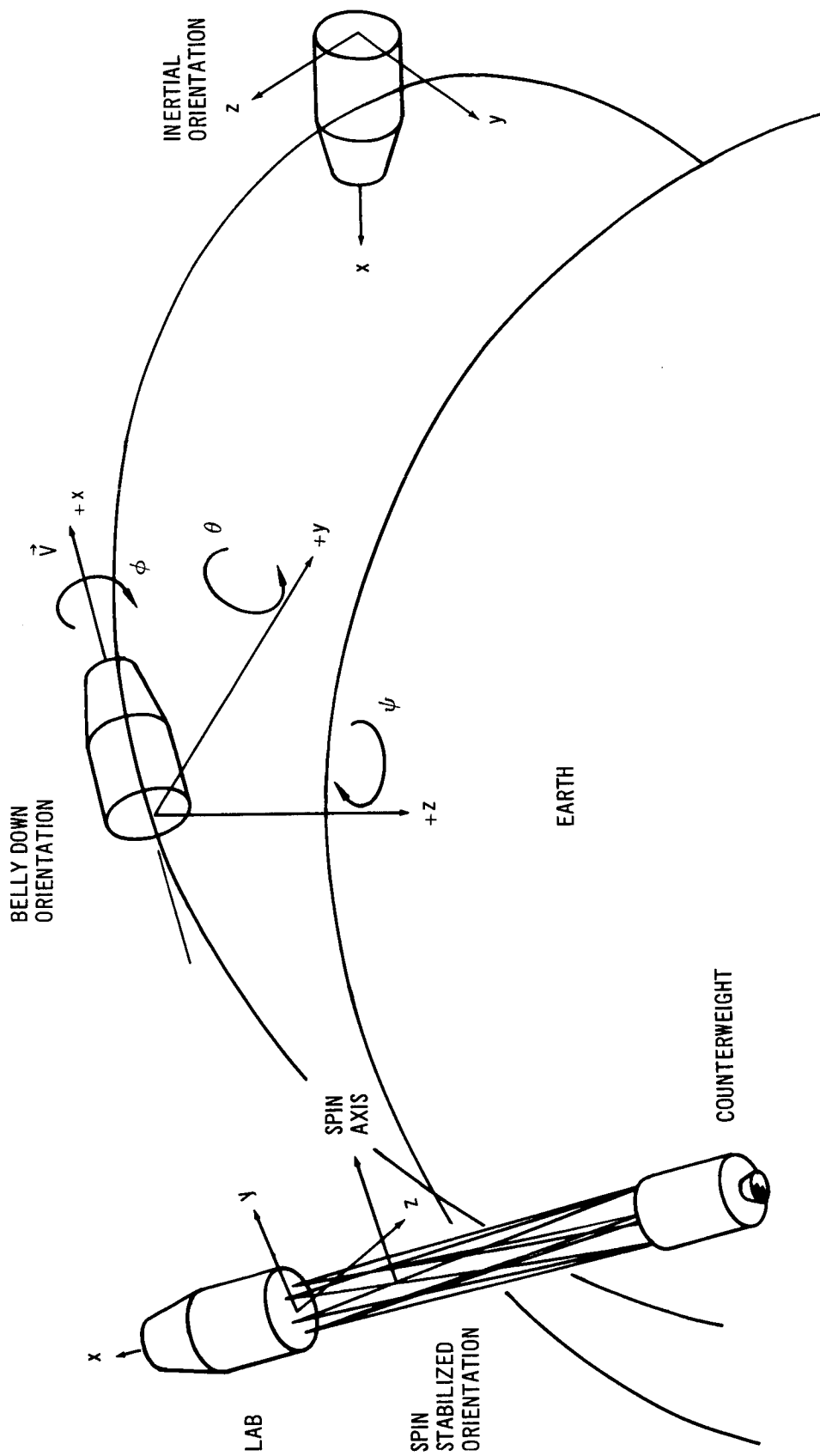


Figure 3-1. MORL Reference Axes

selected as the primary orientation for most operational events and experimental activities. This orientation minimizes aerodynamic drag and allows one side of the laboratory to face the Earth at all times--this is a major advantage because most of the pointing-type experiments require an Earth-surface orientation.

For those experiments requiring an inertially stabilized platform, such as that needed for astronomical observations, the inertial orientation is provided as shown in Figure 3-1. This terminology is used to describe any nonrotating position of the spacecraft axes.

Deletion of solar panels also eliminates the major orientation requirement for the rotating artificial gravity mode. The orientation for the MORL when operating in the rotating mode will, therefore, be established at initial spin-up to meet the immediate needs of the experimental program. The laboratory will then remain inertially fixed, subject to gravity gradient and other disturbance torques. This mode of operation is termed spin-stabilized and is illustrated in Figure 3-1.

A redefinition of the vehicle axes with respect to the orbital parameters, to comply with the more accepted Earth orientation definitions, has been carried out during Phase IIb and is as shown in Figure 3-1. During the previous study phases, the laboratory's pitch, or Y-axis, lay in the orbit plane and was directed toward the center of the Earth. The roll, or X-axis, was directed along the orbit velocity vector ( $V$ ), and the yaw, or Z-axis, was directed normal to the orbit plane, making a right-handed coordinate set. This orientation was also defined as the belly-down orientation. The axes definition previously used was a carry-over from Phase I studies. The present definition interchanges the laboratory's pitch and yaw axes so that the Z-axis now lies in the orbit plane and is directed toward the center of the Earth. The Y-axis is normal to the orbit plane. The X-axis orientation remains the same.

### 3.2 FUNCTIONAL DESCRIPTION

Figure 3-2 shows the basic functional components which comprise the Stabilization and Control system. Inertial rate integrating gyros provide the attitude information for normal use. Alignment of the laboratory in the belly-down orientation is done using a horizon scanner for the pitch and roll axes and gyrocompassing for the yaw axis. Precision attitude information is

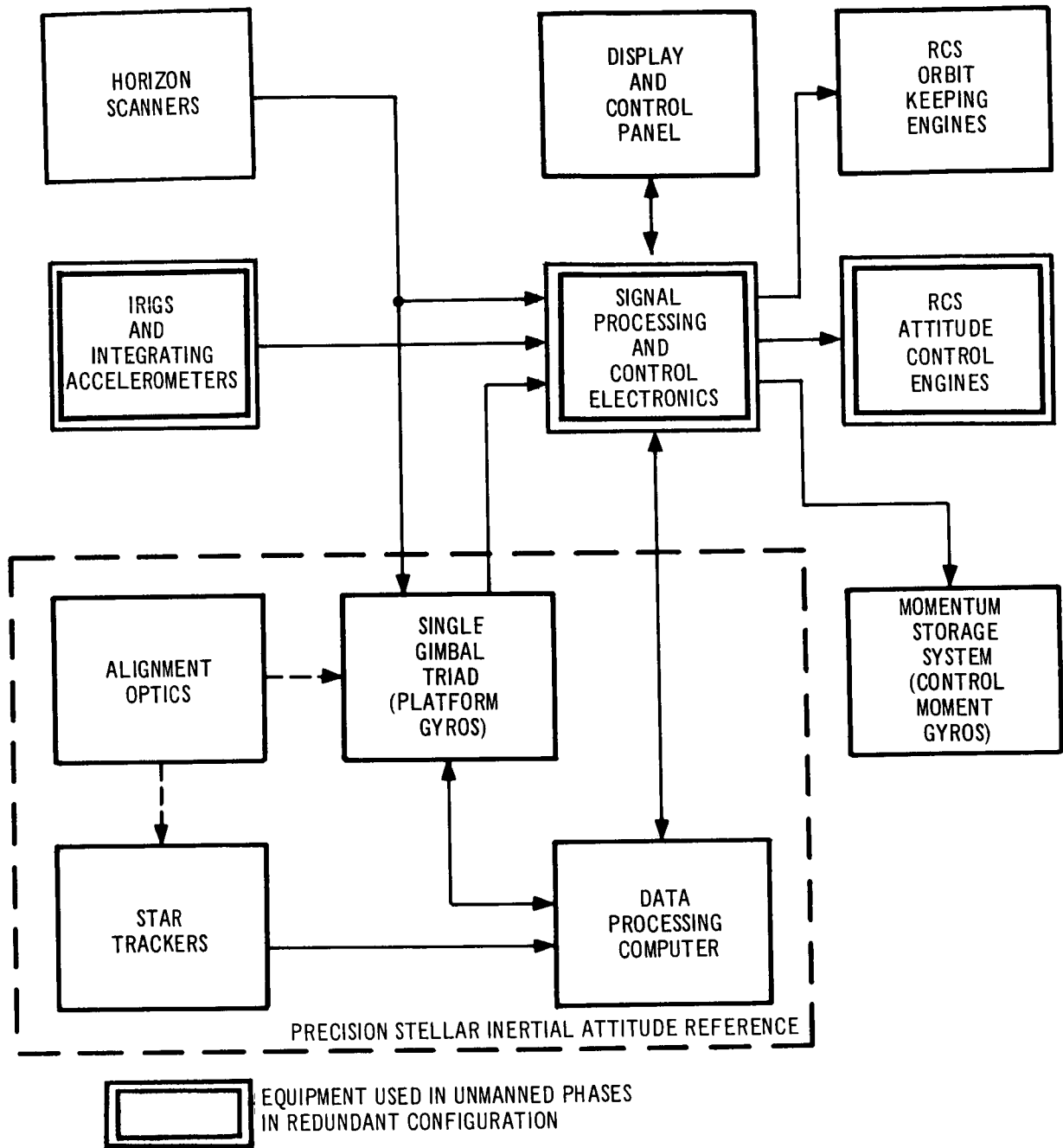


Figure 3-2. Simplified Block Diagram – Stabilization and Control System

provided by a stellar-inertial system consisting of a single-gimbal-triad (SGT) platform gyro package, two star trackers, and a special-purpose digital computer.

Control actuation is provided by the Reaction Control system's (RCS) attitude control engines and by a momentum storage system of four control moment gyros. Orbit injection thrust and subsequent orbit altitude maintenance is provided by the RCS orbit-keeping engines, with an integrating accelerometer supplying the necessary  $\Delta V$  information. Electronics packages provide the switching logic, gain, compensation, failure detection, and other functions necessary for system operation. The display and control panel provides the crew/SCS interface. An electro-optical system is provided to align the star trackers and experiment sensors with the SGT inertial reference.

As compared with the Phase IIa baseline system, the SCS as presently configured deletes both the manned and unmanned roll solar modes and incorporates rate control as a basic mode of operation. The solar detectors and sensors, previously necessary for solar orientations, have likewise been deleted.

### 3.2.1 Orbit Injection

In the boost phase, the SCS is essentially in a standby mode. Upon separation from the Saturn IVB booster, the SCS is activated and it takes control of the pitch, roll, and yaw of the vehicle by using attitude and rate information from the redundant pair of body-mounted inertial rate integrating gyros (IRIG). During this initial phase of operation, control torques required for maneuvering the laboratory and counteracting dynamic disturbances are supplied by the bipropellant RCS.

At booster separation, the pitch IRIG, or attitude gyro, is torqued through a preprogrammed attitude change to align the laboratory for orbit circularization using the orbit injection engines. Thrust is initiated after the appropriate time delay and terminated after the required  $\Delta V$  is obtained as measured by the integrating accelerometer.

After the preprogrammed orbit circularization, the gyros are switched to a rate mode and rate control is initiated. The RCS is used to keep the attitude drift rate below a threshold of  $0.03^\circ/\text{sec}$  to simplify the docking operation.



### 3.2.2 Manned Operation in the Long-Term Belly-Down Orientation

Subsequent to laboratory boarding and initial checkout, the display and control panel is activated and the laboratory is maneuvered into the belly-down orientation by supplying manual input commands to the RCS. The horizon sensor and gyrocompassing control are initiated by selecting the horizon-hold mode, which is the autopilot mode for the belly-down orientation. Spin-up of the control moment gyros is initiated but RCS actuation is continued until the gyros have acquired enough angular momentum to provide effective control. At this point, the RCS is switched from a limit cycle mode to a desaturation mode. Desaturation, or momentum dump, is required wherever a CMG reaches its gimbal angle limit, indicating that its momentum storage capability is saturated. The two double-gimbal CMG's, used for control about the pitch and yaw axes, will require desaturation a maximum of two times per orbit under the worst case gravity gradient and aerodynamic torque conditions. Roll axis disturbances, other than centrifuge operation, are negligible and, since the two roll CMG's are sized to control the centrifuge during 1-g operation, desaturation of the roll axis will seldom be necessary.

In the belly-down orientation, the double-gimbal CMG desaturation impulse can be used for orbit keeping. Asymmetrical mass loading, which should generally cause a large momentum accumulation on the pitch axis, will result in the need for frequent operation of the pitch-axis RCS engines. The desaturation control moment is then applied with the thrust acting in the direction of the laboratory's velocity vector, which increases orbit energy and compensates for aerodynamic drag. If more desaturation impulse is needed than that required for orbit keeping, the engines are fired in a pure couple so that no net thrust acts on the vehicle.

### 3.2.3 Rendezvous and Docking

The same horizon-hold mode is used in the belly-down orientation when a rendezvous event is scheduled. However, a crew member must stand by to provide manual control in case the logistic vehicle enters the horizon sensor's field of view and causes loss of horizon lock-on. A manual maneuver to a new orientation may also be desired to obtain better illumination of the docking port and to keep the solar disk out of the required field of view.

The docking transient is likely to cause a large angular momentum transfer to the laboratory, requiring use of the RCS to reduce the resulting body rate and accumulation of attitude error. Following the transfer of cargo, the RCS will again stabilize the laboratory during the rotation of the cargo module and spacecraft to the stowage position.

#### 3.2.4 Experiment Support

The belly-down orientation is utilized for most experiments having Earth-centered objectives or which simply require the maintenance of zero-g aboard the laboratory. The  $1/2^\circ$  accuracy of the horizon-hold mode accommodates over 50% of the experiments shown in Figure 2-1. For experiments requiring better accuracy, the use of the precision attitude reference is required.

The first procedure performed when using the precision attitude reference in support of experiments, following orientation of the laboratory to the normal belly-down mode, is to check the mechanical alignment of the star trackers and experiments with the SGT inertial reference. This is done by means of the on-board autocollimators, optical wedges, and optical flats mounted on the sensor packages, which form the electro-optical alignment system.

Once the mechanical alignment has been established and the electrical nulling/biasing adjustments completed, vehicle coarse attitude information, obtained from horizon sensing and gyrocompassing, is inserted by means of the SCS control console into the data processing computer (DPC). The DPC, with this coarse attitude information and precise orbit parameters (vehicle position, velocity, and time), received via the Earth communication link, determines which are the most desirable stars available for sighting by the two star trackers. The DPC then computes the required star tracker inner and outer gimbal angles, based on the presently assumed attitude. Because vehicle attitude is known to within  $0.5^\circ$ , these commanded gimbal angles are sufficiently accurate to bring the stars into the  $1^\circ$  fields of view of the star trackers.

Once the stars come within the fields of view of the tracker telescopes, the trackers are switched to a closed-loop tracking mode and their boresights zeroed in on each selected star line of sight. The trackers' actual inner and

outer gimbal angles are then transmitted to the DPC, along with the inertial platform gimbal angles, to update the attitude reference computation.

In the belly-down orientation, the reference coordinates are a rotating inertial set, and an orbit rate correction, computed on the ground or in the DPC, must be applied to the inertial reference computation. Vehicle pitch rate must equal orbit angular rate to maintain the vehicle fixed with the rotating inertial reference set of coordinates.

The modes of system operation are both selected and displayed on the command and display panel, where preselected and manual maneuvers may also be initiated. Commands so initiated are operated on through the signal processing and control electronics.

Various alternate and backup capabilities are provided, such as employing the redundant equipment on board during the unmanned phase so it can be used as wired-in spares during the manned phase, using the RCS attitude jets for control in case of momentum storage system shutdown, or using the body-mounted IRIGs to provide the display and control torque command signals in the inertial hold mode when the inertial reference system is not in operation.

The system retains the previously configured rotating mode of operation, thus allowing the laboratory booster to be deployed and the system spun to create the desired artificial gravity.

### 3.3 EQUIPMENT SUMMARY

The Stabilization and Control system mechanization study, accomplished during Phase IIb, has resulted in a more accurate and realistic appraisal of weight, power, and space requirements.

Table 3-1 summarizes these system characteristics which indicates an increase in weight, power, and volume from those previously quoted. Although the sensor complement has been reduced by the deletion of the sun sensors previously required for the solar orientation, total weights and volumes for sensors, electronics, and actuators have increased. In addition, the alignment optics weight, power, and volume have been introduced into the SCS during this phase.

Sensor weight and volume increases, approximately 25 lb and 1/2 cu ft, are primarily the result of the incorporation of the two Apollo attitude gyro accelerometer packages (AGAP). The incorporation of this package, in addition to providing improved maintenance characteristics and thermal design over the previous baseline IRIGs as well as separately mounted accelerometer, gives exact detail in terms of weight, size, and power. Power requirements were reduced by approximately 25%.

Table 3-1  
SYSTEM CHARACTERISTICS SUMMARY

	Volume (cu ft)	Weight (lb)	Connected Power	
			ac (W)	dc (W)
Zero-g mode				
Sensors	2.2	109.0	32.8	206.8
Electronics	4.7	184.9	75.9	218.5
Actuators	42.6	628.0	118.0	33.0
Controls and displays	0.8	30.2	-	39.8
Alignment optics	0.3	74.0	-	22.5
Totals	50.6	1,026.1	226.7	520.6
Rotating mode				
Sensors	0.2	13.0	17.0	46.0
Electronics	0.4	11.0	-	32.0
Totals	0.6	24.0	17.0	78.0
Complete SCS complement	51.2	1,050.1	243.7	598.6
Changes from Phase IIa baseline complement				
Sensors	+0.5	+26	-5	-44
Electronics	+0.4	+52	+37	+88
Actuators	+9.7	+66	+81	+3
Controls and displays	-0.5	-32	-20	+10
Alignment optics	+0.3	+74	-	+23
Totals	+10.4	+186	+93	+80

Slight weight and volume increases result from a new horizon scanner packaging approach, which incorporates the four sensors into a single (quadded head) assembly. This assembly eliminates the necessity for separate head alignment. In addition, windows have been provided to allow element repair or replacement without resorting to extravehicular activity.

The SCS electronics increase in weight, power, and volume may be attributed to a more definitive design, a better grouping of functional elements, and the packaging philosophy adopted for the entire system's electronics. The Apollo-type modules required for coupling the flight director and attitude indicator (FDAI) to the body-mounted IRIGs are also added to the complement.

The electronics are contained in cold-plate rack-mounted assemblies (eight including the rotating mode electronics), each capable of in-flight maintenance through the use of built-in test equipment and replaceable modules. The packaging technique alleviates the high-humidity environment problem, prevalent on present-day spacecraft, by utilizing a pressure-tight container.

Actuator changes have resulted in the largest increases in SCS equipment weight and volume (approximately 110 lb and 10 cu ft). These increases are the result of the increased torque and momentum storage capacity incorporated in the control moment gyros to allow maneuvering of the laboratory with the CMG's. Wheel spin power has increased approximately 20 W, partly because of the higher torque capability and partly because of more definitive design data resulting from the Langley CMG development program (contracted with Bendix, Eclipse-Pioneer).

The controls and displays designed for MORL during this phase of the program exhibit a decrease in weight, power, and volume, and are the result of more detailed studies of system operation and the man-machine interface. The separation of the controls and displays into packaged function assemblies provides the capability to remove individual assemblies for maintenance and repair.

The rotating-mode mechanization was not iterated during this phase of the program effort except for combining the mode electronics into a single package consistent with zero-g system electronics.

In summary, the SCS weight has been increased approximately 3% because of better equipment definition, and increased approximately 18% because of improved maintenance features and added capability. Volume has also increased approximately 25%. This increase is almost entirely caused by the increase in the momentum storage system.

### 3.4 EFFECT OF DISTURBANCES ON TORQUE AND IMPULSE SIZING

The sizing of the SCS actuators is dependent on: (1) the disturbing forces and resulting impulse imposed on the orbiting space laboratory, (2) the desired response to these disturbances, and (3) the maneuvering capability required. This section evaluates the first category of sizing influence, which is predominant in estimating propellant consumption, and CMG torque and momentum requirements. The effects of the other two influences are discussed in subsequent sections.

#### 3.4.1 Analysis of Dynamic Disturbances

The major external disturbances are the aerodynamic forces and gravity gradient torques that are dependent on the space laboratory configuration, orientation, and orbital parameters. To assist in evaluating these disturbances, two digital computer programs were written. One program describes the aerodynamic drag and torques, and their impulse histories for the space laboratory in a belly-down orientation. The second computer program is used for the inertial and roll solar orientations' torque and impulse histories. The advantage of the computer programs is their capability to determine the SCS requirements for many space laboratory configurations with speed and accuracy. The SCS requirements obtained from these programs are the propellant quantities necessary for maintaining orbital altitude, the propellant required to counteract the bias disturbing torques, and the impulse-time histories needed to obtain the momentum storage size requirements for external disturbance control.

The results of the computer studies, in terms of propellant and momentum storage requirements, are presented in the following paragraphs. Several vehicle configurations with two different methods of storing modules on the space laboratory are considered. The propellant requirements are based on an average taken over a period of 6 months for each of several of the years during the 11-year solar cycle. The momentum storage sizing is based on the maximum impulse history encountered during the solar cycle. A detailed explanation of the propellant and momentum storage requirements caused by the major disturbances (aerodynamics and gravity gradients) is given in the Appendix A, Control System Analysis.

Several miscellaneous disturbances are encountered during the mission which have negligible effects on the space laboratory. These disturbances are solar radiation, Earth magnetic field, and micrometeorites. The order of magnitude for these disturbances ranges between  $10^{-2}$  and  $10^{-8}$  when compared to the gravity gradient and aerodynamic disturbances.

Another source of external disturbance is that caused by docking a logistic spacecraft on the space laboratory. For longitudinal docking (along the roll axis) the anticipated impact rates are 0.5 ft/sec in translation and  $0.25^\circ/\text{sec}$  in rotation. If radial docking (normal to the longitudinal axis) is employed, an angular rate of  $2.5^\circ/\text{sec}$  is expected as a result of the impact.

Internal disturbances resulting from crew motion are limited by the laboratory volume, and assumed to be random in nature. Maximum angular rates and attitude errors resulting from the movement of one crew member from one side of the laboratory to the other are  $0.06^\circ/\text{sec}$  and  $0.13^\circ$ , respectively.

Of the internal disturbances arising from equipment motion, the centrifuge operation imposes the maximum requirement on the SCS. To negate the effect of the centrifuge at a 1-g environment requires an angular momentum of 2,940 lb-ft-sec from the roll axis control moment gyros (CMG). The centrifuge requirement is summed with the requirements for the other major disturbances to obtain the total momentum storage sizing for the roll axis. Operation at 9 g, to follow the re-entry profile, applies a disturbance torque of 9.7 lb-ft to the roll axis and generates an angular momentum vector

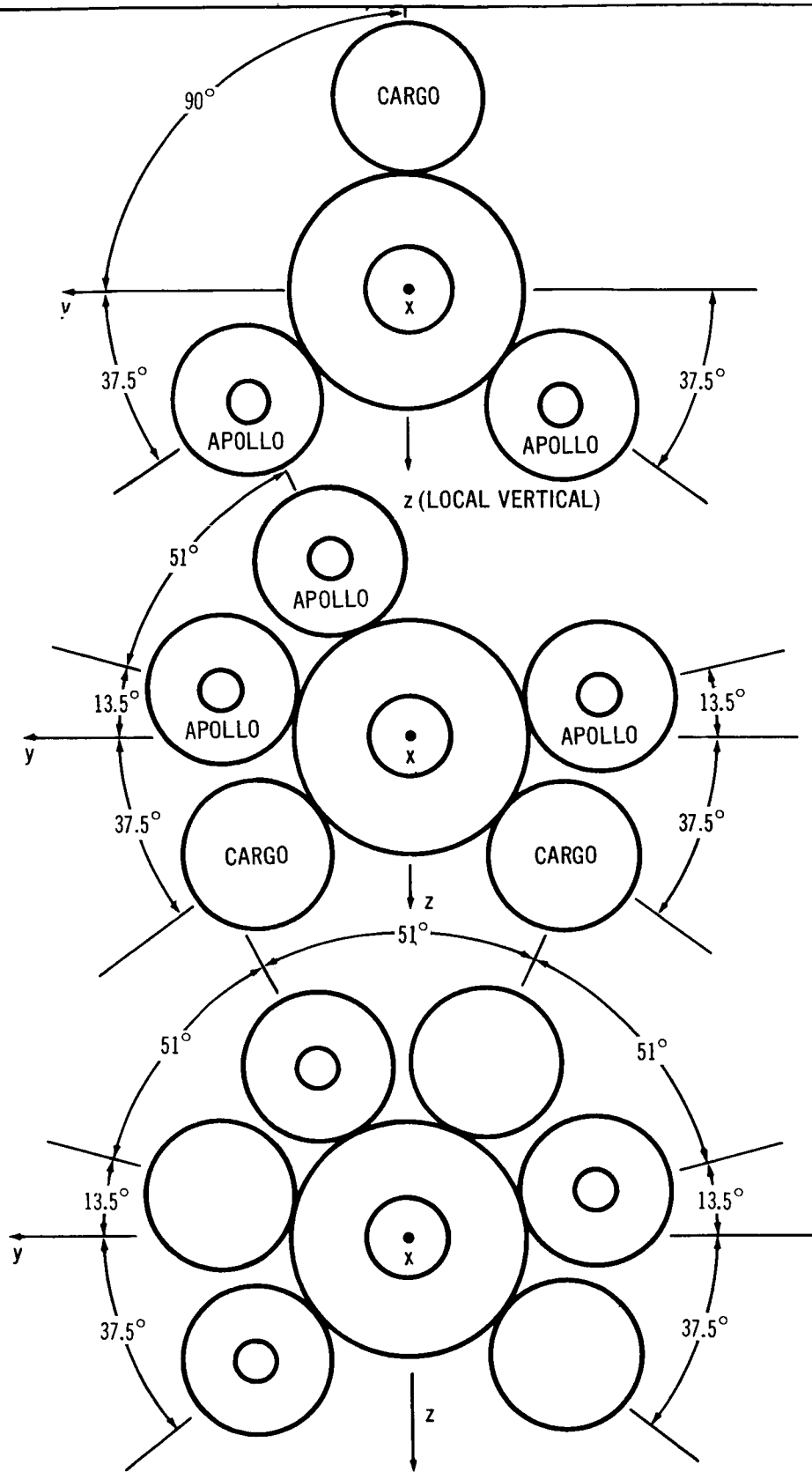
of 8,800 lb-ft-sec. To eliminate any cross-coupling torques, it is assumed that the centrifuge will be operated above 1-g only when the vehicle is in an inertial orientation.

#### 3.4.2 Effect of Laboratory Configuration on Sizing

Propellant consumption estimates and momentum storage sizing requirements are based on only the effects of aerodynamic and gravity gradient disturbances, and the centrifuge control problem. Because the aerodynamic and gravity gradient torques are a function of mass distribution, it is necessary to evaluate the effects of each major vehicle configuration on the SCS requirements. Several schemes of stowing cargo and Apollo command modules on the laboratory are shown in Figures 3-3 and 3-4. The method of longitudinal stowing is shown in Figure 3-3. Figure 3-4 illustrates the concept of radial stowing. The inertia data for each configuration, on which the gravity gradient torques are based, are also given in these figures.

For the belly-down orientation, the products of inertia are the source of the gravity gradient torques because the body roll axis is to be aligned with the orbital velocity vector. The product of inertia,  $I_{xz}$ , rotates the principal roll axis towards the local vertical and produces a constant gravity gradient torque about the pitch axis. Since the pitch axis is fixed with respect to the orbit, the time history of the impulse appears as a ramp function. This represents a bias impulse which must be either continuously removed, or stored and removed periodically. To store the impulse for any length of time requires a momentum storage unit; to remove the impulse requires the RCS. The other product of inertia that produces a gravity gradient torque for the belly-down orientation is the  $I_{yz}$  term. This produces a constant gravity gradient torque about the roll axis of the laboratory. Since the roll axis is not inertially fixed with respect to the orbit (as is the pitch axis), the constant roll torque will produce a cyclic impulse (with respect to the orbit period) about both the roll and yaw axes. Because these impulses (as a result of the  $I_{yz}$  term) are cyclic, they can be negated by momentum storage devices.



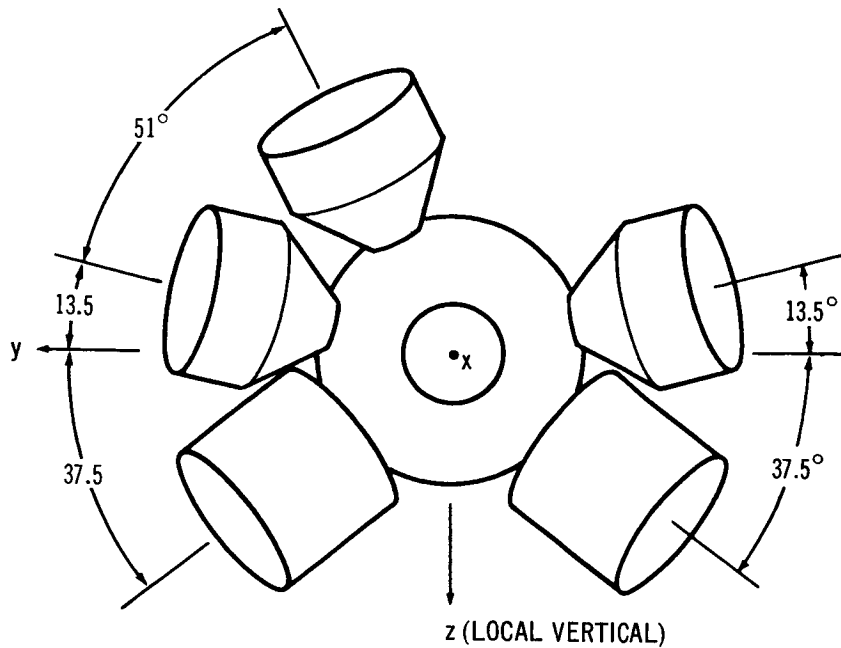


CONFIGURATION X  
 $I_x = 0.5 \times 10^6 \text{ SLUG-FT}^2$   
 $I_y = 0.8 \times 10^6 \text{ SLUG-FT}^2$   
 $I_z = 0.67 \times 10^6 \text{ SLUG-FT}^2$   
 $I_{xz} = 0.035 \times 10^6 \text{ SLUG-FT}^2$

CONFIGURATION L-5  
 $I_x = 0.89 \times 10^6 \text{ SLUG-FT}^2$   
 $I_y = 0.98 \times 10^6 \text{ SLUG-FT}^2$   
 $I_z = 0.58 \times 10^6 \text{ SLUG-FT}^2$   
 $I_{xy} = 0.013 \times 10^6 \text{ SLUG-FT}^2$   
 $I_{xz} = 0.01 \times 10^6 \text{ SLUG-FT}^2$   
 $I_{yz} = 0.045 \times 10^6 \text{ SLUG-FT}^2$

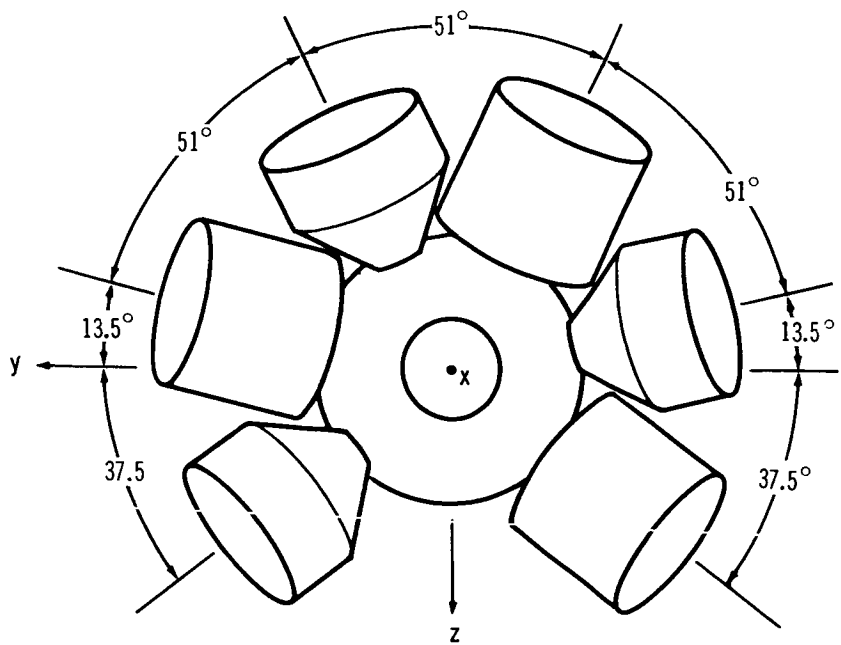
CONFIGURATION L-6  
 $I_x = 1.14 \times 10^6 \text{ SLUG-FT}^2$   
 $I_y = 0.72 \times 10^6 \text{ SLUG-FT}^2$   
 $I_z = 0.48 \times 10^6 \text{ SLUG-FT}^2$   
 $I_{xy} = 0.038 \times 10^6 \text{ SLUG-FT}^2$   
 $I_{xz} = 0.003 \times 10^6 \text{ SLUG-FT}^2$   
 $I_{yz} = 0.023 \times 10^6 \text{ SLUG-FT}^2$

Figure 3-3. Longitudinal Stowing Configurations



CONFIGURATION R-5

$$\begin{aligned}
 I_x &= 0.69 \times 10^6 \text{ SLUG-FT}^2 \\
 I_y &= 0.84 \times 10^6 \text{ SLUG-FT}^2 \\
 I_z &= 0.72 \times 10^6 \text{ SLUG-FT}^2 \\
 I_{xy} &= 0.011 \times 10^6 \text{ SLUG-FT}^2 \\
 I_{xz} &= 0.013 \times 10^6 \text{ SLUG-FT}^2 \\
 I_{yz} &= 0.038 \times 10^6 \text{ SLUG-FT}^2
 \end{aligned}$$



CONFIGURATION R-6

$$\begin{aligned}
 I_x &= 0.88 \times 10^6 \text{ SLUG-FT}^2 \\
 I_y &= 0.94 \times 10^6 \text{ SLUG-FT}^2 \\
 I_z &= 0.84 \times 10^6 \text{ SLUG-FT}^2 \\
 I_{xy} &= 0.052 \times 10^6 \text{ SLUG-FT}^2 \\
 I_{xz} &= 0.003 \times 10^6 \text{ SLUG-FT}^2 \\
 I_{yz} &= 0.014 \times 10^6 \text{ SLUG-FT}^2
 \end{aligned}$$

Figure 3-4. Radial Stowing Configurations

In the belly-down orientation with solar panels, the major disturbance is caused by the aerodynamic forces on the solar panels. These forces result in large momentum storage and propellant requirements. Because the baseline electrical power supply for the space laboratory is changed to the Isotope Brayton Cycle, the detailed description and formulation for the belly-down orientation with solar panels is given in Appendix A.

Without the solar panels, the aerodynamic moments are small (between 5% and 10% of the gravity gradient) for the laboratory in the belly-down orientation. These aerodynamic moments are caused by the relative displacement between the center of pressure and the center of mass.

#### 3.4.3 Use of CMG Desaturation Propellant for Orbit-Altitude Maintenance

As noted in the previous paragraph, the product of inertia,  $I_{xz}$ , produces a bias impulse about the pitch axis which must be removed periodically by the RCS. By utilizing one aft-firing thruster to remove the bias impulse, thereby desaturating the pitch axis control moment gyros, the effect of drag can be counteracted and orbit-altitude maintenance can be accomplished.

This represents a substantial propellant saving. The drag makeup during desaturation can be accomplished throughout the orbit by both pitch and yaw thrusters because the vehicle roll axis is aligned with the orbital velocity vector. Since orbit-keeping should be accomplished with two equal impulses spaced  $180^\circ$  apart in the orbit (to maintain circularity), the desaturation intervals will be selected accordingly. The momentum storage CMG requirement for this bias moment on the pitch axis is obtained by dividing the impulse accumulated over one-half of an orbit by  $2 \sin 60^\circ$ . This latter factor assumes that the CMG gimbals are deflected  $60^\circ$  in each direction. At this point, desaturation, or momentum dump, is accomplished. The propellant requirements given in the next paragraph are based on the use of this desaturation scheme.

### 3.4.4 Propellant Consumption and Momentum Storage Sizing for Selected Laboratory Configuration

Figure 3-5 shows the propellant consumption as a function of the year for Configuration X of Figure 3-3. (The nomenclature is a carry-over from Phase IIa, where this configuration was originally identified.) The solid curve is the total propellant required and the dashed curve shows the amount of propellant required for orbit keeping. The propellant requirements are based on a 10-ft lever arm and an  $I_{sp}$  of 270 sec. After the year 1969, the total propellant requirement is determined by the attitude control requirements. This is shown to be practically independent of the year because the aerodynamic bias moment at 200 nmi is only 5% of the gravity gradient moment; at 164 nmi the orbit-keeping requirement dominates until 1971. Beyond that time, the attitude control requirement is more than enough to satisfy the orbit-keeping needs.

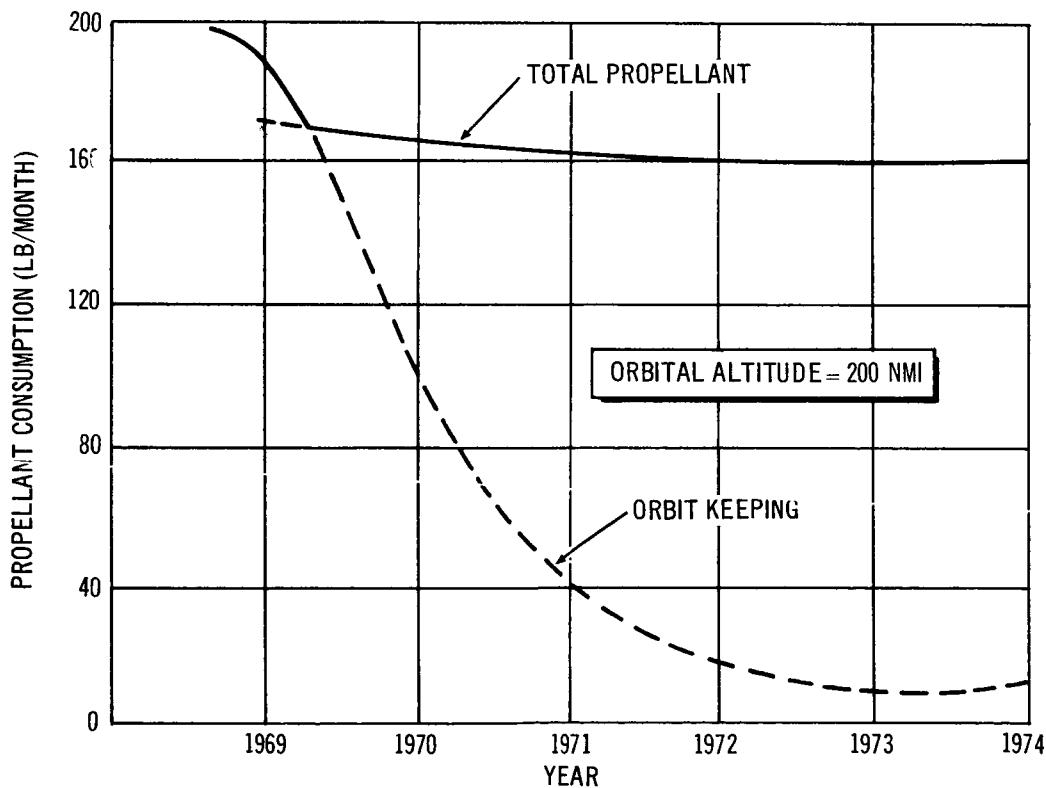


Figure 3-5. Effect of 11-Year Solar Cycle on Propellant Requirements

Table 3-2 lists the propellant requirements and momentum storage requirements for all of the configurations shown in Figures 3-3 and 3-4. All of these requirements are based on the year 1969, a propulsion  $I_{sp}$  of 270 sec, a 10-ft control lever arm, and a 200 nmi orbit altitude.

As a comparison for Configuration X, shown in Table 3-2, the propellant consumption with solar panels is 260 lb/month, which is essentially the orbit-keeping requirement. The increase of the SCS requirements for the laboratory with solar panels is presented in Appendix A.

Orbit keeping while in the belly-down orientation is preferred since, in this orientation, the pitch and yaw thrusters are always aligned with the velocity vector. In the inertial orientation, all RCS functions for attitude control are to be provided for by couples. The drag makeup requirement, while in the inertial orientation, will be made up in the belly-down orientation.

The impulse requirements for the inertial orientation, with the Isotope Brayton Cycle power supply, are mainly dependent on the gravity gradient torques. For the year of maximum solar activity, the aerodynamic torques are approximately 40% of the gravity gradient torques. The SCS requirements for the inertial orientation are determined from a worst-case condition of the gravity gradient torques (a description of this particular orientation is given in Appendix A). The SCS external disturbance control requirements for Configuration X in the inertial orientation, with the Isotope Brayton Cycle power supply, are as follows:

1. Roll momentum storage: 3,030 lb-ft-sec.
2. Pitch and yaw momentum storage: 910 lb-ft-sec.
3. Attitude control propellant: 310 lb/month.

Since a set of two double-gimbal gyros is to be used for both the pitch and yaw axes, the pitch and yaw momentum storage requirements are combined. The propellant is again based on an  $I_{sp}$  of 270 sec, the year 1969, and a control lever arm of 10 ft. The additional orbit-keeping requirement for the inertial orientation is 0.67 lb/orbit, which is accomplished in the belly-down orientation.

Table 3-2  
 PROPELLANT CONSUMPTION AND MOMENTUM STORAGE REQUIREMENTS

Storage Configuration	No. of Modules	Momentum Storage (lb-ft-sec)*				Propellant (lb/mo)*		
		Roll	Pitch	Yaw	Attitude Control	Orbit Keeping	Total	
Longitudinal	Two Apollos and one cargo (Config X)	2, 940 (Centrifuge)	240	0	170	190	190	
	Three Apollos and two cargo	3, 100	80	310	80	250**	250	
	Three Apollos and three cargo	3, 020	240	160	180	280**	280	
Radial	Three Apollos and two cargo	3, 070	70	260	50	260**	260	
	Three Apollos and three cargo	3, 030	320	180	240	290**	290	

\*Values are for the belly-down orientation, year 1969, orbit altitude, 200 nmi.  
 \*\*The orbit-keeping requirements are based on preliminary drag coefficients for these configurations.

The worst-case momentum storage requirements, obtained from both the belly-down and inertial orientations, and for the highest solar activity are as follows:

1. Roll momentum storage: 3,100 lb-ft-sec.
2. Pitch and yaw momentum storage: 910 lb-ft-sec.

These external disturbance momentum storage requirements, which satisfy any of the configurations presented in Figures 3-3 and 3-4, are to be combined with the recommended maneuvering momentum (as defined in Section 4.4) for the purpose of sizing the CMG system.

### 3.5 SYSTEM PERFORMANCE

The ultimate laboratory steady-state attitude and rate stabilization accuracy obtainable by the SCS is primarily dependent on the sensing device employed for the particular mission event. On a transient basis, this stabilization and control accuracy is primarily dependent on the severity of the disturbance inputs. The accuracies quoted in the following paragraphs are based on predicted external disturbances and estimated crew-motion disturbances. The SCS, as defined, is capable of meeting all the nonexperimental performance requirements. There are, however, a number of experiments which call for attitude and rate requirements which are beyond the capability of the SCS. Section 2 details the performance requirements and the MORL concept responsiveness analysis, reported in Task Area III, details the total accommodation assessment. This assessment can be summarized as follows:

1. The SCS has an attitude control accuracy of  $0.5^\circ$  using horizon scanner and gyrocompassing (horizon-hold mode). Body rates which are dependent on transient disturbances, are expected to be nominally  $0.01^\circ/\text{sec}$ .
2. Using the inertial reference system, the SCS has an attitude control accuracy of  $0.1^\circ$  for (at least) 1 hour, a stabilization capability of  $0.01^\circ/\text{sec}$  after star tracker update (inertial and orbital hold modes), and a celestial-hold accuracy of  $0.1^\circ$  for an indefinite period using the star tracker directly through the DPC (celestial-hold mode).
3. The SCS has an attitude measurement accuracy of  $0.01^\circ$  and a rate measurement capability of  $0.0006^\circ/\text{sec}$  using the star tracker and the body-mounted inertial rate integrating gyros (in a rate mode), respectively.

4. Propellant consumption is excessive for maneuvering the MORL to accommodate Earth-tracking experiments (on the order of 10 lb/maneuver) and other experiments requiring slew rates above  $1^\circ/\text{sec}$ ; therefore, experiments having slewing requirements above  $1^\circ/\text{sec}$  will have their sensor elements mounted on gimbals and the laboratory will be held at a fixed attitude. This essentially eliminates the laboratory-attitude-hold requirement for 8 of the 14 experiments shown in Figure 2-2 needing  $0.1^\circ/\text{sec}$  or better and the stabilization requirements for the two experiments needing  $0.0006^\circ/\text{sec}$  or better.
5. The remaining eight experiments, six from the attitude chart (Figure 2-1) and two from the rate chart (Figure 2-2), that can not be accommodated by the SCS, must provide their own error sensing and must be gimballed to provide for slewing and dynamic isolation.

The SCS laboratory control and measurement capabilities are indicated on the experiment requirements charts (Figures 2-1 and 2-2) along with crew-motion-rate limits.



Section 4  
SYSTEM IMPROVEMENT STUDY

A major portion of the Task Area IV effort has been devoted to analysis of possible improvements to the baseline Stability and Control system (SCS) concept, determined at the completion of the MORL Phase IIa program.

4.1 STUDY SOURCES

The present system concept does not differ fundamentally from the baseline SCS developed in the MORL Phase IIa study. The changes incorporated in the current design are in the nature of desired refinements which have been identified by examining the following:

1. Task III responsiveness analysis study.
2. Task III 48-hour study.
3. Task IV improvement analysis.
4. Effects of launch date extensions.
5. Effects of changes in interfacing MORL subsystems.

Each of these areas has contributed recommended changes or improvement studies. Since implementation of the total list of recommendations was not within the scope of the Phase IIb effort, only the critical subjects from each of these areas were selected for analysis or implementation. The recommended changes or improvement studies resulting from each of the five topics are noted in the following text.

4.1.1 Task III Responsiveness Analysis

This study was mainly concerned with the ability of the SCS to accommodate experimental requirements. It was concluded that the Stabilization and Control system design concept is adequate if the specified attitude reference and control accuracies can be met and if experiments which require high slewing rates and high pointing or rate control accuracies are mounted on

separately-stabilized gimballed platforms. This latter approach allows the laboratory SCS to provide the basic attitude reference information and control commands but isolates the experiments from laboratory transient disturbances. To guarantee a high probability of success in meeting the accuracy specification, the following changes to the Phase IIa baseline SCS were recommended:

1. Relocate the attitude reference sensors and experiments requiring high accuracy on a common, rigid-mount base.
2. Develop an in-flight alignment and calibration method for the attitude-reference and experiment sensors.

These subjects are reported in Subsection 4.8. Item 2 is covered in further detail in Appendix C. In addition to these changes, the following areas were recommended for further study:

1. Further substantiation analysis of the  $\pm 0.5^\circ$  horizon sensor/gyrocompass accuracy.
2. Further substantiation analysis of the  $\pm 0.1^\circ$  attitude control accuracy in the stellar-inertial mode.
3. Further investigation of the crew motion category of transient disturbance.
4. Further substantiation analysis of the  $0.01^\circ$  attitude sensing and experiment control accuracy in the stellar-inertial mode and the  $0.0006^\circ/\text{sec}$  rate measurement accuracy.

Since detailed study in all of these areas was not within the scope of the present effort, the following actions were taken:

1. Analysis of the horizon sensor/gyrocompass mode was initiated and is reported in Subsection 4.3 and in detail in Subsection A.2 of Appendix A.
2. Further substantiation analysis of the  $0.1^\circ$  attitude-hold accuracy was accomplished by investigation of the error sources associated with the precision attitude reference and by investigation of the experiment sensor alignment errors. The precision attitude reference, which contains inertial platforms, star trackers, and a computer, is reported in Appendix C and D. Experiment sensor alignment is discussed in Appendix C.
3. Further investigation of the crew motion disturbances is outside the scope of this study and is recommended for a follow-on effort.
4. Further substantiation of  $0.01^\circ$  accuracy attitude sensing and control capability is given in the attitude reference and alignment studies noted in (2), above. Further analysis of rate measurement accuracy has been postponed.

#### 4. 1. 2 Task III 48-Hour Study

The 48-hour study, which involved a detailed examination of the operations associated with a brief segment of the mission, was designed to identify problem areas not readily discernable from a gross examination of the total mission. This study illuminated several problems associated with the SCS experiment interface and resulted in the following recommendations for change or follow-on study:

1. Further expansion of the experiment integration study, incorporating the complete spectrum of experiment types and investigation at a more detailed functional level. The objective is to refine experimental support requirements to be imposed on the SCS and to develop a more detailed definition of the total experiment/laboratory interface. This would require a significant amount of effort and it is recommended as a post-Phase IIb study.
2. Relocation of attitude reference sensors and development of an attitude reference to experiment alignment concept, as also noted in the Task Area III responsiveness analysis study.
3. Detailed analysis of the performance of the combined SCS experiment control loop, including all significant error sources and all significant variations of the experiment pointing, tracking, and control problem.

Item 2, above, was identified as a serious problem, requiring immediate investigation. The ability to accurately control experiment sensors located several feet from the laboratory attitude reference sensors is influenced by the pressure and temperature changes which distort the mounting structure and cause misalignment between the attitude reference and the remote experiments. Two approaches have been taken to resolve this problem: (1) incorporation of a separate attitude reference and experiment mounting beam designed to minimize effects of pressure and temperature variations, and (2) incorporation of an electro-optical alignment system to measure alignment deviations and permit their compensation. Design features of the attitude reference beam are discussed in Book 1, SM48815, and summarized in Appendix C, with details of the electro-optical alignment scheme.

Item 3, above, has been postponed for future study, although the first steps toward identifying error sources have been taken in the error analyses (given in Appendices C and D).

#### 4.1.3 Task IV Improvement Analysis

As part of the overall objective to improve the design concept for MORL and its subsystems, an SCS design review was conducted. This resulted in identification of several items recommended for study as part of the Task Area IV effort, including the following:

1. Optimization of the control moment gyro size for attitude maneuvering.
2. Updating of the CMG design.
3. Improving the estimates for attitude control propellant, orbit maintenance propellant, and momentum storage impulse requirements imposed by aerodynamic and gravitational gradient disturbances.
4. Investigation of manual control modes.
5. Further definition and integration of the total system hardware mechanization.
6. Updating of the display and control functional and equipment requirements.
7. Review of equipment selection to increase utilization of existing and in-development hardware, with emphasis on Apollo usage.
8. Re-evaluation of the precision inertial attitude reference selection.

Items 1 and 2 have been investigated and are included in Subsection 4.4 and Appendix A. Item 3 is discussed in 4.2 and Appendix A. Item 4 is summarized in 4.5 and Appendix A. Items 5, 6 and 7 are summarized in 4.6 and Appendix B. The last, Item 8, is briefly summarized in 4.7 and presented in depth in Appendix D.

#### 4.1.4 Effects of Launch Date Extensions

While the improvements identified in Subsections 4.1 through 4.8 are concerned with use of present technology and assume a fixed program schedule, it is of interest to examine the effects of extensions in the launch date of from 1 to 5 years. Possible changes in technology in this period, which may be of advantage to the SCS, are described in Subsection 4.9. These include the following:

1. Incorporation of improved accuracy angle encoders in the inertial reference.

2. Use of gas-bearing gyros or electrostatic gyros.
3. Use of improved-accuracy horizon sensors.
4. Use of mono-pulse radar for determining the local vertical and orbit plane.
5. Use of advanced electronic packaging concepts (for instance, integrated circuits).
6. Use of improved CMG configurations which yield greater torque and momentum per unit of weight and power.
7. Use of low-thrust, high specific impulse reaction control systems.

#### 4.1.5 Effects of Changes in Interfacing MORL Subsystems

This final consideration has revealed the need for an investigation of the following:

1. Re-evaluation of the long-term orientation selection because of changeover to a Brayton Cycle Power system.
2. Resizing of propellant consumption and CMG momentum storage requirements because of change to a Brayton Cycle Power system, modification in the logistics module stowage configuration, and a reduction in orbital altitude.

These topics are covered in Subsection A. 1. 2 of Appendix A.

#### 4.2 IMPROVEMENTS IN DISTURBANCE AND SIZING ANALYSES

In Phase IIa, the SCS sizing requirements (CMG sizing and propellant consumption) were derived by hand calculations. These requirements, because of aerodynamic and gravitational gradient disturbances, are dependent on vehicle configuration, orientation, and position. As a consequence, procedures were established to determine the SCS requirements with reasonable mathematical approximations of the actual phenomena.

When the SCS requirements are hand-calculated, only a limited number of orbital conditions which describe the location of the orbit plane with respect to the ecliptic plane can be examined. CMG sizing is then based on the maximum impulse history for all three body axes. In general, this is difficult to determine, since the aerodynamic and gravitational gradient disturbances do not reach extremes at the same time; however, successive trials can be used to reach a near-maximum condition for a given vehicle configuration.

To reduce the limitations inherent in hand calculations, two digital computer programs were developed in Phase IIb. These programs include an accurate description of the atmospheric bulge with respect to the orbital position for the purpose of computing the aerodynamic forces. The diurnal bulge is assumed to be symmetrical in two dimensions and moves in the ecliptic plane, lagging the sun line by  $28^\circ$ . The orbital conditions used in the hand calculations were limited to the condition of the orbit plane passing through the maximum bulge of the atmosphere. This, of course, is not realistic and leads to higher than average propellant consumption rates. The digital programs give a true simulation of the orbital position with respect to the diurnal bulge for any selected orbital altitude. Elliptical orbits can be simulated in the range of 180- to 500-nmi orbits. In the program operations, aerodynamic pressure is computed on the basis of the orbital altitude and diurnal bulge descriptions. The programs describe the aerodynamic moment and force coefficients as a function of orbital position and celestial parameters, from which the aerodynamic moment and drag values are obtained. With the aerodynamic moments and the gravitational gradient moments combined (which are computed throughout the orbit for the specific celestial parameters), the total disturbing moment is defined. Time integrations of these disturbing moments and the drag force yield the total impulse-time histories needed for determining the CMG momentum storage requirements and RCS propellant estimates.

One of these digital programs is for the belly-down orientation and the other is for both the roll solar and inertial orientations. Both programs are simulated in a like manner. Starting with a set of initial celestial parameters, the disturbance torques (aerodynamic and gravity gradient) and the drag forces are integrated over equal increments of orbit angle over a complete orbit. After one orbit is completed, a second, larger increment, in the form of number of orbits, is made to describe the regression rate of the orbit, the precession rate of the perigee, and the autumnal equinox. In this manner, several orbits could represent an average of several days, or weeks, or whatever the case, with a minimum of computer time and data printout.

With this simulation of the varying celestial parameters, a maximum impulse history to determine the CMG sizing and the average propellant consumption can readily be obtained.

Figure 4-1 is a sample of the results from the solar program and shows the drag impulse in lb-sec/orbit for Configuration X in the roll solar orientation, as a function of days. This particular computer run is for a perigee altitude of 200 nmi at an inclination of  $53^\circ$  for the 1969 solar activity. The celestial parameters are  $\Omega_0$  (angle between autumnal equinox and direction to the sun) =  $-48.3^\circ$ ;  $\lambda_0$  (the angle between the autumnal equinox and the line of nodes of the orbit) =  $-211.3^\circ$ ;  $e$  (orbit eccentricity) = 0.001. The curve shows that the drag impulse varies by a factor of nearly two over a period of 18 days.

Figure 4-2 shows the accumulated angular impulse for the pitch and yaw axes as a function of time. This accumulated impulse must be removed by the RCS and it is from this that the attitude propellant requirements are

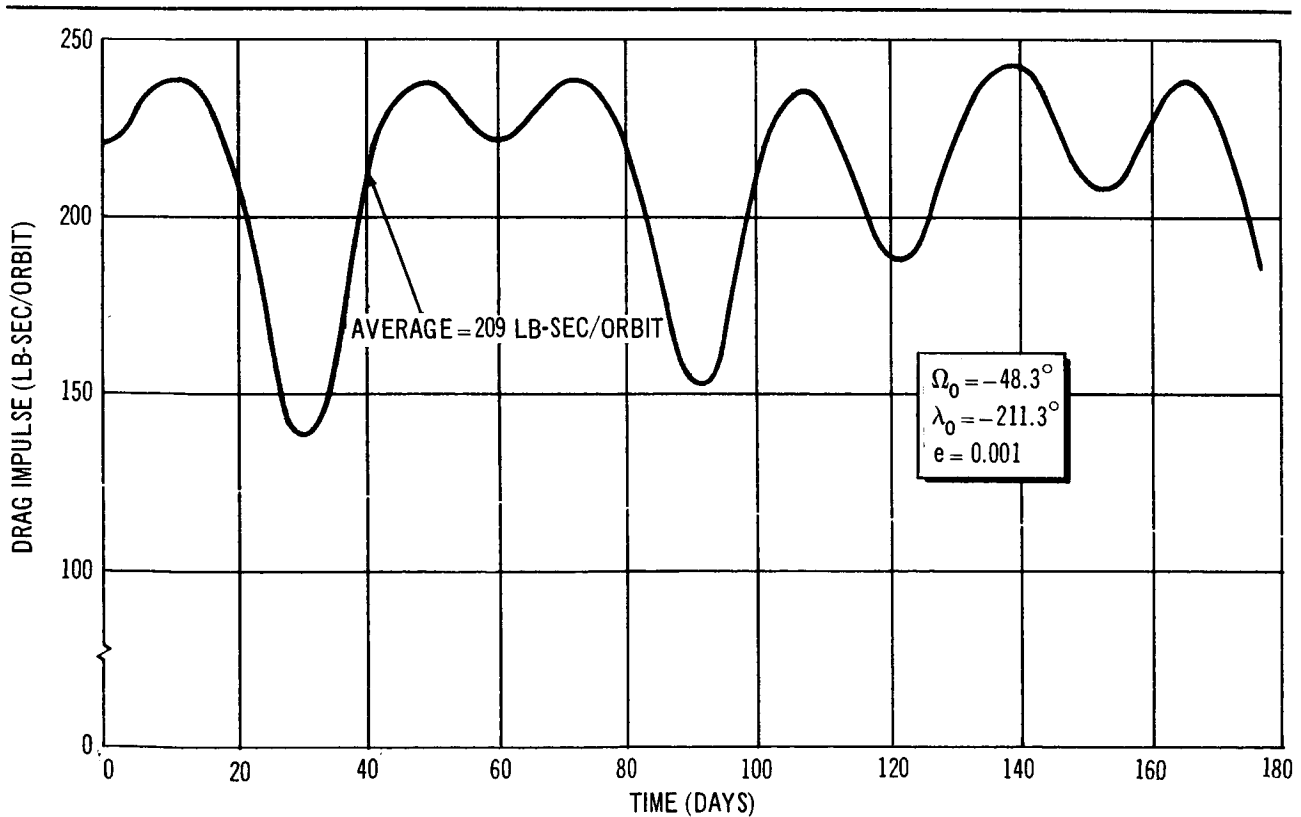


Figure 4-1. Roll Solar Drag Impulse History

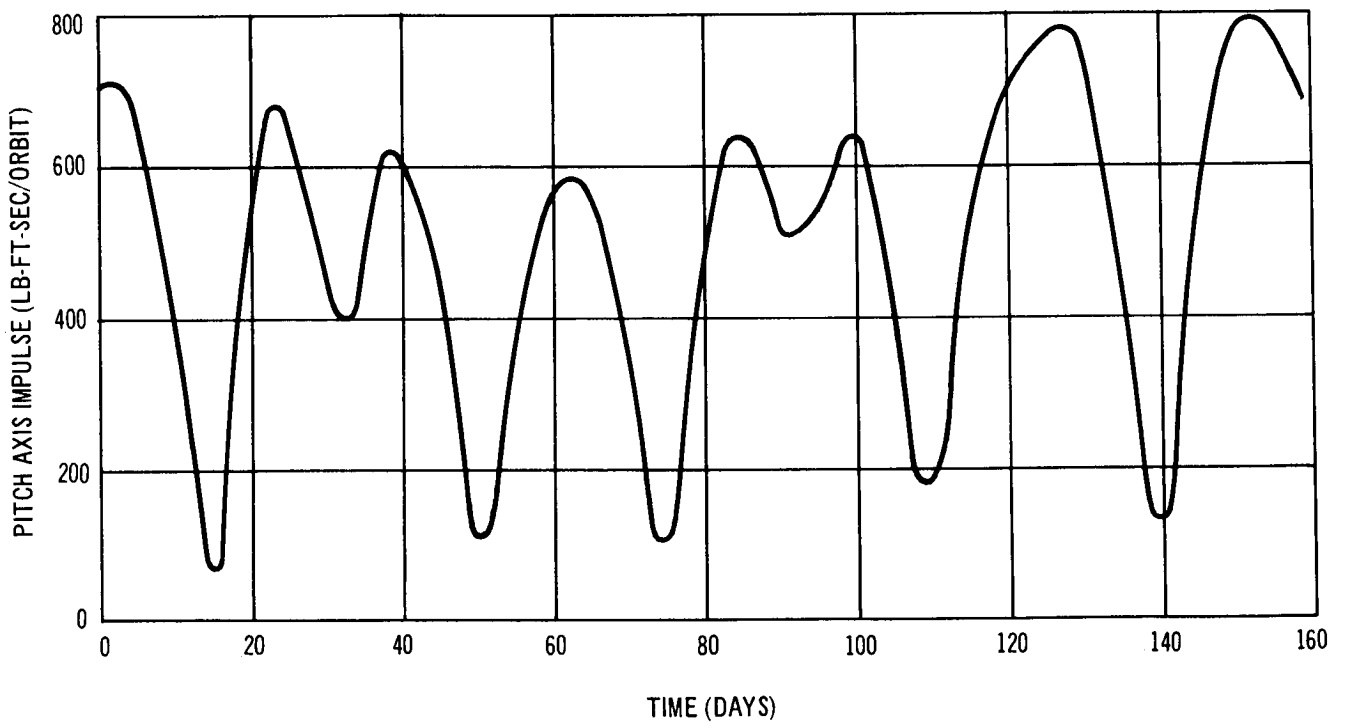
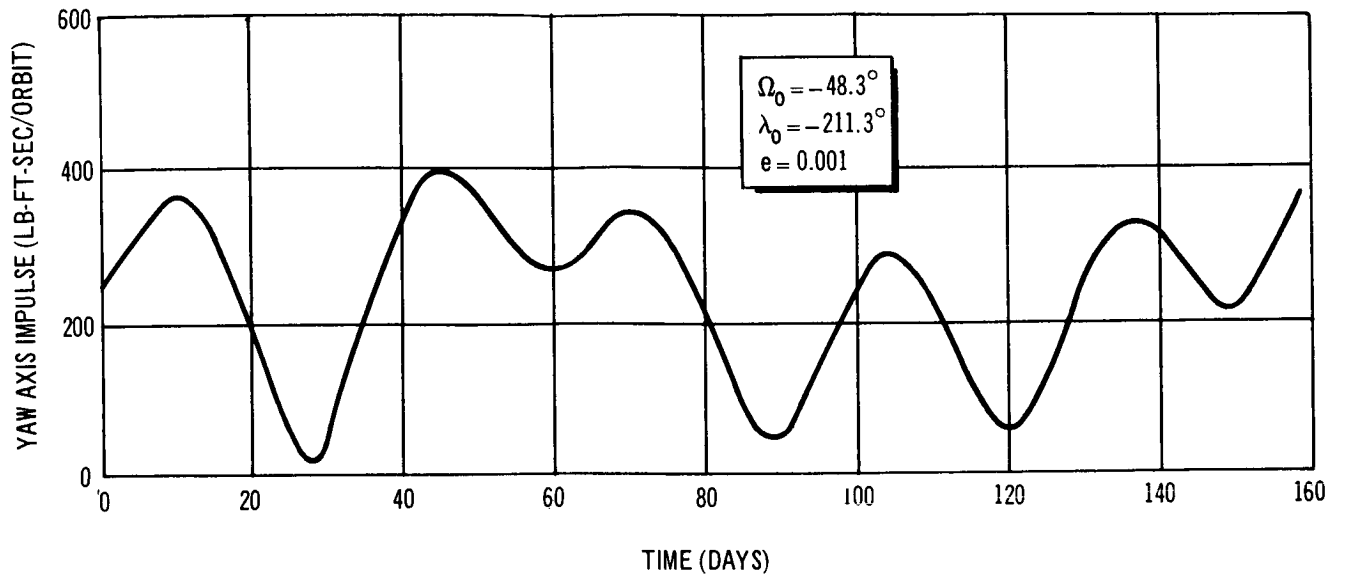


Figure 4-2. Roll Solar Accumulated Angular Impulse History



determined. These plots are for the same vehicle configuration and celestial parameters shown in Figure 4-1. Additional results obtained from these programs are presented in Section A.1.2 of Appendix A.

The use of these computer programs for determining the SCS requirement to compensate for aerodynamic and gravitational gradient disturbances has provided fast and accurate information and produced significant improvements in the estimation of CMG momentum and RCS propellant requirements.

#### 4.3 GYROCOMPASSING PERFORMANCE

In normal long-term operation of the laboratory, an orientation has been selected which aligns the roll, or X, axis with the orbital velocity vector and the yaw, or Z, axis with the Earth's geocenter. This orientation is referred to as the belly-down orientation. For routine operations an attitude accuracy of  $0.5^\circ$  is required. To meet these attitude requirements, a horizon sensor/gyrocompass stabilization technique is utilized.

With this technique (briefly investigated in the Phase IIa study), a two-axis horizon sensor provides the pitch and roll attitude errors. The yaw attitude error,  $\psi$ , is derived from the output of the roll rate gyro,  $\omega_x$ . A yaw attitude error results in a component of orbital rate,  $\omega_o$ , coupled into the roll axis. The derived yaw attitude error,  $\psi$ , is then  $\omega_x/\omega_{orb}$ . The attitude errors and body rates are used to command the control moment gyro gimbal rates for vehicle stabilization. The limiting factors of this system are the accuracy to which the vehicle can be controlled with respect to the local vertical and the rate threshold of the gyroscope. Horizon scanner accuracy establishes the limiting accuracy of the local vertical alignment. The roll gyro rate threshold is the limiting factor in alignment about the yaw axis. As described in Section 2, routine operations in the belly-down orientation require an attitude hold accuracy of  $\pm 0.5^\circ$ . This accuracy requirement, when operating with an orbit rate ( $\omega_{orb}$ ) =  $-0.001162$  radians/sec, requires roll rate gyro with a sensing threshold of  $0.00058^\circ$ /sec. This threshold is within the capability of an inertial grade integrating gyro operating in a rate mode.

In Phase IIb, an analysis of the horizon sensor/gyrocompass technique was initiated to evaluate the Phase IIa design and identify improvements, where necessary. This analysis, accomplished mainly with an analog computer, placed various types of disturbances in the system to determine their effects on performance. It was found that to achieve the required  $0.5^\circ$  attitude accuracy, some modifications of the Phase IIa baseline system were necessary.

#### 4.3.1 Description of Phase IIa Baseline Gyrocompassing Mechanization

Figure 4-3 shows the Baseline Phase IIa belly-down mechanization. As shown, the yaw attitude error is derived from the output of the roll rate gyro. The roll axis is controlled by commanding the single gimbal control moment gyro (SG CMG) gimbal rates as a function of the roll attitude error,  $\phi$ , and body roll rate,  $\omega_x$ . The pitch and yaw axes are controlled with the double gimbal control moment gyro (DG CMG) in the same manner as the roll axis. The pitch, or Y, axis control logic is not affected by the gyrocompass implementation.

The Phase IIa baseline gimbal rate control laws are given as follows:

$$\dot{\alpha}_{1c} = K_\phi \phi_m + K_{\omega_x} \omega_{x_m} \quad (\text{SG CMG gimbal rate, roll control}) \quad (4-1)$$

$$\dot{\alpha}_{2c} = K_\psi \psi_m + K_{\omega_z} \omega_{z_m} \quad (\text{DG CMG gimbal rate, yaw control}) \quad (4-2)$$

$$\dot{\beta}_c = K_\theta \theta_m + K_{\omega_y} (\omega_{y_m} - \omega_{orb}) \quad (\text{DG CMG gimbal rate, pitch control}) \quad (4-3)$$

where

$\omega_{x_m}$  = measured vehicle roll rate

$\omega_{y_m}$  = measured vehicle pitch rate

$\omega_{z_m}$  = measured vehicle yaw rate

$\phi_m$  = measured vehicle roll attitude



$\theta_m$  = measured vehicle pitch attitude

$$\psi_m = \frac{\omega_{x_m}}{\omega_{orb}} = \text{derived vehicle yaw attitude}$$

and the Phase IIa baseline system gains for the above control logic are  $K_\phi = 0.203$ ,  $K_{\omega_x} = 18.3$ ,  $K_\theta = 2.83$ ,  $K_{\omega_y} = 124.0$ ,  $K_\psi = 2.83$ , and  $K_{\omega_z} = 124.0$ . The control loop responses for these gains are shown in Table 4-1.

#### 4.3.2 Evaluation of Phase IIa Mechanization

In the performance evaluation of the Phase IIa baseline gyrocompass technique, system transient response was determined for both step and sinusoidal disturbance torques and for initial attitude errors. In addition, the extent to which roll angle transients couple into the yaw channel was determined. The results showed the gyrocompassing performance to be inadequate, and investigation of several methods of improving the mechanization was initiated.

In the Phase IIa baseline mechanization, if the vehicle has an inertial roll rate as well as a yaw attitude error, the derived yaw attitude error will be incorrect. One possibility for correcting the yaw attitude information is to attenuate the high-frequency roll rates with a filter network so that the filter output is again approximately proportional to the yaw attitude error. This output is combined with the yaw rate signal to provide control of the vehicle yaw axis. However, the network was found to be ineffective and has been omitted in the Phase IIb baseline system.

For the Phase IIa baseline system it was found that the responses of the roll and yaw channels could not be separated sufficiently in frequency to permit filtering to have a significant effect. Also, if the control gains in the roll channel are too small, system instability will result. The effect is produced by the CMG gimbal angle coupling. This coupling is between the orbital rate vector and the CMG momentum vector. In addition, sinusoidal torque disturbances at the orbital frequency cause the system to resonate. To

Table 4-1  
**PERFORMANCE SUMMARY OF PHASE IIa BASELINE AND PHASE IIb BASELINE  
 SCS SYSTEMS OPERATING IN THE BELLY-DOWN MODE\***

SCS System	Control Parameters					Control Loop Response				Performance (Maximum Allowable Disturbances)					
	$K_\phi$	$K_{\omega_x}$	$K_\psi$	$K_{\omega_z}$	$K_c$	$\phi_{DB}$	Natural frequency (rad/sec)		Dumping ratio		$\phi(0)$ (degrees)	$\phi(0)$ (degrees)	Step (ft-lb)	Sinusoid A sin $\omega t$	$T_{cZ}$
							x channel (roll)	z channel (yaw)	x channel (roll)	z channel (yaw)					
Phase IIa baseline	0.203	18.3	2.83	124	0		0.042	0.066	1.9	1.45	0.05	0.5	0.62	A $\approx$ 0.3 lb-ft, all $\omega$	Greater than 13.9 lb-ft
Phase IIb baseline	4.55	86.5	1.03	74.8	55	0.05	0.2	0.04	1.9	1.45	0.5	0.5	13.9	A = 2 lb-ft, 0.0035 < $\omega$ < 0.07 rad/sec A = 11.9 lb-ft, all $\omega$	Greater than 13.9 lb-ft

\*Belly-down stabilization requires an attitude accuracy of 0.5°

Gimbal control laws

$$\dot{\alpha}_{1c} = K_\phi \dot{\phi}_m + K_\omega \omega_{xm} + \frac{H}{H_x} \omega_{orb} \alpha_{2c}$$

$$\dot{\alpha}_{2c} = + \frac{K_\psi}{\omega_{orb}} \omega_{xm} + K_\omega \omega_{zm} - \frac{H_z}{H} \omega_{orb} \alpha_{1c} - K_c \phi_c \quad \text{where } \phi_c = \begin{cases} \phi_m & \text{for } |\phi_m| > \phi_{DB} \\ 0 & \text{otherwise} \end{cases}$$

avoid the gimbal angle coupling difficulties with initial angle disturbances and the resonance from sinusoidal torque disturbances, the gimbal control law equations were modified as shown below:

$$\dot{\alpha}_{1_c} = K_{\phi} \phi_m + K_{\omega_x} \omega_{x_m} + \frac{H}{H_x} \omega_{orb} \alpha_{2_m} \quad (4-4)$$

$$\dot{\alpha}_{2_c} = K_{\psi} \psi_m + K_{\omega_z} \omega_{z_m} - \frac{H_x}{H} \omega_{orb} \alpha_{1_m} \quad (4-5)$$

where

$H_x$  = angular momentum of the SG CMG

$H$  = angular momentum of the DG CMG

$\alpha_{1_m}$  = measured gimbal angle of SG CMG

$\alpha_{2_m}$  = measured yaw control gimbal angle of DG CMG

This modification eliminates the CMG dynamic coupling through the gimbal angles. Performance achieved with this modification shows that the non-zero steady-state problems for initial condition disturbances and the resonance for sinusoidal disturbances at the orbit frequency are eliminated.

Although no problems exist for disturbances in the yaw (Z) and pitch (Y) channels with this modification, disturbances in the roll channel still couple into the yaw channel, causing yaw angle transients which exceed the 0.5° attitude hold specification. For the initial condition,  $\phi(0) = 0.1^\circ$ , the yaw angle reached a maximum value of 1.0° before decreasing the settling back to zero; for a 2 lb-ft step torque input in the roll channel, the heading angle,  $\psi$ , reached a maximum of 1.6°, and, for a 2 lb-ft sinusoidal ( $\omega = 0.01$  cps) torque disturbance, the heading angle was a sinusoid of 0.63° amplitude. Since the system is approximately linear, an initial roll angle,  $\phi(0) = 0.05^\circ$ , will cause  $\psi$  to reach a maximum of 0.5°. Hence, according to the attitude requirements,  $\phi(0) > 0.05^\circ$  cannot be tolerated; by the same reasoning, a step torque disturbance  $T_{Dist} > 0.62$  lb-ft cannot be tolerated. It was also

determined that 2 lb-ft amplitude disturbances at frequencies between 0.0035 and 0.07 rad/sec cannot be tolerated. The largest torque amplitude disturbance that can be tolerated for all frequencies is 0.3 lb-ft.

The results of the study for x channel disturbances using Phase IIa baseline system gains are summarized in Table 4-1. Disturbances in the Y and Z channels of the above magnitude are not significant.

#### 4.3.3 Modifications which Produced the Phase IIb Baseline System

To improve the performance of the Phase IIa baseline system, it was necessary to modify the control law gains and insert roll angle cross feed into the yaw channel when the roll angle exceeded  $0.05^\circ$ . This modification resulted in the following control law equations:

$$\dot{\alpha}_{1c} = K_\phi \phi_m + K_{\omega_x} \omega_{x_m} + \frac{H}{H_x} \omega_{orb} \alpha_{2m} \quad (4-6)$$

$$\dot{\alpha}_{2c} = +\frac{K_\psi}{\omega_{orb}} \omega_{x_m} + K_{\omega_z} \omega_{z_m} - K_c \phi_c - \frac{H_x}{H} \omega_{orb} \alpha_{1m} \quad (4-7)$$

where

$$\phi_c = \begin{cases} \phi_m & \text{for } |\phi_m| > \phi_{DB} \\ 0 & \text{otherwise} \end{cases}$$

$$\phi_{DB} = 0.05^\circ$$

$$K_\phi = 4.55, \quad K_{\omega_x} = 86.5$$

$$K_\psi = 1.03, \quad K_{\omega_z} = 74.8$$

$$K_\theta = 2.83, \quad K_{\omega_y} = 124.0$$

The mechanization of the Phase IIb baseline system is shown in Figure 4-4. Allowable input disturbance levels were determined as described previously. Table 4-1 summarizes the performance of the baseline system defined at the conclusion of the Phase IIa effort and the modified Baseline Phase IIb system.





It can be seen that satisfactory gyrocompassing performance can be achieved with the Phase IIb baseline system. The addition of gimbal angle feedback effectively reduces gimbal dynamic cross coupling and eliminates resonance for sinusoidal torque disturbances at or near orbital frequency. Separation of the roll and yaw channel natural frequencies, achieved by increasing the roll channel response by a factor of 5 and decreasing the yaw channel response by 30% significantly reduces yaw channel sensitivity to roll channel torque disturbances, but preserves satisfactory overall dynamic response capability in the yaw channel.

The introduction of roll angle cross feed into the yaw control channel significantly reduces the magnitude of the yaw angle transient in response to a roll angle initial condition or step input disturbance arising, for example, from sensor output discontinuities. System response for  $10^\circ$  initial roll angle is damped out within approximately 3 min. Hence, when transferring from any other orientation to belly-down, only a gross attitude alignment is necessary before the automatic stabilization mode is activated. It should be emphasized that, for this gyrocompass study, the gimbal angular rate of the DG CMG was limited to  $1.15^\circ/\text{sec}$ , which corresponds to maximum torque output of 11 lb-ft. Limiting the gimbal rate at this value is not necessary if increased control moment gyro torque output capacity is incorporated. However, the results of the gyrocompass study would remain valid for increased torque capabilities.

#### 4.4 USE OF CONTROL MOMENT GYROS FOR ATTITUDE MANEUVERING

In Phase IIa, the momentum storage system (MSS) torque and momentum values were sized primarily to counteract the external disturbances and to control the centrifuge disturbances. This resulted in some limited capability for counteracting crew motion disturbances and for performing attitude maneuvers.

During Phase IIb, in addition to using the momentum storage system to counteract the disturbances, studies were made to determine the feasibility of expanding the control moment gyro (CMG) capabilities to provide the

control torques and moments necessary to maneuver the MORL through a realistic attitude maneuver profile. Tradeoff studies were conducted to determine if it would be profitable, from the standpoint of total mission resource, to use CMG rather than jets to perform the required maneuvers. These tradeoff studies, summarized in Subsection 4.4.1 with supporting details in Subsection A.3 of Appendix A, showed that the use of CMG for performing maneuvers is profitable if approximately 100 maneuvers are performed during the total mission life.

A detailed study, beyond the scope of the Phase IIb effort, is required to accurately estimate the number and type of maneuvers likely to be required during an entire mission. For the Phase IIb CMG sizing task, the value of 100 pitch or yaw maneuvers, averaging  $90^\circ$  per maneuver, was assumed.

#### 4.4.1 Sizing of CMG for Maneuvering

Studies of maneuvering techniques which use jet actuation indicated that maneuvers could be accomplished more economically when executed at relatively low slewing rates and with a thrust-coast-reverse thrust sequence. These results were based on the relative costs to the total laboratory resources of crew time and payload weight. The dollar values established during Phase IIa studies were \$19,000/pound and \$63,000/hour.

These cost factors were very preliminary, but the value ratio between crew time and weight of approximately 3:1 (hours to pounds) established with dollar cost as the common denominator, can be considered as a reasonably realistic ratio. With this ratio, a figure of merit designated laboratory resource usage factor (LRUF) was established which allowed a tradeoff to be made between jet and CMG actuation. Optimization of the CMG torque and momentum parameters was also done with the above figure of merit. This LRUF is essentially equivalent to the total laboratory resources used to provide a function. The lower the LRUF, the more economical or efficient the device.

As noted in Subsection A.3 of Appendix A, the studies showed that, with jet actuation, the maneuver rate required to minimize the LRUF for various maneuver angles up to 1 rad was approximately  $0.1^\circ/\text{sec}$ . Maneuver rates

on this order of magnitude make the use of control moment gyros a distinct possibility, provided torque requirements are not excessive, since the low rates imply low momentum storage requirements. The minimized LRUF occurring at these low rates, and for large angle maneuvers, is such that the crew time used while making the maneuver can be on the order of 10 min. and still be economical in terms of total laboratory resources. This means that for the fixed laboratory inertia involved ( $0.8 \times 10^6$  slug-ft<sup>2</sup>), the fixed maneuver rate specified,  $0.1^\circ/\text{sec}$ , and with approximately 10 min. available to make the maneuver economically, only a relatively low torque need be applied via the control moment gyros. These conclusions are only true, however, if the laboratory resources consumed by the CMG are less than or comparable to those consumed by the reaction jets.

An attitude maneuver profile to support both planned mission events and the experimental program was statistically modelled in terms of probability densities, to conduct the tradeoff study to optimize the MSS size on a basis of cost and as a function of the number of maneuvers. Two classes of attitude maneuvers were considered, pitch and yaw, and roll.

Pitch and yaw points the vehicle to astronomical objects in any direction. Roll moves the vehicle away from the belly-down attitude to Earth targets off the ground track. The hypothetical model for pitch and yaw limits rotation to  $180^\circ$ , while roll rotation is limited to  $75^\circ$ . For the distributions assumed, the average pitch and yaw rotation is  $90^\circ$ , while for roll, the average is  $25^\circ$ .

The average LRUF for both CMG and jet actuation was obtained by assigning resource usage to operational time, and to incremental or delta weight chargeable to the maneuvers (jets and CMG are already on the laboratory, and the CMG is sized to handle the impulse caused by the centrifuge and external disturbances). To obtain an approximate weight chargeable to maneuvers, the Phase IIa baseline configuration of two DG CMG for pitch and yaw and two SG CMG for roll was assumed. The orientation of the CMG with respect to the body axes is shown in Figure 4-5. However, since the increase in weight per unit,  $H$ , is approximately the same for both the double gimbal and single gimbal CMG in the areas of interest (1,000 lb-ft-sec to

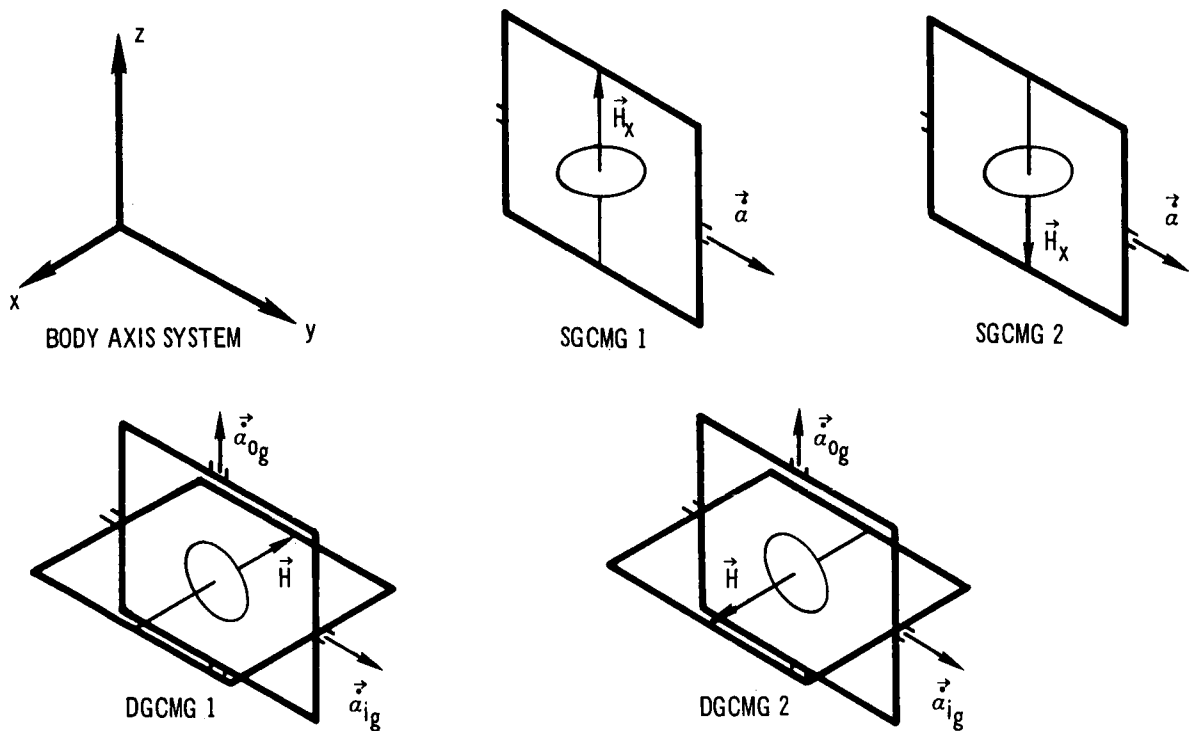


Figure 4-5. CMG Configuration

3,000 lb-ft-sec per unit) the weights used in minimizing the maneuver LRUF in this study apply to all configurations which use combinations of double and single gimbal control moment gyros.

Resources used for power and equipment volume requirements were not included in the tradeoff. CMG spin power does not increase significantly with  $H$ , nor does average torque power change significantly with torquer size. There is no increase in CMG volume in the range of interest, and there is no increase in jet power or volume.

Both of the CMG parameters considered, angular momentum,  $H$ , and torque,  $T$ , involve the use of laboratory resources in terms of weight and the average crew time required to perform vehicle rotations during the mission. Since the ratio of weight increase between  $H$  and  $T$  over the range of interest is approximately 10 to 1, only  $H$  is considered significant in contributing to resource usage via a weight allowance. Accordingly, average

or expected mission lifetime resource usage was computed with available angular momentum,  $H$ , adjusted to minimize the LRUF for a given number,  $N$ , of maneuvers in a mission and a given torque,  $T$ , available for accelerating the vehicle. Two extremes in vehicle inertia,  $I = 500,000$  and  $800,000$  slug-ft<sup>2</sup> were considered. Figure 4-6 summarizes the numerical evaluations of the minimized LRUF for CMG pitch and yaw maneuvers.

Figure 4-6 shows that 50 lb-ft of torque provides nearly the minimum usage factor. Beyond 50 lb-ft, little change occurs in the LRUF, since the rate of decrease in maneuver time per unit of available torque becomes less as torque is increased, and tends toward a constant value in the neighborhood of 50 lb-ft. The average lifetime LRUF for jet actuation was similarly computed as functions of jet actuation parameters and number of maneuvers.

To compare the cost of jet and CMG maneuvering, the average LRUF for jet actuation, which depends on the generated angular momentum,  $H$ , the number of maneuvers,  $N$ , in a mission, and vehicle inertia,  $I$ , was computed with the LRUF minimized with respect to  $H$ . The CMG mission lifetime average LRUF, which depends on the optimized angular momentum, and on  $N$  and  $T$ , as well as  $I$ , was also computed. Figure 4-7 compares the minimized LRUF for the jet and CMG actuation, with the latter set at 50 lb-ft. The much greater divergence of the usage factors for pitch and yaw as  $N$  increases reflects that the average angular rotation used for pitch and yaw is greater than for roll. From these plots, it is seen that the CMG are more efficient if 75 or more pitch or yaw maneuvers, or approximately 275 roll maneuvers are required.

While the number of maneuvers over the mission life cannot be firmly defined, one maneuver every 3 days is assumed as a minimum. Since mission life may be extended to 5 years, the total number of maneuvers could easily vary from approximately 100 to 1,000 or more. For Phase IIb CMG sizing purposes, the CMG momentum and torque values have been selected on the basis of 100 as the minimum total of maneuvers.

The required momentum for the roll axis is noted to be less than 1,500 lb-ft-sec and the pitch and yaw axis momentum for the  $8 \times 10^5$  slug-ft<sup>2</sup> inertia

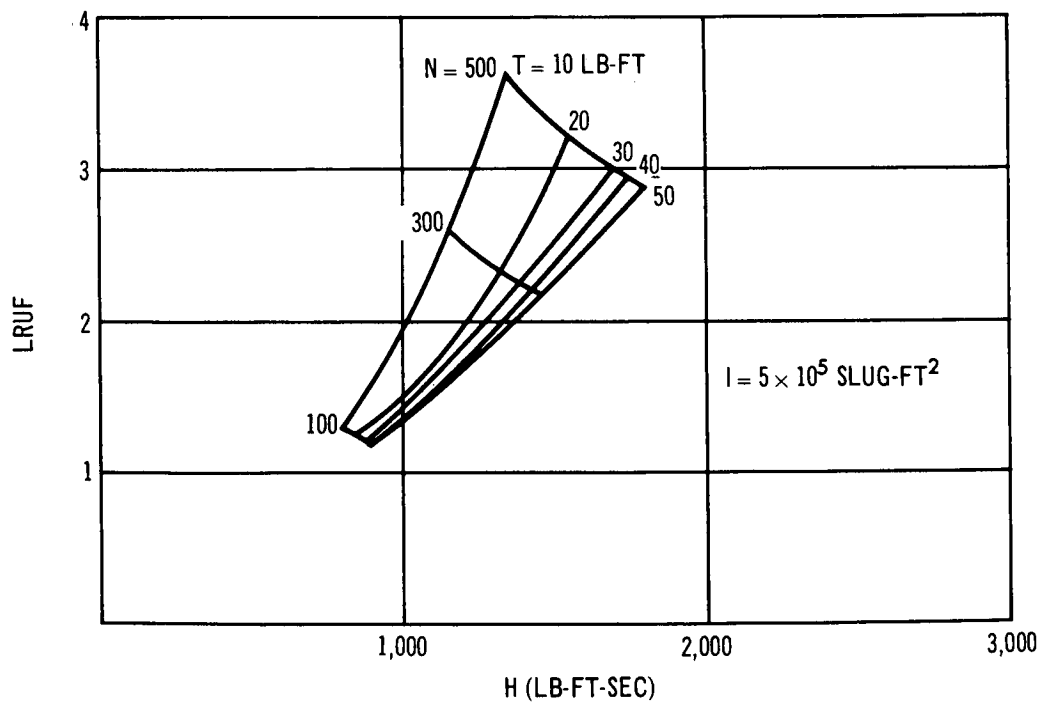
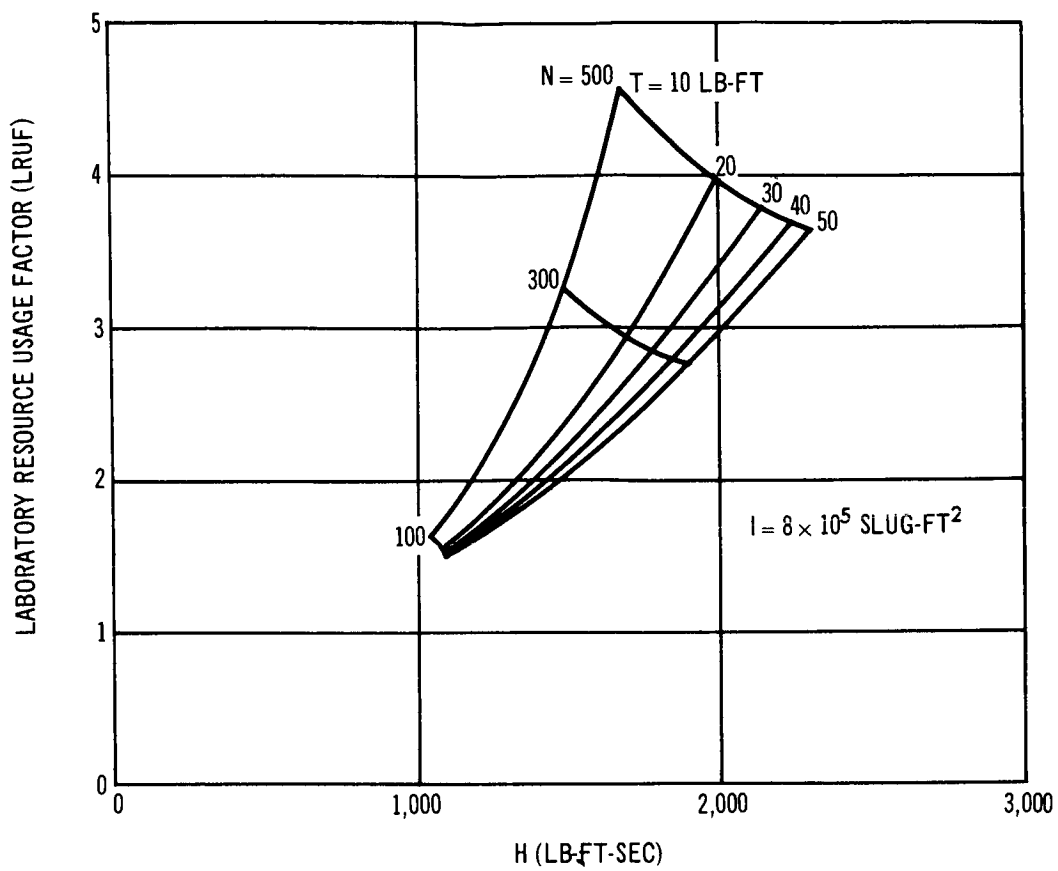


Figure 4-6. Resource Usage for CMG Pitch-Yaw Maneuvers

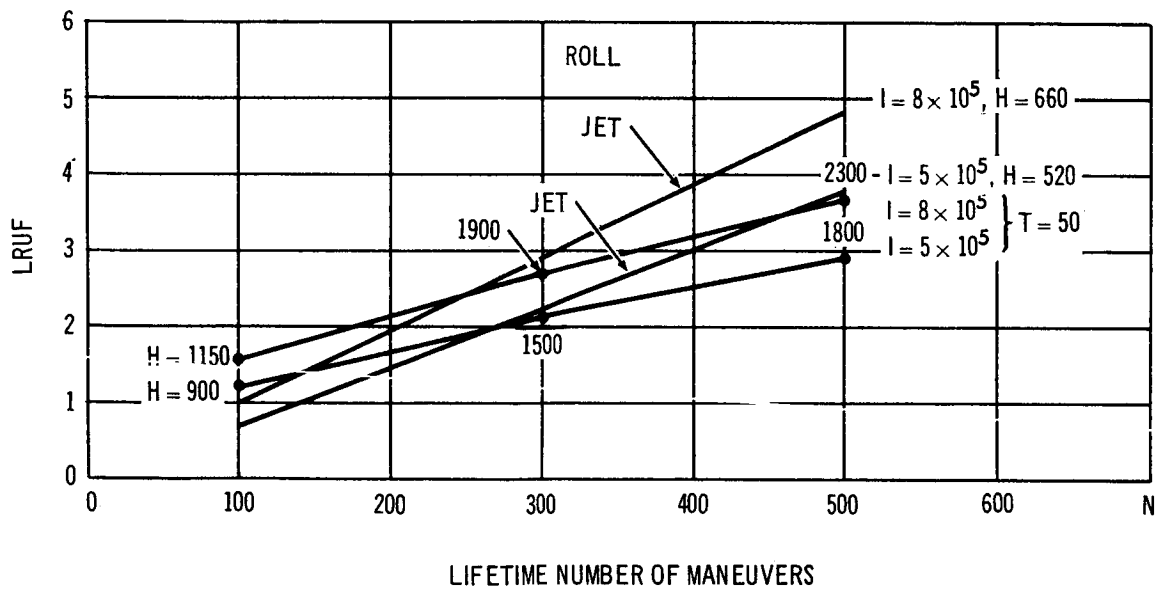
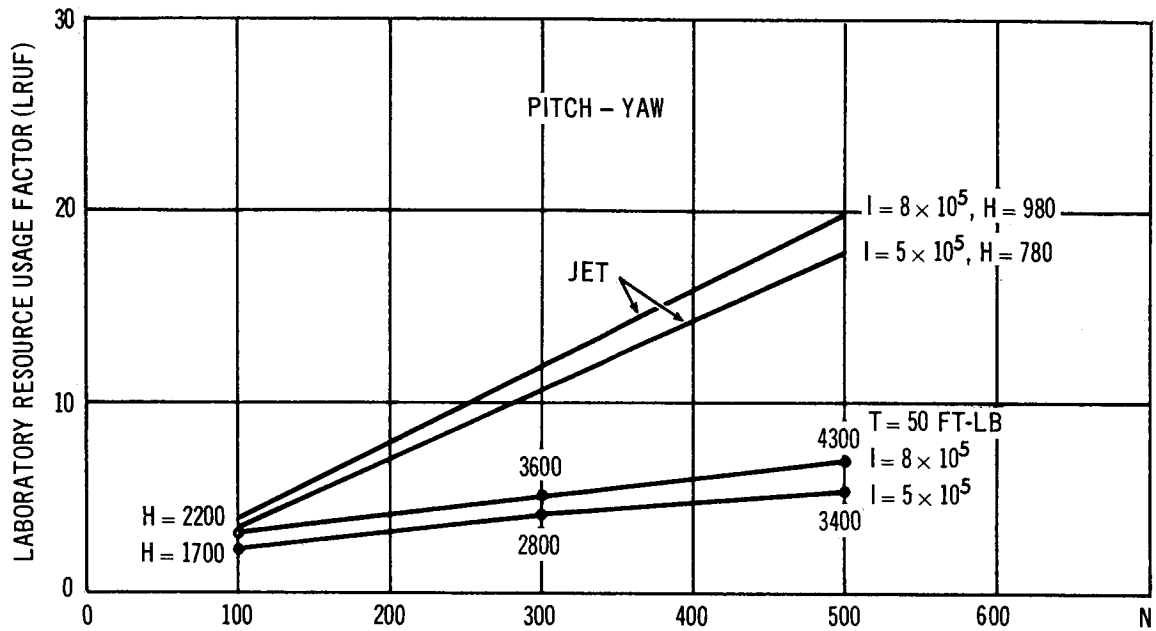


Figure 4-7. Comparison Between Optimum CMG and Jet Resource Requirements for Maneuvering

is 2,200 lb-ft-sec. If more than the number of maneuvers indicated by these momentum values are performed, the CMG will be undersized in terms of minimum laboratory resource usage. However, the greater the total number of maneuvers, the more efficient or the more savings incurred by using CMG in place of reaction jets. This is strikingly clear in the case of pitch and yaw maneuver; for 500 maneuvers, the estimated total laboratory resource usage factor would be 20 using the jets, and only 6.8 using optimized CMG. Using CMG sized for 100 maneuvers, the total LRUF for 500 operations would be approximately 15.

#### 4.4.2 Updating the Momentum Storage System Design

With the momentum requirements established for disturbances (Subsection 4.2.2), and for maneuvering (Subsection 4.4.1), the CMG total requirements and physical characteristics can be determined.

By restricting maneuvers about the roll axis when the centrifuge is in operation, no increase in x-axis momentum storage capacity is necessary to accommodate maneuvers, since the maneuver H is only about half as large as the H needed to counteract the centrifuge impulse. However, the pitch and yaw axis H required to support the maneuver profile is more than twice as large as that needed for counteracting the external disturbances, or 2,200 compared to 910. This large momentum storage requirement for the pitch and yaw axis, coupled with the 3,100 lb-ft-sec roll axis requirement, indicates that the choice of a momentum storage configuration should be reopened for future examination. In addition to the eight CMG configurations investigated in MORL Phase IIa, other configuration concepts, including the six-pack configuration developed by NASA-Langley, should be considered in the tradeoff study.

For the present, the baseline configuration of two counteracting double CMG for pitch and yaw control and two counteracting single-gimbal CMG for roll control will be used.

In combining the momentum requirements for disturbance control with those sized for maneuvering, the two values must be added to permit simultaneous



absorption of the disturbance impulse with maneuvering about the same axis. Using  $\pm 60^\circ$  gimbal travel, the 910 lb-ft-sec for disturbance control requires two 525 lb-ft-sec CMG ( $910/2 \sin 60^\circ = 525$ ).

The 2,200 lb-ft-sec for maneuvering already contains the factor for  $\pm 60^\circ$  gimbals and need only be divided between 2 double-gimbal CMG; thus  $525 + 2,200/2 = 1,625$  lb-ft-sec. This is the total momentum required for each of the two pitch/yaw units. The roll axis units are each sized for 1,790 lb-ft-sec for centrifuge control, and no increase is required. Note also that the full DG CMG capability ( $2 \times 1,625 \times \sin 60^\circ = 2,820$  lb-ft-sec) can be applied for maneuvering when partial capacity is not being used for disturbance control.

CMG development, sponsored by NASA-Langley and contracted to Bendix (Eclipse-Pioneer Division), has produced more realistic design data on which to update the CMG design for Phase IIb. Of most importance are the results of torquer studies and refined system weight analyses.

The performance advantages of direct drive DC torquers were established in the Phase IIa design study. Continuing studies have established the feasibility of using single and compound planetary gearing with DC torque motors to control the CMG gimbals.

The range of torquers from which to select includes three different sizes (7, 11.5 and 14.3 lb-ft) with either 1 or 2 gear passes (a single-pass planetary with an 8:1 ratio and a compound planetary with a 20.7:1 ratio). The actuator weight per gimbal as a function of the output torque is plotted in Figure 4-8 for these six combinations of torque and gear pass considered. Any one of the torquer-gear pass combinations can supply the 50 lb-ft torque. However, because of electronic considerations, a practical limitation on torquer input current of 10 amps has been set. This limitation reduces the potential available output torque to the values noted in Figure 4-8.

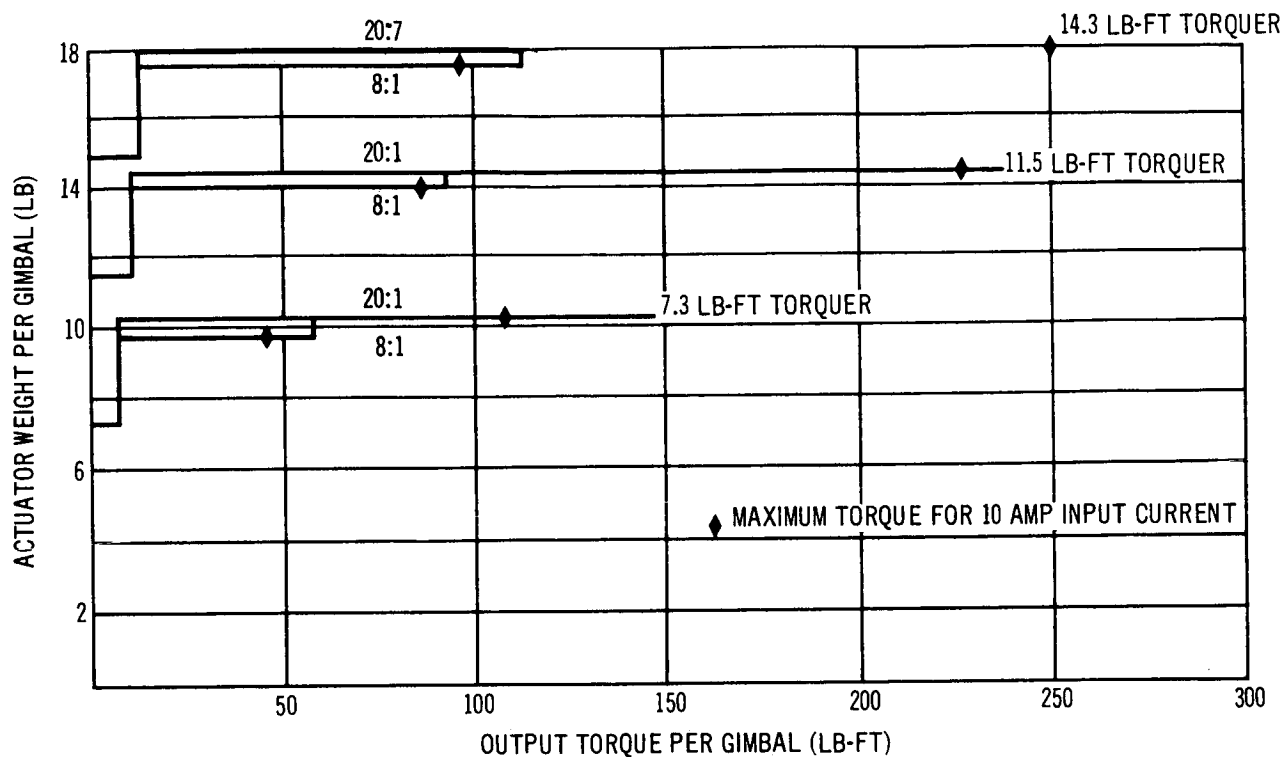


Figure 4-8 CMG Actuator Weight as a Function of Output Torque

The 11.5 lb-ft torquer with the 8:1 gear pass has been selected, for the following reasons:

1. The torquer characteristics are such that the 10-amp electronic limitation provides almost full-rated torque capacity.
2. The 11.5 lb-ft torquer has a better torque per Watt rating than the 7.3 lb-ft torquer by a factor of 2:1, while the 14.3 lb-ft torquer has an advantage of only 1.2:1 over the 11.5 torquer.
3. The 11.5 lb-ft torquer with the 8:1 gear ratio provides a torquing capacity more than 3 times that required, providing adequate design margin for growth potential.

Figure 4-9 shows the relationship between momentum, H, and total control moment gyro weight (including torquers) for both the single- and double-gimbal units.

As the result of further design studies with NASA-Langley CMG evaluation program, a more accurate assessment of the CMG parameters has been

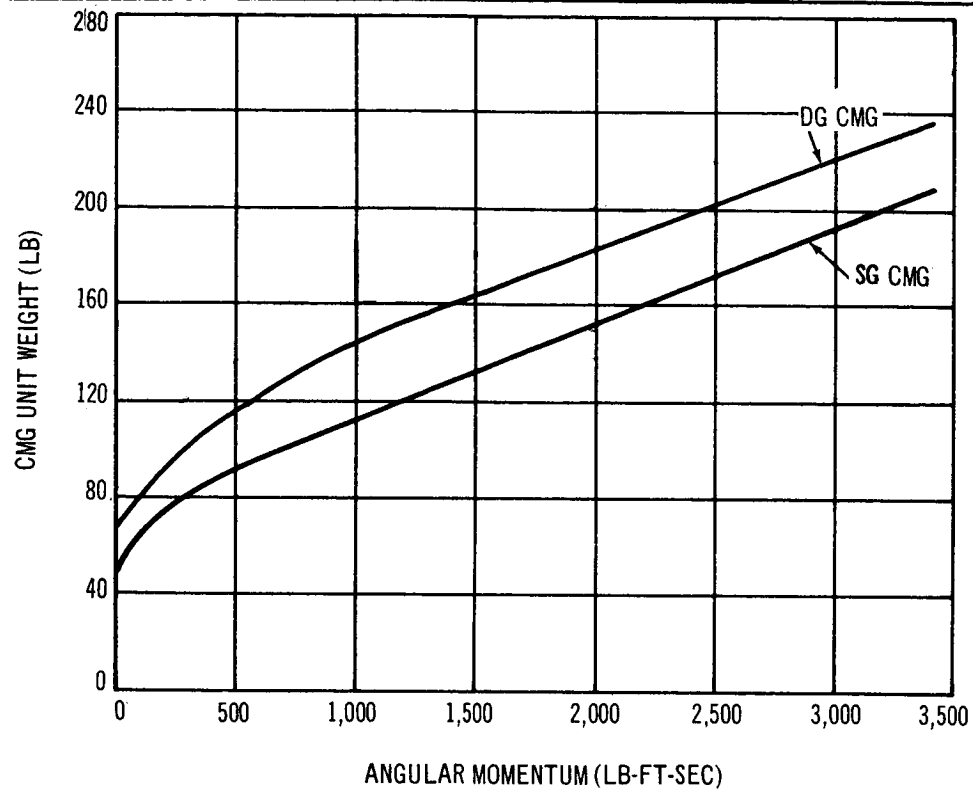


Figure 4-9. CMG Unit Weight as a Function of Angular Momentum

made and has produced an appreciable decrease in the weight associated with a given momentum for the double-gimbal CMG. This decrease, due primarily to a reduction in the weight of the DG CMG outer gimbal as a result of more detailed stress analysis, has resulted in an approximate 18-lb reduction in the weight of the DG CMG per unit of momentum. There has been no appreciable change in single-gimbal CMG weight, since there is no outer gimbal on the SG CMG.

From the curves in Figure 4-9, the weight per DG CMG (1,625 lb-ft-sec) is 168 lb. The single-gimbal units (1,790 lb-ft-sec) are each 146. Total size, weight, and power requirements are tabulated on the following page.

Table 4-2  
CMG CHARACTERISTICS

Parameter	DG CMG (2)	SG CMG (2)	Total
Axis controlled	Y-Z	X	
H per unit (lb-ft-sec)	1,625	1,790	
Torque per unit (lb-ft)	25	25	50 lb-ft/axis
Weight per unit (lb)	168	146	628 lb
Volume per unit (cu ft)	11.24	10.08	42.64 cu ft
Ac power per unit (W)	30	29	118 W
Dc power per unit (W)	11	5.5	33 W

#### 4.5 MANUAL CONTROL

The analysis and simulation of MORL manual control established the feasibility of the proposed concepts. Comparisons were made of various controllers on the basis of the displayed data and required control accuracy. With these results, an MORL manual control logic was formulated. A detailed study was also made of an Earth-tracking maneuver, which considered both single- and three-axis control. In general, propellant expenditure was large (approximately 15 lb per maneuver) and accurate control was difficult. The use of CMG for attitude reorientation under manual control was also studied as part of the Phase IIb effort. In one of these studies, only small reorientation angles were considered because of torque, angular momentum, and gimbal limitations then in existence. However, the results which established feasibility are applicable to larger reorientations, where increased torque and angular momentum are available.

The results of the manual control study are summarized below:

1. Manual command of attitude reorientation, which uses rate proportional to stick deflection, yields best performance.
2. Acceleration control is feasible but takes longer and requires more propellant.
3. In general, manually controlled maneuvers are too costly in propellant to be performed unless there is a severe requirement.
4. The Earth-tracking maneuver should be accomplished by gimbaling the equipment rather than rotating the vehicle.

5. If Earth-surface tracking by rotating the vehicle (with the RCS) is required, the use of pushbutton-operated acceleration control is best.
6. Manual control which uses CMG is feasible.

#### 4.6 SYSTEM HARDWARE MECHANIZATION IMPROVEMENTS

The SCS mechanization review has been held to incorporate modification caused by the change in the baseline electrical power system (EPS) from a solar panel to an Isotope Brayton Cycle Power system. The review also identified needed improvements in definition of the system and in total integration of the hardware elements. In addition, hardware already developed or being developed, will be investigated for application to related programs.

##### 4.6.1 Effects of Change to Isotope Power

Use of the Isotope Brayton Cycle Power source in place of the solar panel power system has eliminated the SCS requirement of maintaining the laboratory X axis along the sun line during both unmanned and manned modes. The solar modes were provided to eliminate the need for continuously gimbaling the panels and thereby increased the life and reliability of this subsystem. With this requirement deleted, the long-term laboratory orientation is now changed to the more efficient (in terms of attitude control and orbit-keeping propellant) belly-down mode.

The use of belly-down as the long-term mode also simplifies the orbit-keeping function because the vehicle, in the belly-down mode, is always in a favorable orientation for orbit-keeping thrusting. In the previous long-term orientation (roll solar) mechanization, the most efficient manner of obtaining proper orientation required waiting until orbit sunrise or sunset, at which time a single-axis maneuver (yaw) of up to 73° was necessary to align the thruster with the orbit velocity vector.

In the new SCS mechanization, it is no longer necessary to provide the logic, switching, and timing functions that were required to establish the laboratory Y axis in the orbit plane by means of a horizon sensor and the X axis along the sun line with the sun sensors. This updating of the roll solar orientation occurred once per orbit in the vicinity of orbit sunrise.

Similarly, the electronics hardware elements required for mechanizing the solar rotating mode in which the laboratory spin axis was aligned with the sun line are no longer required.

The Phase IIa baseline stabilization and control system mechanization equipment to be deleted as a result of the elimination of the roll solar manned and unmanned modes, and the rotating solar mode, are tabulated below:

1. Solar detectors and electronics.
2. Wide angle sun sensors and electronics.
3. Narrow angle sun sensors and electronics.
4. Solar acquisition and operational logic electronics.
5. Orbit keeping and orientation update electronics.
6. Masked sun sensor (rotating mode).
7. Precession controller electronics (rotating mode).
8. Sensor indicators and switching panel.

The total weight of the above equipment is 13.6 lb. The deletion of the sensors represents the elimination of seven sensor/vehicle interfaces, in itself desirable, and also eliminates in-orbit extravehicular maintenance required in the event of failure.

#### 4.6.2 System Design

The baseline stabilization and control system has been revised to reflect a more refined definition of the hardware inter-relationships, incorporating, where applicable, equipment developed for current manned spacecraft programs. A more efficient grouping of functional elements (as shown in Figure 4-10) has resulted in simplification of the subsystem mechanization and a more clearly defined man-machine control interface.

The overall design philosophy is reflected in the mechanization characteristics tabulated below:

1. The system provides for individual selection of sensors, actuators, control channels, and instrumentation.
2. The system provides monitoring of each separate control or display element for operability.

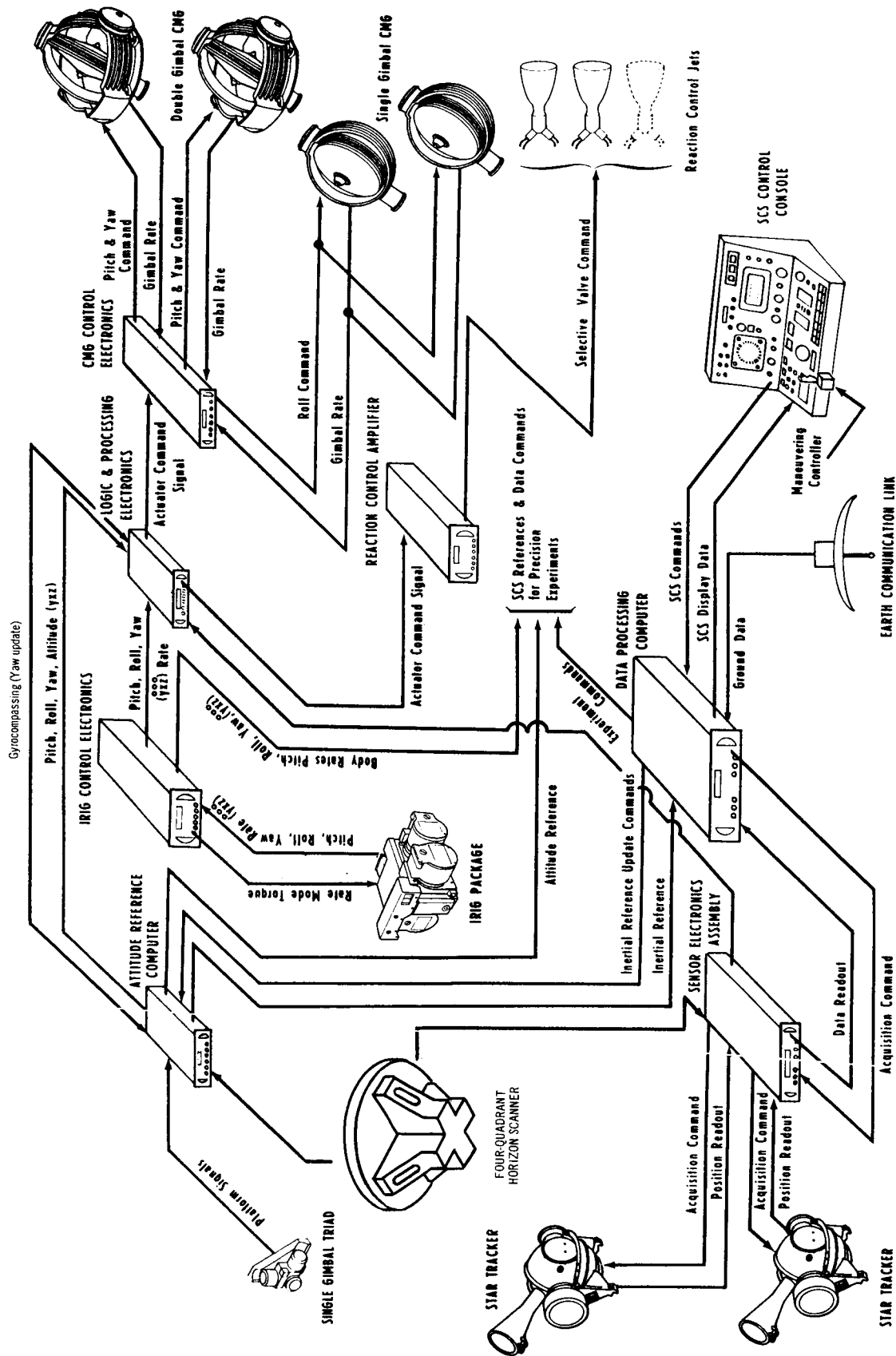


Figure 4-10. SCS Mechanization

3. Individual element selection and their proper operation is indicated prior to selection of their using mode.
4. Conflicting modes are interlocked.
5. For economy in fuel and power, normal maneuvering is to be at a low rate. Where possible, maneuvers are performed through automatic preselection to conserve crew time and to reduce operator fatigue.
6. Command, and accomplishment of command, is displayed.
7. Mode of operation, and its effectiveness, is continuously displayed or otherwise indicated.
8. Vehicle attitude is displayed in a reference frame appropriate to the operational mode.
9. A single warning, and a single corrective action, is required in the event of a serious system malfunction.
10. Manual maneuvering, as provided, is logical in input motion, and command capability is within the range of the primary reference employed.
11. At least one backup is instantly available for each automatic mode of operation.
12. The primary SCS controls and display are arranged for rapid assessment of system status, the initiation of commands, and the indication of system failure. Individual element controls and monitors retain a secondary status and are located in a secondary position.

#### 4.6.2.1 Man-Machine Design Philosophy

The SCS mechanization study has included the man-machine interface needed to provide the most efficient and effective application of man's capabilities in performing laboratory control functions. Investigation of the functional and performance requirements has been supplemented by the manual control studies summarized in Subsection 4.5 and reported in detail in Subsection A.1.4 of Appendix A. The results have been integrated into an overall manual control philosophy which forms the basis for the control and display mechanization for the MORL SCS.

#### 4.6.2.2 Modal Requirements

In refining the mechanization, the Phase IIa baseline SCS modes of operation (orbit injection, unmanned control, belly-down, experimental/inertial, and rendezvous) were examined for common requirements. Orbit injection



remains unchanged in that the laboratory is stabilized to an attitude and rate reference where redundant sensors and electronic elements are used, and an automatic sequencing program directs the control events.

The unmanned phase, formerly a solar-stabilized orientation, has been replaced by a rate stabilization mode. In this mode, the simplicity of rate threshold control and the continued utilization of redundant sensing and electronic elements results in high reliability during the unmanned phase.

The modal requirements of a manned laboratory stem primarily from four sources: (1) a requirement to maintain the laboratory in the baseline 164-nmi orbit, (2) a requirement to minimize orbit-keeping and attitude control propellant, (3) possible attitude maneuver and pointing requirements during rendezvous with the logistics spacecraft, and (4) support of the experiment pointing and stabilization requirements.

In support of these requirements, the control modes employed during manned phases of operation have as their basis a belly-down orientation, the preferred orientation from both a minimum propellant and Earth-centered experiment accommodation point of view. These mode requirements are as follows:

1. Belly-down, with a horizon-sensing reference.
2. Experimental, using a horizon-updated inertial reference.
3. Rendezvous, with a horizon-updated inertial reference.
4. Inertial reference, celestially updated.
5. Celestial tracking, with star tracker vehicle control.

Each represents a sensor and an updating method selection.

The revised modal selections are as follows:

1. Horizon hold, which uses direct horizon sensor control.
2. Orbital hold, which uses the inertial reference with an horizon scanner update.
3. Inertial hold, which uses the inertial reference with star tracker update.
4. Celestial hold, which uses direct star tracker control.

A prerequisite of each of these modes is that a specific sensor be turned on, and the long life requirement dictates that these sensors be energized only when needed; hence, a simple, basic operation mode is necessary for transition. For this purpose, a rate stabilization mode has been chosen for the transition. As a result, the lack of a specific selection returns the system to the rate stabilization mode, in which the vehicle is rate limited about all three body axes with a maximum drift rate of  $0.03^{\circ}/\text{sec}$ .

The integration task further defined the mode selectors, the maneuvering command devices, and astronaut displays. An interlocking philosophy has been established, a command priority system organized, and astronaut procedures have been defined. This work has resulted in the complete description of the necessary control panels, command devices, and displays. (See Appendix B)

#### 4.6.2.3 Electronics Refinement

The stabilization and control system has been functionally regrouped into seven packaged assemblies (eight, including the rotating mode electronics). The zero-g packages are as follows:

1. Sensor electronics assembly (SEA).
2. IRIG control electronics (ICE).
3. Reaction control amplifier (RCA).
4. Logic and processing electronics (LPE).
5. CMG control electronics (CCE).
6. Attitude reference computer (ARC).
7. Regulated power supply (RPS).

The packages have been grouped to keep like functions in the same assembly to facilitate failure detection, maintenance, and repair. The assemblies conform to cold-plate rack-mount configuration, and are provided with a gasket seal for environmental (moisture) protection. The lower surfaces are smooth for positive contact with the laboratory rack cold plate.

#### 4.6.2.4 Utilization of Related Program Hardware

A review of the sensors, electronics, controls, and display equipment now in use or in development on several current related space programs was conducted to assess the ability of these elements to meet the requirements of the MORL stabilization and control system. In all cases, evaluation of suitability for MORL use was heavily influenced by whether it possessed the required maintainability potential.

The Gemini, Apollo, and Lunar Orbiter systems were considered in this study. Of these systems, the Apollo was found to have the greatest applicability and several components were selected for incorporation into the MORL.

In surveying the Apollo stabilization and control system, it has been determined that Block I equipment generally meets the MORL on-board maintenance requirement. The equipment reflects a modular design with easily replaceable subassemblies and carries provision for on-board troubleshooting. Block I was in fact developed for ease of maintenance. Block II, the current design, employs hermetic seals, potting, and hard-wired subassemblies to overcome an anticipated high humidity environment. Thus, Block II components, to be deemed applicable to MORL, must be those for which complete replacement can be justified in terms of life, spares provisioning, basic weight, and equipment and skill necessary for on-board repair/replacement.

In terms of direct applicability, the following selections and recommendations are made:

1. The Block I three-axis attitude gyro and accelerometer package, Type DGG 245C, is directly applicable to the MORL SCS system. It will replace the previously specified IRIG and in addition will provide longitudinal acceleration sensing for the orbit-keeping functions. As Block I, it meets the present MORL maintenance criteria.
2. The Block I three-axis rotational controller, Type DCG 146G, is applicable and was on the previous MORL equipment list. The unit provides the necessary interlocking and command functions required by the MORL SCS. Its force/command operation may relegate this device to a back-up role in the future, since present maneuvering trends favor extremely slow (fuel-efficient) changes and a hand-operated force stick may be tiring to the operator.

3. The flight director attitude indicator (FDAI) of Block I or II is applicable and is specified for use in the MORL system. Block II represents a more rugged version of the Block I device; final choice depends on the results of detailed maintenance studies.
4. The Block I velocity change indicator, Type DCG 148G, (used on Apollo) provides all the functions required by the MORL SCS system, and, in addition, provides for MORL orbit-keeping propulsion; only subassemblies of this device are deemed directly applicable.
5. The Block I electronic control amplifiers provide many of the functions required by the MORL SCS. Their direct applicability as complete assemblies is marginal. As far as MORL electronics are concerned, the use of modular subassemblies of these packages appears more probable. The final decision requires additional depth in MORL system design, the selection of the basic electronics technology to be employed, the establishment of firm packaging concepts, and the development of detailed maintenance and spares provisioning requirements.

#### 4.7 INERTIAL REFERENCE SYSTEM SELECTION

The inertial reference systems studied in this review were the Phase IIa baseline single-gimbal triad (SGT), the Gemini inertial measurement unit (IMU), the gimbaless inertial reference unit (IRU) proposed for NASA Lunar Orbiter System, and the Air Force standardized space guidance system (SSGS). The Apollo inertial reference system, a three-gimbal platform system, was not included for detailed review; the system is not designed to meet the MORL all-attitude reference requirement and is not designed with in-orbit maintenance and repair capabilities, because of its relatively short (compared to MORL) mission life requirements.

The systems studied were evaluated for applicability to the MORL mission on the basis of a technique developed during the Phase IIa study effort. The systems are compared on the basis of the following factors:

1. Weight.
2. Power.
3. Volume.
4. Reliability.
5. Maintenance (crew time).
6. Spares provisioning requirements.
7. Cost.
8. Performance.

Penalty factors based on these criteria (except performance) were established for each of the evaluated systems. These penalty factors were based on the percentage of the available laboratory resources required by each of the

different inertial reference systems. (This is possible, since each system makes a predictable demand on the laboratory resources in terms of weight, power, crew time, and so forth.) In addition, the percentage of data bank experiments that each of the contending systems can accommodate is included as a weighting factor in the system comparison. These penalty factors, when considered in conjunction with other nonquantifiable factors, provide a realistic basis for determining the best potential mechanization. Appendix D contains the detailed system descriptions and tabulations of characteristics, weighting factors, and analyses used in deriving the tradeoff data for making the preferred system selection. The results of the study point out that the Gemini IMU, although possessing an advantage in terms of accuracy, was not selected because of the greater weight, power, and volume required. In another and perhaps more significant aspect, this system, because of its mechanical complexity, does not lend itself to in-flight maintenance and repair and, in the case of failure, the entire platform assembly would have to be replaced. With the SGT and gimbaless IRU, only components associated with a single control axis need be replaced after a system failure.

The decision to make a choice between the SGT and IRU is not as evident. The IRU is somewhat better than the SGT in terms of weight and power, but its accuracy under dynamic condition ( $0.5^\circ/\text{hour}$ ) does not meet the inertial reference system design requirements. It therefore appears that under the conditions of current technology, the single-axis concept is better suited to the MORL requirements than the strap-down rate measurement concept. For this reason, no change is recommended in the present basic configuration of the MORL inertial reference system, and the Phase IIa baseline single-gimbal triad remains the best potential IRS mechanization at the present time.

#### 4.8 INSTALLATION AND ALIGNMENT OF SENSORS

Experimental operations require provision and maintenance of a precision attitude reference installation on board the laboratory. In previous installation concepts, the attitude sensors were not located so that alignment consistency could be assured. In Phase IIb, a new sensor installation concept

has been developed incorporating all attitude reference components on a single mounting base, isolated from major pressure and temperature influences. Figure 4-11 is a conceptual drawing emphasizing the installation of the inertial reference and the star tracker components, and showing the equipment used for checking the alignment between these devices in flight. The single-gimbal triad (SGT) inertial reference includes an optical cube that is the absolute reference for the system. The alignment autocollimators are used to measure errors between the star tracker axes and this optical cube.

Once the stellar/inertial reference has been accurately aligned, remotely located experiment sensors can be aligned relative to it. For this purpose, secondary reference targets are located on the rigid mounting beam to which the SGT and star trackers are attached. The secondary reference targets are calibrated relative to the SGT and then used as reference points for aligning the experiment sensors.

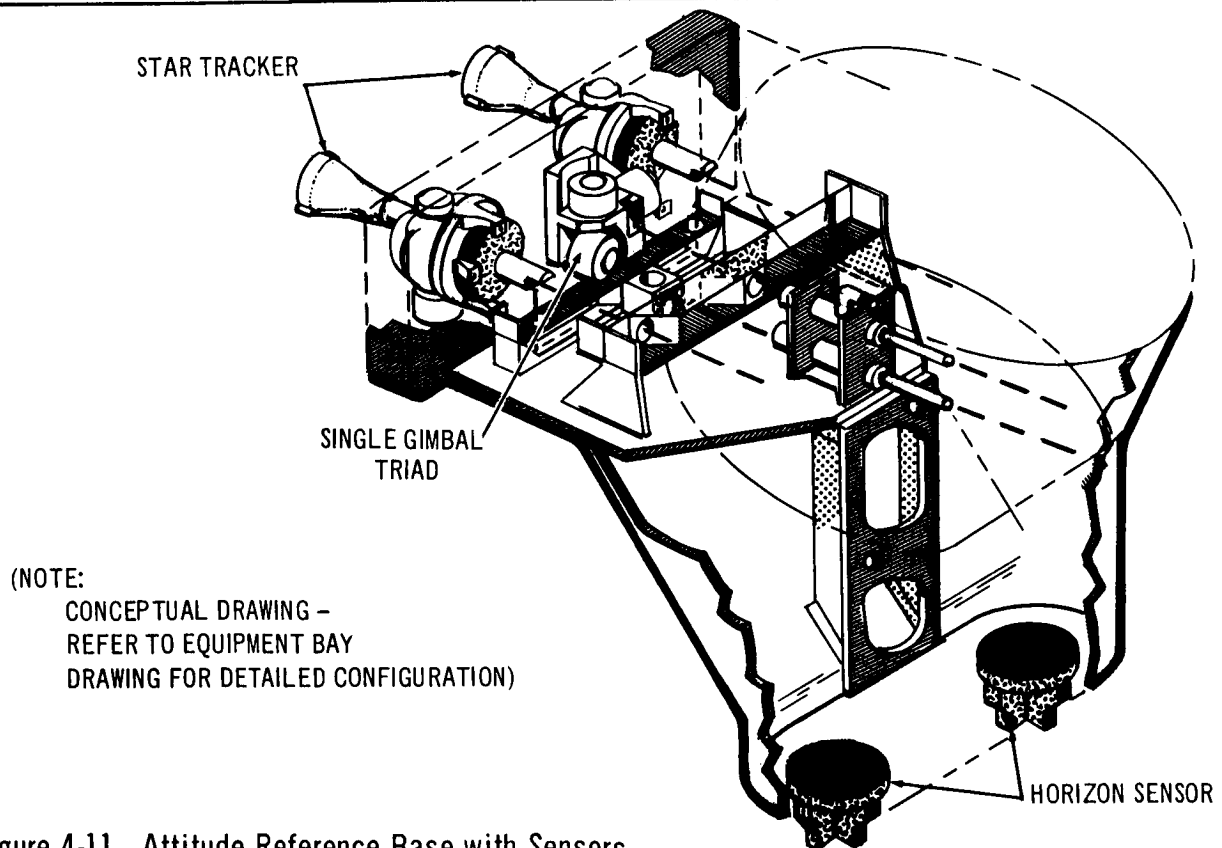


Figure 4-11. Attitude Reference Base with Sensors

The expected accuracy with this arrangement is  $0.01^\circ$ . Mechanical mounting pads at each sensor installation should provide initial alignment to  $\pm 0.1^\circ$ . Vernier alignment calibration data are read out electronically and used to update correction matrices in the data processing computer. Manual readout is also provided for initial installation and checkout purposes.

#### 4.9 IMPROVEMENTS MADE POSSIBLE BY THE LAUNCH DATE EXTENSION

There are several areas in the MORL stabilization and control system mechanization where launch date extensions of from 1 to 5 years might result in the availability of improved system elements as a result of current development activities on other programs.

##### 4.9.1 Sensor Development

The following projections are made of some of the more promising technical developments which could be incorporated to improve the SCS performance, reliability, or efficiency.

##### 4.9.1.1 Inertial Reference System

The single-gimbal triad system selected for the MORL SCS mechanization is subject to further improvements in accuracy and reliability. The most important single improvement would be the substitution of higher accuracy digital output encoders. The use of an encoder in the 30-arc sec resolution range is required to meet the desired system accuracy. Improvements in encoder resolution and accuracy to the 1- to 10-arc-sec range would permit added margin, and increase the accuracy growth potential for the system.

Another potential improvement involves the use of gas-bearing gyros in place of the conventional mechanical-bearing models. Both random drift and power consumption are very low in this type of gyro, although some of the power saved is required for the air pumps. The use of a gyro of this type should result in longer life and improved drift characteristics.

#### 4.9.1.2 Electrostatic Gyros

An inertial reference system sensor which shows considerable promise (even though it is in the experimental prototype stage) is the electrostatic gyro (ESG). This employs a spinning sphere supported by electric fields for attitude reference. These devices can be used to provide a complete all-attitude reference with an extremely low drift rate ( $\approx 0.01^\circ/\text{hour}$ ), long running times ( $\approx 1$  year), and virtually no wear. Problems remain in their development, particularly in the area of readout. They would seem to be most valuable in long-term inertially fixed applications, such as manned planetary fly-by missions.

#### 4.9.1.3 Horizon Sensors

Current studies are under way by both NASA and the Air Force to more precisely define the radiometric gradient of the Earth's atmosphere. These programs are gathering radiometric data for use in the design of more accurate horizon sensor systems. Horizon sensor instrument accuracies of less than  $0.1^\circ$  are obtainable, but because of incomplete knowledge of the Earth's horizon radiance profile, errors of up to  $0.5^\circ$  and larger are possible during in-orbit operation. More complete knowledge of the Earth target characteristics will lead to the development of new optical filters, detectors, and signal processing techniques tailored to minimize horizon-anomaly induced errors.

High-accuracy horizon sensors currently in use employ some form of optical chopping or scanning. This is true of the MORL baseline sensor. Optical scanning is obtained mechanically by means of a rotating or oscillating mirror which sweeps the Earth horizon image across the detector elements. The elimination of this mechanical motion would result in increased life and reliability. There are several current development programs for the fabrication and test of electronic scan horizon sensors which, if successful, could be incorporated into the MORL SCS.



#### 4.9.1.4 Mono-Pulse Radar Systems

A mono-pulse radar system, employing a single, small-diameter (1.5 ft) antenna, is being developed for use in the determination of the local pitch and yaw errors from altitudes up to 300 nmi. This system is completely autonomous and flight test (25,000 ft) data extrapolated to near-Earth orbits indicate accuracies approaching  $0.02^\circ$ . Development activities are centered around the fabrication of a compact, lightweight system using microelectronic circuitry. Estimates of power for this system are less than 35 W. Successful development of this system would require tradeoff studies to determine whether this system or the baseline horizon sensor system is better suited to the MORL mission.

#### 4.9.2 Electronics

Development of new electronic components, circuits, and techniques is being continued to realize reduced weight, size, power, and cost through the use of integrated microcircuits. Testing indicates a considerable increase in reliability over discrete component circuits. Multiple redundancy with such circuits involves little weight penalty and the resultant increases in reliability may justify this approach over the spares provisioning philosophy used in the baseline MORL system.

#### 4.9.3 Actuators

A development program is now under way for the design, fabrication, and test of double-gimbal control moment gyro systems. These studies should, in the next several months, uncover inadequacies in the baseline CMG design, configuration, and control philosophy. The program aim is the development of a minimum weight, power, and size system that will be used to provide control torques during precision maneuvers in an orbiting vehicle. The program includes the investigation of various configurations of CMG systems and the complexity of the control and unload logic mechanizations required. As developments in this type of actuator continue, figures of merit, such as momentum/lb should be increased beyond the current MORL estimates.

The successful development of low-thrust (Resistojet, Poodle, and so forth), high  $I_{sp}$  reaction control systems should be considered for the MORL system. These control systems, with potential propellant weight savings of three to one over the baseline high-thrust hypergolic system, could be used for orbit-keeping impulse requirements as well as momentum storage system unload impulse requirements. The fact that these are relatively low-thrust devices (0.01 to 0.1 lb) requires that, for orbit keeping, they be fired for long periods of time while the laboratory SCS (using CMG) maintains the thrust vector along the orbit velocity vector.

Section 5  
TECHNOLOGICAL REQUIREMENTS

The research and development work identified in the first iteration of this task were concerned with the baseline laboratory as defined at the time. These research and development (R&D) tasks included development items that could be accommodated by AES in-orbit testing.

In the second iteration, the first output was reviewed for modifications, additions, or deletions resulting from baseline Stabilization and Control system (SCS) changes generated in this phase. As such, it represents an up-dated version of the original study. Although a second iteration of the experiments for AES testing was not conducted, the need for in-orbit data collection still exists for those items that ground-testing alone might not provide the necessary high level of confidence for MORL SCS development.

#### 5.1 SUMMARY

The MORL SCS technology requirements chart, Figure 5-1, identifies the research and development tasks that need to be initiated prior to authority to proceed. The chart shows the evolution from functional requirements to equipment definition, and the associated research and development, progressing from design studies through ground and orbital tests. Alternate research and development approaches are identified for areas where particularly difficult problems are foreseen or where more than one approach appears feasible.

The required research and development tasks are divided into three levels of effort: (1) studies/analyses, (2) ground tests/simulations, and (3) orbital tests. It is intended that the effort be only enough to provide sufficient confidence that a satisfactory solution exists for the problem posed under the area of investigation.

← REQUIRED RESEARCH AND DEVELOPMENT (TO BE INITIATED PRIOR TO ATP) →										
GENERAL FUNCTION	SPECIFIC FUNCTIONAL REQUIREMENT	TECHNIQUE EMPLOYED	BASILINE EQUIPMENT TO BE USED	CRITICAL PERFORMANCE AND DESIGN REQUIREMENTS	EQUIPMENT/FUNCTION INVOLVED	AREA OF INVESTIGATION	STUDIES / ANALYSES	GROUND TESTS/SIMULATIONS	ORBITAL TEST	NOTES
ATTITUDE SENSING	SENSE THE LOCAL VERTICAL	BAROMETRIC SENSOR	TWO AXIS HORIZON SENSOR	LOCATE LOCAL VERTICAL TO WITHIN 0.5 DEG.	SCANNER DETECTOR/FILTER	HORIZON SPECTROMETRY	ANALYZE AVAILABLE ATMOSPHERIC DATA FOR FILTER/DETECTOR SELECTION		INVESTIGATE HORIZON RADIATION CHARACTERISTICS	NOTE 1 INCREASED KNOWLEDGE OF HORIZON SPECTRAL + GEOMETRIC PROPERTIES WILL LEAD TO IMPROVED ACCURACY
				LONG LIFE IN SPACE ENVIRONMENT	OPTICAL-MECHANICAL VEHICLE INTERFACE	ALIGNMENT	INVESTIGATE STRUCTURAL BENDING EFFECTS ON ALIGNMENT	EVALUATE TEST ARTICLE OF SELECTED ALIGNMENT MECHANISM		
					MAINTENANCE	HUMAN FACTORS	ANALYSIS + DESIGN OF ALTERNATE ALIGNMENT CONCEPTS			
					SEALS	HIGH VACUUM RADIATION MAINTAINABILITY	INVESTIGATE FEASIBILITY OF AIR-LOCK DEVICES FOR INTERNAL MAINTENANCE	EVALUATE TEST ARTICLE + MAINTENANCE PROCEDURES IN VACUUM CHAMBER	TEST INTRAVEHICULAR MAINTENANCE EQUIPMENTS + PROCEDURES	NOTE 2 HUMAN FACTORS DESIGN HANDBOOK IS REQUIRED FOR ITEMS REQUIRING INTRAVEHICULAR MAINTENANCE
				OPTICS	METEOROID IMPINGEMENT RADIATION HIGH VACUUM MAINTAINABILITY	PERFORM MAINTAINABILITY DESIGN STUDIES	PERFORM ENVIRONMENTAL TESTS ON OPTICS, SEALS + PROTECTIVE DEVICES	EVAL. TEST ARTICLES IN SPACE ENVIRONMENT	SEE NOTE 2	
ATTITUDE SENSING	SENSE DEVIATIONS FROM INERTIAL REFERENCE	GYROSCOPE	INERTIAL RATE INTEGRATING GYRO (IRIG)	OPERATION IN NULL GRAVITY DRIFT RATES LESS THAN .02 DEG/HR LONG LIFE IN SPACE ENVIRONMENT	LUBRICATION	FLUID BEHAVIOUR	USE APOLLO IN-FLIGHT REPLACEMENT TECHNIQUE (NO PRE-ATP WORK REQ.)	PERFORM EVALUATION TESTS ON ALTERNATE DEVICES	DETERMINE IN-ORBIT DRIFT CHARACTERISTICS + EVALUATE AUTO/MANUAL DRIFT COMPENSATION TECHNIQUES	
					IN-ORBIT DRIFT COMPENSATION	GYRO DRIFT	INVESTIGATE USE OF ALTERNATE (AIR BEARING) DEVICES			
					BEARINGS	WEAR-OUT				
ATTITUDE SENSING	SENSE STELLAR REFERENCE LINE-OF-SIGHT	BAROMETRIC SENSOR	TWO-AXIS STAR TRACKER	VEHICLE ALIGNMENT TO 0.1 DEG. FOR EXPERIMENTS	OPTICAL-MECHANICAL VEHICLE INTERFACE	ALIGNMENT	INVESTIGATE STRUCTURAL BENDING EFFECTS ON ALIGNMENT	EVALUATE TEST ARTICLE OF SELECTED ALIGNMENT MECHANISM		NOTE 3 HUMAN FACTORS DESIGN HANDBOOK IS REQUIRED FOR ITEMS REQUIRING EXTRAVEHICULAR MAINTENANCE
				LONG LIFE IN SPACE ENVIRONMENT	MAINTENANCE	HUMAN FACTORS	ANALYSIS + DESIGN OF ALTERNATE ALIGNMENT CONCEPTS			
							INVESTIGATE EXTRA VEHICULAR MAINTENANCE	SIMULATE VARIOUS MAINTENANCE OPERATIONS + TECHNIQUES	TEST EXTRAVEHICULAR MAINTENANCE EQUIPMENT + PROCEDURES	
							INVESTIGATE FEASIBILITY OF AIR-LOCK DEVICES FOR INTERNAL MAINTENANCE	EVALUATE TEST ARTICLE + MAINTENANCE PROCEDURES IN VACUUM CHAM	TEST INTRAVEHICULAR MAINTENANCE EQUIPMENT + PROCEDURES	SEE NOTE 2
				OPTICS	METEOROID IMPINGEMENT RADIATION HIGH VACUUM MAINTAINABILITY	PERFORM MAINTAINABILITY DESIGN STUDIES	SIMULATE MAINTENANCE TASKS ON TEST ARTICLES	EVALUATE TEST ARTICLES IN SPACE ENVIRONMENT	SEE NOTE 2	
				BEARINGS	HIGH-VACUUM MAINTAINABILITY		PERFORM ENVIRONMENTAL TESTS ON OPTICS, BEARINGS + PROTECTIVE DEVICES			
ATTITUDE SENSING	PROVIDE INERTIAL REFERENCE	GYROSCOPE	THREE SINGLE AXIS PLATFORMS (WITH RATE INTEGRATING GYROSCOPES + DIGITAL COMPUTER)	MAN/MACHINE EFFICIENCY PERFORMANCE OPTIMIZATION	DISPLAYS INERTIAL-OPTICAL SENSORS DATA PROCESSING TECHNIQUES + EQUIPMENT	SUBSYSTEM INTEGRATION	PERFORM DETAIL STUDIES FOR INTEGRATION OF INERTIAL, OPTICAL, ELECTRICAL + DISPLAY ELEMENTS. INCLUDE INVESTIGATION OF USE OF CENTRAL VS SEPARATE COMPUTER			
				LONG LIFE IN SPACE ENVIRONMENT	MECHANICAL + ELECTRONIC COMPONENTS	MAINTAINABILITY	INVESTIGATE USE OF ALTERNATE ATTITUDE REFERENCE SYSTEMS (INCLUDE GIM-BALLED + STRAPPED-DOWN TYPES)			
							PERFORM INERTIAL REFERENCE SYSTEM MAINTAINABILITY DESIGN STUDIES FOR BASELINE + ALTERNATE SYSTEMS	SIMULATE MAINTENANCE TASKS ON TEST ARTICLES	SEE NOTE 2	
							ALIGNMENT TO VEHICLE AXES TO 0.05 DEG.	EQUIPMENT/VEHICLE INTERFACE	ALIGNMENT	INVESTIGATE EQUIPMENT REQUIREMENTS FOR ALIGNMENT TO VEHICLE AXES. INVESTIGATE ALTERNATE ALIGNMENT TECHNIQUES INCLUDING OPTICAL-MECHANICAL, ELECTRICAL + INTEGRAL MOUNT FOR INERTIAL + OPTICAL ELEMENTS

Figure 5-1. MORL SCS Technology Requirements (Page 1 of 2)

GENERAL FUNCTION	SPECIFIC FUNCTIONAL REQUIREMENT	TECHNIQUE EMPLOYED	BASELINE EQUIPMENT TO BE USED	CRITICAL PERFORMANCE AND DESIGN REQUIREMENTS	EQUIPMENT / FUNCTION INVOLVED	AREA OF INVESTIGATION	REQUIRED RESEARCH AND DEVELOPMENT (TO BE INITIATED PRIOR TO ATP)			NOTES
							STUDIES / ANALYSES	GROUND TESTS / SIMULATING	ORBITAL TEST	
ATTITUDE SENSING	SENSE ORBIT PLANE	GYROCOMPASSING	GYROSCOPES + ELECTRONIC FILTERING	SENSE ALIGNMENT WITH ORBIT PLANE TO WITHIN 0.5 DEG	GYROSCOPE + ELECTRONIC FILTER	GYRO DRIFT + FILTER NOISE	INVESTIGATE APPLICATION OF SINGLE AXIS PLATFORM + OTHER TECHNIQUES	EVALUATE PROPOSED GYRO COMPASSING SYSTEM BY SIMULATION EVALUATE SELECTED ALTERNATE SYSTEM OF SIMULATION		
ATTITUDE SENSING	ALIGNMENT REFERENCE	OPTICAL SIGHTINGS	BACK-UP (NOT PART OF BASELINE)	VEHICLE ALIGNMENT TO 0.1 DEG FOR EXPERIMENTS	TELESCOPE + DISPLAYS	HUMAN FACTORS EQUIPMENT INTERFACE REQUIREMENTS	INVESTIGATE BACK-UP (MANUAL) REF ALIGNMENT TECHNIQUES. CONSIDER EXISTING (APOLLO) + NEW SYSTEMS	EVALUATE PROTOTYPE OF SELECTED SYSTEM		
ACTUATION	CONTROL TORQUE GENERATION	MOMENTUM EXCHANGE	CONTROL MOMENT GYROSCOPES (CMG)	COUNTERACT EXTERNAL DISTURBANCE EFFECTS	SYSTEM SIZING (TORQUE + IMPULSES)	DETERMINATION OF AERODYNAMIC GRAVITY GRADIENT DISTURBANCES	DEVELOP IMPROVED COMPUTER TECHNIQUES FOR EVALUATING DISTURBANCES + SIZING MOMENTUM STORAGE + PROPELLANT CONSUMPTION REQUIREMENTS IN EACH ORIENTATION	OPERATE COMPUTER PROGRAMS TO ESTIMATE SIZING REQUIREMENTS	MEASURE LONG PERIOD (EXTERNAL) DISTURBANCE TORQUES IN ORBIT	
				COUNTERACT INTERNAL DISTURBANCE EFFECTS	SYSTEM SIZING (TORQUE + IMPULSES)	CREW EQUIPMENT, CENTRIFUGE DISTURBANCES	PERFORM CREW + EQUIPMENT OPERATIONS TIME LINE ANALYSES + DERIVE DISTURBANCE DATA	EVALUATE CREW AND EQUIPMENT DYNAMIC EFFECTS IN SIMULATED NULL GRAVITY	MEASURE SHORT PERIOD (INTERNAL) DISTURBANCE TORQUES IN ORBIT	
				GENERATE HIGH TORQUE FOR SLEWING + CONTROL TORQUE SHORT PERIOD, INTERNAL DISTURBANCES	CONTROL MOMENT GYROSCOPES + GIMBAL TORQUERS	ELECTRICAL TORQUER DEVICES, EFFECTS OF HIGH TORQUE ON CMG DESIGN	INVESTIGATE ALTERNATE CMG CONFIGURATIONS + TORQUER DESIGNS	EVALUATE TEST ARTICLE OF SELECTED DESIGN		
				WITHSTAND STRESSES AT SPEEDS TO 12,000 RPM	FLYWHEEL	STRESS ANALYSIS MATERIALS SAFETY BALANCING	PERFORM ANALYSIS + DESIGN STUDIES FOR SELECTION OF WHEEL SPEED, CONFIGURATION, MATERIAL IN VIEW OF EXPANDED REQUIREMENTS	EVALUATE TEST ARTICLE OF SELECTED DESIGN		
				OPERATING EFFICIENCY	SPIN MOTOR, BEARINGS + HOUSING	SPEED CONTROL SPIN UP + SPIN DOWN POWER REQUIREMENTS MOTOR EFFICIENCY AERODYNAMIC DRAG VISCOUS DRAG HEAT DISSIPATION	PERFORM DETAILED TRADE STUDIES OF SELECTED + ALTERNATE MOTOR, BEARING LUBRICANT + HOUSING DESIGNS	EVALUATE PERFORMANCE OF SELECTED + ALTERNATE DESIGNS		
				LONG LIFE IN SPACE ENVIRONMENT	MOTORS BEARINGS PACK-OFFS MAINTENANCE	BEARING DESIGN LUBRICATION (HIGH VACUUM) MAINTAINABILITY HEAT DISSIPATION COMPONENT RELIABILITY	PERFORM TRADE STUDIES OF ALTERNATE CONFIGURATIONS CONSIDER AIR-BEARING TECHNIQUES PERFORM MAINTAINABILITY DESIGN STUDIES	PERFORM ENVIRONMENTAL + LIFE TESTS ON PROTOTYPE UNITS SIMULATE MAINTENANCE ON TEST ARTICLES OF SELECTED DESIGN	SEE NOTE 2	
ACTUATION	ORBIT KEEPING + REACTION CONTROL	MASS EXPULSION	HYDRAULIC REACTION CONTROL SYSTEM	ORBIT KEEPING MOMENTUM UNLOAD	ELECTRIC PROPULSION ION ENGINES ARC JET RESISTO-JET PODS	EFFICIENCY POWER REQUIREMENTS THROTTLING RESPONSE THREE LEVELS MAINTENANCE	INVESTIGATE FEASIBILITY OF APPLICATION OF ADVANCED SYSTEMS FOR MOMENTUM UNLOAD + CONTROL	EVALUATE PERFORMANCE OF SELECTED PROTOTYPE SYSTEMS		
ELECTRONICS	SIGNAL PROCESSING LOGIC FUNCTION TIMING FUNCTIONS	DIGITAL-ANALOG	COMPUTERS LOGIC CIRCUITRY POWER SUPPLIES SIGNAL PROCESSING	LONG LIFE IN SPACE ENVIRONMENT	ELECTRONICS	RELIABILITY MAINTAINABILITY COST PERFORMANCE	PERFORM RELIABILITY / MAINTAINABILITY STUDIES FOR ELECTRONICS COMPONENTS / SUB-SYSTEMS. CONSIDER COST REDUCTIONS THROUGH UTILIZATION OF APOLLO / OTHER HARDWARE	EVALUATE SELECTED COMPONENTS, CIRCUITS + MAINTAINABILITY TECHNIQUES	SEE NOTE 2	
ENVIRONMENT PROGRAM SUPPORT	PROVIDE STABILIZED EXPERIMENT	GIMBAL ISOLATION OF PACKAGE FROM LAB	SCS - STABILIZER FOR REFERENCE ACQUISITION	PROVIDE ATTITUDE REFERENCE TO G1 PROVIDE RATE HOLD TO 0005/SEC	GIMBALLED EXPERIMENT MOBILE STABILIZATION + CONTROL	MECHANICAL / OPTICAL / FUNCTIONAL INTERFACE DISPLAYS + AUTOMATIC TECHNIQUES ALIGNMENT	PERFORM ANALYSIS AND DESIGN STUDIES REQUIRED TO DEVELOP CONTROL TECHNIQUES, PROCEDURES + EQUIPMENT + ESTIMATE PERFORMANCE			
SIMULATION	SCS TEST FACILITIES	THREE-AXIS MOTION SIMULATOR	SCS SUBSYSTEMS	SIMULATE LABORATORY RESPONSE + PROVIDE DISPLAYS, CONTROLS, ETC. FOR INTEGRATED SCS PERFORMANCE EVALUATION	LARGE-THREE GIMBAL TEST FACILITY	GIMBAL DESIGN BEARING DESIGN COMPUTER REQUIREMENTS SIMULATED SENSOR TARGETS	DETERMINE SIMULATOR REQUIREMENTS + PERFORM DESIGN STUDIES	BUILD AND TEST SIMULATOR	NOTE 4 SIMULATOR IS USED TO EVALUATE CMG CONFIGURATIONS	
MORL SCS DEVELOPMENT	PROVIDE DESIGN DATA FOR MORL SCS DEVELOPMENT	SCS IN-FLIGHT PERFORMANCE EVALUATION	STABILIZATION + CONTROL SYSTEM	SCS OVERALL PERFORMANCE	STABILIZATION + CONTROL OF SPACE VEHICLES	ATTITUDE HOLD ACCURACY RATE HOLD ACCURACY	STUDY RESULTS OF SCS IN-ORBIT PERFORMANCE FOR INPUT TO MORL SCS SUBSYSTEM DESIGN			
CONTROL	MANUAL / AUTO CONTROL	MAN-MACHINE INTERFACE EQUIPMENT	DISPLAYS CONTROLS	LONG-TERM OPERATION IN ORBITAL ENVIRONMENT	REDEVELOP TRACKING DISPLAY MONITORING REACTION TIME LOGICAL SEQUENCING	ENVIRONMENTAL EFFECTS ON CREW PERFORMANCE		MONITOR CREW PERFORMANCE IN THE EXECUTION OF VARIOUS CONTROL TASKS		

Figure 5-1. MORL SCS Technology Requirements (Page 2 of 2)

The identified research and development activities remain essentially unchanged from the first iteration of this task. The primary differences stem from the following three baseline system changes:

1. The deletion of the development tests associated with the former baseline system's externally mounted sun-sensors.
2. The relocation of the SCS star trackers, horizon sensor, and inertial reference system.
3. The modification of the baseline system's horizon sensor packaging concept.

The baseline SCS sun sensors have been deleted because, with the deletion of the solar panels, there is no longer a requirement to align the laboratory with the sun-line.

Studies initiated during this phase have resulted in the relocation of the externally mounted SCS sensors. These studies were begun because of a need for precise alignment of the SCS sensors and the sensors used for experiments. Preliminary studies have produced an attitude reference base (ARB) concept in which critical inertial/optical sensors are mounted on a common, rigid base, in close proximity to each other and to the experimental sensors.

As a result of the increased emphasis on the belly-down orientation, because of the deletion of solar orientation requirements, the problem of maintaining horizon sensors has been explored during this phase. A concept in which critical sensor elements may be replaced from within the laboratory has evolved. This development has resulted in decreased emphasis on the need for extravehicular maintenance experience for these sensors.

In all but six cases, studies and analyses are required as the initial level of effort. In these six cases, extensive studies and analyses have already been conducted and actual testing of prototype hardware is necessary to provide advancement in the particular technology.

Orbital testing has been recommended in most cases because of the difficulty of simulating, for extended periods of time, the zero-g and hard vacuum environment and, thus, the inability to ascertain the effects of these environments on the equipment under investigation. Effects of other space

phenomena (such as radiation, meteoroid, and jet exhaust impingement), which in most cases are expected to have less severe effects on the equipment under investigation but which are difficult or impossible to simulate, contributed to the decision to perform orbital testing.

It becomes obvious by examination of the 11 experiments recommended for orbital test that a number of them are quite similar; therefore, a single experiment, modified only slightly, could accomplish the same results as 2 or 3 separately proposed experiments. The extravehicular maintenance experiments which have been recommended for the star tracker could be combined into one experiment. This is also the case for the intravehicular maintenance experiments.

The two experiments recommended for evaluating the effects of the space environment on materials used in externally mounted sensors can also be combined into one experiment. This can be done by including all those materials peculiar to the particular sensors in the experiment package.

Two other candidate experiments that could be combined are the long-term and short-term disturbance (aerodynamic and gravity gradient) measurement experiments associated with the control moment gyros, because the equipment required for these experiments are similar. However, since the disturbances associated with the two experiments are considerably different in dynamic characteristics and magnitude, closer consideration must be given to the sensitivities and dynamic ranges of the disturbance sensing elements to ensure the success of integrating them into one experiment package.

The need for the long-term disturbance measurement experiment can be eliminated by performing the CMG in-orbit performance evaluation before the long-term disturbance experiment. The control moment gyro experiment could, through proper instrumentation, provide the data required to derive the aerodynamic and gradient disturbance characteristics.

The 11 recommended orbital experiments could be reduced to the following eight experiments:

1. Investigation of the Earth's horizon radiance characteristics.
2. Evaluation of extravehicular maintenance equipment and procedures for SCS externally mounted sensor equipment (horizon and star sensors).
3. Evaluation of intravehicular maintenance equipment and procedures for SCS internally mounted sensors (horizon sensors).
4. Evaluation of optical sensor materials in long-term exposure to the space environment (horizon and star sensors).
5. Investigation of inertial rate integrating gyro performance characteristics in a zero-g environment.
6. Measurement of short-term orbital disturbances.
7. Evaluation of the performance of a control moment gyro system and determination of long-term orbital disturbances.
8. Investigation of crew control performance after long-term exposure to orbital environment.

## 5.2 TASK DESCRIPTIONS

The following sections describe the research and development activities represented in the MORL SCS technology requirements chart, Figure 5-1.

### 5.2.1 Horizon Sensors

The following paragraphs discuss the horizon sensors concept.

#### 5.2.1.1 Performance Characteristics

The accuracy to which the horizon sensor device can determine the local vertical is heavily dependent on the actual radiometric signature presented by the horizon defined by the Earth's limb. Most of the radiometric data to date are based on indirect measurements of atmospheric density, pressure, carbon dioxide content, and so forth, and these data are used in conjunction with empirical formulas to derive the radiometric gradient of the Earth's horizon. The design of critical components in the horizon sensor system, such as filters, detectors, and the signal processing techniques used, are heavily dependent on the accurate definition of the horizon gradient profile. For this reason, it is recommended that horizon radiometric testing be extended to provide a better match between current instrument accuracy ( $0.05^\circ$ ) and horizon definition ( $0.5^\circ$ ).



### 5.2.1.2 Long-Life Considerations

The proposed horizon sensor concept, in which maintenance of the sensors may be performed from within the laboratory, needs further definition. Preliminary considerations to date indicate that such a technique is feasible but that the detailed design studies required have not been performed. Tradeoff studies comparing this and other concepts should be performed, and test articles fabricated and tested both in ground simulation facilities and in orbit.

### 5.2.1.3 Alignment

A large number of experiments require accurate determination of the local vertical. The number of experiments that can be accommodated by the horizon sensor system is affected by the accuracy to which the horizon sensor can be aligned to the experiment package and inertial reference system. The proposed attitude reference base concept requires more refined analysis and test to determine effects of structural misalignment, such as those caused by thermogradients, launch vibration, and transition to zero-g, to establish the adequacy of this technique.

Analysis of alternate alignment concepts and calibration techniques should be pursued. Ground test of selected alignment systems is recommended.

## 5.2.2 Inertial Rate Integrating Gyros

The following paragraphs discuss the inertial rate integrating gyros concept.

### 5.2.2.1 Performance Characteristics

The behavior of the motor bearing lubricant and the gimbal float fluid in precision inertial-grade rate-integrating gyros, when operating for extended periods in a zero-g environment, can cause disturbing torques about the gyro gimbal which result in drift rates. Determination of the performance characteristics of inertial rate-integrating gyros in a zero-g environment is recommended. In-orbit AES testing is required to provide the necessary long-term zero-g. Automatic and manual compensation techniques should be developed to help reduce these gyro drifts in the space environment.

#### 5.2.2.2 Long-Life Considerations

Gyro motor bearing life is the limiting factor in gyro life. Present inertial-grade rate-integrating gyros reach the wear-out region after approximately 3,000 hours. The zero-g environment should tend to increase the gyro motor bearing life because it reduces the load on the spin motor bearings. However, even doubling the gyro life by operating in a zero-g environment would still be insufficient for MORL applications. Apollo in-flight replacement techniques should be studied for application to the MORL mission. An alternate investigation of the applicability of long-life air-bearing gyros to the MORL should be made and ground evaluation tests conducted.

#### 5.2.3 Two-Axis Star Tracker

The following paragraphs discuss the two-axis star tracker concept.

##### 5.2.3.1 Alignment

Pointing accuracies for certain experiments require that star trackers be used to provide a precise attitude reference. Structural misalignment effects caused by thermogradients, pressure differentials, launch vibration, and transition from one g through launch g's to zero g need to be investigated to determine if adequate structural stability between the attitude reference and experiment sensors can be maintained with the proposed attitude reference base.

Analysis and design of alternate alignment concepts and development of alignment and calibration techniques for in-flight use should be pursued. Ground tests, using breadboards of the selected alignment system, are recommended.

##### 5.2.3.2 Long-Life Considerations

The two-axes star tracker has a reliability of approximately 0.98 for a 1-year mission. This reliability, without repair, is unacceptable for MORL and indicates the need for developing designs with in-flight maintenance capability. Simulation and test of extravehicular maintenance procedures, techniques, and equipment is recommended. A basic human factors handbook for design of equipment for extravehicular maintenance is required.

As an alternate to extravehicular maintenance, the feasibility of airlock devices for internal maintenance should be investigated. It may be possible to mount the star trackers in an airlock device, normally exposed to vacuum but sealable and accessible from the laboratory interior, to facilitate maintenance. Ground and orbital testing of prototype equipment is recommended. A human factors handbook for design of equipment requiring intravehicular maintenance is needed.

Knowledge of the effects of prolonged exposure to the space environment on materials and devices used on the star tracker, primarily optical devices and bearings, is needed. Ground and orbital tests are recommended to gather data on the effects caused by phenomena such as exhaust and meteoroid impingement, radiation, and high vacuum. Design and analysis of these sensor components to facilitate on-board maintenance and subsequent ground evaluation of these designs are desirable.

#### 5.2.3.3 Man-Machine Interface

The total MORL mission success depends on the successful execution of the planned experiments, and the conduct of these experiments depends largely on the efficiency of the man-machine interface. Detail performance studies to ensure optimum interfacing of the star tracker with the inertial reference system, displays, data processing equipment, and the precision experimental packages are recommended.

#### 5.2.4 Inertial Reference System

The following paragraphs discuss the inertial reference system concept.

##### 5.2.4.1 Integration of the Inertial Reference and Experiment System

Total integration of the Earth and star sensors with the inertial reference system, the various experiment packages, and the space crew is essential for complete mission success. Determination of the detailed computational requirements and tradeoff studies is needed to decide whether the on-board central computer or the present baseline special purpose computer can perform the required inertial reference system calculations more efficiently.

The investigation to determine the applicability of other presently available inertial reference systems, including gimbaled as well as strapped-down types, should be continued. These studies should be of sufficient depth to define and detail changes required to adapt existing reference systems for application to the MORL.

#### 5.2.4.2 Long-Life Considerations

The gyro motor bearing is the limiting factor in gyro life and thus in inertial reference system life. Maintenance considerations must be included in the design of any of the inertial reference systems under consideration. Because present inertial-grade rate-integrating gyros have a life expectancy of approximately 3,000 hours, maintenance of the inertial reference system on a scheduled basis will be necessary. Simulated maintenance tasks should be performed on the selected system to ensure adequate maintenance capability.

#### 5.2.4.3 System Alignment

Current spacecraft attitude reference alignment methods depend on ground alignment and a rigid structure between sensors and the inertial reference system.

Detailed studies of the proposed attitude reference base (ARB) concept and other techniques and procedures for alignment of the Earth and star sensors to the inertial reference system, as well as the experiment packages, must be investigated. Structural misalignment effects caused by thermogradients, pressure differentials, launch vibration, and transition from one g through maximum launch g's to zero g need to be investigated to determine what techniques are most applicable to the MORL. Ground evaluation tests, using prototype equipment of the inertial reference system and the sensor alignment technique selected, should be conducted.

#### 5.2.5 Orbit Plane Alignment

Alignment of the MORL X-axis with the orbit plane is required in the Earth-oriented mode (belly-down). A gyrocompassing technique is proposed to maintain the X-axis in the orbit plane. More complex simulations which

include nonlinearities, such as gyro drift, hysteresis, threshold, and filter noise should be conducted. Alternate studies and analyses employing techniques which align the X-axis to the orbit plane should be investigated, and ground simulations should be performed.

#### 5.2.6 Backups for Obtaining Inertial Reference

The baseline system requires that the horizon sensor and gyrocompass circuit operate to establish the inertial reference. Investigation of backup manual optical techniques (telescope and displays) for aligning the inertial reference system is desirable. Prototypes of the selected system should be evaluated.

#### 5.2.7 Control Moment Gyros (CMG)

The following paragraphs discuss the control moment gyros concept.

##### 5.2.7.1 Torque Generation for Counteracting External and Internal Disturbances

The torque required to counteract long-period (external) disturbances and short-period (internal) disturbances is provided by CMGs. More accurate determination of the long-term and short-term disturbance profiles, including the effects of crew motion and other transient disturbances, and evaluation of the CMG ability to counteract these disturbance torques is desirable. Additional studies and simulations are necessary to provide these data. Orbital tests to provide correlation data are recommended.

Investigation of alternate CMG configurations, that can provide additional torque capability and thus allow more growth potential, should be studied and prototypes of selected configurations should be evaluated by ground simulation and testing. These efforts should be oriented primarily toward the use of CMG for laboratory maneuvering rather than the RCS attitude control thrusters.

#### 5.2.7.2 CMG Safety Considerations and Operating Efficiency

The control moment gyros large inertia wheels are spun to as much as 12,000 rpm. Further stress analysis and design studies of the selected wheel material and speed, in view of increased torque capabilities, and tradeoff studies of selected and alternate motor bearing lubricants and housing designs should be continued. Ground and flight testing of prototype hardware is recommended.

#### 5.2.7.3 Long Life in Space Environment

The limiting factor in CMG life is motor bearing life. Tradeoff studies of alternate techniques for providing effective bearing lubrication in a zero-g environment, and consideration of air bearing techniques and maintainability features, should be conducted. Ground environmental and life tests, as well as checkout of the maintainability features, are recommended.

#### 5.2.7.4 Configuration Optimization

Large CMG for the generation of control torques for spacecraft stabilization and control are in the early stages of development. Detailed analysis and tradeoff studies of various CMG configurations and control laws should be performed. Extensive ground testing of the prototype system and flight evaluation are recommended.

#### 5.2.8 Hypergolic Reaction Control System

The baseline RCS is used mainly for orbit keeping and momentum unload. Investigation and ground evaluation of potentially more efficient low-level thrusters and advanced propulsion systems should be performed.

#### 5.2.9 Electronics

Reliability/maintainability considerations and tradeoff studies in electronic circuit design, packaging, and testing must be performed. New electronic components, circuits, and techniques to realize reduced weight, size, power, and cost (that is, micro integrated circuits) should be evaluated.

#### 5.2.10 Experiment Program Support

Investigation of the mechanical, optical, and functional interfaces between the experiment packages and the inertial reference system for those experiments which require precision pointing and hold accuracies should be conducted. Studies to define the feasibility of a universal mount for all, or several, of the precision experiments should be carried out.

#### 5.2.11 Simulation

Adequate simulation of the SCS is necessary to verify the performance of the SCS components functioning as a complete integrated subsystem. A large three-gimbal test platform for complete SCS testing is needed. Design studies are needed to determine requirements for the simulator computer, displays and controls, table mechanization, and sensor targets. It is recommended that the simulator facility be built to provide a total system testing capability for all SCS systems.

#### 5.2.12 MORL SCS Development

It is expected that the AES and MORL stabilization and control systems will be very similar, and will even contain identical components in some areas. Studies and analyses of the AES in-orbit performance should be carried out and the results integrated into the MORL program.

#### 5.2.13 Displays and Controls

The success of the MORL mission depends, to a great extent, on the ability of man to perform his specified tasks. Monitoring and evaluation of man's execution of specified control system tasks, particularly as his length of time in orbit increases, should be conducted on AES. These results should be compared with the results from similar tasks performed in ground simulations.

### 5.3 PROGRAM TIME PHASING

The critical research and development tasks identified in the previous sections have been charted in PERT-type network form (schedule-phasing charts) and are shown in Figures 5-2, 5-3 and 5-4. Each chart identifies the major

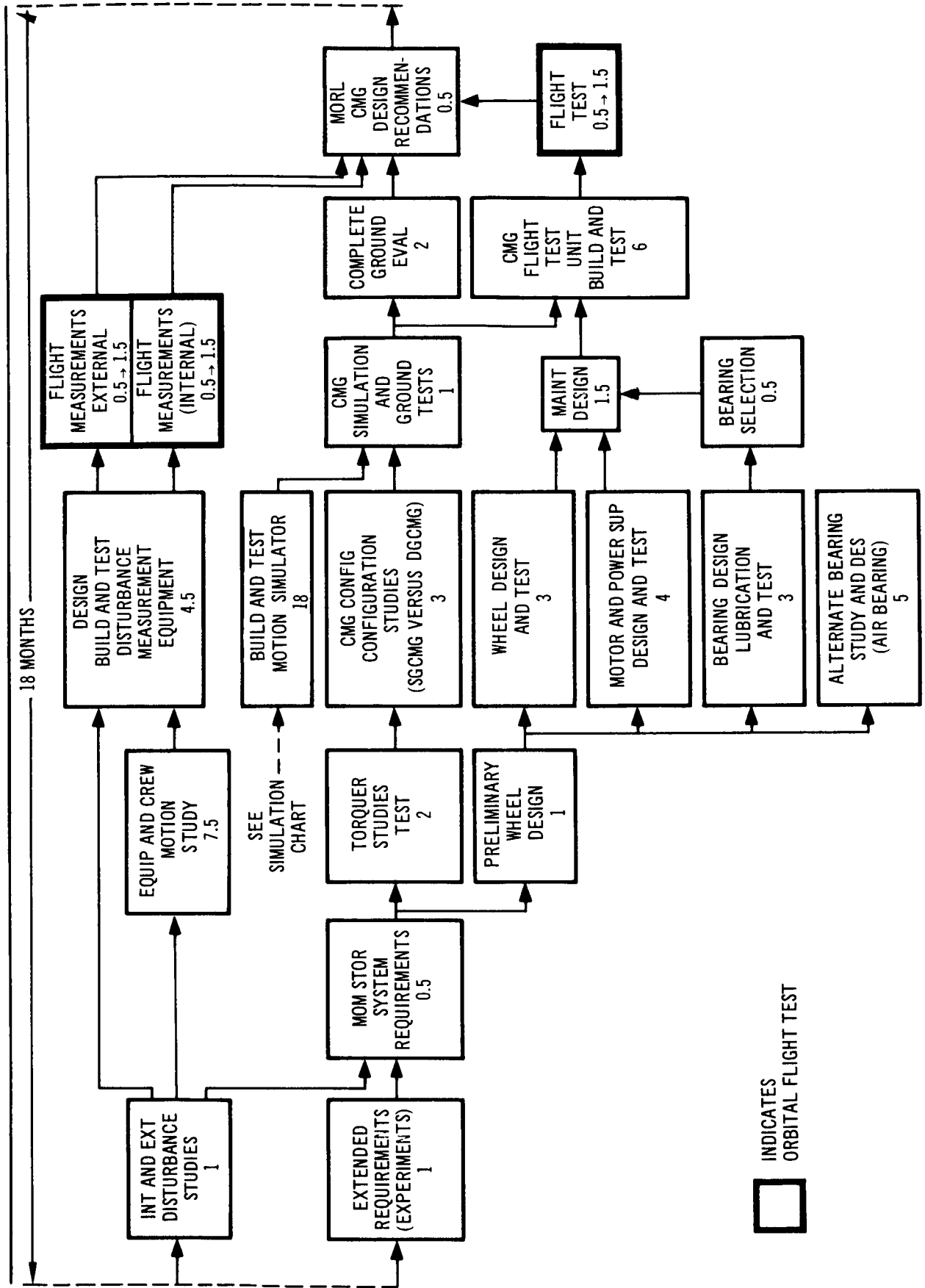


Figure 5-2. Control Moment Gyros



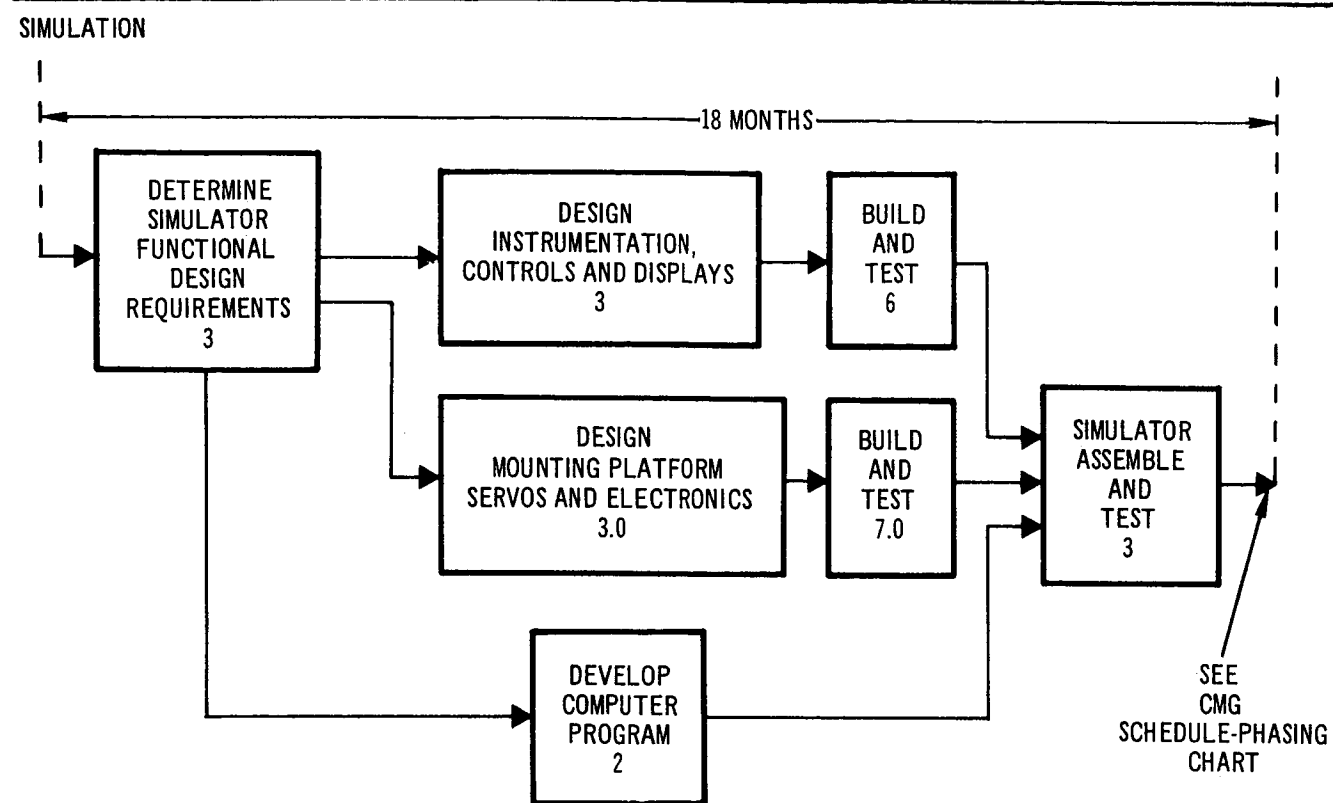


Figure 5-3. SCS Dynamics Simulator

tasks, the time required to accomplish these tasks, and the dependent inter-relationships between these tasks and other related research and development task areas.

Figure 5-2 is a scheduling of tasks associated with the CMG system and indicates the phasing recommended, based on MORL being the first application of large CMG. The CMG development currently in progress at Langley Research Center, although not specifically directed toward the MORL requirements, will furnish the essential data needed to accomplish the objectives of this plan: namely, to prove the feasibility of using large CMG controllers prior to committing them to operational use on the first MORL. Incorporated in this schedule is the critical task of evaluating the effects of crew-motion transients disturbances, which are also under investigation by Langley Research Center.

EXTERNAL SENSORS (HORIZON, STAR) TRACKER

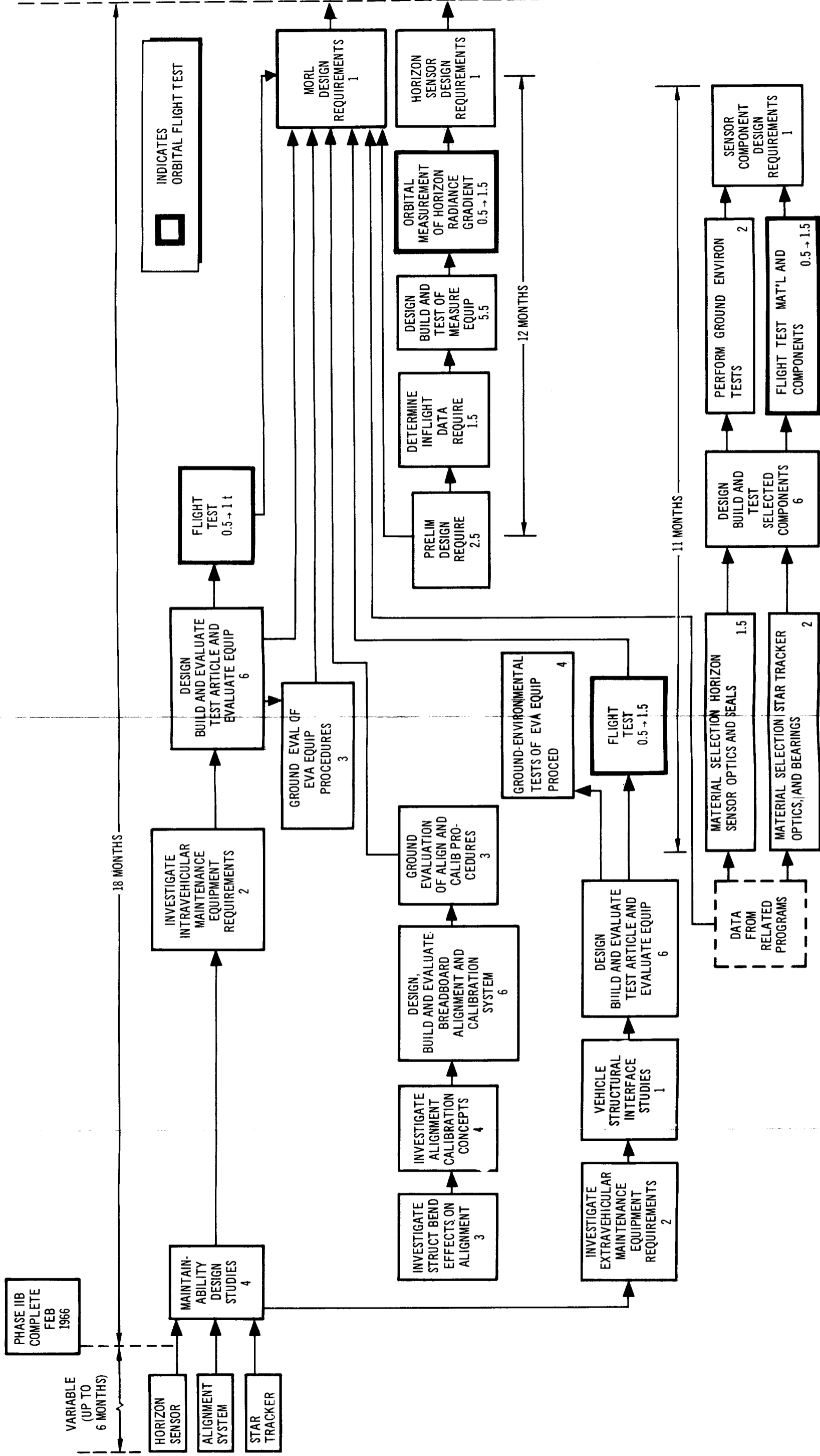


Figure 5-4. Alignment System for the Attitude Reference Sensors

Figure 5-3 shows the phasing for development of the SCS dynamics simulator (three-axis table) system which is critical to the CMG system evaluation shown in Figure 5-2. The initial phases of this activity have already been completed by Langley Research Center. This should reduce the remaining effort to approximately 12 months.

Figure 5-4 shows the tasks related to the long life and maintainability of electro-optical sensors. Included in this sequence is the initial development of an in-flight alignment system for the attitude reference sensors.

## Section 6

### RECOMMENDATIONS FOR FOLLOW-ON STUDIES

The following recommendations for future study are concerned with the analyses required to define and resolve the experiment/SCS interface problems. The recommendations have been derived from an expanded version of the experiment plan, and the studies are required to generate a more sophisticated definition of the SCS requirements on which more realistic hardware definitions can be based.

#### 6.1 EXPERIMENT CONTROL INTERFACE

An expanded version of the 48-hour study is recommended to further define the requirements imposed by a more complete spectrum of experiments. The more complex experiments which require isolation gimbal mounts should be reviewed for similarity, to justify development of a common mounting fixture and control interface. The advantages which result from such a device are reduced operating time (common procedures for similar experiments) and the ability to simultaneously perform several experiments which have the same target. The elimination of separate gimbaling for experiment sensors will produce weight saving and simplify the laboratory/experiment interface.

#### 6.2 MANEUVERING--CMG COMPARED TO RCS

In this phase, a preliminary tradeoff study was conducted to determine whether maneuvering requirements for experiments could be more efficiently met by the attitude thruster reaction control system (RCS), or by the momentum storage system control moment gyros (CMG). This study was based on statistical models of expected roll and pitch/yaw maneuvers, and it assumed multiple mission maneuvers. The two systems were compared on the basis of crew time and system weight. The study indicated an advantage in using CMG for these maneuvers for the assumed maneuvering models and resulted in specific momentum and torque recommendations.

It is recommended that a more realistic experiment maneuver profile be developed which will include maneuver frequency, total angular displacements, and the laboratory axes about which the maneuvers will be performed. These data would be used to perform the tradeoff studies required for more realistic comparison of the RCS and the CMG (with optimized torque and momentum capacities) systems. If the CMG system again proves to be more efficient, the study should include definition of the optimum values for the torque and size parameters.

### 6.3 CMG CONFIGURATION SELECTION

Accurate values for unassigned laboratory resources (volume, weight, power, and so forth) and dollar-cost penalty factors for weight, crew time, and so forth, should be re-evaluated. These values would be used to conduct the tradeoff studies required for an iteration of the CMG system. These studies would include momentum storage systems, sized for the requirements noted above, and new configurations which appear to have merit in view of these new requirements.

### 6.4 CREW MOTION STUDIES

The estimates of crew motion-induced dynamic disturbances are based on simplified assumptions. Further studies, simulation, and in-flight testing are needed to establish a more realistic model of the crew motion disturbance profile. If these disturbances are more severe than expected, major changes in the CMG torque and momentum sizes will be required.

### 6.5 ATTITUDE REFERENCE STUDIES

The ability of the laboratory's precision attitude reference to provide attitude sensing accuracy to  $0.01^\circ$  and rate sensing accuracy to  $0.0006^\circ/\text{sec}$  is estimated on the basis of current technology. More sophisticated studies and simulations are needed to determine if these requirements can be met when realistic error sources associated with the hardware mechanization are taken into account. Such a performance analysis must encompass the navigation errors, mechanical alignment errors, errors in the experimental equipment, and other sources, since these all affect the performance capability of the system.

## 6.6 EARTH OBLATENESS EFFECTS

The ellipticity of the Earth, although slight, is sufficient to cause attitude errors of up to  $0.17^\circ$  for the  $50^\circ$  inclination orbit, which uses horizon-sensing techniques for finding the local geocentric vertical. This error is predictable and is a function of the latitude and altitude of the laboratory at any given moment. Because of the Earth's geometric symmetry, east to west, the local vertical error is always north to west. The amount of error which appears about the roll or the pitch axis is a function of the orbit inclination and instantaneous yaw angle deviation from the orbit plane. If these quantities are known, the errors due to Earth oblateness may be compensated for in the horizon-sensor output signals. Future study is recommended to determine computational mechanization requirements, update data rate, whether the corrections should be performed within the sensor-processing electronics or the attitude reference computer, and the effects of sensor pitch/roll cross-coupling on the selected technique.

## 6.7 LOW-THRUST REACTION CONTROLLERS

Investigations into the use of more efficient, higher  $I_{sp}$  reaction control systems should be continued. The control system analysis studies are needed to determine the mechanization requirements for use of these devices for orbit-keeping on a continuous basis. Also, further studies of the control laws are required to determine the most efficient method of using the thrusters for providing desaturation impulse for the momentum storage system.

Appendix A  
CONTROL SYSTEM ANALYSIS

This section presents additional details of the analysis performed in the Phase IIb study. The work includes: (1) an analysis of worst-case external disturbance torques, (2) an analysis of the gyrocompassing technique, (3) an analysis of the minimal cost of using CMG for attitude maneuvering, and (4) results of the manual control simulation study.

The analysis of worst-case external disturbance torques is presented in Subsection A. 1. Torque and impulse profiles for each orientation are developed for Configuration X shown in Figure 3-3. From these profiles the momentum storage and propellant requirements due to the gravity gradient and aerodynamic disturbances are determined.

The gyrocompassing technique is investigated in detail in Subsection A. 2. It is shown that this technique provides satisfactory vehicle stabilization in the presence of transient disturbances (step torque and initial condition), and steady-state sinusoidal disturbances if certain modifications to the Phase IIa baseline gyrocompassing mechanization are incorporated.

Subsection A. 3 shows that the choice between CMG and RCS for large angular maneuvers can be based on minimizing weight and crew-time. Relationships are developed which show the effect of gyro angular momentum and torque capability on maneuver cost for two different operational modes. In addition, a combination of parameters which minimizes maneuver cost is given as a function of an assumed statistical distribution of angular maneuvers over the entire mission.

The analysis and the simulation of the MORL manual control problem are presented in Subsection A. 4 where comparisons are made of various controllers on the basis of the displayed data and required control accuracy. With these results, an MORL manual control logic has been formulated.

## A. 1 ANALYSIS OF THE IMPULSE REQUIRED FOR EXTERNAL DISTURBANCE AND CENTRIFUGE CONTROL

This section presents the requirements for momentum storage and propellant to compensate for aerodynamic and gravity gradient disturbances on the space laboratory. These requirements are presented for two different orientations, belly-down and inertial, and for vehicle configurations using both solar cell and the Isotope Brayton Cycle power systems. The requirements for these four conditions are based upon Configuration X (with two stowed Apollo command modules and one cargo module, as shown in Figure 3-3), and are presented for the period 1969 to 1974. These requirements are based upon the Phase IIa baseline orbital altitude of 200 nmi. The requirements for the change to the Phase IIb orbital altitude of 164 nmi are presented here.

This study has shown the method for unloading or desaturating the control moment gyros (CMG) while the laboratory is in the belly-down orientation. This method of desaturating the CMG uses two equal impulse expulsions 180° apart in the orbit. In the case of the vehicle with solar panels, the desaturation propellant is dependent upon the relative orbit position of the laboratory at the time of desaturation. This is because of the particular aerodynamic moments on the solar panels (which will be discussed later). For the laboratory without solar panels, desaturation can be accomplished anywhere in the orbit. When desaturating, aft firing thrusters may be used to accomplish orbital drag makeup as well as used to desaturate the CMG. This desaturation scheme can save as much as 50% of the propellant during the years of high solar activity. It is also shown that for some cases the desaturation scheme can reduce the momentum storage requirements.

### A. 1. 1 Analytic Conditions

The summary of the momentum storage and propellant requirements is presented for four conditions; combinations of two orientations and two vehicle configurations based on different electrical power sources.

#### A. 1. 1. 1 Belly-Down with Solar Panels

For the belly-down orientation with solar panels the momentum storage and propellant requirements are based on satisfying the three following



conditions: (1) the solar panels are feathered during occultation, (2) the desaturation impulse is used for orbit keeping, which requires two equal impulses 180° apart in the orbit, and (3) desaturation of the pitch and yaw axis occurs when the roll axis impulse is zero. This occurs when the vehicle yaw axis is in the plane which is normal to the Earth/sun line which passes through the center of the Earth.

Table A-1 presents the momentum storage and propellant requirements for the belly-down orientation. The propellant requirements are based upon an  $I_{sp}$  of 270 sec with an 8-ft lever arm (with solar panels the maximum lever arm is 8 ft).

Table A-1  
MOMENTUM STORAGE AND PROPELLANT REQUIREMENTS

Year	Momentum Storage (lb-ft-sec)				Propellant (lb/mo)		
	Roll	Pitch	Yaw	Pitch and Yaw	Orbit Keeping	Attitude Control	Total
1969	3,530	250	880	910	261	290	290
1970	3,270	250	490	540	144	248	248
1971	3,090	250	220	330	65	218	218
1972	3,010	250	110	270	32	206	206
1973-1974	2,980	250	65	260	19	202	202

The momentum storage figures in Table A-1 do not include an allowance for limited gimbal angle travel for the momentum storage devices. The values are averages for each year noted. In the worst case, which occurs in 1969, the maximum desaturation impulse to be removed by the thrusters for the belly-down orientation is 1,970 lb-ft-sec per orbit, which is a propellant consumption of 430 lb/month.

#### A.1.1.2 Inertial Orientation with Solar Panels

Since the inertial orientation is expected to be used for only short-time durations, no requirements are imposed for combining orbit-keeping with

desaturation. The requirements given in Table A-2 are based on the worst-case (1969) density of the atmosphere and an orbital altitude of 200 nmi.

Table A-2  
INERTIAL ORIENTATION

Momentum Storage (lb-ft-sec)				Propellant (lb/mo)*		
Roll	Pitch	Yaw	Pitch and Yaw	Attitude Control	Orbit-Keeping	Total
3,030	340	620	660	259	435	694

\*Propellant requirements are a maximum and not an average.

For the year 1969, the momentum storage requirements for the inertial orientation are less than those for the belly-down orientation. After 1969, the inertial orientation may impose larger momentum storage requirements than the belly-down orientation, because gravity gradient torques remain constant while the aerodynamic torques decrease with time.

#### A. 1. 1. 3 Belly-Down Orientation without Solar Panels

The only momentum storage and propellant requirement for the belly-down orientation without solar panels is caused by the gravity gradient torque and a small aerodynamic torque about the pitch axis. These torques are due to the asymmetry of the vehicle. These requirements are nearly independent of the year since the aerodynamic torque is small. The pitch axis desaturation impulse will be used for orbit-keeping capability.

Table A-3 presents the momentum storage and propellant requirements for the belly-down orientation without solar panels, based on a 1969 atmosphere and an orbit altitude of 200 nmi. The lever arm for attitude control without solar panels is 10 ft.

Table A-3  
MOMENTUM STORAGE AND PROPELLANT REQUIREMENTS  
WITHOUT SOLAR PANELS

Momentum Storage (lb-ft-sec)		
Roll	Pitch	Total Propellant (lb/mo)
2,940	240	170

A. 1. 1. 4 Inertial Orientation without Solar Panels

Table A-4 presents the momentum storage requirements for the inertial orientation without solar panels.

Table A-4  
INERTIAL ORIENTATION WITHOUT SOLAR PANELS

Year	Momentum Storage (lb-ft-sec)			
	Roll	Pitch	Yaw	Pitch and Yaw
1969	3,030	900	125	910
1970	3,030	850	110	860
1971	3,030	825	100	830
1972	3,030	810	95	820
1973-1974	3,030	800	85	810

For the space laboratory without solar panels, the inertial orientation imposes the largest momentum storage requirements.

Table A-5 presents the maximum required propellant for the inertial orientation without solar panels.

Table A-5  
MAXIMUM REQUIRED PROPELLANT

Year	Orbit-Keeping (lb/mo)	Attitude Control (lb/mo)	Total Propellant (lb/mo)
1969	310	314	624
1970	172	298	470
1971	77	288	365
1972	38	283	321
1973-1974	23	282	305

#### A. 1. 2 Derivation of Requirements

This section discusses system requirements for the four analytic conditions.

##### A. 1. 2. 1 Belly-Down Orientation with Solar Panels

This section presents the propellant and momentum storage requirements for the belly-down orientation with solar panels. The data presented are for an orbital altitude of 200 nmi during the 1969 to 1974 period. These requirements are based on an aerodynamic moment about the vehicle yaw (or Z) axis, and aerodynamic and gravity gradient moments about the vehicle pitch (or Y) axis. The aerodynamic force on the solar panels produces yaw and pitching moments on the vehicle. The gravity gradient moment about the pitch axis is caused by the fact that the roll axis, which is aligned with the orbital velocity vector, is not a principal body axis. This asymmetrical inertia distribution is due to the third resupply craft on top of the vehicle in the X-Z plane.

The aerodynamic moments due to the solar panels were obtained by use of the belly-down orientation computer program described in Section 4. 1. The propellant and momentum storage requirements because of the moments on the solar panels for various vehicle configurations can be obtained from the data presented by ratioing changes in solar panel area and CG locations. Also, the propellant and momentum storage requirements for any year can

be obtained from these data by ratioing the density of the atmosphere for the particular year of solar activity. The gravity gradient moments and the average bias aerodynamic moments caused by vehicle asymmetry are readily obtained analytically and are summed with the panel aero moments obtained from the computer program.

### Aerodynamic Force on Solar Panels

In deriving the aerodynamic moments produced by the solar panels, the normal force coefficient,  $C_N$ , of the panels is assumed to be equal to  $2 \sin^2 \alpha$ , where  $\alpha$  is the angle between the plane of the solar panel and the orbital velocity vector. The normal force,  $F_n$ , on the solar panels is given as:

$$F_n = C_N Q A_{REF} \quad (A-1)$$

with

$$Q = \text{dynamic pressure in lb/ft}^2$$

$$A_{REF} = \text{reference area in ft}^2$$

From the two gimbal angles of the solar panels,  $\delta$  and  $\phi$  shown in Figure A-1, the normal force,  $F_n$ , on the solar panels is resolved into body axes, pitch, roll, and yaw. The force along the roll (or X) axis is almost all due to the aerodynamic drag of the solar panels. Summing the drag of the laboratory with that of the solar panels produces the total drag of MORL. The forces along the yaw (or Z) axis and the pitch (or Y) axis produce moments about the pitch and yaw axes, respectively.

A yawing moment is obtained by the deflection,  $\delta$ , of the solar panels, which is defined in Figure A-1. The deflection,  $\delta$ , is dependent on the inclination of the orbit plane to the ecliptic plane. The yawing moment is directly proportional to  $\sin \delta \sin \alpha |\sin \alpha|$ , where  $\sin \alpha = \cos \delta \cos \phi$ . Assuming a constant density atmosphere, the maximum yawing moment occurs at  $\delta = \pm 35^\circ$  and  $\phi = 0, 180^\circ$ . The yawing moment is zero at  $\phi = 90^\circ, 270^\circ$ . Where the solar panels are feathered in occultation, the yawing moment is zero for  $180^\circ + \phi_c \leq \phi \leq 360^\circ - \phi_c$ , as shown in Figure A-1.

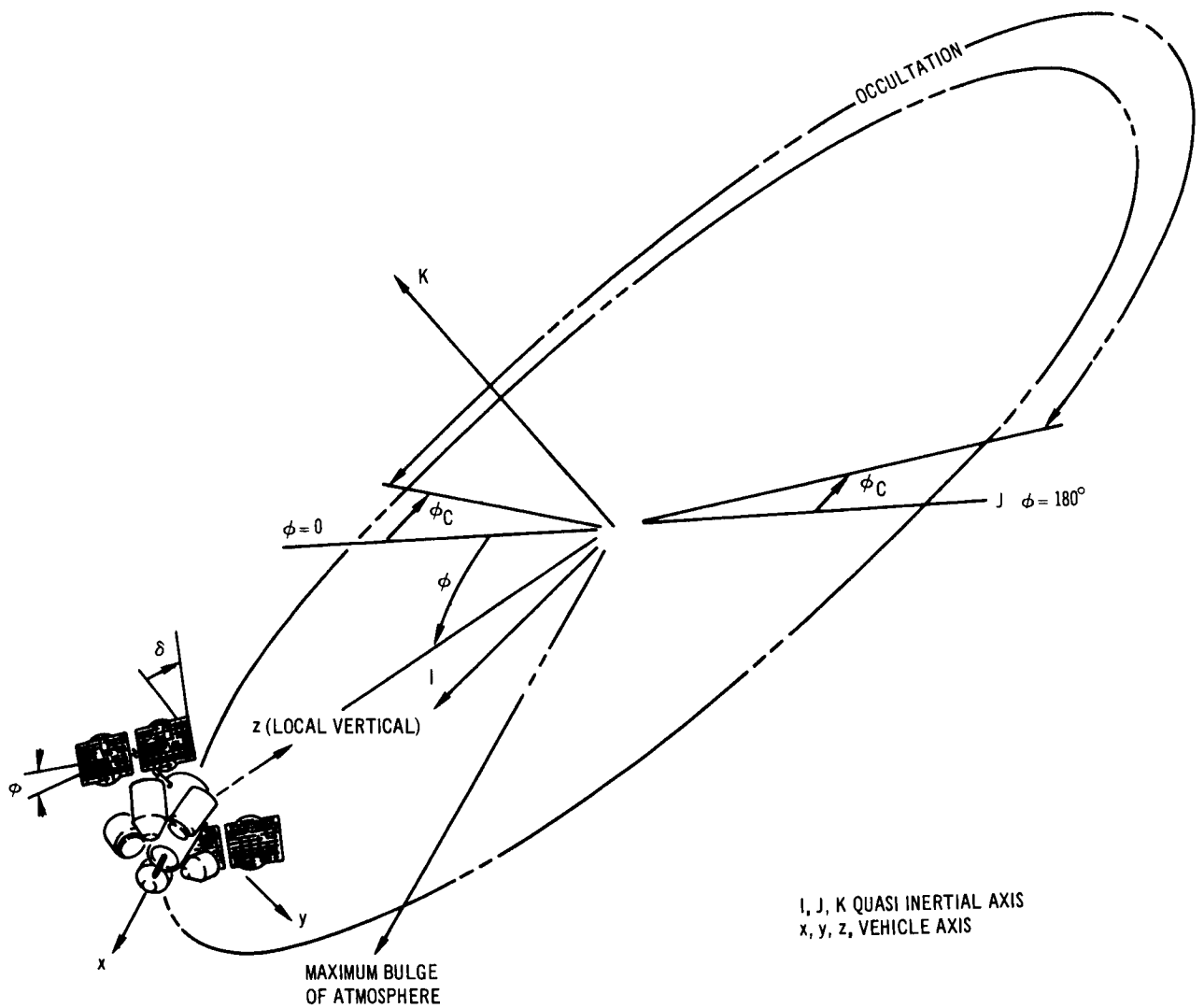


Figure A-1 Coordinate System

The aerodynamic pitching moment caused by the solar panels is directly proportional to  $\sin \phi \cos \delta \sin \alpha |\sin \alpha|$ , and again  $\sin \alpha = \cos \delta \cos \phi$ .

With a constant density atmosphere, the maximum pitching moments occur for a  $\delta = 0^\circ$  and  $\phi = \pm 35^\circ, 145^\circ, \text{ and } 215^\circ$ .

#### Effect of the Diurnal Bulge

The effect of the diurnal bulge of the atmosphere displaces the positions in orbit of peak yawing and pitching moments. The amplitudes of the negative and positive peak moments are also dependent on their position relative to the bulge; positions of zero moments in the orbit are unaffected by the bulge.

Figure A-2 is a plot of the yaw,  $M_Z$ , and pitch,  $-M_Y$ , moments caused by the aerodynamic forces on the solar panels, as obtained from the computer program. It is noted that the negative peak of the yaw moment,  $M_Z$ , is displaced about  $4^\circ$  from  $\phi = 0$ , whereas the positive peak is displaced  $15^\circ$  from  $\phi = 180^\circ$ . Since the positive peak is closer to the bulge than the negative peak, the bulge has more effect on the amplitude of the positive peak. The position of occultation is also indicated in Figure A-2. With the solar panels feathered in occultation, the pitch and yaw moments are zero in this region.

#### Inertial Momentum Caused by Aerodynamic Moments on Solar Panels

To illustrate the effect of the panel aerodynamic moments, the yaw moment will be considered to be a cosine function of  $\phi$  and the pitch moment a sine function of  $2\phi$ . (Note Figure A-2.) These are reasonable assumptions since the bulge does not shift the moment peaks very much. The largest source of error in these assumptions is the relative difference between the positive and negative peak amplitudes of the aerodynamic moments. The fact that the yaw moment is a function of  $\cos \phi |\cos \phi|$  instead of  $\cos \phi$  can be taken into account by a ratio of the effective values of  $\cos^2 \phi$  to  $\cos \phi$ , which is  $0.5/(2/\pi) = 0.787$ . It is also noted that, at certain times in the regression period when the orbit plane is nearly normal to the sun line, the diurnal bulge has a much smaller distortion effect on the aerodynamic moments.

ALTITUDE = 200 NMI  
 INCLINATION = 53°  
 YEAR: 1969

$\Omega_0 = 48.3^\circ$   
 $\lambda_0 = 211^\circ$

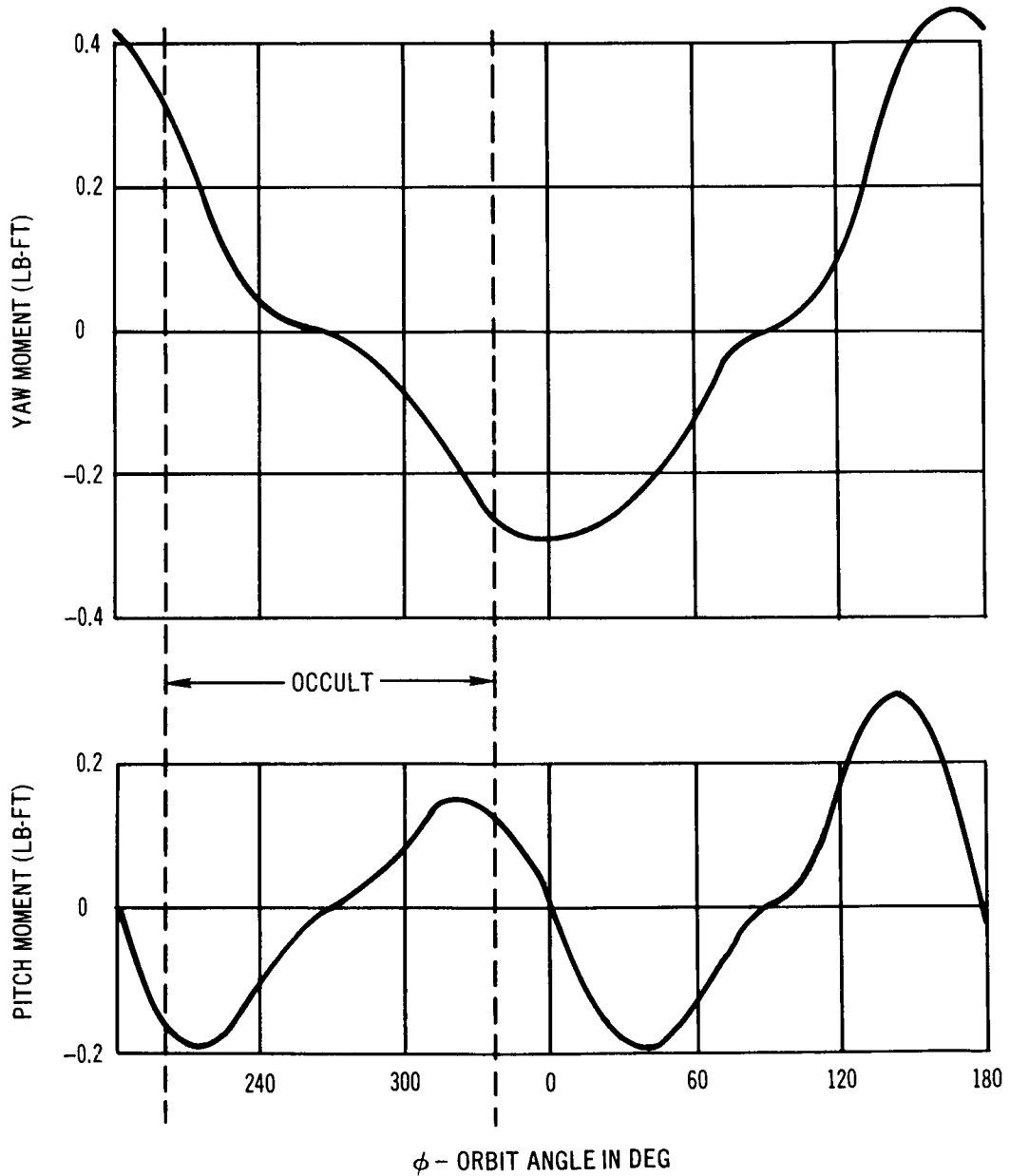


Figure A-2. Belly-Down Solar Panel Moments



The body axes moments caused by the solar panels are as follows:

$$M_X = 0 \quad (A-2)$$

$$M_Z = M_1 \cos \phi \quad (A-3)$$

$$M_Y = -M_2 \sin 2\phi \quad (A-4)$$

From Figure A-1, the quasi-inertial moments (with respect to the orbit plane) are obtained as:

$$M_I = -M_Z \sin \phi = -M_1 \sin \phi \cos \phi \quad (A-5)$$

$$M_J = M_Z \cos \phi = M_1 \cos^2 \phi \quad (A-6)$$

$$M_K = -M_Y = M_2 \sin 2\phi \quad (A-7)$$

Integrating the inertial moments with respect to time, the inertial angular momentum over one orbit is obtained as follows:

$$H_I = -\frac{M_1}{2} \int_0^T \sin \frac{4\pi}{T} t \, dt = 0 \quad (A-8)$$

$$H_J = \frac{M_1}{2} \int_0^T (1 + \cos \frac{4\pi}{T} t) \, dt = \frac{M_1}{2} T \quad (A-9)$$

$$H_K = M_2 \int_0^T \sin \frac{4\pi}{T} t \, dt = 0 \quad (A-10)$$

where  $\phi = \frac{2\pi}{T} t$  and  $T$  is the orbit period in seconds.

This indicates that for a constant density atmosphere there is only an impulse accumulation on the quasi-inertial J axis. With the diurnal bulge

there is some small (compared to the J axis) impulse accumulation along the I and K axes. This impulse accumulation must be removed by jet thrusters to prevent the CMG from reaching saturation. (The desaturation techniques are discussed in a later section.)

### Feathering Solar Panels in Occult

The technique of feathering the solar panels (presenting the minimum area to the relative wind) during occultation was suggested by Bendix for the purpose of reducing the orbit-keeping and attitude control propellant requirements.

Figure A-3 includes a plot of the drag impulse in lb-sec/orbit for the belly-down orientation without feathering the solar panels and a plot of drag on the body only (without solar panels). The actual drag coefficient,  $C_D$ , for this configuration without the solar panels is 4.35, whereas the drag coefficient

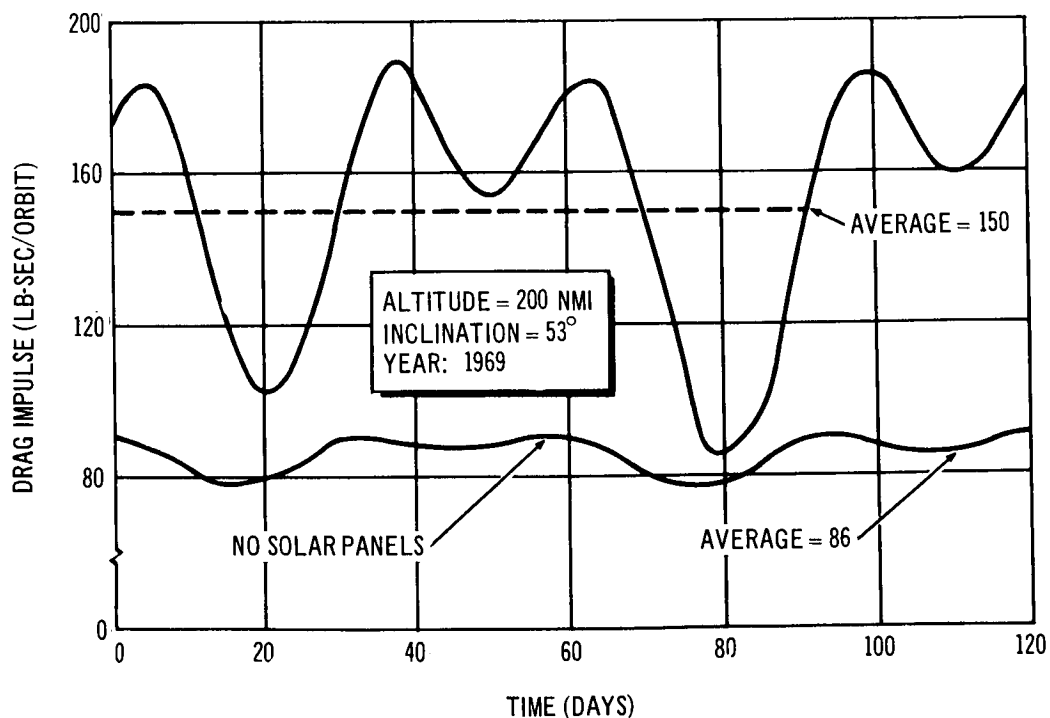


Figure A-3. Belly-Down Drag without Feathering Solar Panels

used in the computer program is 4.0; hence, the drag impulse is obtained from the average values given in Figure A-3 as follows:

$$\text{Average drag impulse} = \left( \frac{4.35}{4} \times 86 \right) + (150 - 86) = 158 \text{ lb-sec/orbit.}$$

The reference area of the space laboratory without solar panels is 368 ft<sup>2</sup> and the solar panel area is 1,700 ft<sup>2</sup>. The drag for any configuration with a different C<sub>D</sub> or solar panel area, or both, can be obtained by ratios of the C<sub>D</sub> and solar panel areas.

The peaks in the plot with solar panels of Figure A-3 occur at times in the regression period where the solar panels are nearly normal to the orbit plane. The plot without solar panels illustrates the effects of the diurnal bulge throughout a regression period.

Figure A-4 is a plot of the drag impulse for feathering the solar panels during occultation. The average drag impulse is obtained in the same manner as noted above.

$$\text{Average drag impulse} = \left( \frac{4.35}{4} \times 86 \right) + (138 - 86) = 146 \text{ lb-sec/orbit.}$$

Both Figures A-3 and A-4 are based upon a maximum atmospheric density, the year 1969 and an orbital altitude of 200 nmi.

As previously mentioned, feathering of the solar panels during occultation reduces the attitude control propellant requirement. This can be illustrated by noting Equation (A-9), which is the impulse accumulation produced by the solar panel aerodynamic moments without feathering. If the panels are feathered during occultation, then the impulse accumulation along the quasi-inertial J axis is given by

$$H_J = \frac{M_1}{2} \int_{-\phi_c}^{\pi + \phi_c} (1 + \cos 2\phi) \frac{T}{2\pi} d\phi = \frac{M_1}{4\pi} T (\pi + 2\phi_c + \sin 2\phi_c) \quad (\text{A-11})$$

where  $\phi_c$  is described in Figure A-1.

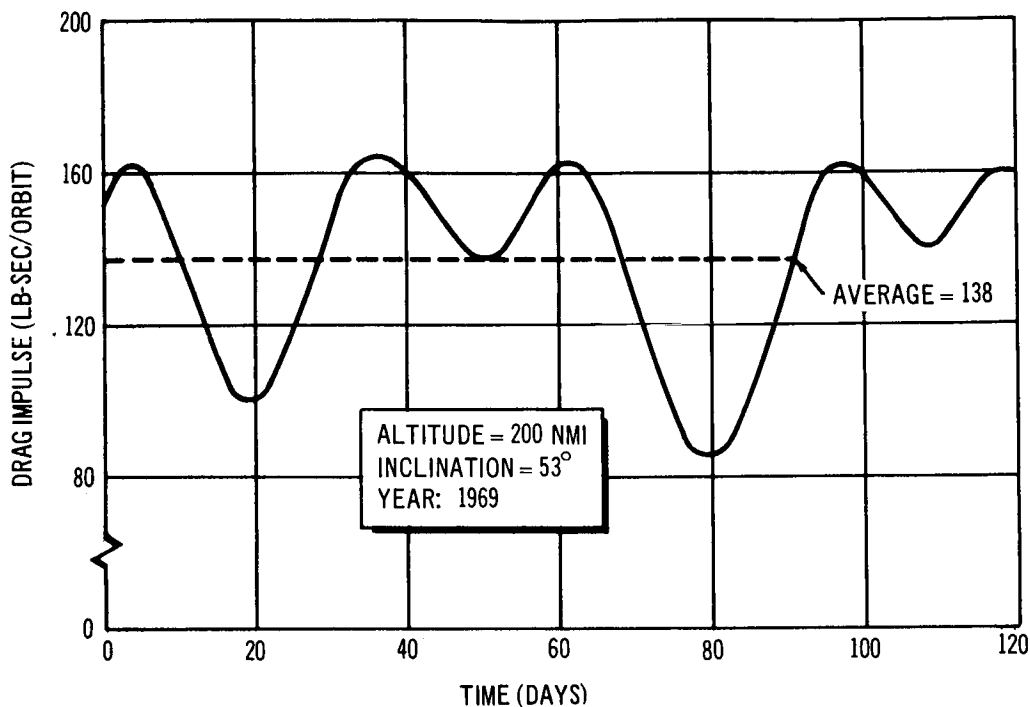


Figure A-4. Belly-Down Drag Feathering Solar Panels in Occult

Since  $\phi_c < \frac{\pi}{2}$ , the maximum value of Equation (A-11) approaches that of Equation (A-9), for  $\phi_c$  approaching  $\pi/2$ . Hence, by feathering the solar panels during occultation, the impulse accumulation along the quasi-inertial J axis can be reduced.

Figure A-5 shows two plots of the accumulated impulse per orbit, as a function of time in days, as obtained from the computer program for the case of not feathering the solar panels. The upper plot shows the vector sum of the quasi-inertial I and J axes impulse. The effect of the diurnal bulge causes a maximum deflection of  $6^\circ$  in the I-J plane between the quasi-inertial J axis and the accumulated impulse vector. This amounts to an accumulated impulse vector along the I axis that is, at most, 10% of the J axis.

The second plot shows the accumulated impulse along the K or body negative pitch axis. This accumulation is produced by the diurnal bulge of the

ALTITUDE = 200 NMI  
INCLINATION = 53°  
YEAR: 1969

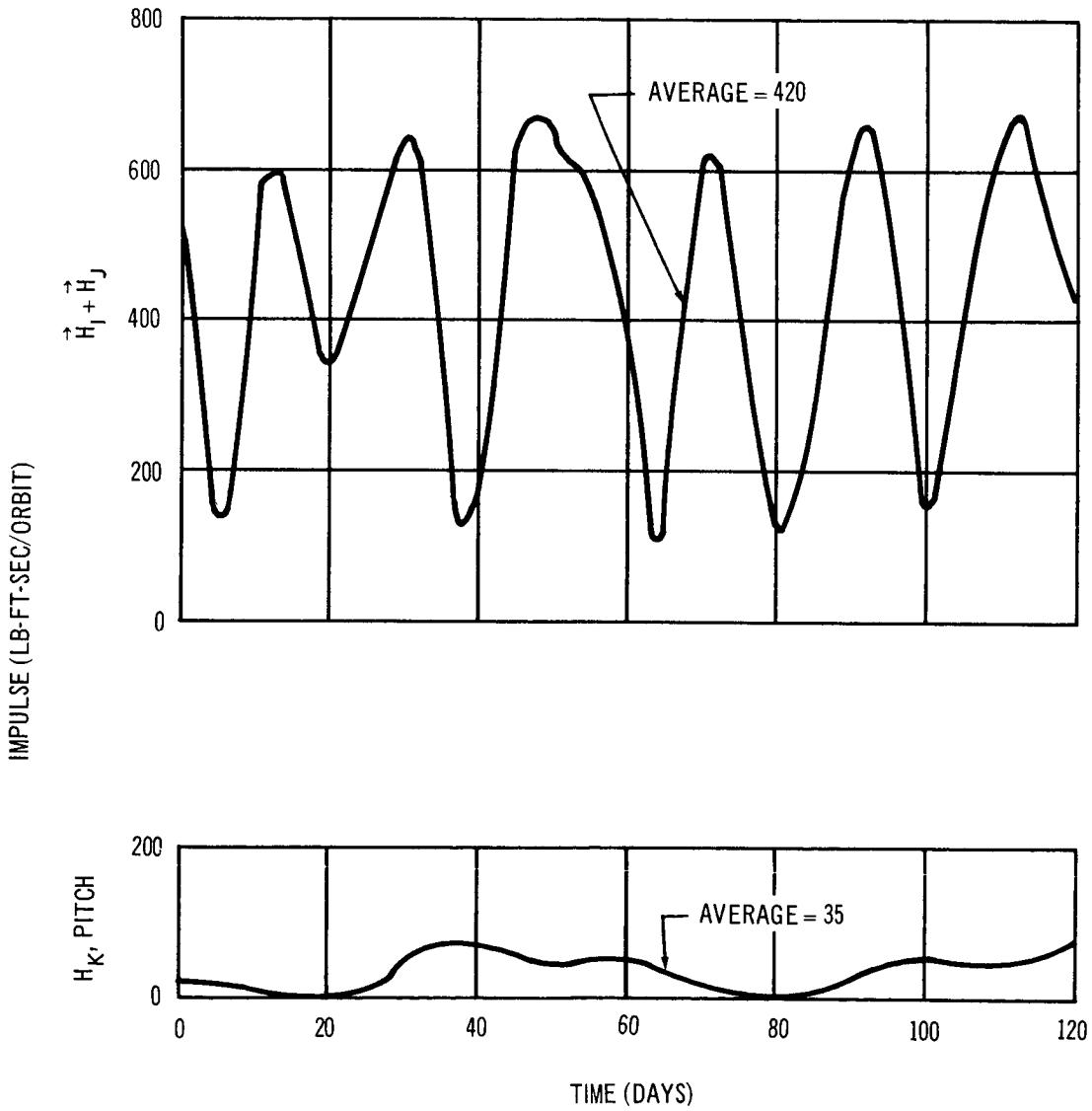


Figure A-5. Belly-Down Accumulated Impulse without Feathering Solar Panels

atmosphere. The total average accumulated impulse is  $420 + 35 = 455$  lb-ft-sec/orbit.

Figure A-6 is the same as Figure A-5 except that the solar panels are feathered during occultation. For this case, the total average accumulated impulse is  $330 + 45 = 375$  lb-ft-sec/orbit. Both Figures A-5 and A-6 were obtained from computer runs which were based on an aerodynamic lever arm of 20 ft. Since the actual lever arm for the most recent vehicle configuration is 26.6 ft, the numbers for the total accumulated impulses must be multiplied by the ratio of  $26.6/20$ .

Table A-6 presents the propellant requirements for the two cases of feathering or not feathering the solar panels during occultation. The propellant requirement consists of the orbit-keeping propellant and the propellant to remove the accumulated impulse obtained from the aerodynamic moments of the solar panels.

Table A-6  
COMPARISON OF PROPELLANT REQUIREMENTS\*

	Orbit Keeping		Accumulated Impulse due to Solar Panels		Total Propellant
	(lb-sec/orbit)	(lb/mo)	(lb-ft-sec/orbit)	(lb/mo)	(lb/mo)
Without feathering	163	284	605	131	415
With feathering solar panels	150	261	499	109	370

\*Values are for Configuration X, 200-nmi orbit, and year 1969.

The propellant weights are based on an  $I_{sp}$  of 270 sec with a control lever arm of 8 ft. By feathering the solar panels during occultation, the propellant consumption is reduced by 45 lb/month.

In the following discussion and analyses, only the case of feathering the solar panels during occultation will be considered.

ALTITUDE = 200 NMI  
 INCLINATION = 53°  
 YEAR: 1969

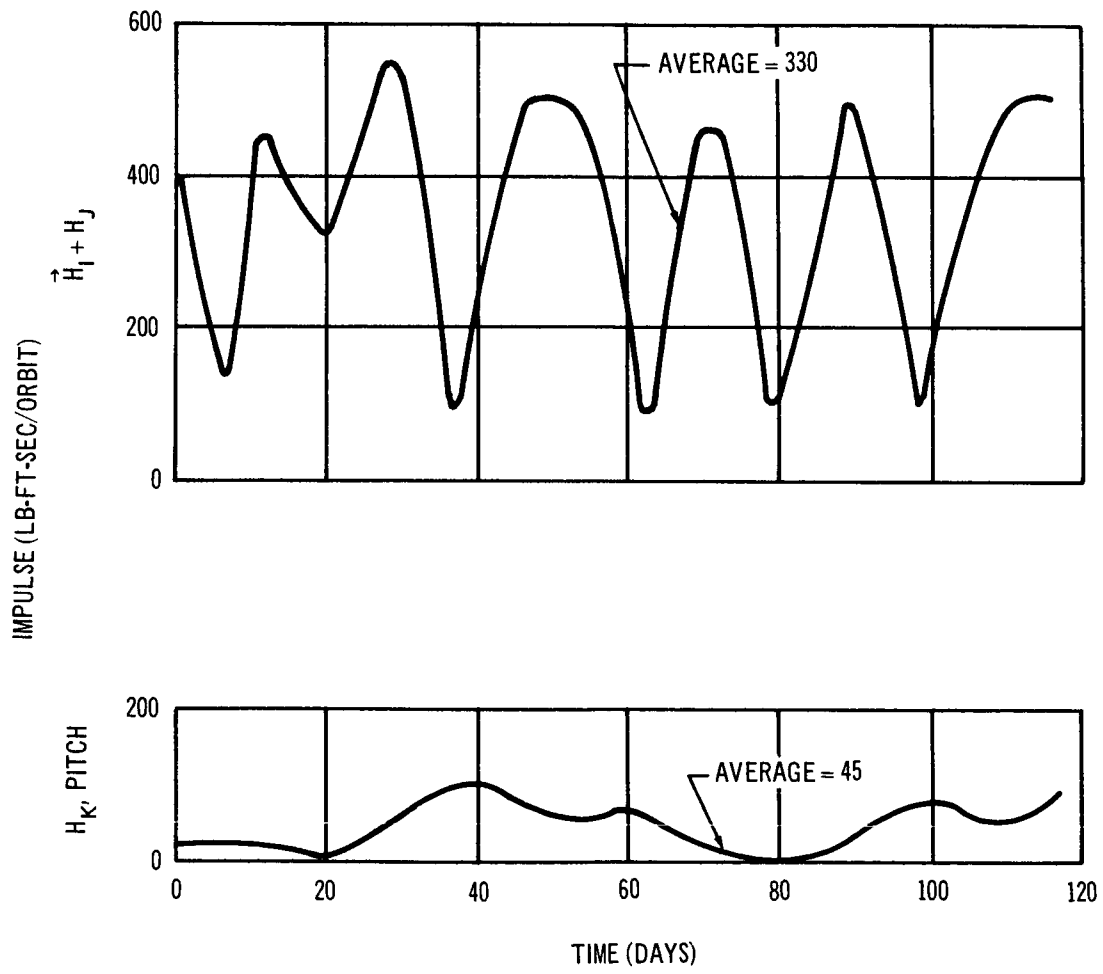


Figure A-6. Belly-Down Accumulated Impulse Feathering Solar Panels in Occult

## Desaturation Schemes

Desaturation is most efficiently accomplished when the yaw axis is aligned with the accumulated impulse vector in the I-J plane. The body yaw axis is chosen instead of the body roll axis since the yaw thrusters have the capability of removing the accumulated impulse and, at the same time, applying thrust for orbit keeping. (This dual purpose is discussed in a later section.) If the body yaw axis is not aligned with the accumulated impulse vector at the time of desaturation, a vector combination of impulse from both the body yaw axis and body roll axis will be required to remove the total amount. Of course, this would give higher requirements for the impulse removal or desaturation since the body impulse components,  $H_X$  and  $H_Z$ , of the impulse vector,  $H_{I-J}$ , are larger than  $H_{I-J}$  itself.

Over a complete orbit, the amount of accumulated impulse on the body pitch axis, which is the quasi-inertial axis K, is independent of the time of desaturation. (This is also discussed further in a later section.)

It was illustrated that with a moment on the body yaw-axis in the form of a cosine function of  $\phi$ , an impulse accumulation is obtained along the quasi-inertial J axis. This means that desaturation should be accomplished when the body yaw axis is aligned with the accumulated impulse which is approximately at  $\phi = 0^\circ$  or  $180^\circ$ .

For the following example of desaturation in the case of feathering the solar panels during occultation, the desaturation takes place at  $\phi = 180^\circ$ .

The dynamic equations are as follows:

$$M_X = 0 = \dot{h}_x + \omega_y h_z \quad (\text{A-12})$$

$$M_Z = -M \cos \omega_y t = -\omega_y h_x + \dot{h}_z \quad (\text{A-13})$$

where

$$-\omega_y t = \phi = \frac{2\pi}{T} t$$



and  $-M \cos \omega t$  is the description of the solar panel aerodynamic moment with  $h_x$  and  $h_z$  representing the roll and yaw angular impulse, respectively.

Solving for  $h_x$  and  $h_z$

$$h_x = h_{x_0} \cos \phi + h_{z_0} \sin \phi - \frac{M}{4\pi} T \phi \sin \phi \quad (\text{A-14})$$

$$h_z = h_{z_0} \cos \phi - h_{x_0} \sin \phi - \frac{M}{4\pi} T (\sin \phi + \phi \cos \phi) \quad (\text{A-15})$$

where

$h_{x_0}$  and  $h_{z_0}$  are the initial conditions.

With  $h_x = h_z = 0$  at  $\phi = 180^\circ$ , the desaturation point, the angular momentum accumulated at occultation is obtained as follows:

At occultation  $\phi = 180^\circ + \phi_c$

$$h_{x_c} = \frac{M}{4\pi} T \phi_c \sin \phi_c \quad (\text{A-16})$$

$$h_{z_c} = \frac{M}{4\pi} T (\sin \phi_c + \phi_c \cos \phi_c) \quad (\text{A-17})$$

During occultation,  $360^\circ - \phi_c > \phi > 180^\circ + \phi_c$  and  $M_Y = 0$ . The angular momentum is given by

$$h_x = -h_{x_c} \cos (\phi - \phi_c) - h_{z_c} \sin (\phi - \phi_c) \quad (\text{A-18})$$

and

$$h_z = -h_{z_c} \cos (\phi - \phi_c) + h_{x_c} \sin (\phi - \phi_c) \quad (\text{A-19})$$

Upon leaving occultation, the roll and yaw axes impulses are given as:

$$h_{x_L} = -h_{x_c} \cos 2 \phi_c + h_{z_c} \sin 2 \phi_c \quad (\text{A-20})$$

$$h_{z_L} = -h_{z_c} \cos 2 \phi_c - h_{x_c} \sin 2 \phi_c \quad (\text{A-21})$$

At  $\phi = 360^\circ - \phi_c$  Equations (A-20) and (A-21) are the initial impulses for Equations (A-14) and (A-15). Hence, for  $\phi > -\phi_c$  where  $M_Z \neq 0$ , the following equations are obtained:

For  $\phi > -\phi_c$

$$\begin{aligned} h_x &= h_{x_L} \cos (\phi + \phi_c) + h_{z_L} \sin (\phi + \phi_c) \\ &\quad - \frac{M}{4\pi} T (\phi + \phi_c) \sin (\phi + \phi_c) \end{aligned} \quad (\text{A-22})$$

$$\begin{aligned} h_z &= h_{z_L} \cos (\phi + \phi_c) - h_{x_L} \sin (\phi + \phi_c) \\ &\quad - \frac{M}{4\pi} T \left[ \sin (\phi + \phi_c) + (\phi + \phi_c) \cos (\phi + \phi_c) \right] \end{aligned} \quad (\text{A-23})$$

at  $\phi = 0$ ,  $h_x$  and  $h_z$  are now obtained

$$h_x = h_{x_z} = h_{x_L} \cos \phi_c + h_{z_L} \sin \phi_c - \frac{M}{4\pi} T \phi_c \sin \phi_c \quad (\text{A-24})$$

$$\begin{aligned} h_z &= h_{z_z} = h_{z_L} \cos \phi_c - h_{x_L} \sin \phi_c - \frac{M}{4\pi} T \left[ \sin \phi_c \right. \\ &\quad \left. + \phi_c \cos \phi_c \right] \end{aligned} \quad (\text{A-25})$$

With the roll,  $h_x$ , and yaw,  $h_z$ , impulses obtained between  $\phi = 180^\circ$  and  $\phi = 360^\circ$ , Equations (A-24) and (A-25) are now substituted for  $h_{x_0}$  and  $h_{z_0}$  in

Equations (A-14) and (A-15). The impulses over a complete orbit, obtained from Equations (A-14) and (A-15) with  $\phi = 180^\circ$ , are the following:

$$h_{x_s} = -h_{x_z} = -h_{x_L} \cos \phi_c - h_{z_L} \sin \phi_c + \frac{M}{4\pi} T \phi_c \sin \phi_c \quad (\text{A-26})$$

$$h_{z_s} = -h_{z_z} + \frac{M}{4\pi} T \pi = -h_{z_L} \cos \phi_c + h_{x_L} \sin \phi_c + \frac{M}{4\pi} T [\pi + \sin \phi_c + \phi_c \cos \phi_c] \quad (\text{A-27})$$

Substituting Equations (A-20), (A-21), (A-16), and (A-17) into (A-26) and (A-27), the accumulated impulse to be removed by the jet thrusters is obtained as follows:

$$h_{x_s} = \frac{M}{4\pi} T \sin \phi_c (\phi_c - \sin \phi_c) \quad (\text{A-28})$$

$$h_{z_s} = \frac{M}{4\pi} T [\pi + (1 + \cos \phi_c)(\phi_c + \sin \phi_c)] \quad (\text{A-29})$$

Since the roll axis impulse,  $h_{x_s}$ , contains the term  $(\phi_c - \sin \phi_c)$ , it will be much smaller than the yaw axis impulse,  $h_{z_s}$ , at the point of desaturation. For  $\pi/2 > \phi_c > 0$ ,  $h_{x_s}$  will be, at most, 10% of  $h_{z_s}$ .

Figure A-7 plots contain the roll and yaw body axes impulses obtained from the computer program. This figure corresponds to the yaw moment plotted in Figure A-2, which is a maximum. From Figure A-7 for desaturation at  $\phi = 180^\circ$ , it is noted that the roll axis impulse,  $h_x$ , is less than 10% of the yaw axes impulse.

For desaturation at  $\phi = 180^\circ$ , two other orbits throughout several regression periods are presented in Figure A-8. These plots illustrate that desaturating the roll axis is not required.

Referring again to Figure A-7, which resulted in a minimum impulse required for desaturation, the positive and negative impulse peaks of the roll and yaw axes are noted to be unequal. For the desaturation point shown

ALTITUDE = 200 NMI	CELESTIAL PARAMETERS
INCLINATION = 53°	$\Omega_0 = 48.3^\circ$
YEAR: 1969	$\lambda_0 = 211^\circ$

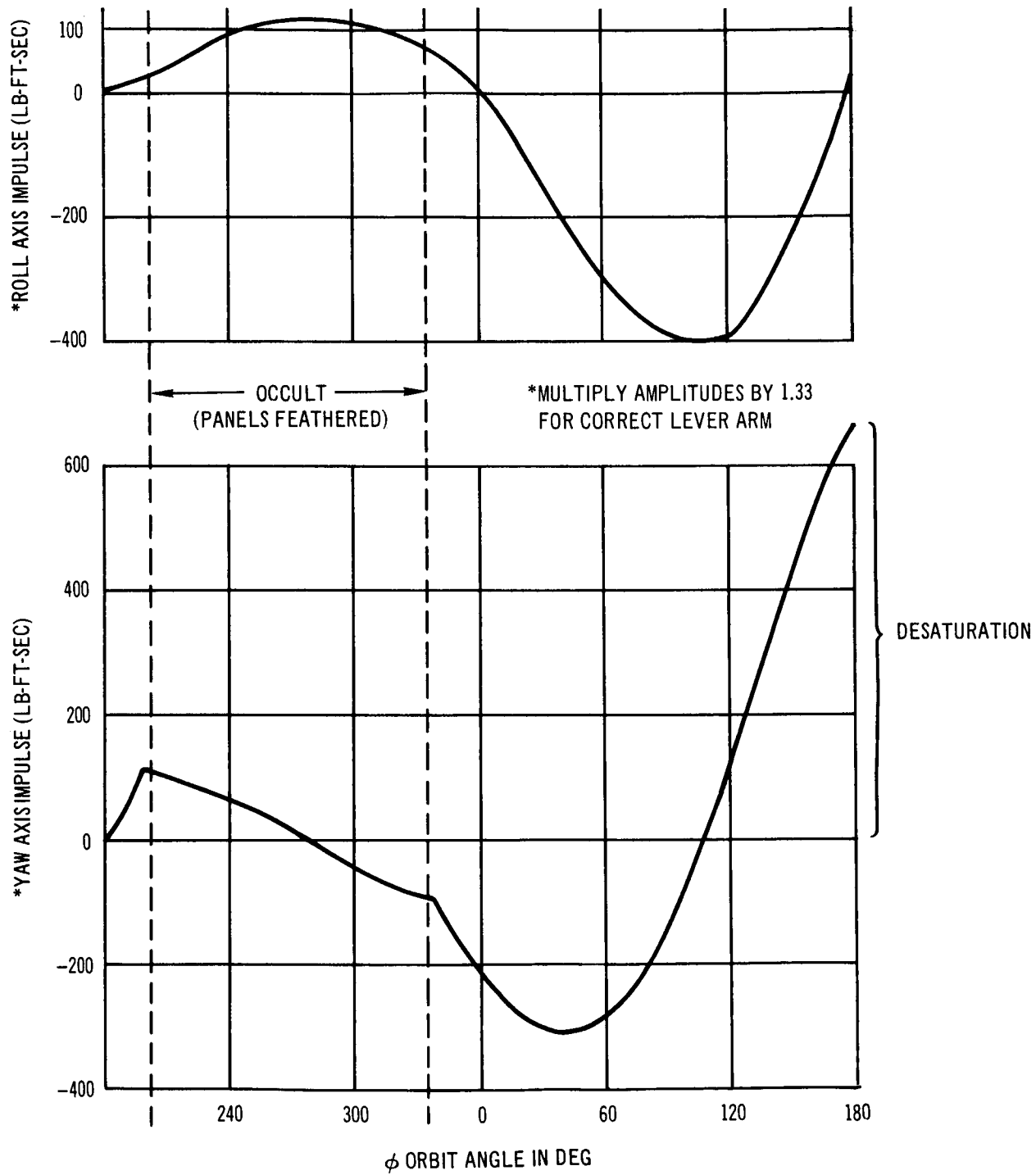


Figure A-7. Belly-Down Roll and Yaw Maximum Impulse (Desaturation at  $\phi = 180^\circ$ )

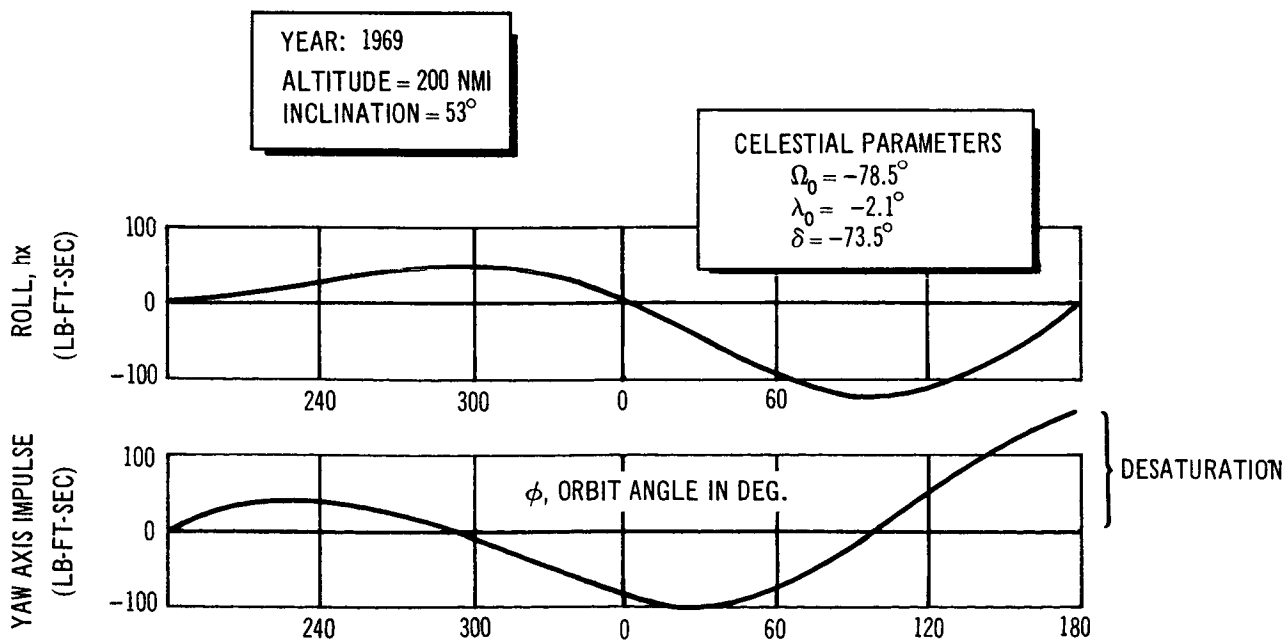
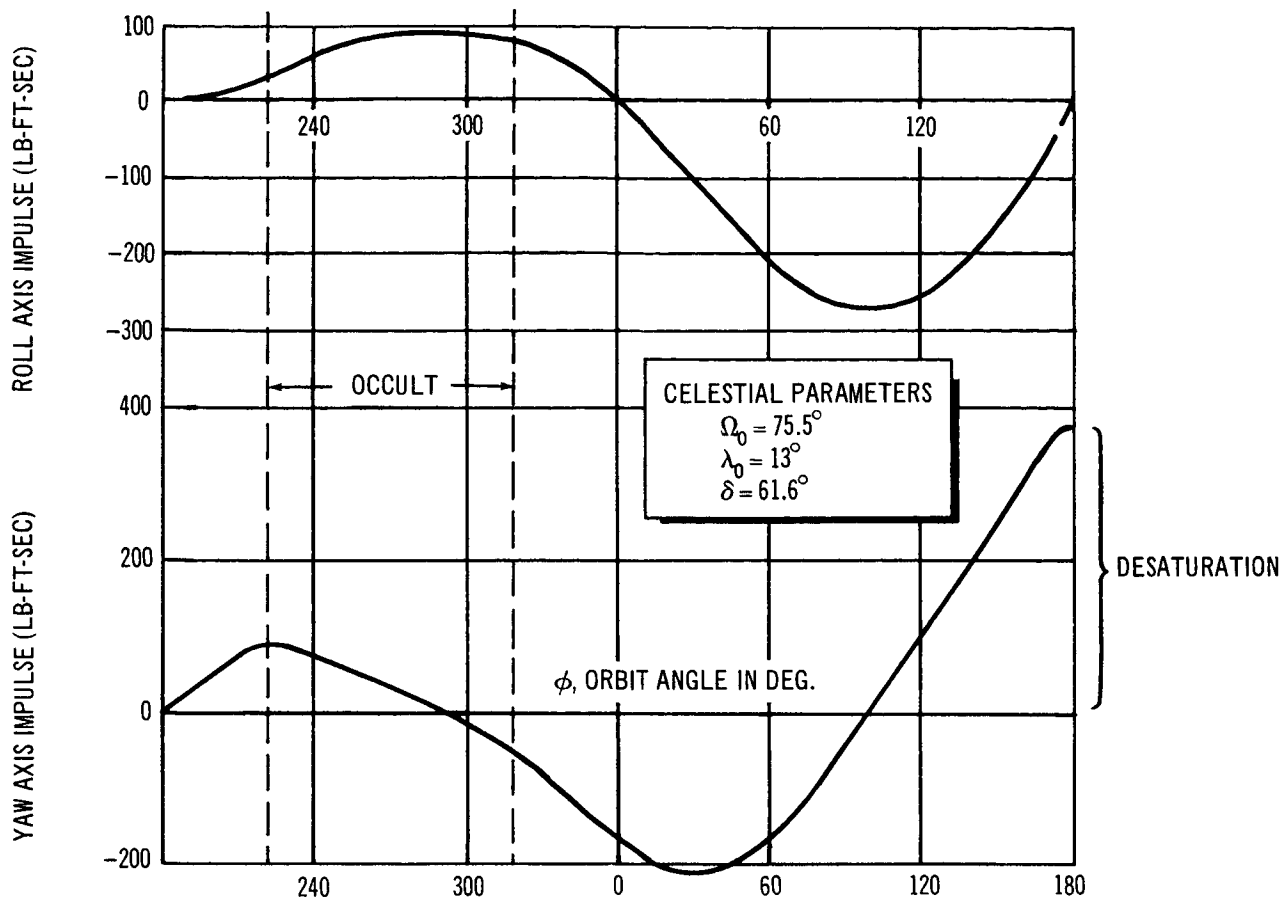


Figure A-8. Belly-Down Roll and Yaw Typical Impulse (Desaturation at  $\phi = 180^\circ$ )

in Figure A-7, the momentum storage requirement would be based upon the maximum peak occurring throughout the orbit. For the roll axis momentum storage, which must be sized for the centrifuge (2,940 lb-ft-sec) as well as the aerodynamic moment impulse, the total momentum storage requirement would be  $1/\sin 60^\circ \times [2,940 + (26.6/20 \times 400)] = 4,010$  lb-ft-sec, where the angle of  $60^\circ$  is the maximum available gimballed angle in one direction of the CMG. This is about  $1/\sin 60^\circ \times (400 - 110) 26.6/20 = 445$  lb-ft-sec more than required for the first half of the orbit. A similar condition exists for the yaw axis momentum storage requirement which is  $26.6/20 \times 660 \times 1/\sin 60^\circ = 1,015$  lb-ft-sec. This is noted to be  $1/\sin 60^\circ (660 - 300) 26.6/20 = 555$  lb-ft-sec more than required for the negative peak of the yaw axis impulse. In other words, for the particular desaturation scheme chosen, which minimized desaturation impulse, the CMG momentum storage requirements are not minimized.

Figure A-9 illustrates the effect of a given desaturation scheme on the angular momentum required which varies as a function of the momentum storage weight. The point of interest is that, for a double-gimbal CMG angular momentum of 400 lb-ft-sec, only an additional 24 lb of weight are required to double the CMG capacity. It will be shown that the minimum weight for desaturation impulse and momentum storage is determined solely by the minimum desaturation impulse.

Figure A-9 presents the roll and yaw axes impulse for desaturation at occultation,  $\phi_c$ , for the same celestial parameters as given in Figure A-7. From Figure A-9, it is noted that the positive and negative impulses of the roll axis are nearly equal. The total momentum storage requirement for the roll axis is  $1/\sin 60^\circ [2,940 + (26.6/20 \times 300)] = 3,860$  lb-ft-sec, which is 150 lb-ft-sec less than the roll impulse required in Figure A-7. The yaw axis momentum storage requirement is noted to be about 10% (76 lb-ft-sec) less than that shown in Figure A-7. With the desaturation shown in Figure A-9, the roll axis as well as the other two axes must be desaturated.

Figure A-10 shows the case of desaturation at a particular place in orbit to make the positive and negative yaw impulses approximately equal. Comparing Figures A-10 and A-7, a decrease of momentum storage for the yaw axis

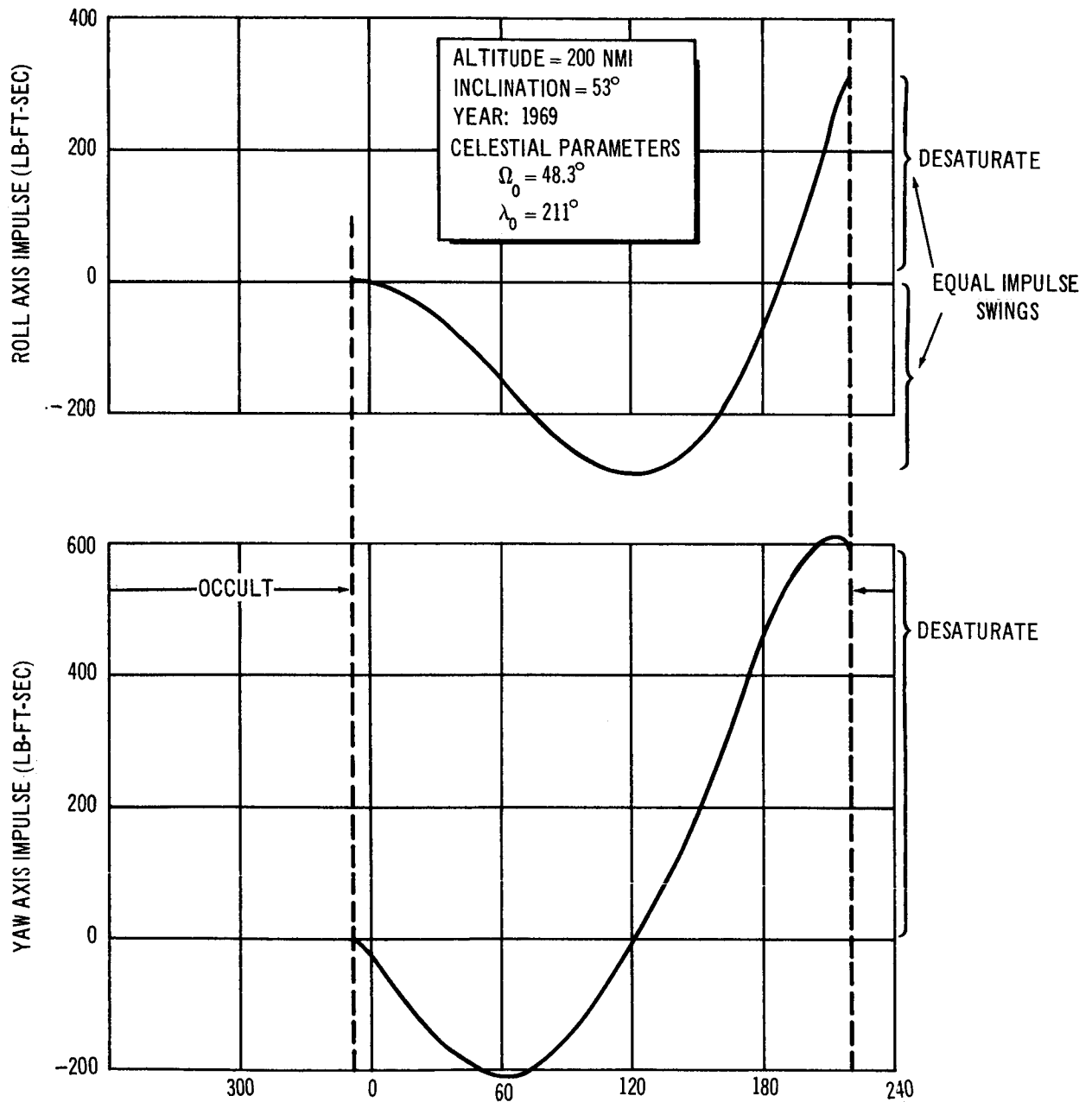


Figure A-9. Belly-Down Roll and Yaw Maximum Impulse (Desaturation at Occult,  $\phi = \phi_C$ )

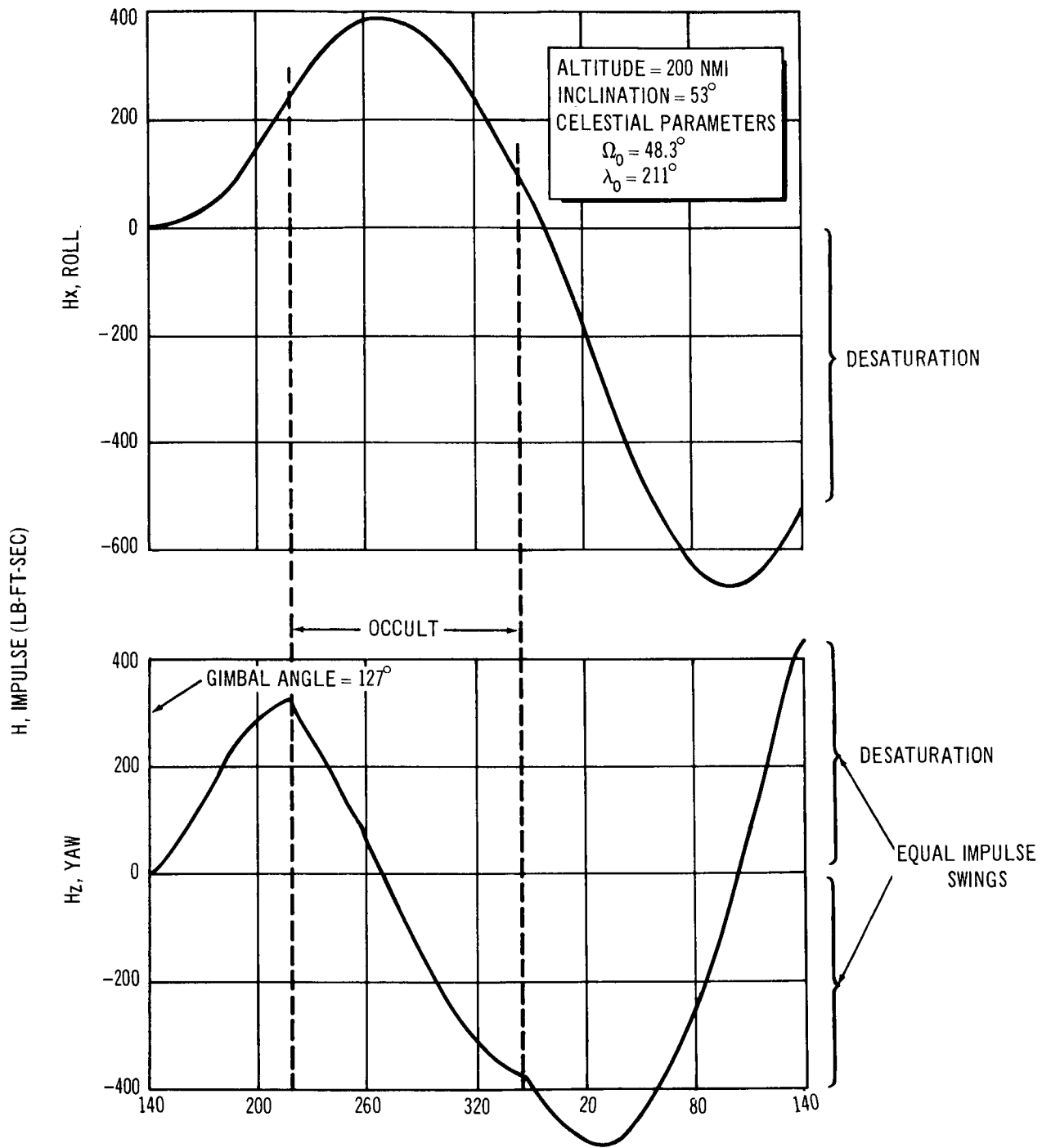


Figure A-10. Belly Down Roll and Yaw Maximum Impulse (Desaturation at  $\phi = 127^\circ$ )



of  $1/\sin 60^\circ \times 26.6/20(660 - 500) = 243$  lb-ft-sec is obtained. However, the roll axis impulse is increased, compared to that shown in Figure A-7, and it must be desaturated.

Table A-7 presents the propellant weight per month required for the desaturation impulse and a weight penalty associated with the momentum storage for the various schemes of desaturation. The propellant weight is based on the average accumulated impulse shown in Figure A-6 with a control lever arm of 8 ft and a propellant  $I_{sp}$  of 270 sec. Since the total impulse has not yet been defined for the pitch axis, a weight penalty is used for the momentum storage in lieu of an actual weight. The reference, or zero weight penalty of the momentum storage weight, is based on the desaturation scheme for  $\phi = 180^\circ$ . A negative weight penalty indicates a weight saving.

Table A-7  
DESATURATING PROPELLANT AND MOMENTUM  
STORAGE WEIGHT PENALTY

Desaturation Scheme	Roll Momentum Storage Penalty (lb)	Yaw Momentum Storage Penalty (lb)	Desaturation Propellant (lb/mo) (Roll and Yaw Only)
Desaturate when $H_x = 0$ ( $\phi = 180^\circ$ )	0	0	$0 + 95.5 = 95.5$
Desaturate at occultation	-6	-5	$45.3 + 84 = 129.0$
Desaturate at $\phi = 127^\circ$ $ +H_z  =  -H_z $	+16	-16	$73.5 + 61 = 134.5$

Table A-7 shows a small weight saving 23 lb, for the first scheme (desaturating at  $\phi = 180^\circ$  or when the roll axis impulse is zero) over the next best method (desaturating at occultation). Considering the lifetime of the space laboratory to be at least a year, a substantial savings in desaturation propellant, using the best desaturation scheme, is possible.

The scheme of desaturation when the roll axis impulse is zero, near  $\phi = 180^\circ$ , is not only the optimum in terms of propellant consumption, but it can be

easily mechanized. This would be mechanized from the pitch gimbal angle,  $\phi$ , of the solar panels and the gimbal deflection of the roll CMG. The condition of centrifuge operation during desaturation would also be integrated into the mechanization of the desaturation scheme.

#### Bias Body Moment of the Pitch Axis

The bias body moment about the pitch axis contains a gravity gradient torque along with an aerodynamic torque. The gravity gradient torque is caused by the fact that the roll axis, which is aligned with the orbital velocity vector, is not a principal body axis for the vehicle loading configuration when considered as a worst case. The bias aerodynamic moment is present because of the relative displacement between the center of pressure and the center of mass along the body yaw axis. These bias moments, which result from vehicle asymmetry, are obtained analytically and are summed with the output of the computer program to obtain the total impulse history. This bias moment for the pitch axis is given as follows:

$$M_y = - \frac{3gR_e^2}{(R_e+h)^3} (I_z - I_x) \frac{\sin 2\delta}{2} - C_m Q A_R L_R \quad (\text{A-30})$$

with

$$\tan 2\delta = \frac{2 I_{xz}}{I_z - I_x} \quad (\text{A-31})$$

where

$g$  = gravitation constant,  $32.2 \text{ ft/sec}^2$

$R_e$  = Earth radius in ft

$h$  = orbital altitude in ft

The parameters for the worst-case inertia distribution are as follows:

$$I_{xz} = 0.042 \times 10^6 \text{ slug-ft}^2$$

$$I_z = 0.77 \times 10^6 \text{ slug-ft}^2$$

$$I_x = 0.49 \times 10^6 \text{ slug-ft}^2$$

$$C_M = \text{moment coefficient} = 0.3$$

$$A_R = \text{reference area} = 368.6 \text{ ft}^2$$

$$L_R = \text{reference length} = 21.67 \text{ ft}$$

$$Q = \text{average dynamic pressure at 200 nmi} = 0.1 \times 10^{-4} \text{ lb/ft}^2$$

Figure 3-3 shows that this worst-case inertia distribution is obtained by rotating both Apollos at  $37.5^\circ$  (in opposite directions) so that they are along the  $\pm Y$  axis.

When Equation (A-30) is evaluated with the given parameters, a bias pitch moment of 0.18 lb-ft results. The total accumulated impulse per orbit with this bias moment is 990 lb-ft-sec. Figure A-11 is a time history of the pitch axis impulse, and indicates that the desaturation required for the pitch axis will be  $800 \times 1.12 = 900 \text{ lb-ft-sec/orbit}$ .

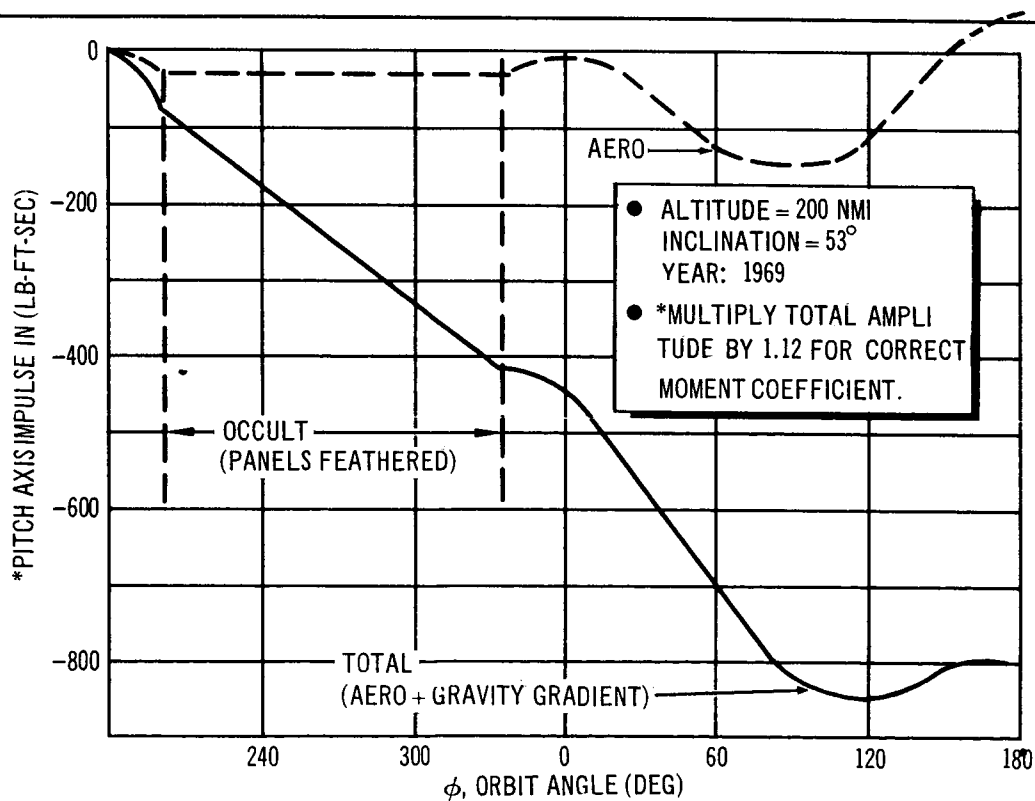


Figure A-11. Belly Down Pitch Body Axis Impulse

An average impulse desaturation is now obtained, with the aid of Figure A-6, as  $900 + 440 = 1,340$  lb-ft-sec/orbit. For a control lever arm of 8 ft and a propellant  $I_{sp}$  of 270 sec, the average desaturation propellant is 290 lb/month.

#### Use of Desaturation Impulse for Orbit Keeping

As noted previously, the average orbit-keeping propellant with feathered solar panels during occultation is 261 lb/month. By using one aft firing pitch jet and one yaw jet, more than the required orbit-keeping velocity could be gained during desaturation. Since orbit keeping requires two equal-velocity increments spaced  $180^\circ$  apart in the orbit, the desaturation would have to be accomplished in the same manner. For the yaw axis desaturation to provide orbit keeping, two equal impulses would be required at  $\phi = 0^\circ$  and  $\phi = 180^\circ$ . (At these two points the roll axis impulse is zero.)

The two equal desaturation impulses,  $180^\circ$  apart, for the pitch axis could be applied anywhere throughout the orbit. Since the two positions,  $\phi = 0^\circ$  and  $\phi = 180^\circ$ , give a minimum solar panel impingement from thruster firing, the desaturation positions for the pitch axis will be made the same as those for the yaw axis.

For equal desaturation impulses at the two prescribed positions in orbit, some previous knowledge of the total amount of the accumulated impulse is required. For the yaw axis, this information can be obtained by completely desaturating the yaw axis at  $\phi = 180^\circ$  and completing an orbit. The yaw axis impulse history will be similar to that shown in Figure A-7. On completion of the orbit,  $\phi = 180^\circ$ , the total accumulated yaw impulse is obtained from the gimbal angle of the control moment gyros. Another way of determining the yaw axis accumulated impulse is from the yaw gimbal angle of the solar panels,  $\delta$ . The yaw axis accumulated impulse from the solar panels is dependent on the  $\delta$  gimbal angle of the solar panels. Figure A-12 is a plot of the yaw axis desaturation impulse for various  $\delta$  gimbal angles. These data were obtained from the computer program.

For equal desaturation impulses of the pitch axis, the momentum storage device (CMG) must be set at one of its maximum gimbal deflections for pitch

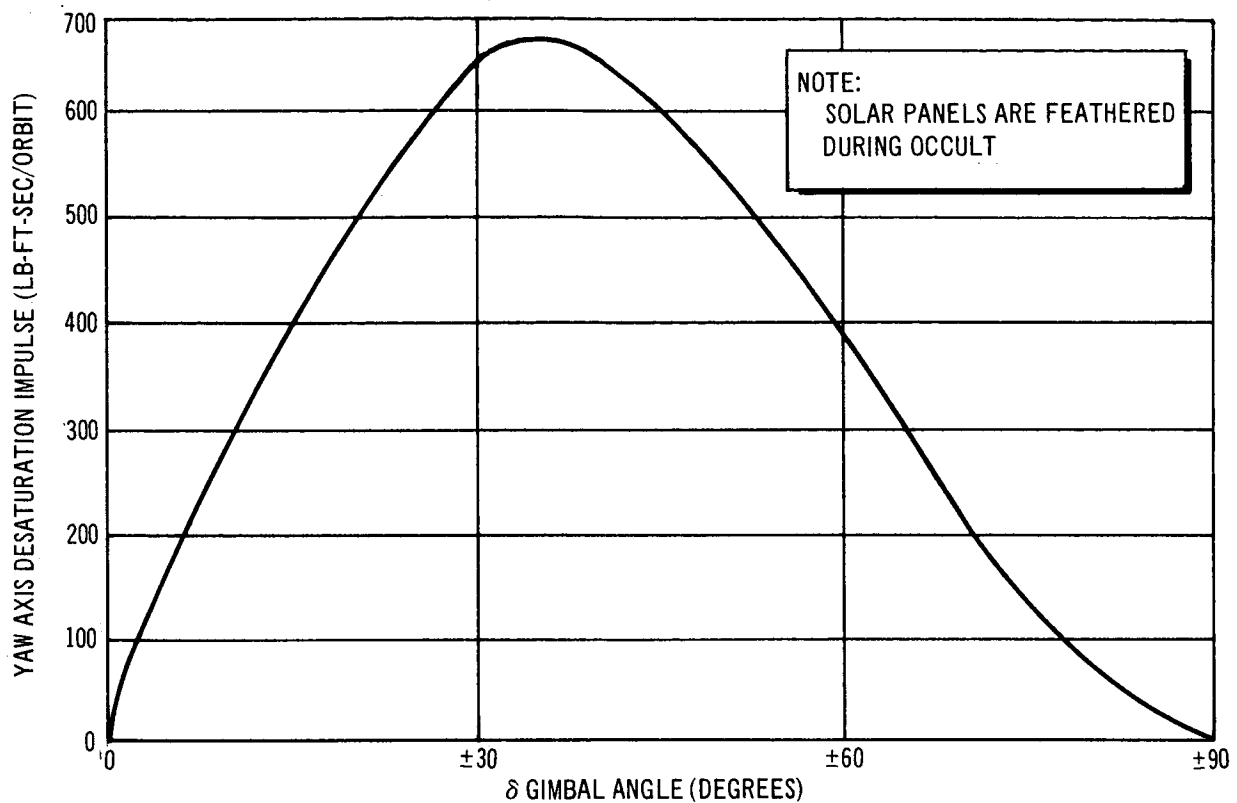


Figure A-12. Belly-Down Yaw Axis Desaturation Impulse as a Function of  $\delta$  Gimbal Angle

impulse storage at  $\phi = 180^\circ$ . (The direction of deflection is easily determined from the asymmetry of the vehicle.) After half an orbit has been traversed, approximately half the accumulated impulse can be obtained from the gimbal deflection of the momentum storage device. From Equation(A-30) and Figure A-11, it is noted that approximately 90% of the total pitch axis accumulated impulse is from the constant gravity gradient torque. Hence, if the asymmetry of the vehicle is known, nearly equal desaturation impulses of the pitch axis can be obtained.

Table A-8 presents the propellant requirements with and without use of the desaturation impulse for orbit keeping.

Table A-8  
 PROPELLANT COMPARISON UTILIZING  
 DESATURATION FOR ORBIT KEEPING

	Total Desaturation Propellant (lb/mo)	Orbit Keeping (lb/mo)	Total Propellant (lb/mo)
Without desaturation impulse for orbit keeping	290	261	551
With desaturation impulse for orbit keeping	290	261	290

Table A-8 indicates a propellant saving of 261 lb/month by using the desaturation impulse for orbit keeping, and by using all the desaturation impulse for orbit keeping, an extra 29 lb/month is available. In effect, this may be used to increase the orbital altitude of the space laboratory. Over a period of a year, the total excess linear impulse would be

$$29 \text{ (lb/mo)} \times 12 \text{ (mo/yr)} \times 270 \text{ sec} = 94,000 \text{ lb-sec/yr}$$

With half of this linear impulse for the altitude change and the other half for circularizing the orbit, a total velocity added at perigee, 200 nmi, is obtained over a period of one year as follows:

$$\Delta V_p = \frac{94,000 \text{ (lb-sec)}}{2 \times 2,800 \text{ (slugs)}} = 16.8 \text{ ft/sec} \quad (\text{A-32})$$

where 2,800 slugs is the mass of the laboratory.

The orbital velocity for a 200-nmi circular orbit is about 25,230 ft/sec. With the added velocity increment, the increase in orbital altitude over a period of one year is approximately 10 nmi.

Figure A-13 is a plot of the desaturation propellant with orbit-keeping capability required, in lb/month, for the period of 1969 to 1974 at an orbital altitude of 200 nmi. The lower curve on the plot is the required impulse for drag. For the year 1973 or 1974, the drag impulse is noted to be only 10% of the impulse required for desaturation. This curve shows that after 1969

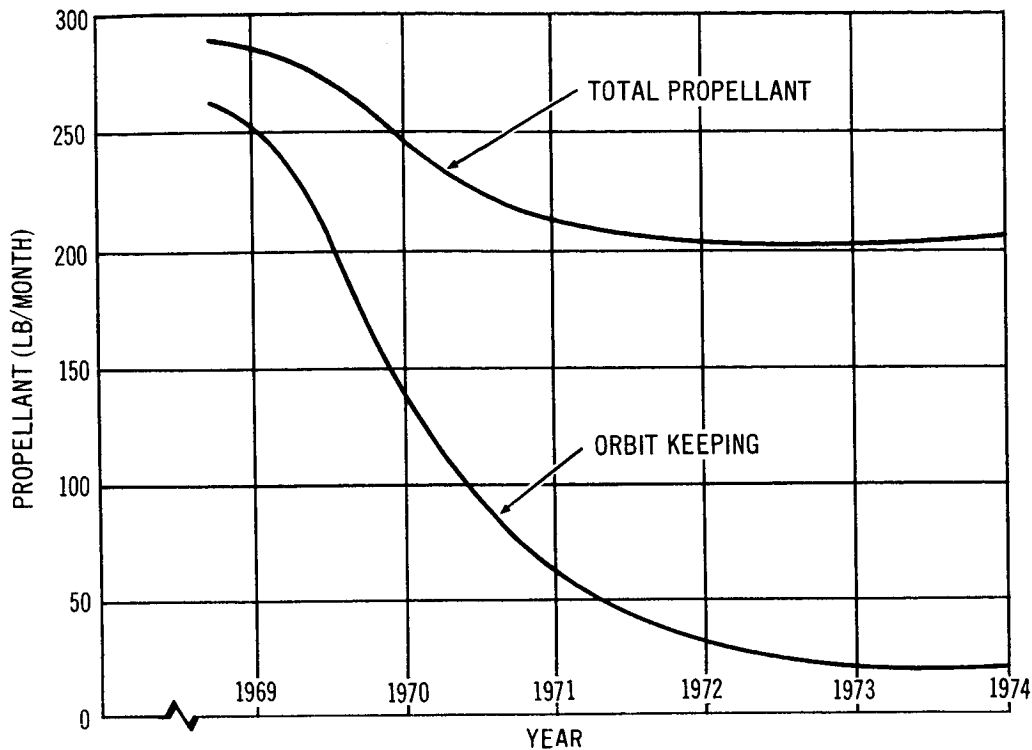


Figure A-13. Propellant Requirement for Belly Down with Solar Panels (Desaturation Propellant is Used for Orbit Keeping)

not all of the desaturation propellant is required for orbit keeping. After the year 1969, desaturation will have to be accomplished by jet thrusting in couples along with single jet thrusting to provide desaturation and orbit keeping. The period and amount of single jet thrusting which provides the orbit-keeping capability with desaturation can be determined by ground tracking stations.

Figure A-14 is a plot of the orbit-keeping propellant for the years 1969 and 1971 as a function of orbital altitude. This illustrates the high propellant consumption for the lower altitudes.

With the use of equal pitch and equal yaw desaturation impulses positioned at  $\phi = 0^\circ$  and  $\phi = 180^\circ$ , the resulting pitch and yaw impulse history is presented in Figure A-15. The yaw impulse history is for the maximum moment shown in Figure A-2. This first portion of the yaw impulse history between  $\phi = 180^\circ$  and  $\phi = 0^\circ$  was obtained by subtracting  $330 \cos \phi$  (lb-ft-sec) from Figure A-7. The pitch axis impulse history was obtained in a similar manner.

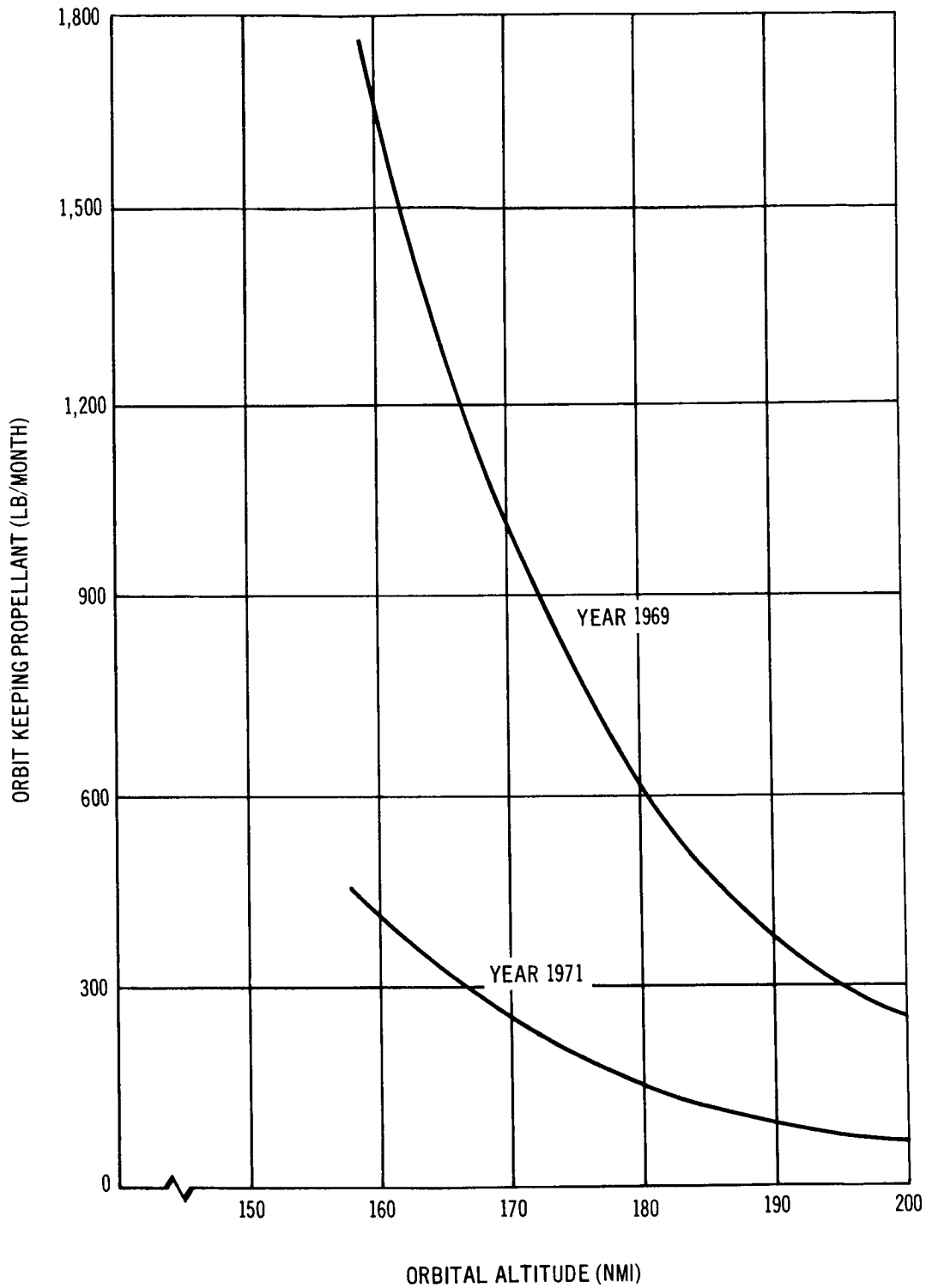
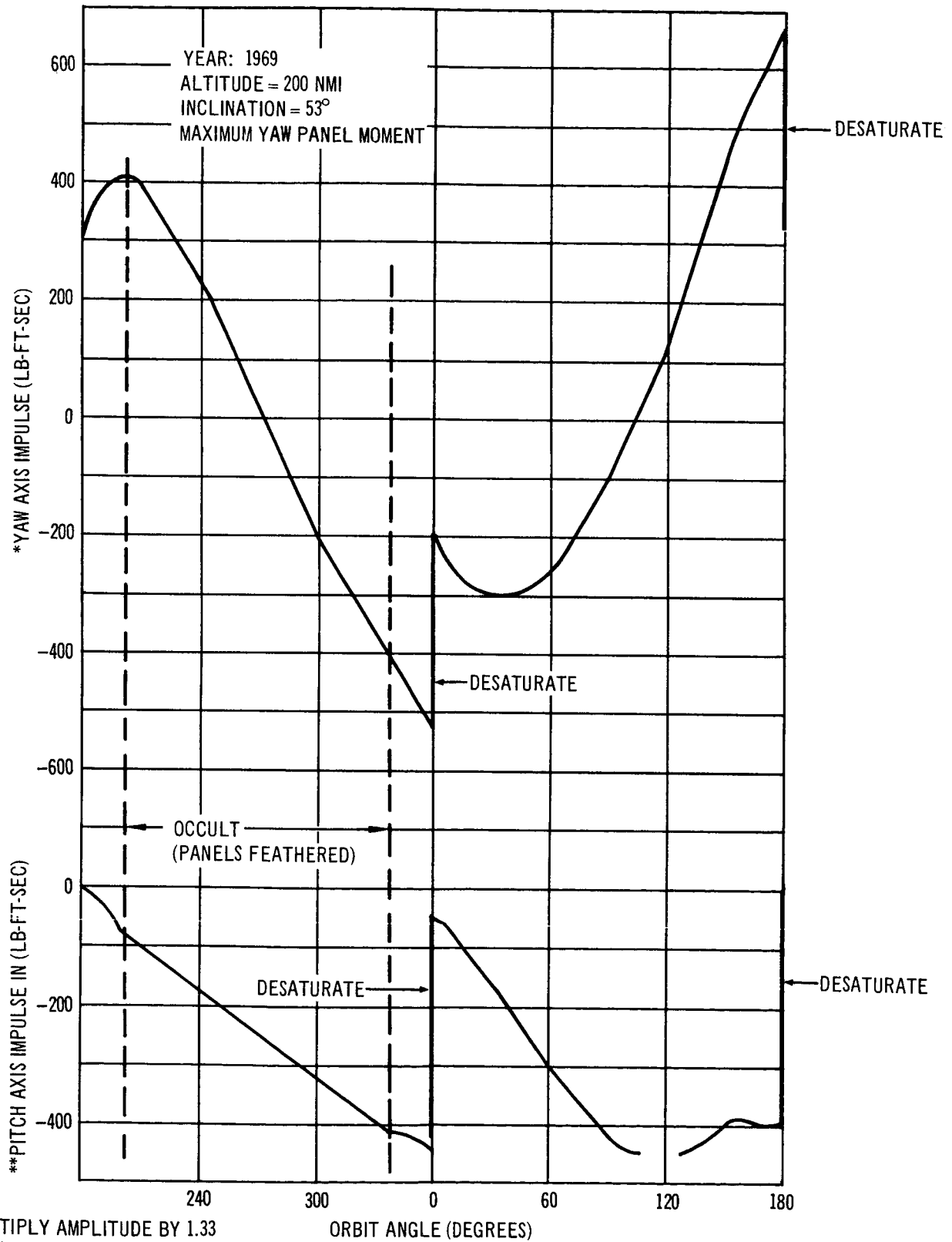


Figure A-14. Orbit-Keeping Propellant for Belly-Down Orientation with Solar Panels as a Function of Orbital Altitude





\*MULTIPLY AMPLITUDE BY 1.33  
 \*\*MULTIPLY AMPLITUDE BY 1.12

Figure A-15. Belly-Down Pitch and Yaw Maximum Impulse

Figure A-7 and the yaw axis impulse in Figure A-15 were obtained from computer runs which were based on an aerodynamic lever arm of 20 ft. Since the actual lever arm is 26.6 ft, the amplitudes of these impulse histories must be multiplied by the ratio of 26.6/20. The yaw axis momentum storage requirement for the belly-down orientation is obtained from Figure A-15 at  $\phi = 180^\circ$  as  $26.6/20 \times 660 = 880$  lb-ft-sec. This is within 10% of the minimum value, since the negative yaw impulse peak is a little smaller than the positive peak.

The pitch axis momentum storage requirement, obtained from Figure A-15, is  $1.12 \times 450/2 = 250$  lb-ft-sec.

If a set of double-gimbal control moment gyros is to be used for both the pitch and yaw axes, the total impulse requirement is then  $(880^2 + 220^2)^{1/2} = 910$  lb-ft-sec. The Phase IIa baseline momentum storage capacity for both the pitch and yaw axes is 950 lb-ft-sec.

Figure A-16 is the roll axis impulse history for the desaturation procedure shown in Figure A-15. The first portion of the roll axis impulse in Figure A-16 between  $\phi = 180^\circ$  and  $\phi = 0^\circ$  is obtained by subtracting  $330 \times \sin \phi$  from the roll axis impulse shown in Figure A-7. Again, the roll axis impulse must be multiplied by the ratio 26.6/20. The roll axis momentum storage requirement for the belly-down orientation is obtained as  $(26.6/20 \times 440) + 2,940$  (centrifuge) = 3,530 lb-ft-sec.

The Phase IIa baseline momentum storage capacity for the roll axis was 3,120 lb-ft-sec. The baseline requirement could be retained, which would limit the centrifuge operation to 29% of the orbit period for the maximum aerodynamic moment case shown in Figure A-16. The average time for the centrifuge operation over an orbit with the baseline system would be 61 min. (92-min. orbit period).

Figure A-17 is a plot of the momentum storage weight from the period of 1969 to 1974. The roll axis impulse is obtained with a pair of single-gimbal control moment gyros (SG CMG), while the pitch and yaw axes impulse is obtained with a pair of double-gimbal CMG. The weights of the CMG are obtained from Figure 4-9. The maximum gimbal angles of the CMG are  $60^\circ$ .

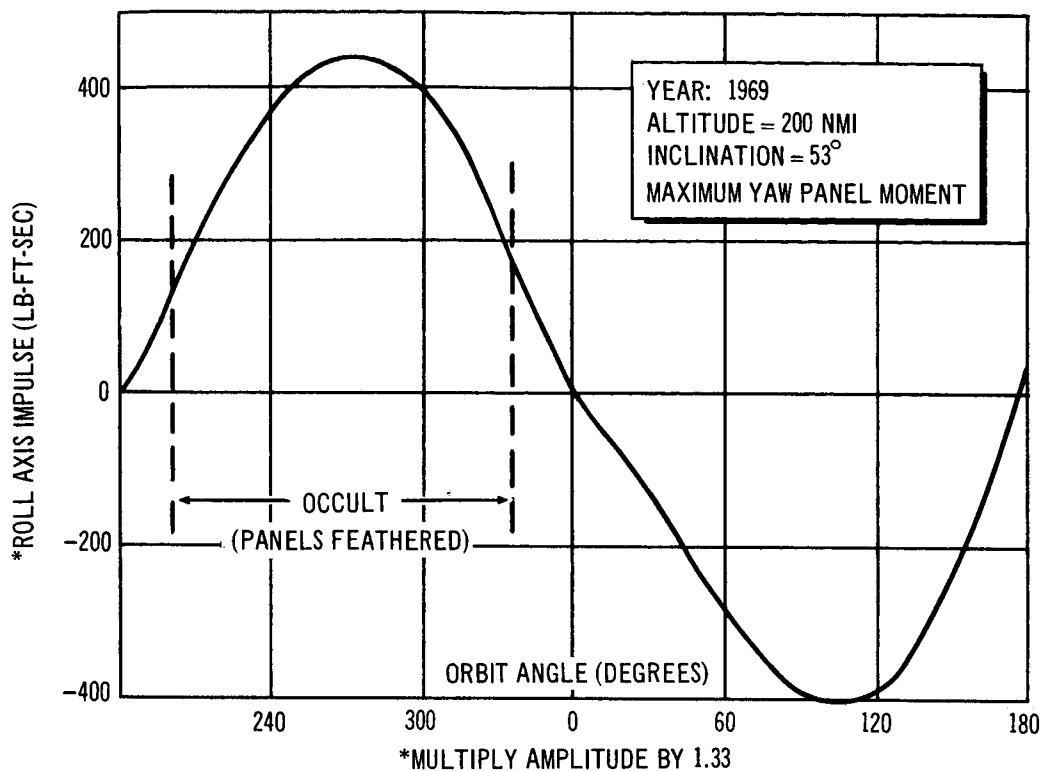


Figure A-16. Belly-Down Roll Axis Impulse

In conclusion, the following operational procedures and requirements are listed for the belly-down orientation with solar panels.

1. The solar panels are feathered during occultation.
2. The desaturation impulse is used for orbit keeping.
3. Equal amplitudes of desaturation impulse for both the pitch and yaw axes will take place when the roll axis impulse is zero. This is at the positions of  $\phi = 0^\circ$  and  $\phi = 180^\circ$ .
4. The average propellant consumption for the year 1969 will be 290 lb/month.
5. The roll axis momentum storage requirement is 3,530 lb-ft-sec for the year 1969.
6. The yaw axis momentum storage requirement is 880 lb-ft-sec for the year 1969.
7. The pitch axis momentum storage requirement is 250 lb-ft-sec (which is independent of the year).
8. The combined pitch and yaw momentum storage requirement is 910 lb-ft-sec.

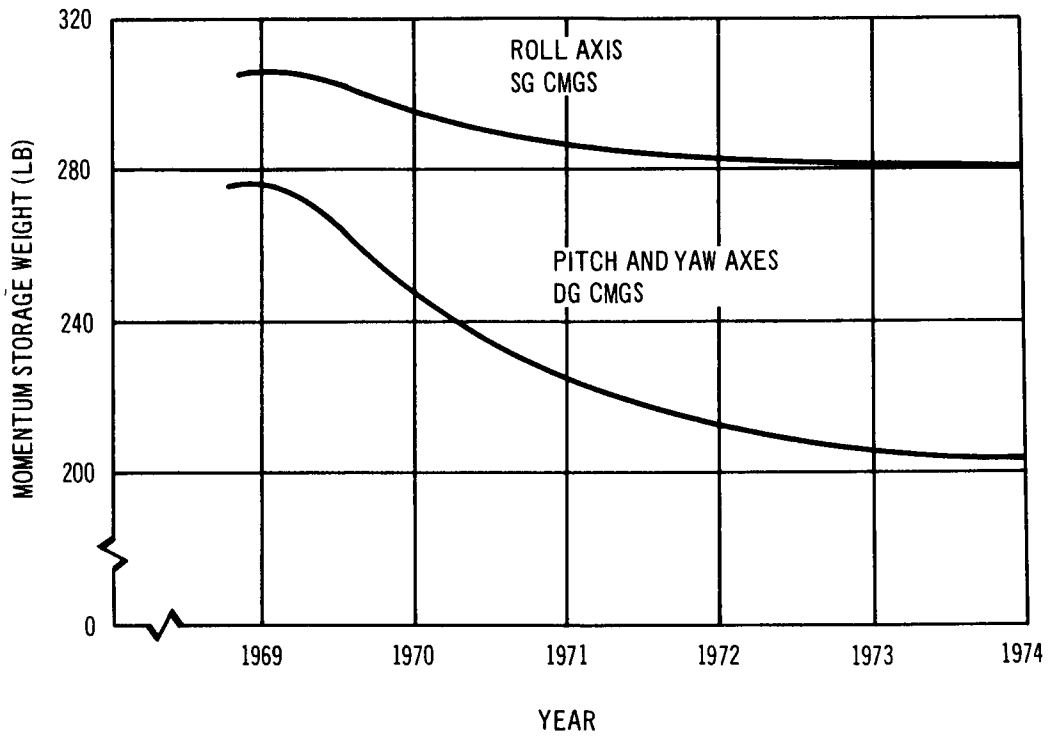


Figure A-17. Belly-Down Momentum Storage Weight as a Function of Year

### A. 1.2.2 Inertial Orientation with Solar Panels

The impulse history for the inertial orientation with solar panels was obtained from the computer program for the roll solar orientation. With the program, a maximum impulse requirement of the vehicle axis is determined at a certain time of the year and at a certain time in the orbital regression cycle. At this point the vehicle is rotated an angle,  $\eta$ , about the roll axis to bring the yaw axis out of the orbit plane. By incrementing the roll angle,  $\eta$ , a maximum impulse requirement for the vehicle axis is obtained. For the conditions examined, the maximum requirement was obtained with a negative roll angle of  $15^\circ$ .

Figure A-18 illustrates the roll and pitch axes impulse history for the inertial orientation. Since the inertial orientation is used for short time durations, no requirement is made to desaturate at equal increments spaced  $180^\circ$  apart in the orbit. Hence, the roll and pitch axes momentum storage obtained from Figure A-18 are 90 lb-ft-sec and 335 lb-ft-sec, respectively.

The portion of the pitch axis impulse between  $\phi = 340^\circ$  and  $\phi = 360^\circ$  is plotted on the left of the ordinate to obtain the correct momentum storage capacity.

Figure A-19 shows the yaw axis impulse history for the inertial orientation. The momentum storage requirement for the yaw axis is 620 lb-ft-sec. If the momentum storage requirements for the pitch and yaw axes are to be met with one set of two CMG, the total momentum storage is  $(235^2 + 620^2)^{1/2} = 660$  lb-ft-sec. The momentum storage requirements are higher for the belly-down orientation than the inertial orientation.

### A. 1.2.3 Belly-Down Orientation with Brayton Cycle Power Supply

The only momentum storage requirement for the belly-down orientation without solar panels, other than the centrifuge, is for the pitch axis. This storage requirement results from the vehicle asymmetry about the pitch axis. The impulse requirement is obtained analytically by the use of Equation (A-30). All the parameters given under Equation (A-30) are the same except for the body axis inertias and the product of inertia and the moment coefficient,

YEAR: 1969 ALTITUDE = 200 NMI INCLINATION = 53°	CELESTIAL PARAMETERS $\Omega_0 = -199^\circ$ $\lambda_0 = -244^\circ$ $\eta = 15^\circ$
---	--

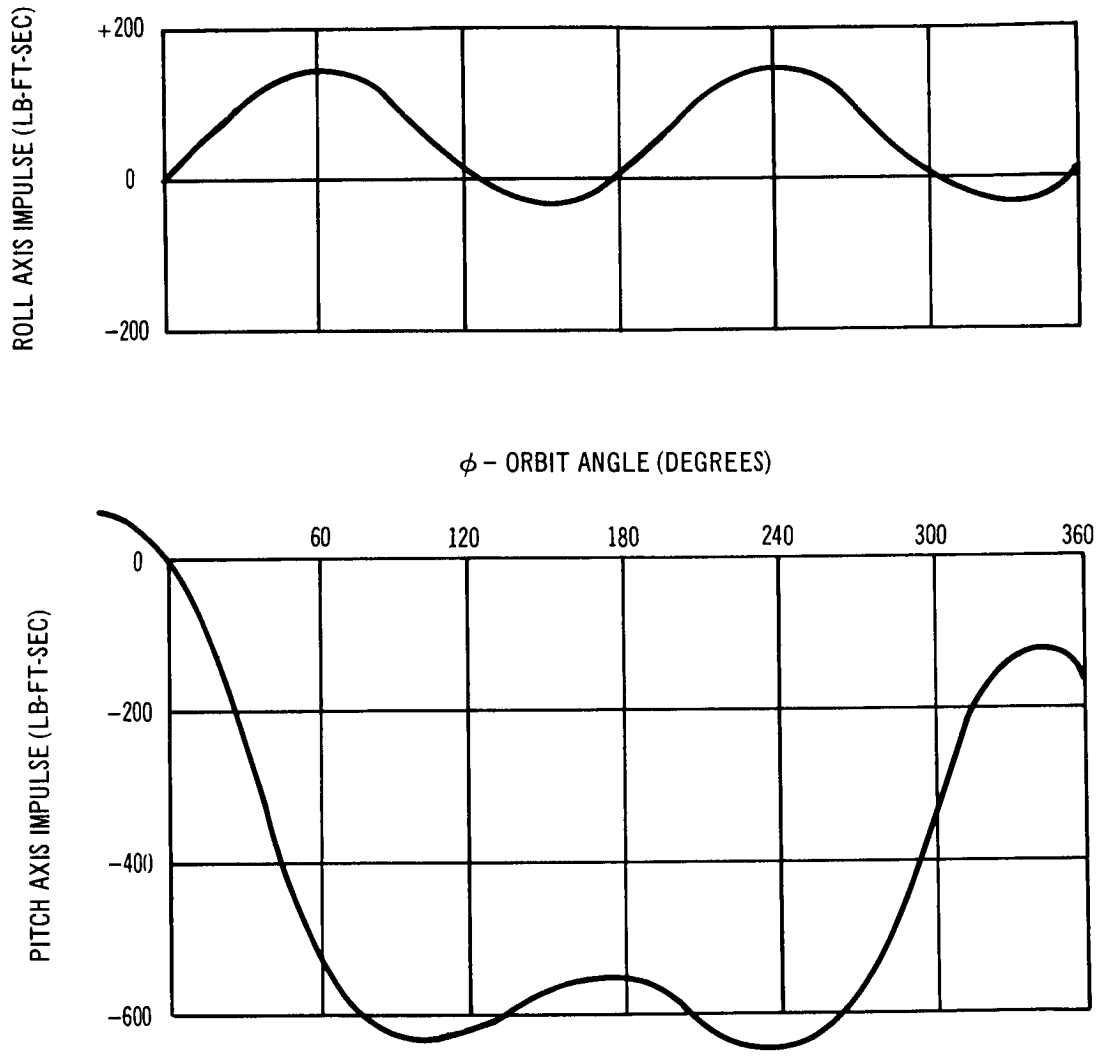


Figure A-18. Inertial Orientation Roll and Pitch Axes Impulse

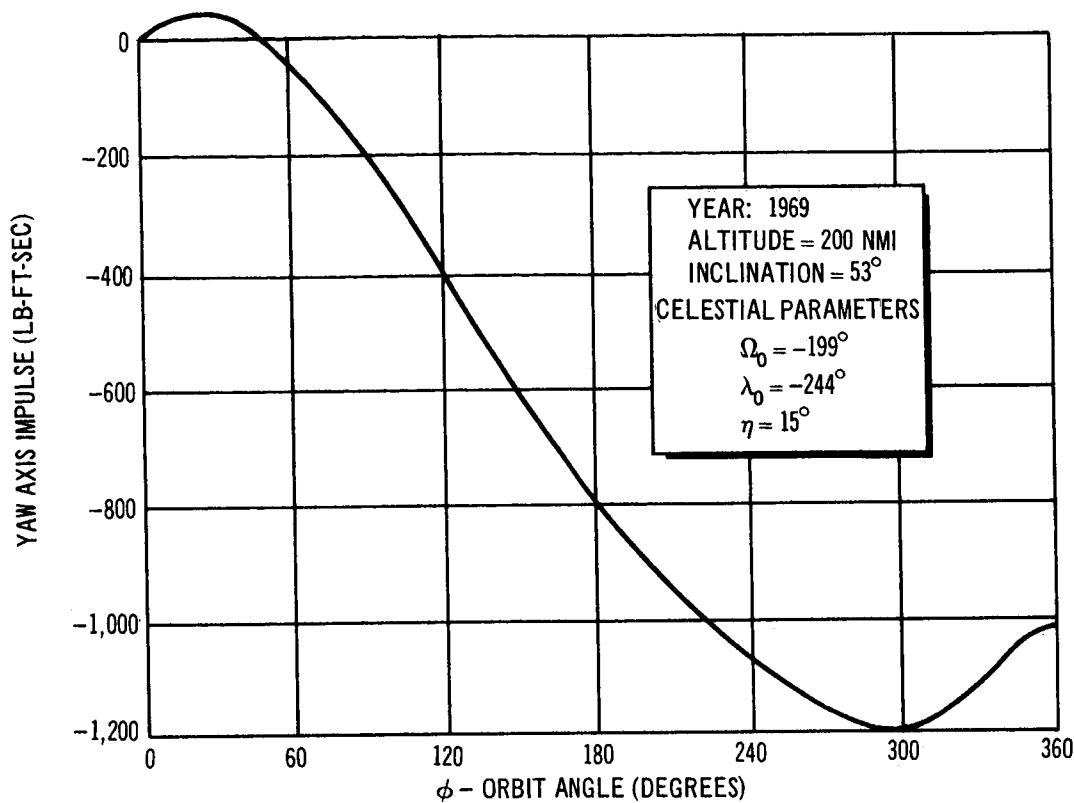


Figure A-19. Inertial Orientation Yaw Axis Impulse

$C_m$ . These values of body axis inertias are for Configuration X, shown in Figure 3-3.

$$I_{xz}, \text{ POI} = 0.035 \times 10^6 \text{ slug-ft}^2$$

$$I_{\text{pitch}}, \text{ MOI} = 0.8 \times 10^6 \text{ slug-ft}^2$$

$$I_{\text{roll}}, \text{ MOI} = 0.5 \times 10^6 \text{ slug-ft}^2$$

$$I_{\text{yaw}}, \text{ MOI} = 0.67 \times 10^6 \text{ slug-ft}^2$$

$$C_m = 0.13$$

The constant pitch axis moment is obtained from Equation (A-30) as

$$M_{\text{pitch}} = 0.15 \text{ lb-ft.}$$

The total accumulated impulse per orbit with this bias moment is 820 lb-ft-sec for the pitch axis. Figure A-20 shows the pitch axis impulse for the

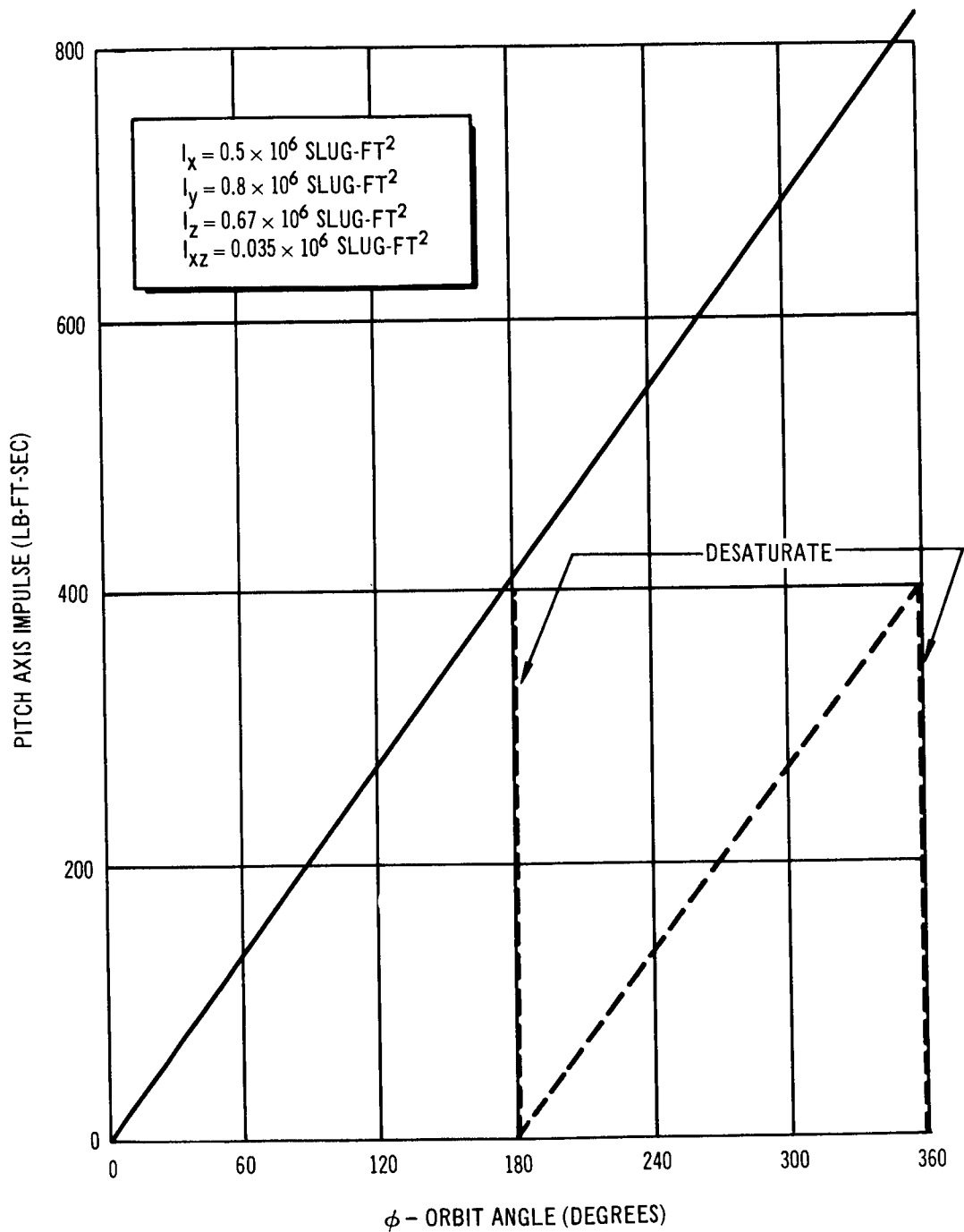


Figure A-20. Belly-Down Pitch Axis Impulse with Brayton Cycle Power Supply



belly-down orientation without solar panels. The solid line shows the impulse history without desaturation. The dashed lines show the impulse history for equal desaturation impulse spaced  $180^\circ$  apart in orbit. The particular desaturation method shown in Figure A-20 permits gimbaling the momentum storage device from a maximum deflection in one direction to a maximum deflection in the opposite direction. The approximate amount of desaturation impulse required at  $\phi = 180^\circ$  and  $\phi = 360^\circ$  can be obtained with known vehicle body axes of inertia and products of inertia.

The momentum storage requirements for the belly-down orientation are:

pitch axis	240 lb-ft-sec (includes 20% contingency factor)
roll axis	2,940 lb-ft-sec

It is noted that the momentum storage requirements for the belly-down orientation without solar panels are independent of the year. The desaturation propellant requirements for orbit keeping for the belly-down orientation will be practically independent of the year. Figure A-21 shows the total propellant requirement and the amount of desaturation propellant required for orbit keeping as a function of year for the belly-down orientation without solar panels.

#### A. 1. 2. 4 Inertial Orientation with Brayton Cycle Power Supply

The impulse requirement for the inertial orientation without solar panels are computed analytically. Without the solar panels the maximum gravity gradient moment is 2.5 times the maximum aerodynamic moment for the year 1969. Hence, for worst-case computation, an orientation was chosen to maximize the gravity gradient moments without regard to maximizing the aerodynamic moments. This orientation places the pitch axis in the orbit plane parallel with the orbital line of nodes with the roll and yaw axes inclined  $45^\circ$  to the orbit plane. Since the largest difference of body axis inertias is between the roll and yaw axes, a maximum bias gravity gradient torque is obtained about the pitch axis.

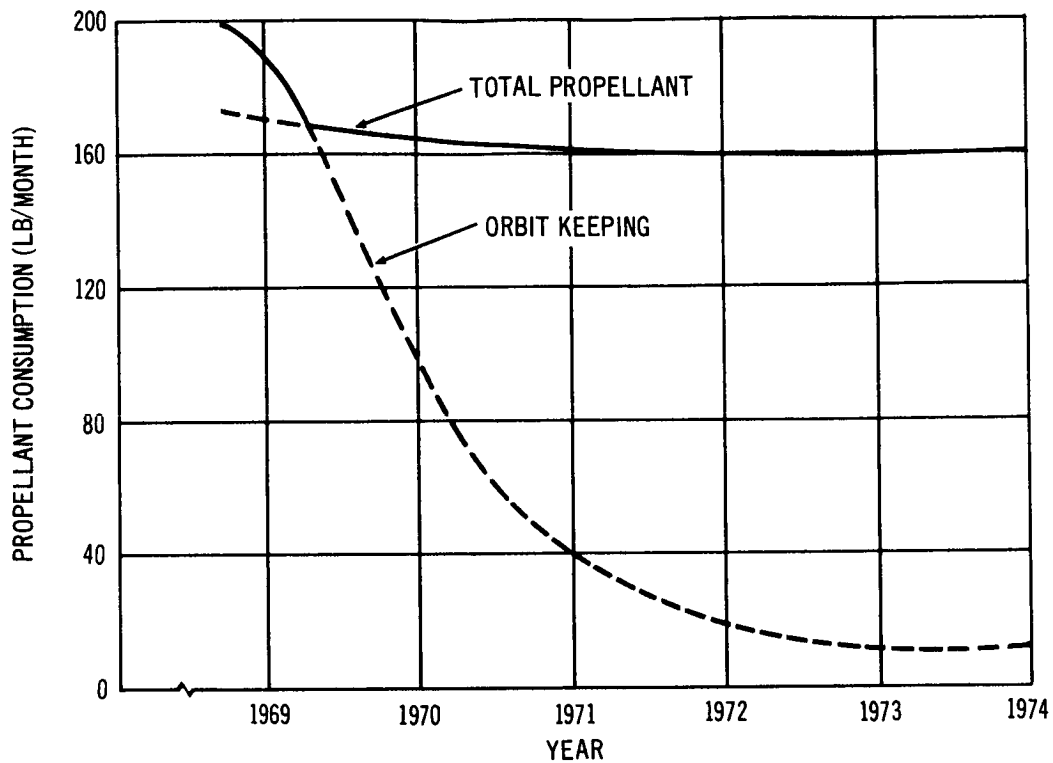


Figure A-21. Belly-Down Propellant Requirement with Brayton Cycle Power Supply

The gravity gradient torque expressions are given by the following equations:

$$M_{\text{pitch}} = \frac{3gR_e^2}{(R_e + h)^3} (I_{\text{yaw}} - I_{\text{roll}}) \left( \frac{1 - \cos 2\phi}{4} \right) \quad (\text{A-33})$$

$$M_{\text{roll}} = \frac{3gR_e^2}{(R_e + h)^3} (I_{\text{pitch}} - I_{\text{yaw}}) \times 0.707 \frac{\sin 2\phi}{2} \quad (\text{A-34})$$

$$M_{\text{yaw}} = \frac{3gR_e^2}{(R_e + h)^3} (I_{\text{roll}} - I_{\text{pitch}}) \times 0.707 \frac{\sin 2\phi}{2} \quad (\text{A-35})$$

where  $\phi$  is the orbit angle measured from the line of nodes and the other parameters are the same as previously described.

The aerodynamic moments are given by the following equations:

$$M'_{\text{pitch}} = 0.707 Q A_R L_R C_M (\alpha) \cos \phi \quad (\text{A-36})$$

$$M'_{\text{yaw}} = -Q A_R L_R C_M (\alpha) \sin \phi \quad (\text{A-37})$$

where  $Q$ ,  $A_R$ , and  $L_R$  are the same as previously defined.

The angle of attack,  $\alpha$ , is computed throughout the orbit. With this, the moment coefficient,  $C_M (\alpha)$ , is obtained throughout the orbit. The aerodynamic moments are then computed throughout the orbit and summed with the gravity gradient moments. These aerodynamic moments are based upon a constant density atmosphere.

Figure A-22 is a plot of the impulse history for the inertial orientation without solar panels. With desaturation accomplished at only one position in orbit, the body axis impulses are given by the following:

Pitch axis momentum storage--900 lb-ft-sec

Roll axis moment storage--2,940 + 90 = 3,030 lb-ft-sec

Yaw axis momentum storage--125 lb-ft-sec

Again, if a set of double-gimbal control moment gyros is used for both the pitch and yaw axes, the total impulse requirement is  $(900^2 + 125^2)^{1/2}$   
= 910 lb-ft-sec.

For the laboratory without solar panels, the inertial orientation imposes the largest momentum storage and propellant requirements. Figure A-23 is a plot of the momentum storage weight as a function of years for the inertial orientation without solar panels. The roll axis requirement is obtained with a pair of single-gimbal CMG while the pitch and yaw axes requirement is obtained with a pair of double-gimbal CMG. The maximum gimbal angles of the gyros used are  $\pm 60^\circ$ .

Figure A-24 is a plot of the maximum desaturation and orbit-keeping propellant requirements, as a function of years, for the inertial orientation without solar panels. The attitude control or desaturation propellant is nearly

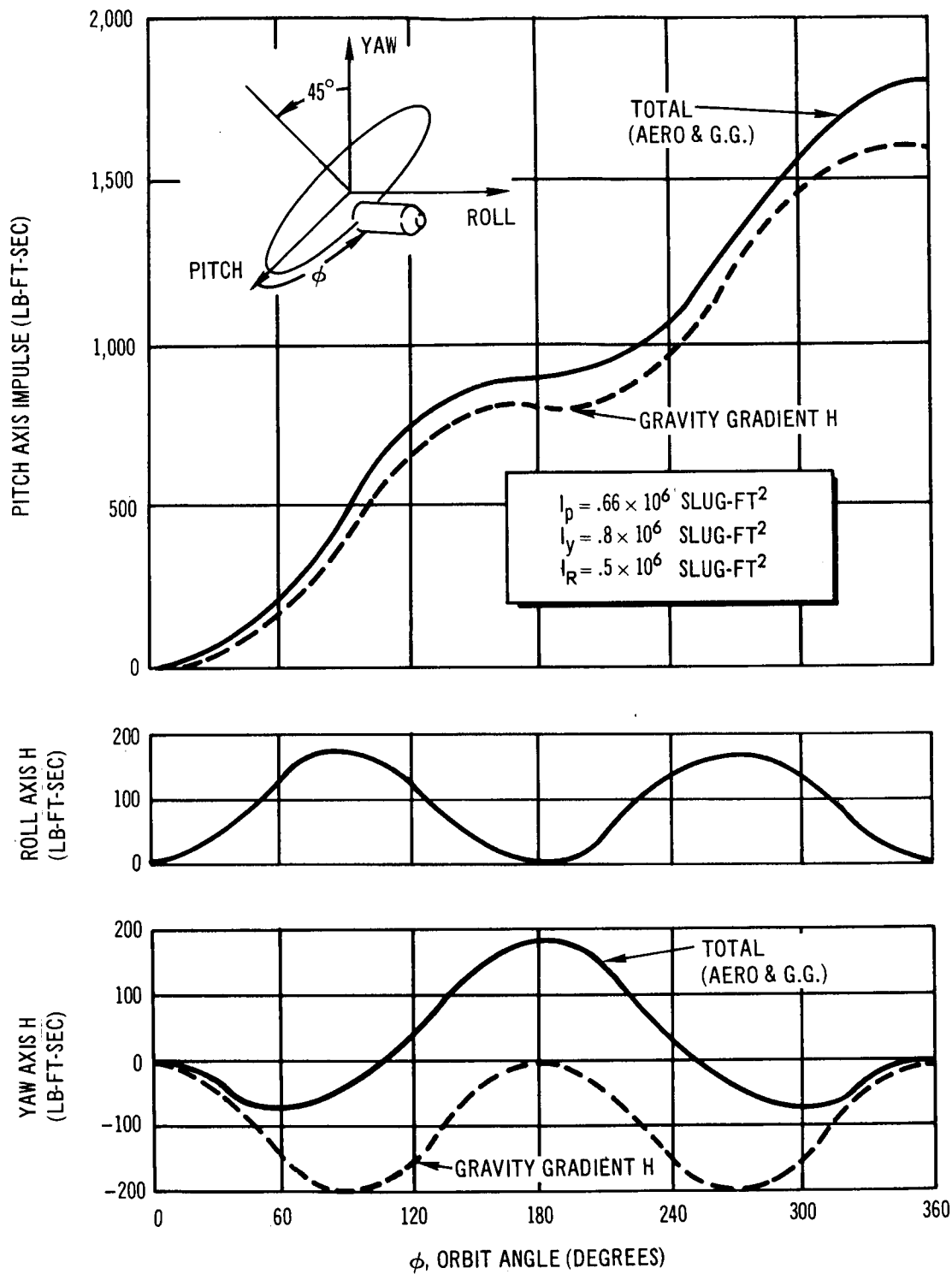


Figure A-22. Inertial Orientation Impulse with Brayton Cycle Power Supply

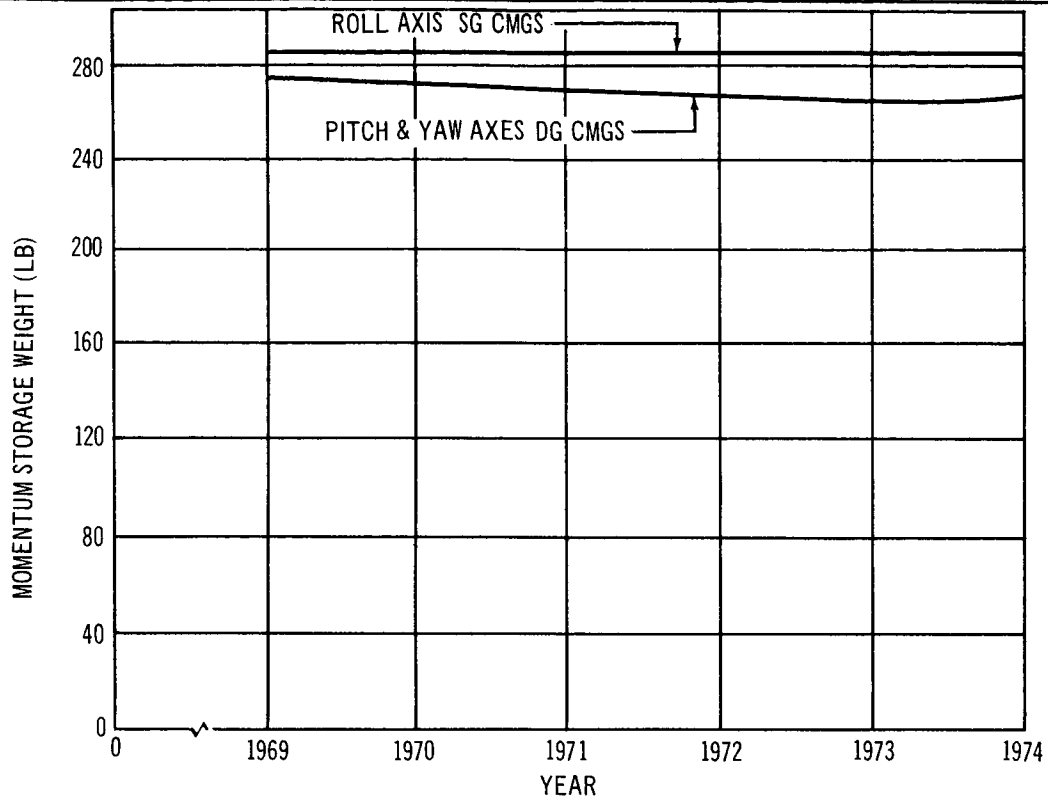


Figure A-23. Inertial Orientation Momentum Storage Weight with Brayton Cycle Power Supply

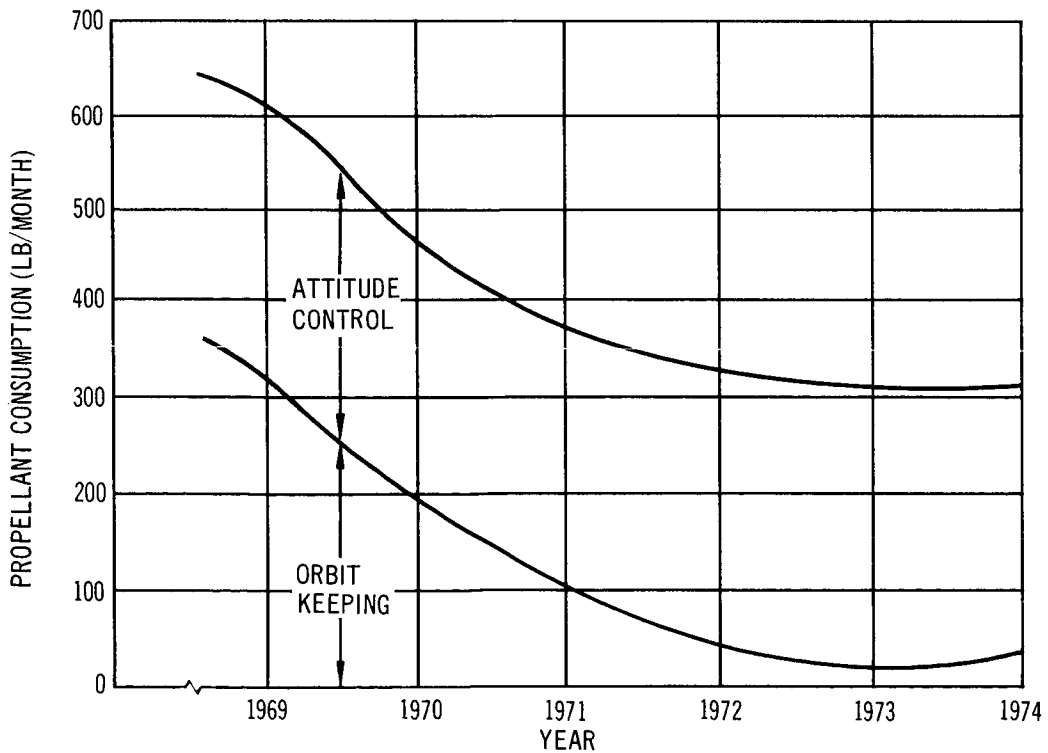


Figure A-24. Maximum Propellant Requirements for Inertial Orientation with Brayton Cycle Power Supply

independent of the year, since the aerodynamic portion of the impulse is small compared to the gravity gradient portion. The orbit-keeping requirement for the short-term inertial orientation will be accomplished while in the belly-down orientation.

Although much of the data presented in this section has been for one particular vehicle configuration, the SCS requirements for other vehicle configurations may be determined by ratioing body inertias and aerodynamic moments and drag coefficients. Also, there is sufficient data presented to determine the SCS requirements for orbital altitudes between 160 and 200 nmi throughout maximum and minimum solar activity.

## A.2 GYROCOMPASS STUDY

This section presents the analysis and results of the horizon sensor gyrocompass study.

### A.2.1 Introduction

The analysis of the study shows that the MORL vehicle can be attitude-stabilized within  $\pm 0.5^\circ$  with control moment gyros which use the horizon sensor gyrocompass technique. This capability meets the requirement of SCS performance in the presence of the anticipated disturbances.

During the long-term belly-down orientation, the course attitude information is provided by the gyrocompass technique. Basically, this technique aligns the roll (or X) axis of the space laboratory with the orbital velocity vector and aligns the yaw (or Z) axis with the Earth's center. Figure A-25 shows the body axes definition for the belly-down orientation. The four lines from the front of the laboratory to the Earth simulate horizon sensor beams. The horizon sensor provides the attitude information about two normal axes (the roll attitude,  $\phi$ , and the pitch attitude,  $\theta$ ). The heading, or yaw attitude,  $\psi$ , is derived by the gyrocompass technique. This technique consists of measuring a component of the orbital rate on the roll (or X) axis which will exist for a yaw attitude error. The derived yaw attitude error,  $\psi_m$ , for small angles is obtained by dividing the measured roll rate by the orbital

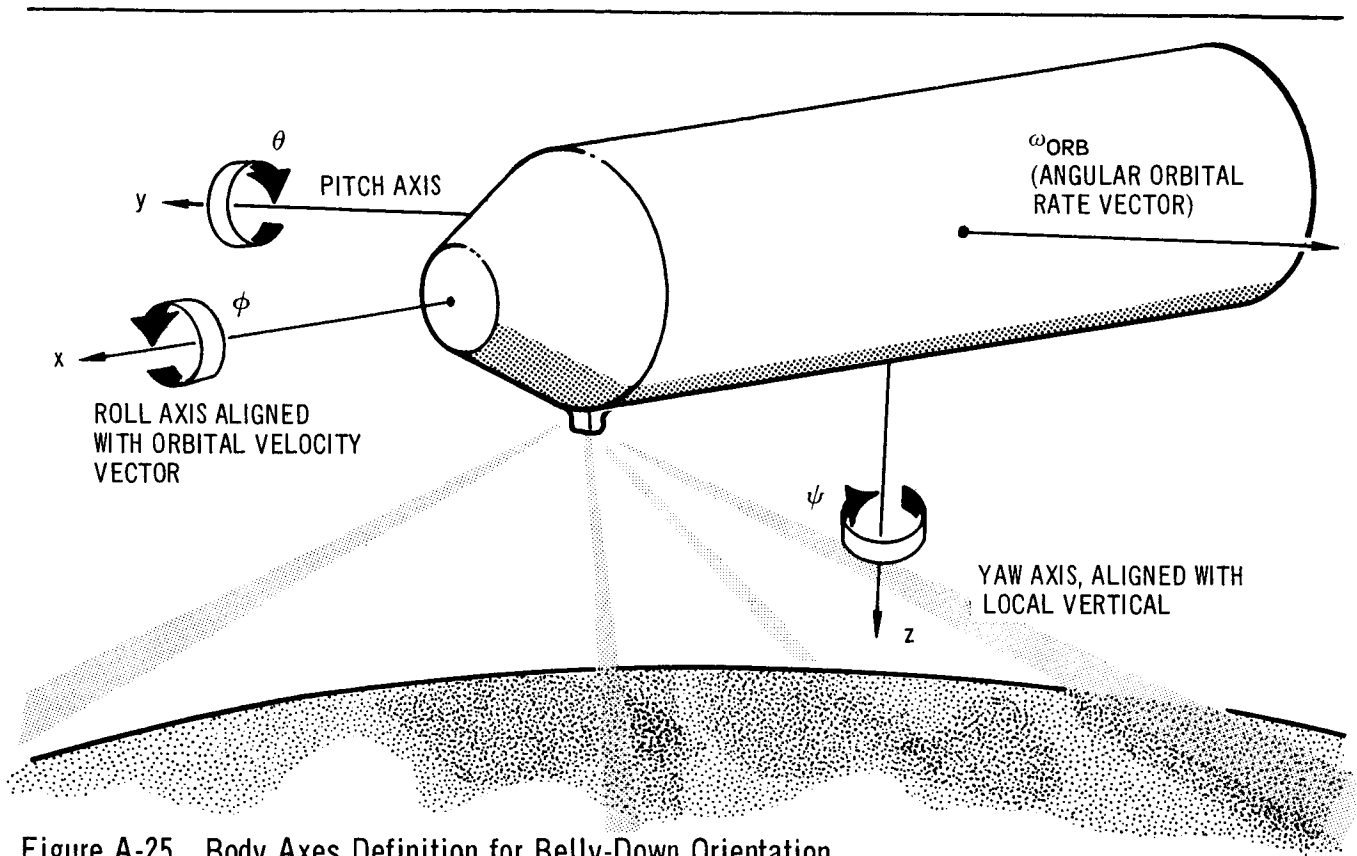


Figure A-25. Body Axes Definition for Belly-Down Orientation

rate. If body roll rate is present, then the derived yaw attitude error,  $\psi_m$ , will be incorrect. The roll axis must be perfectly stabilized to obtain the correct heading or yaw attitude.

The gyrocompass technique is evaluated with the assumed use of horizon sensors and rate gyros, to obtain angle and rate information for the control moment gyro actuators. This evaluation considers the effect of various disturbances and variations in control laws on the performance of the space laboratory.

To achieve this satisfactory performance, three changes in the control laws described in the Phase IIa report were made. These were as follows:

- (1) the rate and attitude gains were changed to obtain a satisfactory response,
- (2) gyro gimbal angle feedback was added to eliminate the dynamic coupling, and
- (3) the yaw channel gimbal control equation was changed to include a roll angle term when the roll angle error is greater than  $0.05^\circ$ . This last change further reduces the yaw response to roll disturbances.

### A.2.2 Mathematical Model

A block diagram of the two-axis gyrocompassing simulation is presented in Figure A-26. The dashed paths and blocks are the additions in the Phase IIa baseline gyrocompassing diagram.

The horizon scanner shown in the block diagram is assumed to have a scale factor error of 4% and a time constant of 0.05 sec. The noise level is Gaussian with zero mean and the rms = 0.033°. White noise is also used in the range of 0.01 to 1.0 cps.

The model for the roll rate gyro includes a scale factor error of 1%, with a natural frequency of 1.0 cps which has a 0.7 damping ratio. Two different types of noise in the output of the roll rate gyro are considered. These are: (1) a Gaussian noise with zero mean and the rms = 0.333°/hour and (2) white noise in the range of 0.01 to 1.0 cps.

The yaw rate gyro is assumed to be perfect. The model of the yaw rate gyro is not as sensitive to system performance as the roll rate gyro.

In deriving the two-axis equations of motion, a constant orbit rate for the pitch axis of  $\omega_y = -\omega_{orb} = -0.0662^\circ/\text{sec}$  is assumed along with only the CMG control torques and disturbances torques acting on the vehicle.

Since the attitude hold requirement of the space laboratory is  $\pm 0.5^\circ$ , small angle approximations are used for the Euler angle expressions. The roll attitude error,  $\phi_m$ , is measured with the horizon scanner while the yaw attitude error,  $\psi_m$ , is derived from the small-angle approximation of the roll rate divided by the orbit rate.

The control torques are obtained from the control moment gyros. The particular CMG configuration used consists of two single-gimbal CMG for the roll (or X) axis and two double-gimbal CMG for the yaw and pitch axes. Each gyro of the SG CMG has an angular momentum of 1,800 lb-ft-sec and each gyro of the DG CMG has an angular momentum of 550 lb-ft-sec. These are Phase IIa baseline sizes. This CMG configuration is shown in Figure 4-5 Section 4. The CMG control torque equations are approximated by assuming



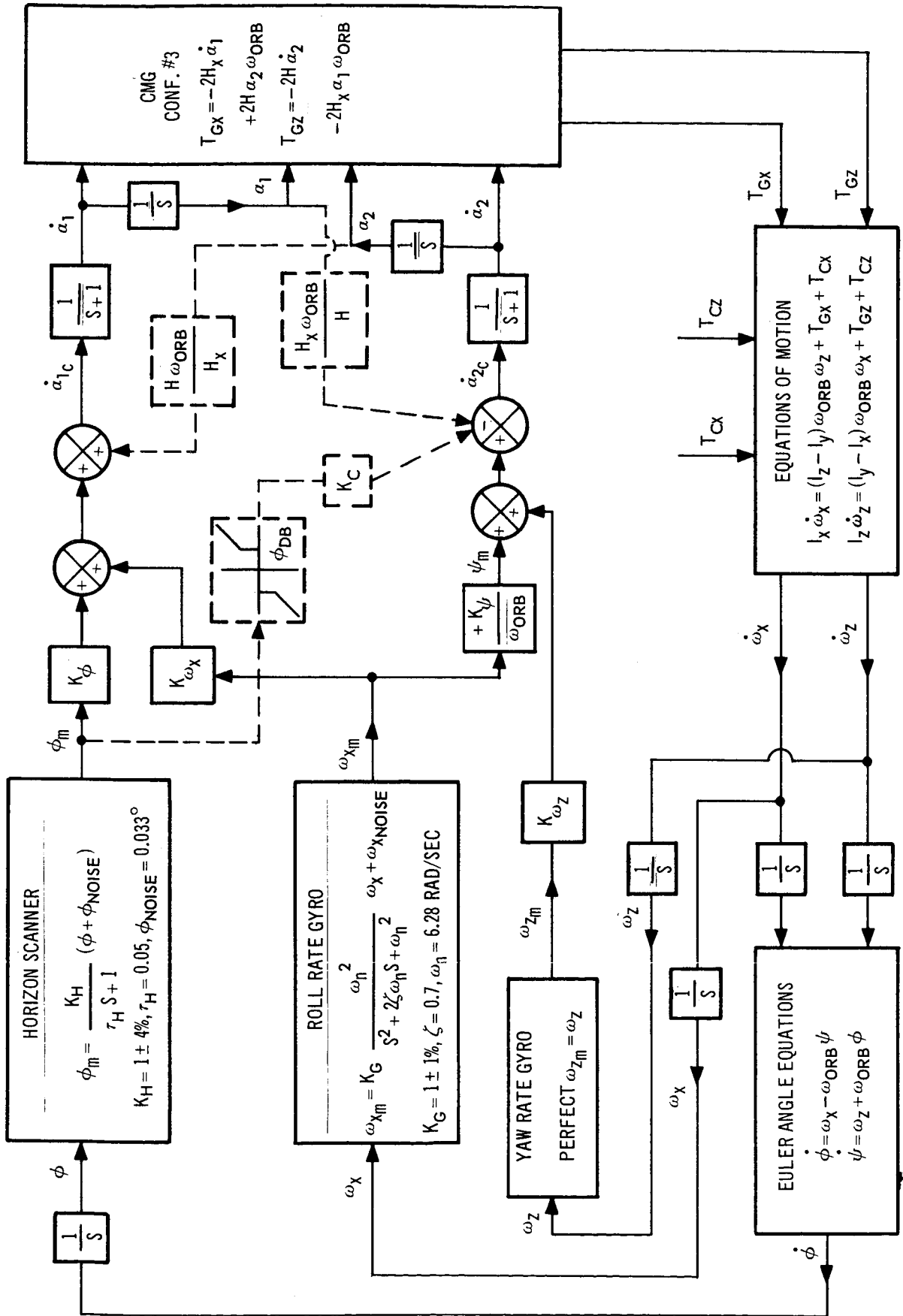


Figure A-26. Two Axes Block Diagram

small gimbal angles and zero roll and yaw angular body rates. In the latter assumption, only the gyro coupling torques caused by the orbital angular rate are considered.

The actual gimbal rates of the CMG,  $\dot{a}_1$  and  $\dot{a}_2$ , are assumed to lag the commanded gimbal rates,  $\dot{a}_{1c}$  and  $\dot{a}_{2c}$ . The model for the CMG gimbal actuators are represented by a 1-sec first-order lag response. This is illustrated in Figure A-26.

The system equations are summarized as follows:

$$I_x \dot{\omega}_x = (I_z - I_y) \omega_{orb} \omega_z + T_{GX} + T_{CX} \quad (A-38)$$

$$I_z \dot{\omega}_z = (I_y - I_x) \omega_{orb} \omega_x + T_{GZ} + T_{CZ} \quad (A-39)$$

Euler angle equations (small angles)

$$\dot{\phi} = \omega_x - \omega_{orb} \psi \quad (A-40)$$

$$\dot{\psi} = \omega_z + \omega_{orb} \phi \quad (A-41)$$

Sensors (the subscript, m, denotes a measured quantity)

$$\phi_m = \frac{K_H}{\tau S + 1} (\phi + \phi_{noise}) \quad (A-42)$$

$$\omega_{xm} = K_G \frac{\omega_n^2}{S^2 + 2\zeta \omega_n S + \omega_n^2} \omega_x + \omega_{xnoise} \quad (A-43)$$

$$\omega_{zm} = \omega_z \quad (A-44)$$

CMG control torques

$$T_{GX} = -2 H_x \dot{a}_1 + 2 H_x a_2 \omega_{orb} \quad (A-45)$$

$$T_{GZ} = -2 H_x \dot{a}_2 - 2 H_x a_1 \omega_{orb} \quad (A-46)$$

Gimbal actuators

$$\dot{a}_1 = \frac{1}{S+1} \dot{a}_{1c} \quad (A-47)$$

$$\dot{a}_2 = \frac{1}{S+1} \dot{a}_{2c} \quad (A-48)$$

### A.2.3 Control Laws

The Phase IIa baseline control laws are given as

$$\dot{a}_{1c} = K_\phi \phi_m + K_{\omega_x} \omega_{xm} \quad (A-49)$$

$$\dot{a}_{2c} = K_\psi \psi_m + K_{\omega_z} \omega_{zm} \quad (A-50)$$

where

$$\psi_m = \frac{\omega_x}{\omega_{orb}}$$

The Phase IIa baseline gains, natural frequencies, and damping for the roll and yaw channels are given in Table A-9.

Table A-9  
PHASE IIa BASELINE GAINS AND RESPONSE

Channel	System Gains	Natural Frequency radians/sec	Damping
X (roll)	$K_\phi = 0.203, K_{\omega_x} = 18.3$	0.042	1.9
Z (yaw)	$K_\psi = 2.83, K_{\omega_z} = 124$	0.066	1.45

These gains have been modified for the Phase IIb baseline and are given in Table A-10.

Table A-10  
PHASE IIb BASELINE GAINS AND RESPONSE

Channel	System Gains	Natural Frequency (radians/sec)	Damping
X (roll)	$K_\phi = 4.55, K_{\omega_x} = 86.5$	0.20	1.9
Z (yaw)	$K_\psi = 1.03, K_{\omega_z} = 74.8$	0.04	1.45

In addition to the gain changes, gimbals angle feedback was introduced into the control laws to reduce the gyro gimbal angle coupling. Also, a roll attitude crossfeed is introduced into the yaw channel to further reduce the roll-yaw coupling.

The Phase IIb control laws are given by the following equations

$$\dot{a}_{1c} = K_\phi \phi_m + K_{\omega_x} \omega_{x_m} + \frac{H}{H_x} \omega_{orb} a_{2m} \quad (A-51)$$

$$\dot{a}_{2c} = K_\psi \psi_m + K_{\omega_z} \omega_{z_m} - \frac{H_x}{H} \omega_{orb} a_{1c} - K_c \phi_c \quad (A-52)$$

where

$$\psi_m = \frac{\omega_x}{\omega_{orb}}$$

$$\phi_c = \begin{cases} \phi_m & \text{for } |\phi_m| \geq \phi_{DB} \\ 0 & \text{for } |\phi_m| \leq \phi_{DB} \end{cases} \quad (A-53)$$

with

$$K_c = 55$$

$$\phi_{DB} = 0.05^\circ$$

#### A.2.4 Study Results

The Phase IIa and IIb evaluation results are discussed in the following subsections.

##### A.2.4.1 Phase IIA Baseline Evaluation Results

The Phase IIa baseline system was evaluated to determine necessary improvements. In the Phase IIa mechanization, the implementation of the gyrocompass technique was represented by  $\psi_m = + \frac{\omega_{xm}}{\omega_{orb}}$  and sensor noise was assumed to be zero. When disturbances were used to perturb the system, unsatisfactory transient and steady-state behavior resulted. For an initial roll angle disturbance, the roll angle,  $\phi$ , did not stabilize at zero and the yaw angle transient exceeded specifications ( $0.5^\circ$ ) if the roll angle disturbance was larger than 0.05. For small control gains in the roll channel system instability will result. This is produced by the CMG gimbal angle coupling. In addition, a sinusoidal torque disturbance in the X channel at the orbital frequency was found to be a resonant frequency. This is verified from the frequency response of the system illustrated in Figures A-27 and A-28. (This resonant peaking of the amplitude ratios of  $\psi/T_{CX}$  and  $a_1/T_{CX}$  is also shown in these illustrations.) The elimination of the CMG gimbal angle coupling removes the resonance near the natural frequency of 0.001 rad/sec. To avoid the effects of this gimbal angle coupling, the gimbal control law equations were modified as shown below:

$$\dot{a}_{1c} = K_\phi \phi_m + K_{\omega_x} \omega_{x_m} + \frac{H}{H_x} \omega_{orb} a_{2m} \quad (A-54)$$

$$\dot{a}_{2c} = K_\psi \psi_m + K_{\omega_z} \omega_{z_m} - \frac{H_x}{H} \omega_{orb} a_{1m} \quad (A-55)$$

Wherein the terms  $+\frac{H}{H_x} \omega_{orb} a_{2m}$  and  $-\frac{H_x}{H} \omega_{orb} a_{1m}$  were added to the Phase IIa control equations.

These modifications eliminate the CMG dynamic coupling through the gimbal angles. Performance achieved with these modifications is illustrated in Figures A-29 through A-32, where analog computer time histories are shown.

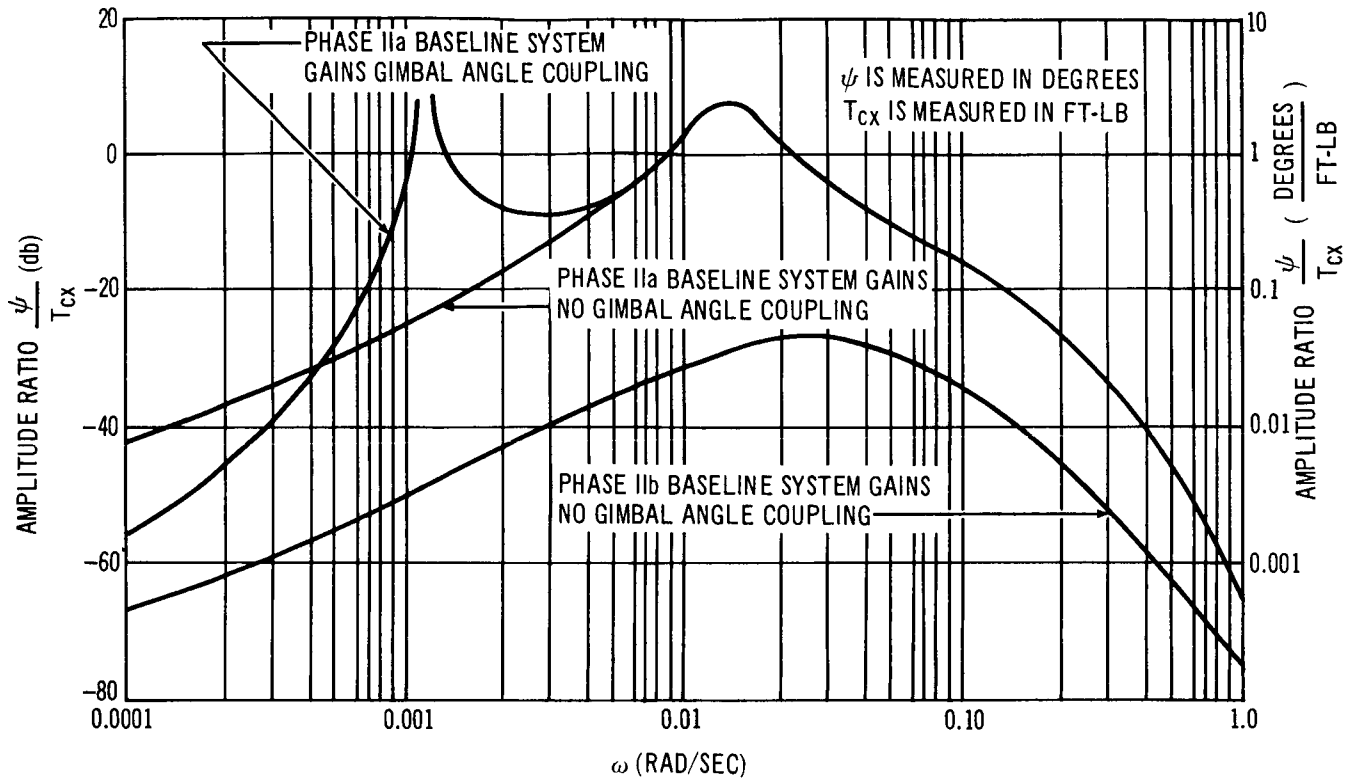


Figure A-27. Effect of Roll Torque Disturbance on Yaw Attitude

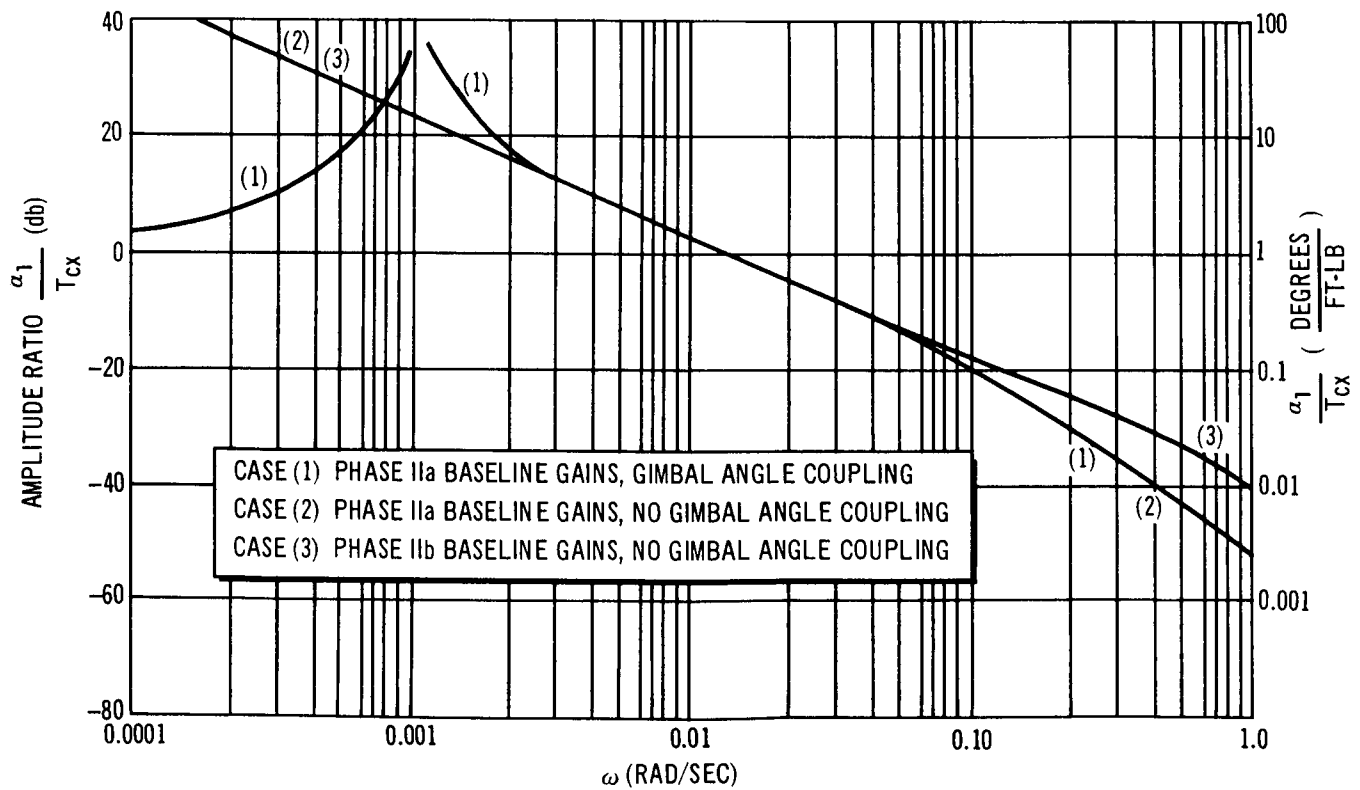


Figure A-28. Effect of Roll Torque Disturbance on Gimbal Angle

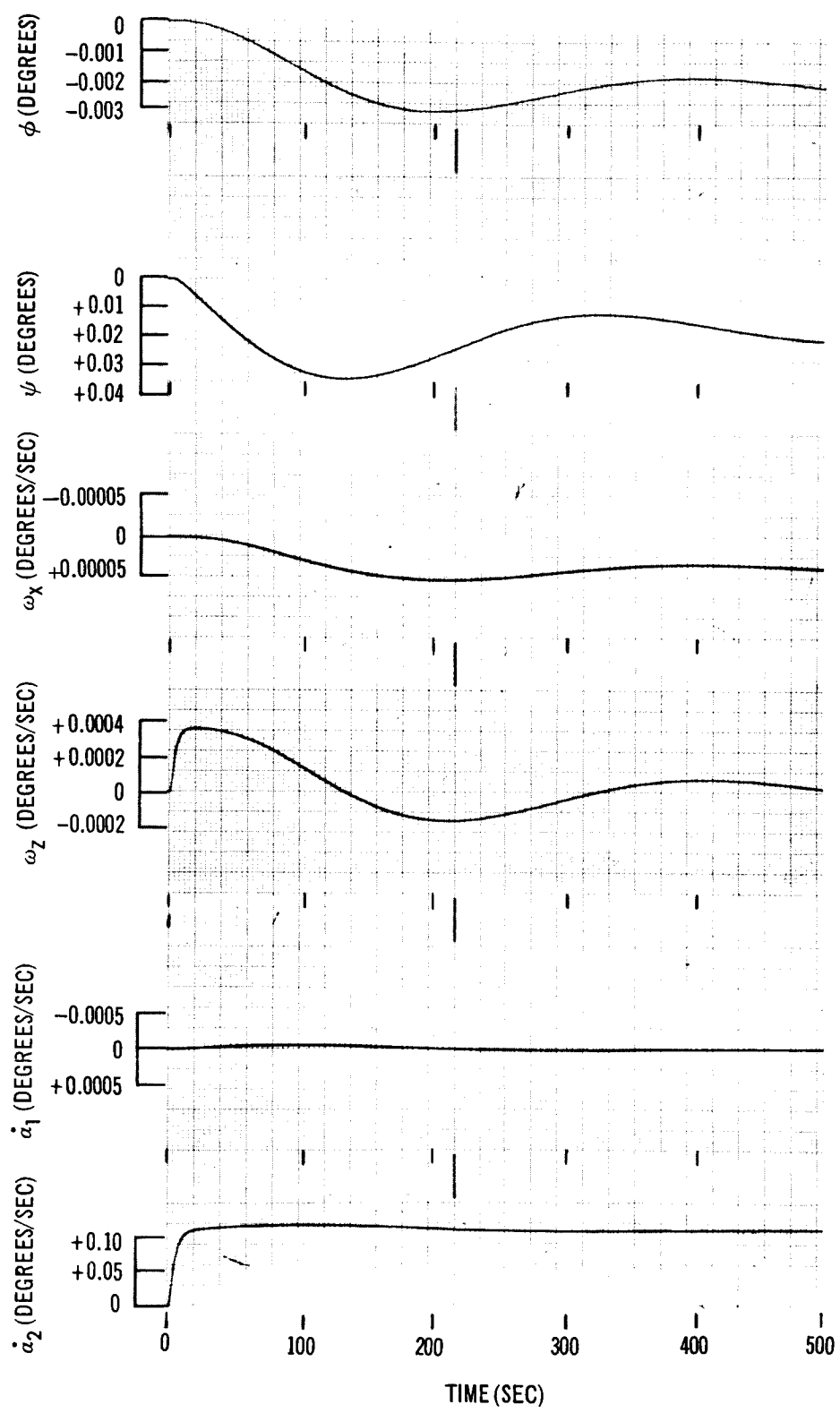


Figure A-29. Phase IIa Baseline Gains;  $T_{CZ} = 2$  lb-ft; No Gimbal Angle Coupling

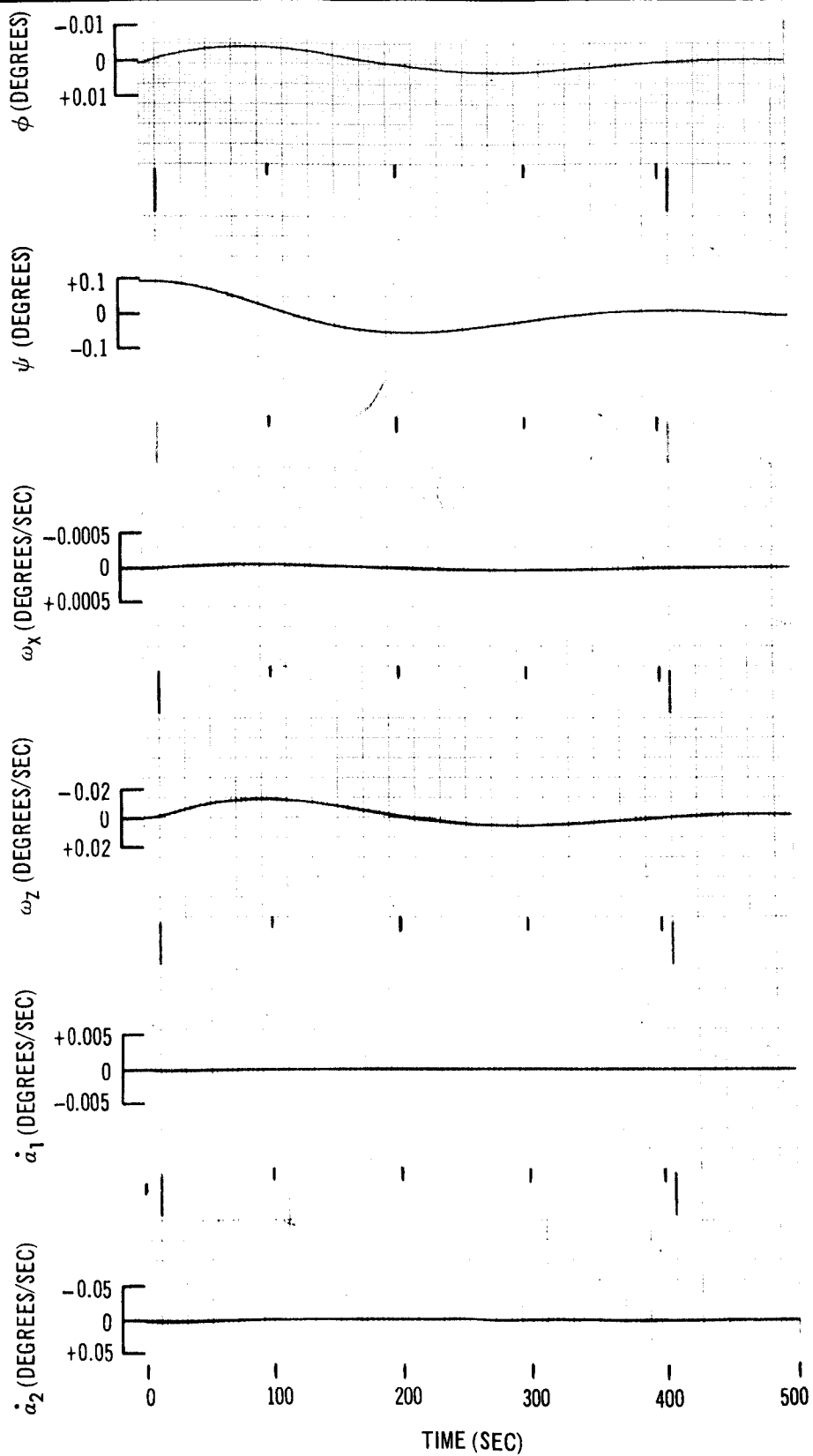


Figure A-30. Phase IIa Baseline Gains  $\psi(0) = 0.1^\circ$ ; No Gimbal Angle Coupling



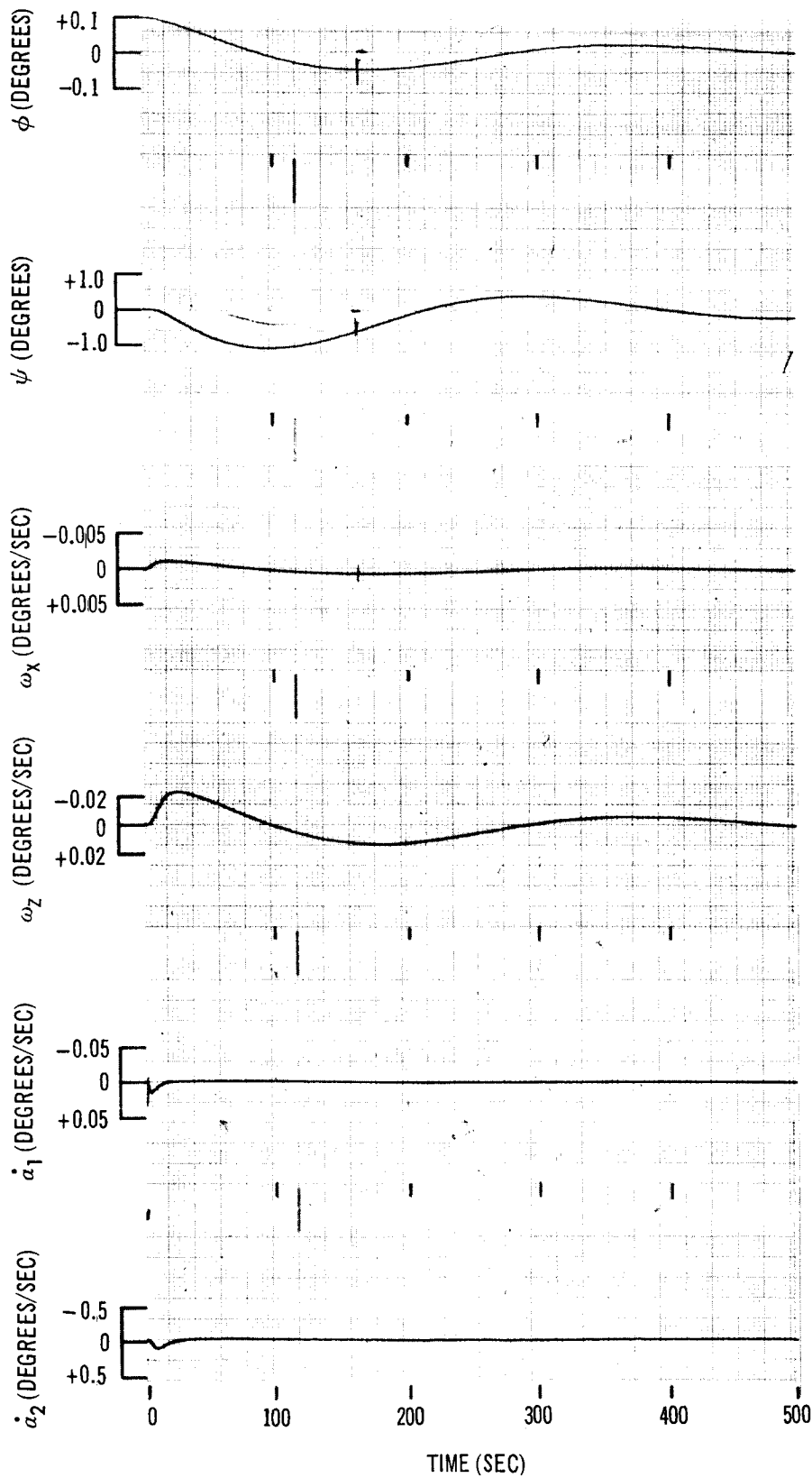


Figure A-31. Phase Ila Baseline Gains  $\phi(0) = 0.1^\circ$ ; No Gimbal Angle Coupling

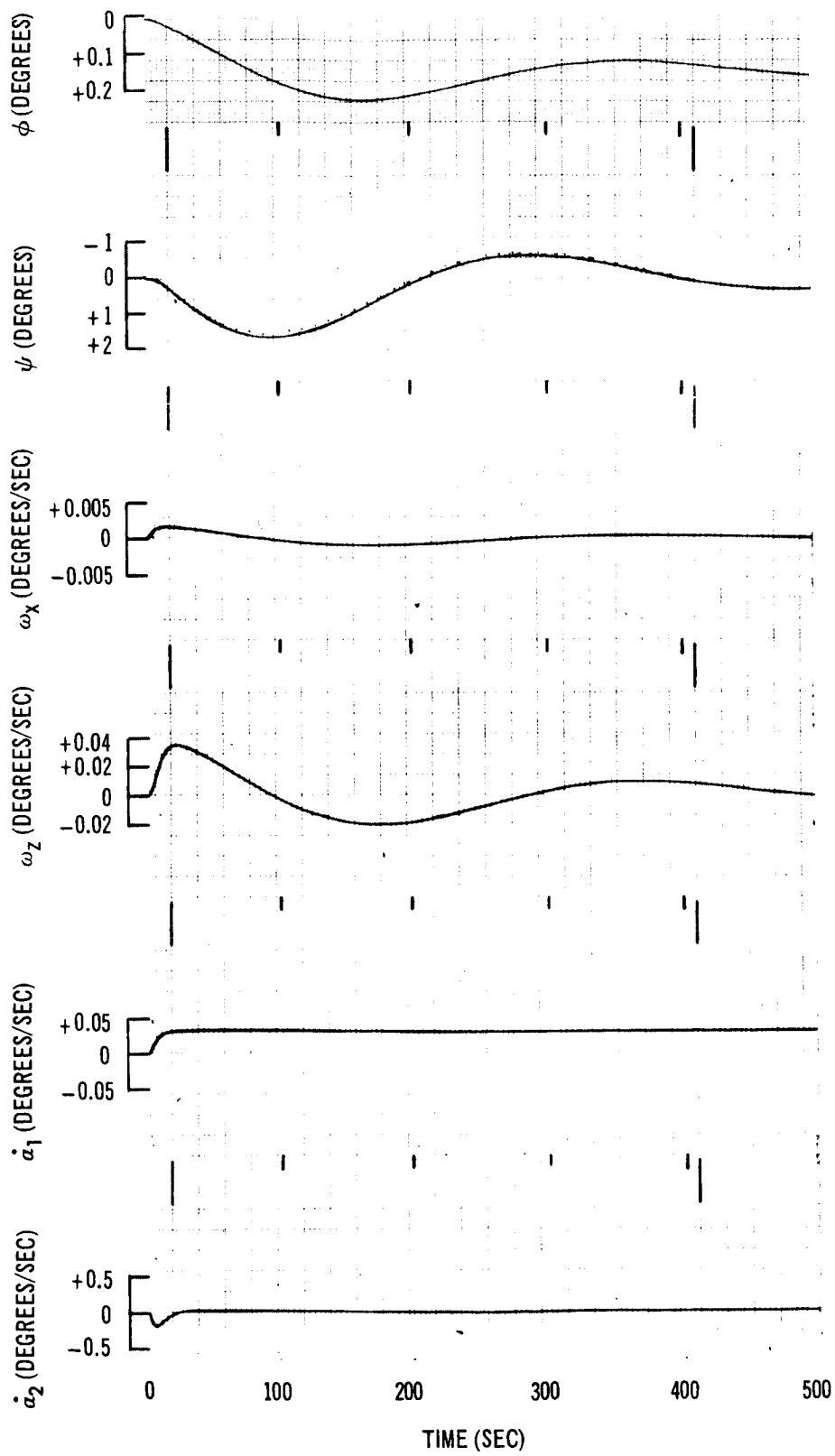


Figure A-32. Phase IIa Baseline Gains;  $T_{CX} = 2$  lb-ft; No Gimbal Angle Coupling

These illustrations show that the non-zero steady-state problems for initial condition disturbances were eliminated but that performance of the system is still not adequate. For example, Figure A-29 shows the response of the system to a step yaw torque of 2 lb-ft. This torque is about four times the maximum value of the aerodynamic and gravity gradient torques. The response of the system is slow, with a maximum yaw attitude error of about  $4^\circ$ . For the actual disturbance torques encountered, the yaw attitude error would be approximately  $1.0^\circ$ , which is out of specification. Additionally, Figure A-29 shows the effect of gyrodynamic coupling between the roll and yaw axes of the space laboratory, which results in a roll attitude error from a yaw disturbance. This particular roll attitude error is shown to be within the  $0.5^\circ$  requirement.

In this example, the yaw attitude error accumulated after the transient is over is caused by the difference in the disturbance and gyro torque profiles. Noting the  $\dot{\alpha}_2$  plot, after 20 sec the gyro torque,  $2 H \dot{\alpha}_2$ , equals the yaw disturbance torque,  $T_Z$ . With this accumulated yaw attitude error still present, a steady-state roll rate,  $\omega_x$ , will also be present with an amplitude of  $\omega_{orb} \sin \psi$  if  $\dot{\phi} = 0$ .

The response of the system to an initial yaw attitude error is illustrated in Figure A-30. Again, the response is slow and the coupling in the roll axis is small. It shows that an initial yaw attitude error can be reduced to zero.

Figure A-31 shows the system response to an initial roll attitude error of  $0.1^\circ$ . With this initial condition, the yaw attitude error is  $1.0^\circ$ , which is unacceptable for the system response. This type of initial condition, which can be produced by crew motion, must be controlled. The initial condition assumed is realistic since the maximum attitude error produced by one crew member is  $0.06^\circ$ . The large yaw error exists since, in reducing the roll attitude error to zero, the vehicle is rotated, which produces a body roll rate that appears as an error input to the yaw channel. Therefore, the yaw attitude errors can only be reduced to zero after the roll axis is stabilized. To meet the system specifications, the maximum initial roll attitude error that can be tolerated is  $0.05^\circ$ .

Figure A-32 shows the system response to a step disturbance torque of 2 lb-ft about the roll axis. The system response is similar for the condition of a yaw torque disturbance. The roll attitude error accumulated after the transient is caused by the difference between the disturbance and gyro torque profiles. The plot of  $\dot{\alpha}_1$  (gimbal rate) and after about 20 sec shows that the gyro torque,  $2H\dot{\alpha}_1$ , is equal to the roll disturbance torque. To meet the system specifications of holding the attitude error to  $\pm 0.5^\circ$ , the largest roll torque tolerable is 0.62 lb-ft.

It was also determined with the frequency response model described in Subsection A.2.2 that 2 lb-ft amplitude disturbances at frequencies between 0.0035 and 0.07 rad/sec cannot be tolerated. This can be seen in Figure A-27, where the amplitude ratio  $\psi/T_{CX}$  is plotted. It is also observed that the amplitude ratio is at a maximum at  $\omega = 0.016$  rad/sec. At this frequency the largest torque amplitude disturbance that can be tolerated is 0.3 lb-ft. The results of the study for X-channel disturbances, which use Phase IIa baseline system gains, are summarized in Table A-11. As described previously, disturbances of the above magnitude in the Z channel are not significant.

Table A-11  
ALLOWABLE X-CHANNEL INPUT DISTURBANCE LEVELS FOR  
THE PHASE IIA BASELINE SYSTEM GAINS  
(NO GIMBAL ANGLE COUPLING)

Type of Disturbance in X Channel	Magnitude of Allowable Disturbance
Initial attitude angle $\phi(0)$	$\phi(0) < 0.05^\circ$
Step torque $T_{CX}$	$T_{CX} < 0.62$ lb-ft
Sinusoidal torque $T_{CX} = A \sin \omega t$	<ol style="list-style-type: none"> <li>1. <math>A &lt; 0.3</math> lb-ft, all <math>\omega</math></li> <li>2. <math>A &lt; 2</math> lb-ft, <math>0.0035 &lt; \omega &lt; 0.07</math> rad/sec</li> </ol>

#### A.2.4.2 Modifications Resulting in the Phase IIb Baseline Gyrocompassing Mechanization

The Phase IIa baseline system does not meet the attitude accuracy requirements of  $0.5^\circ$  for all disturbance levels that the laboratory is expected to experience. In addition, the system response is slow and underdamped. In order to improve this situation, the roll channel response was increased a factor of five and the yaw channel response was decreased by 30%. This was accomplished by using the modified control gains (Subsection A.2.3). The results of this modification are shown in Figures A-33 through A-36. Figure A-33 shows the system response to a step torque in the yaw channel. It can be seen that the response is much faster and is much better damped. Also, the coupling into the roll axis is decreased considerably. The 2.1 lb-ft step torque causes a steady-state yaw attitude error of  $0.1^\circ$ . This yaw attitude error produces a small roll rate of  $\omega_x = \omega_{orb} \sin \psi$  which is observed on the plot. Again, according to linear theory and the attitude requirement accuracy, a maximum 10 lb-ft step torque disturbance in the yaw channel can be tolerated. Figure A-34 shows the response of the system to an initial yaw angle. It can be seen that this disturbance is easily handled by the system. The effect of a step torque disturbance in the X channel is shown in Figure A-35. This illustration shows that the sensitivity of the yaw attitude to roll channel step torques is significantly decreased with the use of the Phase IIb baseline control gains. Instead of tolerating a step torque of 0.62 lb-ft with the Phase IIa baseline control gains, it is possible to tolerate a step torque of 13.9 lb-ft. It can also be seen from the frequency response plots in Figure A-27 that the effect of sinusoidal torques in the X channel on the yaw angle is significantly decreased with the use of the modified control gains. In fact, sinusoidal torque amplitudes as large as 11.9 lb-ft at all frequencies can be tolerated.

These results indicate that the horizon sensor gyrocompass mode of belly-down stabilization with the Phase IIb baseline control equation gains performs satisfactorily for all expected disturbances except initial roll errors. The system response for an initial roll attitude error is shown in Figure A-36. As shown, the yaw attitude is still highly sensitive to initial roll angle disturbances. For an initial roll angle of  $0.1^\circ$ , the yaw attitude reaches a

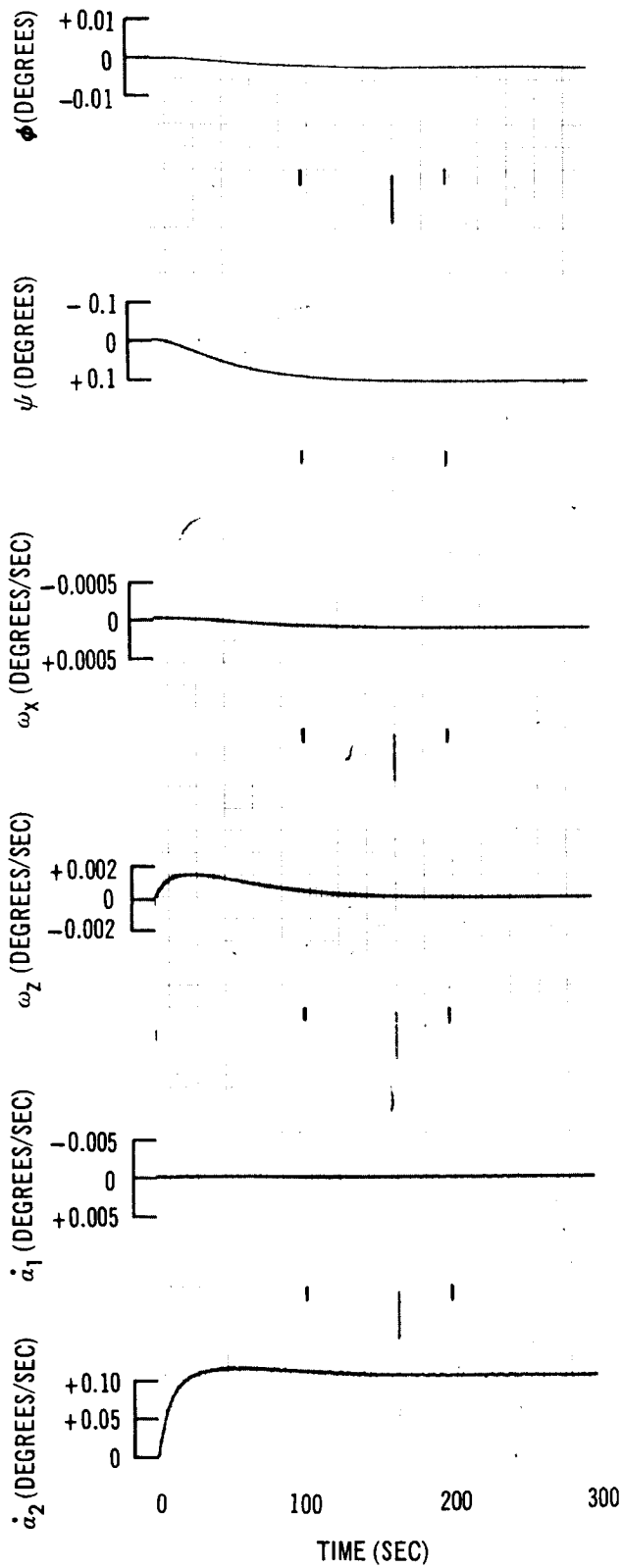


Figure A-33. Phase IIb Baseline Gains;  $T_{CZ} = 2$  lb-ft; No Gimbal Angle Coupling

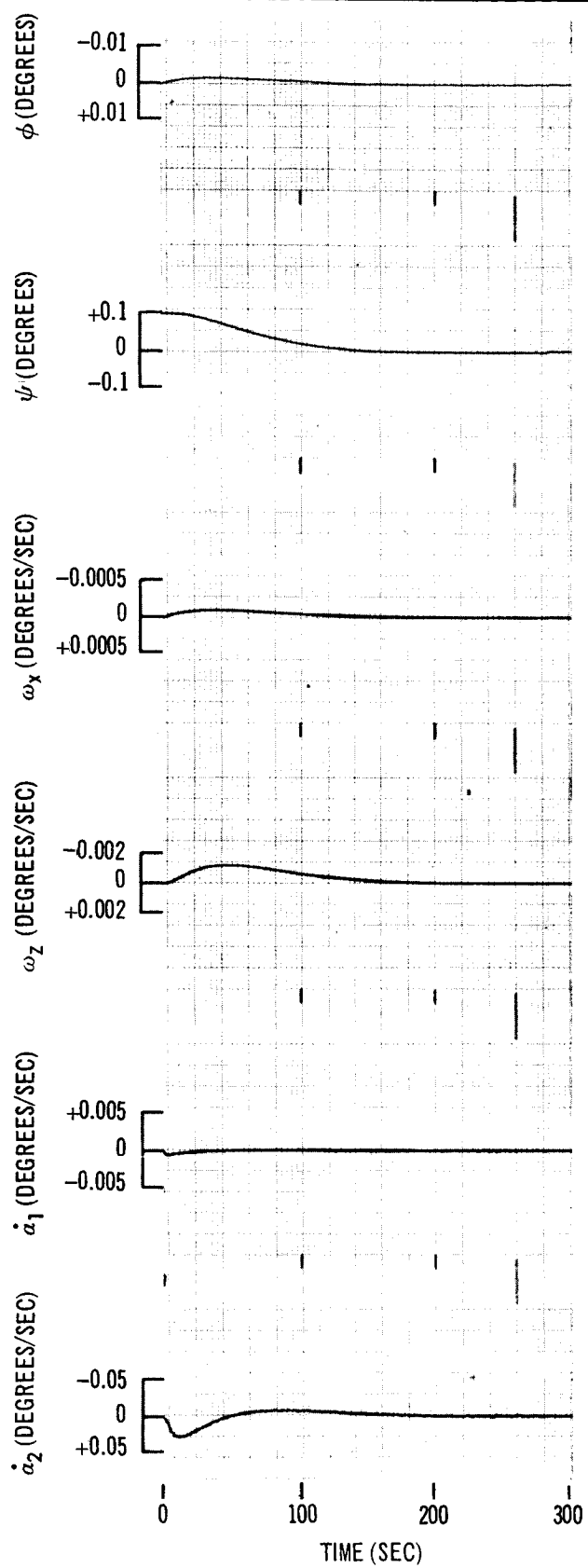


Figure A-34. Phase IIb Baseline Gains;  $\psi(0) = 0.1^\circ$ ; No Gimbal Angle Coupling

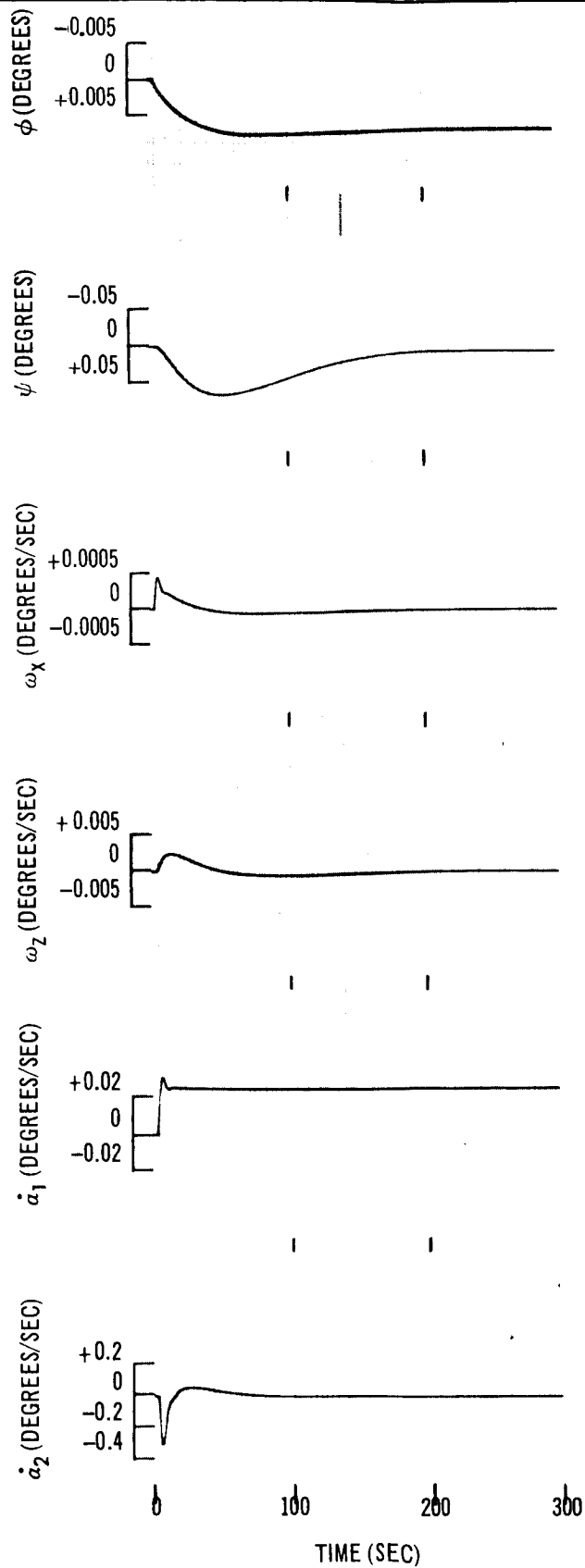


Figure A-35. Phase IIb Baseline Gains;  $T_{CX} = 2$  lb-ft; No Gimbal Angle Coupling.



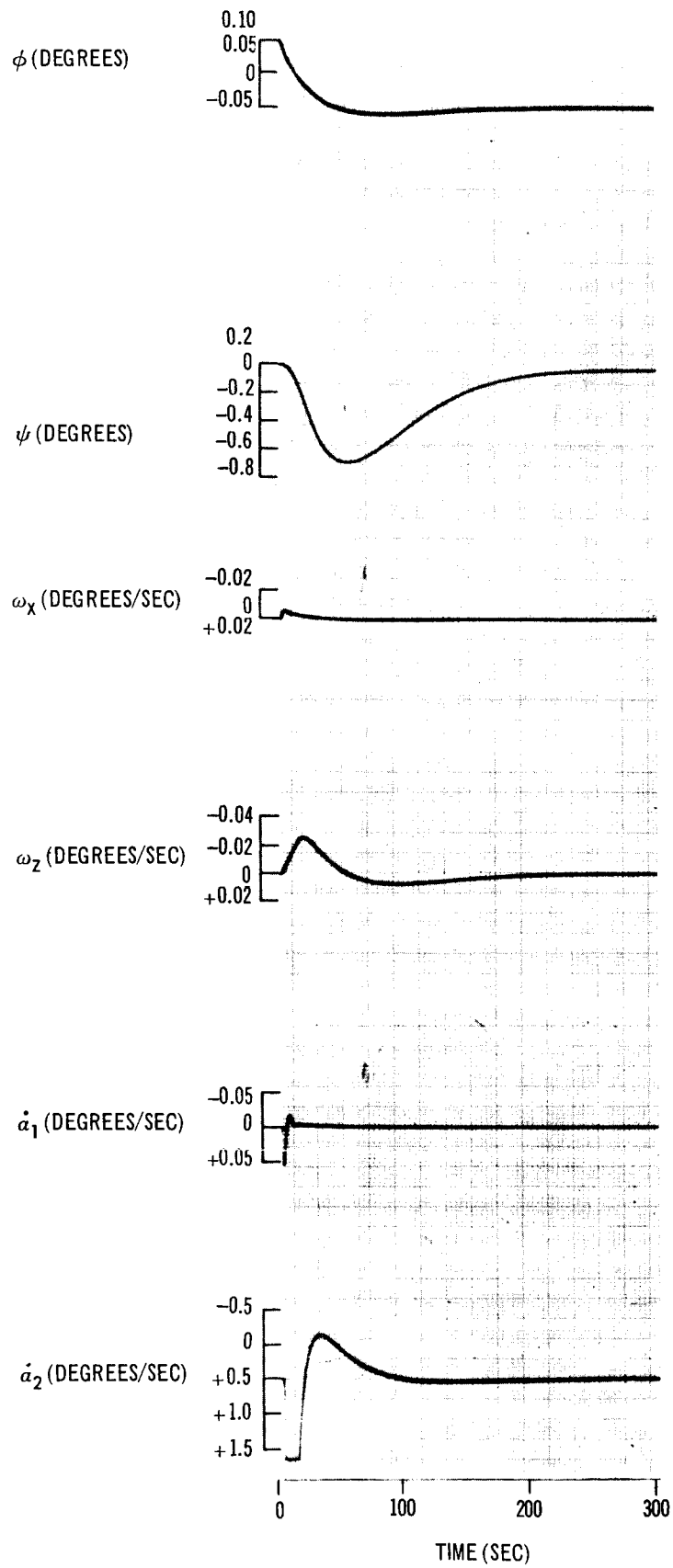


Figure A-36. Phase IIb Baseline Gains;  $\phi(0) = 0.1^\circ$ ; No Gimbal Angle Coupling

maximum of  $0.7^\circ$ . It is noted that  $\dot{a}_2$  is limited to  $1.15^\circ/\text{sec}$  which corresponds to a maximum CMG torque output of 11 lb-ft.

The sensitivity to initial roll angles is caused by the large gain on the roll rate signal being used in the gyrocompass mode to compute the yaw attitude. However, this is an undesired signal when it has been generated to null the roll attitude. To eliminate this false signal when the roll angle is being nulled, a compensation signal proportional to the roll attitude error is subtracted from the yaw control signal. The outer gimbal rate command equation for the yaw axis is therefore modified as shown below:

$$\dot{a}_{2c} = + \frac{K_\psi}{\omega_{\text{orb}}} \omega_{x_m} + K_{\omega_z} \omega_{z_m} - \frac{H_x}{H} \omega_{\text{orb}} a_{1m} - K_c \phi_c \quad (\text{A-56})$$

where

$$\phi_c = \begin{cases} \phi_m & \text{for } |\phi_m| > \phi_{\text{DB}} \\ 0 & \text{otherwise} \end{cases}$$

and where

$$\phi_{\text{DB}} = 0.05^\circ$$

The results of this modification are shown in Figures A-37 and A-38. In Figure A-37, the initial roll angle is  $0.1^\circ$  and  $K_c = 55$ . This illustration shows that the roll crossfeed term causes  $\dot{a}_2$  to be initially positive. This in turn causes the yaw angle to be disturbed in the negative direction. When the roll angle decreases below  $\phi_{\text{DB}} = 0.05^\circ$ , the roll crossfeed term drops out. By this time the undesired roll rate signal, which causes a positive rate, has decreased sufficiently so that the yaw angle remains within the  $0.5^\circ$  attitude accuracy requirement. Similar observations can be made about Figure A-38, where  $\phi(0) = 0.5^\circ$ . The maximum yaw attitude error in this case is nearly  $0.4^\circ$ .

In summary, the Phase IIb baseline system is obtained by changing the Phase IIa control law gains and adding the additional feedback terms as

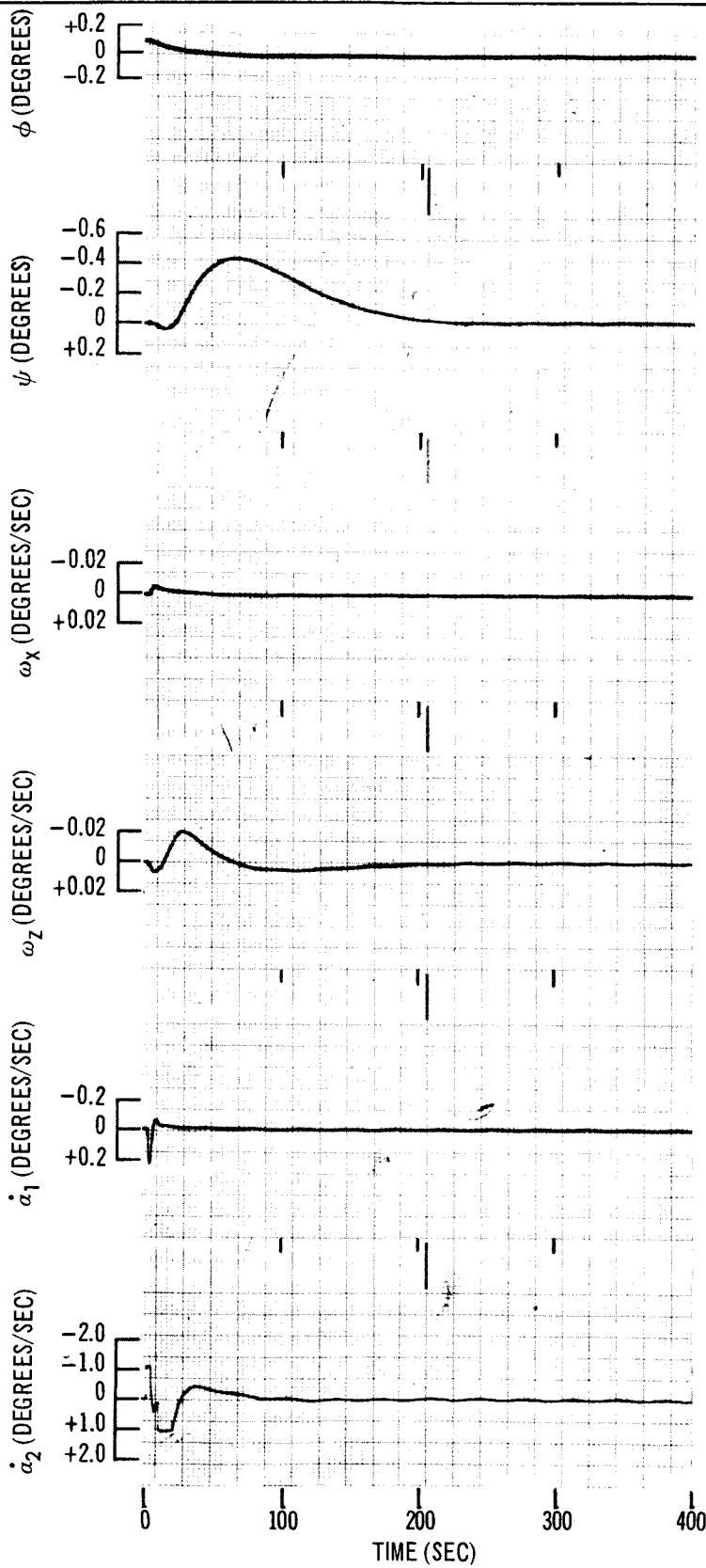


Figure A-37. Phase IIb Baseline System;  $\phi(0) = 0.1^\circ$ ;  $K_C = 55$ ;  $\phi_{DB} = 0.05^\circ$

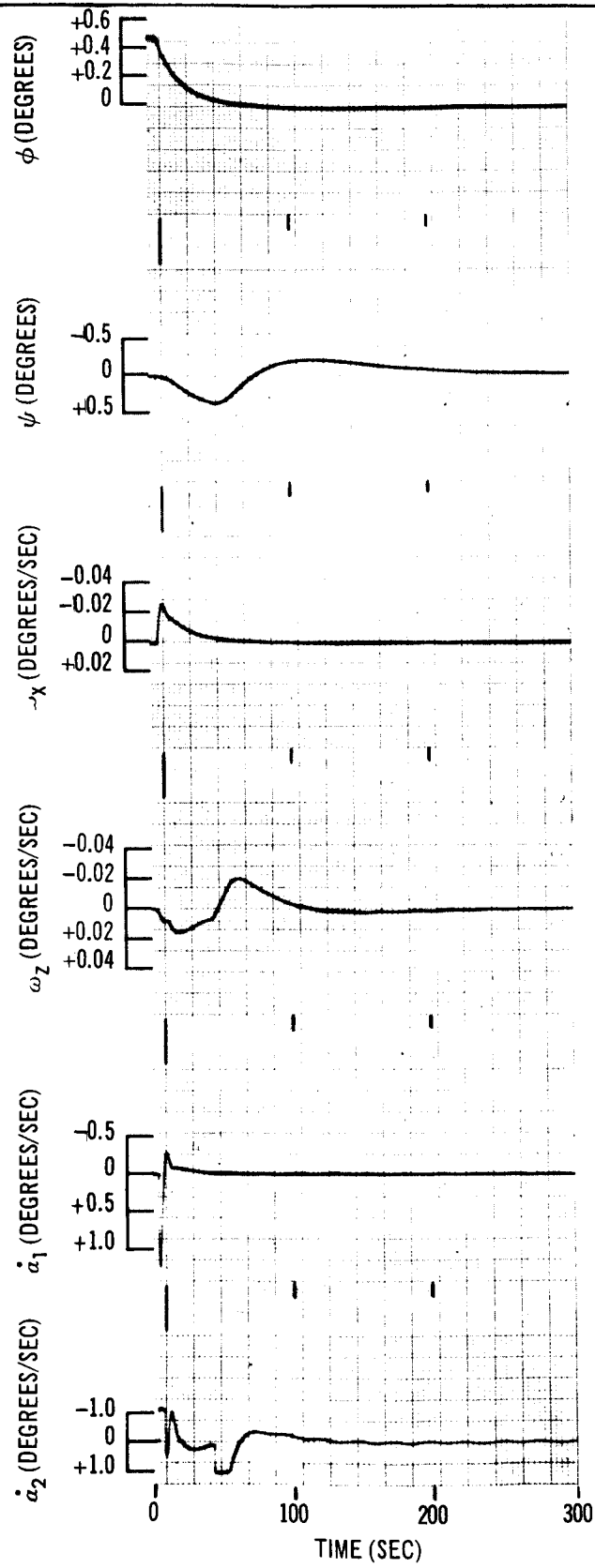


Figure A-38. Phase IIb Baseline System;  $\phi(0) = 0.5^\circ$ ;  $K_C = 55$ ;  $\phi_{DB} = 0.05^\circ$

described in Subsection A. 2. 3. This results in the following control laws and system gains.

$$\dot{a}_{1c} = K_{\phi} \phi_m + K_{\omega_x} \omega_{x_m} + \frac{H}{H_x} \omega_{orb} a_{2m} \quad (A-57)$$

$$\dot{a}_{2c} = + \frac{K_{\psi}}{\omega_{orb}} \omega_{x_m} + K_{\omega_z} \omega_{z_m} - \frac{H_x}{H} \omega_{orb} a_{1m} - K_c \phi_c \quad (A-58)$$

$$K_{\phi} = 4.55 \quad K_{\omega_x} = 86.5$$

$$K_{\psi} = 1.03 \quad K_{\omega_z} = 74.8$$

$$K_c = 55$$

$$\phi_m \text{ for } |\phi_m| > 0.05^{\circ}$$

0 otherwise

(A-59)

Allowable input disturbance levels are determined as previously described. The results are summarized in Table A-12 for the Phase IIb baseline system.

Table A-12  
ALLOWABLE INPUT DISTURBANCE LEVEL  
FOR THE PHASE IIb BASELINE SYSTEM

Type of Disturbance	Magnitude of Allowable Disturbance
Initial attitude angle $\phi(0)$	$\phi(0) < 0.5^{\circ}$
Step torque $T_{CX}$	$T_{CX} < 13.9 \text{ lb-ft}$
Sinusoidal torque $T_{CX} = A \sin t$	$A < 11.9 \text{ lb-ft, all}$
Step torque $T_{CZ}$	$T_{CZ} < 10 \text{ lb-ft}$

Note: Yaw channel disturbances are not significant

It can be seen that satisfactory gyrocompassing performance can be achieved with the Phase IIb baseline system. The addition of gimbals angle feedback effectively reduces gimbal dynamic cross coupling and eliminates resonance for sinusoidal torque disturbances at or near orbital frequency. Separation of the roll and yaw channel natural frequencies achieved by increasing the roll channel response by a factor of five and decreasing the yaw channel response by 30%, significantly reduces yaw channel sensitivity to roll channel torque disturbances and yet preserves satisfactory overall dynamic response capability in the yaw channel. The introduction of roll angle crossfeed into the yaw control channel significantly reduces the magnitude of the yaw angle transient in response to a roll angle initial condition or step input disturbance arising for example from sensor output discontinuities. System response for a  $10^\circ$  initial roll angle is shown in Figure A-39. It can be seen from this illustration that the stabilization system can null comparatively large attitude errors. Hence, when the laboratory is transferring from any other attitude to the belly-down orientation, only a gross attitude alignment is necessary before the automatic stabilization mode is activated. It is emphasized that, for this gyrocompass study, the gimbal angular rate,  $\dot{\alpha}_2$ , was limited to  $1.15^\circ/\text{sec}$ , which corresponded to a maximum torque output of 11 lb-ft. The gimbal rate does not have to be limited to this value because of increased control moment gyro torque output capacity. However, the results of the gyrocompass study are valid for increased torque capabilities.

#### A.2.5 Effects of Sensor Characteristics

The roll rate gyro and the horizon sensor were assumed to have the characteristics described in Section A.2.2. These characteristics, except for the horizon scanner noise, have a negligible effect on the system behavior. Horizon scanner noise causes the coupling into the yaw channel to increase. Figure A-40 shows the system variables with horizon scanner noise. The maximum value of the yaw angle,  $\psi$ , increases slightly. The maximum value of the gimbal rate,  $\dot{\alpha}_2$ , increases to  $0.55^\circ/\text{sec}$ . However, it was found that a first-order filter network on the horizon scanner output will decrease  $\dot{\alpha}_{2\text{max}}$  satisfactorily, and may be added if required.

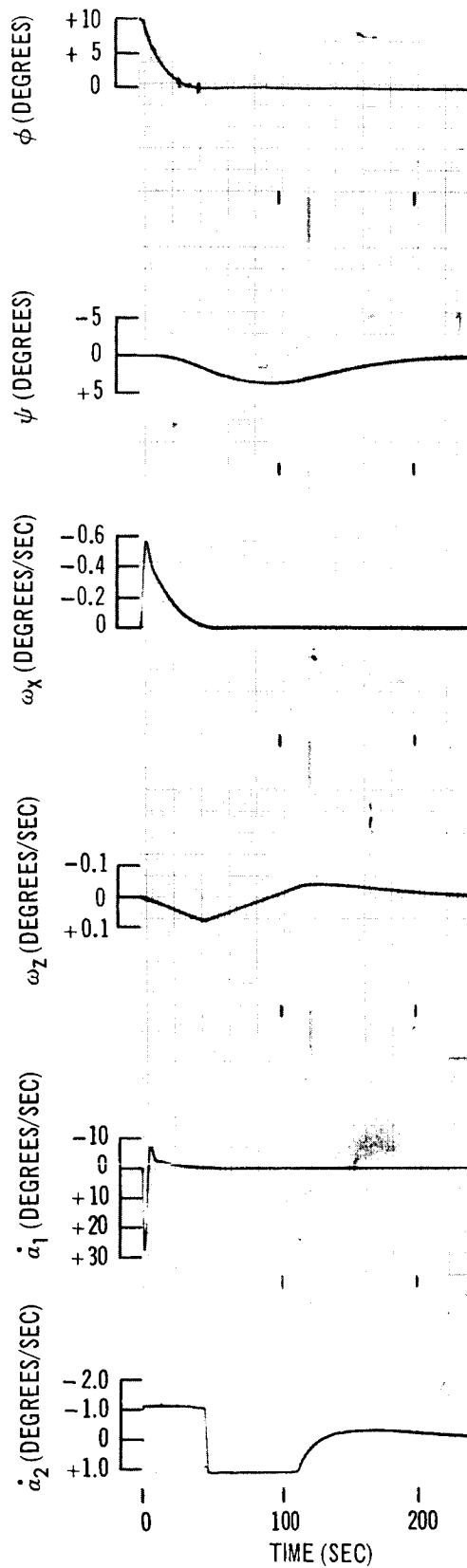


Figure A-39. Phase IIb Baseline System;  $\phi(0) = 10^\circ$ ;  $K_C = 55$ ;  $\phi_{DB} = 0.05^\circ$

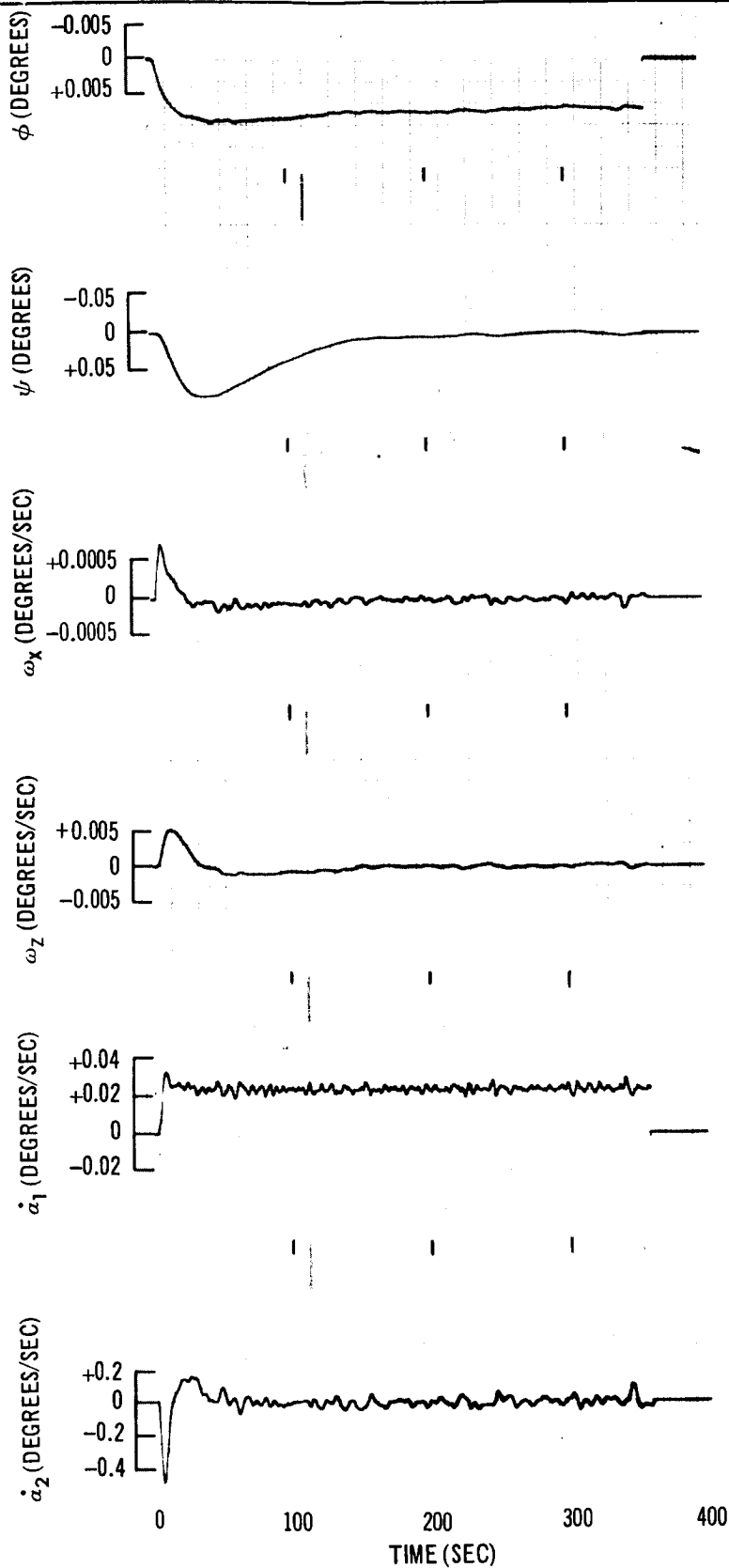


Figure A-40. Phase IIb Baseline System  $T_{CX} = 2$  lb-ft Horizon Sensor Noise



### A.3 COMPARISON OF CMG AND REACTION JET MANEUVER COSTS

This section presents a cost comparison of an estimated maneuver profile for the two actuator systems, CMG and reaction jets.

#### A. 3.1 Introduction

An approach for estimating this mission profile is presented along with the requirements derived from the profile. This cost comparison is based upon minimizing the system resources (maneuver time and weight) required for maneuvering. To determine the minimum cost of a given maneuver which uses CMG, the CMG parameters of angular momentum and gimbal torque are optimized. In order to effectively optimize these CMG parameters, the total mission impulse and torque profile must be known (that is, internal and external disturbances, crew motion disturbances, and mission event and experimental support maneuver requirements). For maneuvering with the reaction jets, only the maneuver rate is optimized with respect to maneuver angle, to yield the minimum cost of the system resources.

Two classes of attitude maneuvers are considered: pitch and yaw, and roll. The first class points the vehicle to astronomical objects in any direction, and the second class rolls the vehicle away from the belly-down orientation. Both types of maneuvers are statistically modeled in terms of probability densities in their respective rotational angles.

Costs of maneuvers are estimated on the bases of (1) time to execute the maneuver, (2) weight of propellant required to execute the maneuver, and (3) the total number of maneuvers required during the life of the laboratory. These estimates of average cost for both CMG and reaction jet actuation follow from the assignment of cost weightings (1) to operational time, and (2), to weight chargeable to the maneuvers on a delta basis (that is, jets and CMG are already on the laboratory and the CMG sized to handle the impulse caused by external and worst-case internal disturbances.)

To obtain an approximate weight chargeable to maneuvers for cost estimates, it was necessary to assume some momentum storage configuration. The Phase IIa baseline configuration of two DG CMG for pitch and yaw and two

SG CMG for roll was assumed. However, since the increase in weight per unit,  $H$ , is approximately the same for both the double- and single-gimbal CMG (1,000 to 3,000 lb-ft-sec per unit), the weights used to minimize the maneuver cost in this study apply sufficiently well to all configurations which use combinations of double- and single-gimbal control moment gyros.

Costs of power and equipment volume requirements were not included in the cost estimates, since CMG spin power does not increase significantly with  $H$ , nor does average torque power change significantly with torquer size. There is no increase in CMG volume in the range from approximately 1,000 to 3,000 lb-ft-sec, and of torques from 5 to 200 lb-ft per unit. There is no increase in reaction jet power or volume.

Both of the CMG parameters (available angular momentum,  $H$ , and available torque,  $T$ ) are factors which, with time required to perform the maneuver, are used to estimate costs. Since the ratio of weight increase between  $H$  and  $T$  over the range of interest is approximately 10 to 1, only  $H$  is considered significant in increasing average cost by weight allowance. Only angular momentum is involved in a tradeoff of cost of both operation time, and cost of equipment weight must be allowed. Accordingly, average or expected operational time costs were computed, with available angular momentum,  $H$ , adjusted to minimize these costs for a given number,  $N$ , of maneuvers in the operational time, and a given torque,  $T$ , available for accelerating the vehicle. Two extremes in vehicle inertia,  $I = 500,000$  and  $800,000$  slug - ft<sup>2</sup>, serve to indicate results over the range of interest. Figures A-41 and A-42 summarize the evaluations of laboratory resource usage factor for CMG pitch-yaw and roll maneuvers, respectively. For these figures, the relative costs of crew time and weight are approximately 3:1.

The expected times for a single maneuver have been computed under the cost optimization constraint, and are indicated in Figures A-43 and A-44 for pitch-yaw and roll maneuvers, respectively. These quantities are indicated, as are the expected costs, for three values of  $N$  (100, 300, and 500) and for five values of available torque (10, 20, 30, 40, and 50 lb-ft). The upper limit in the torque range, 50 lb-ft, was based on the observation that little is gained in reducing costs by increasing CMG available torque beyond this

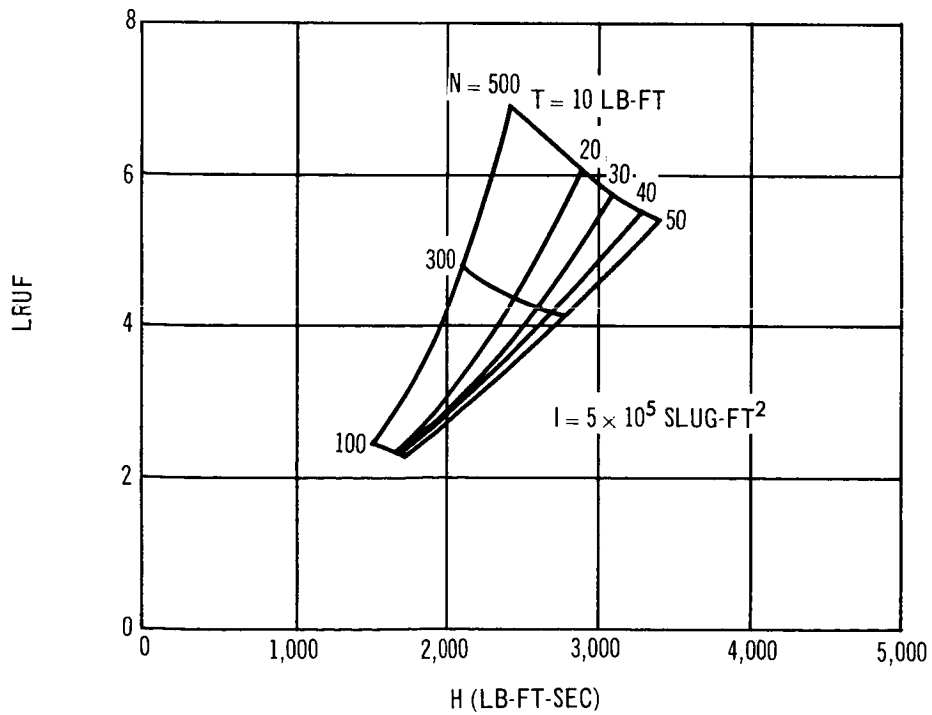
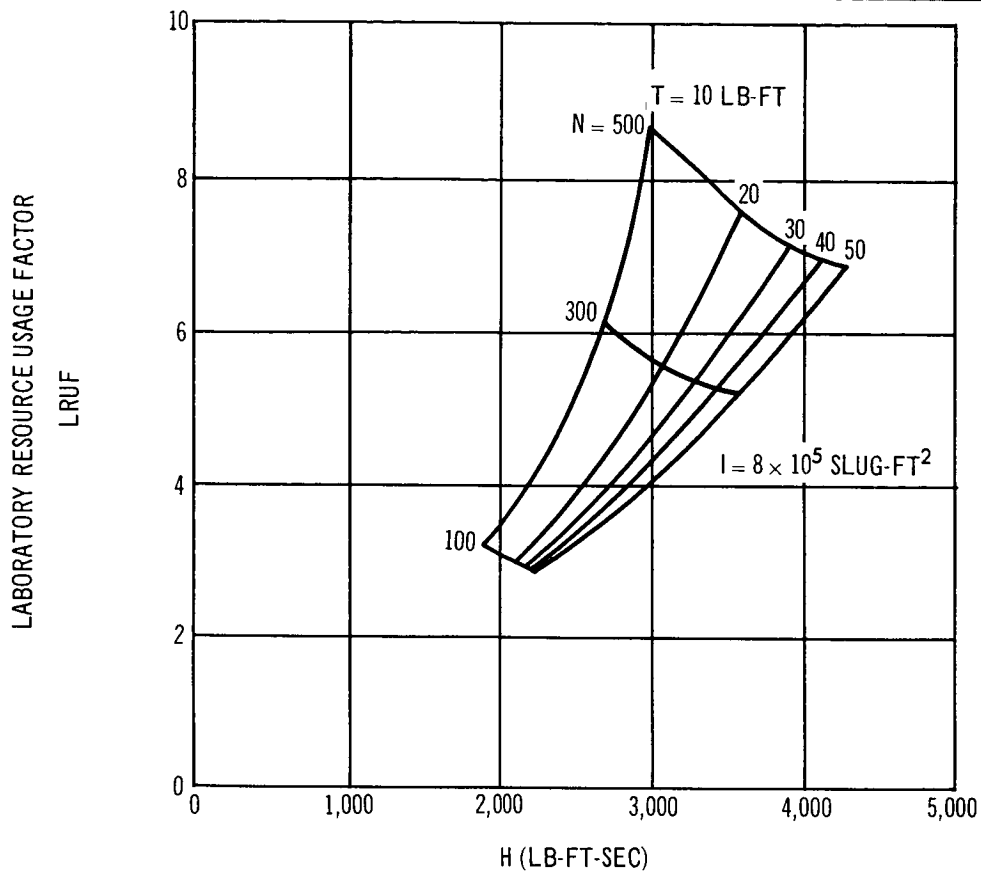


Figure A-41. Resource Usage for CMG Roll Maneuvers

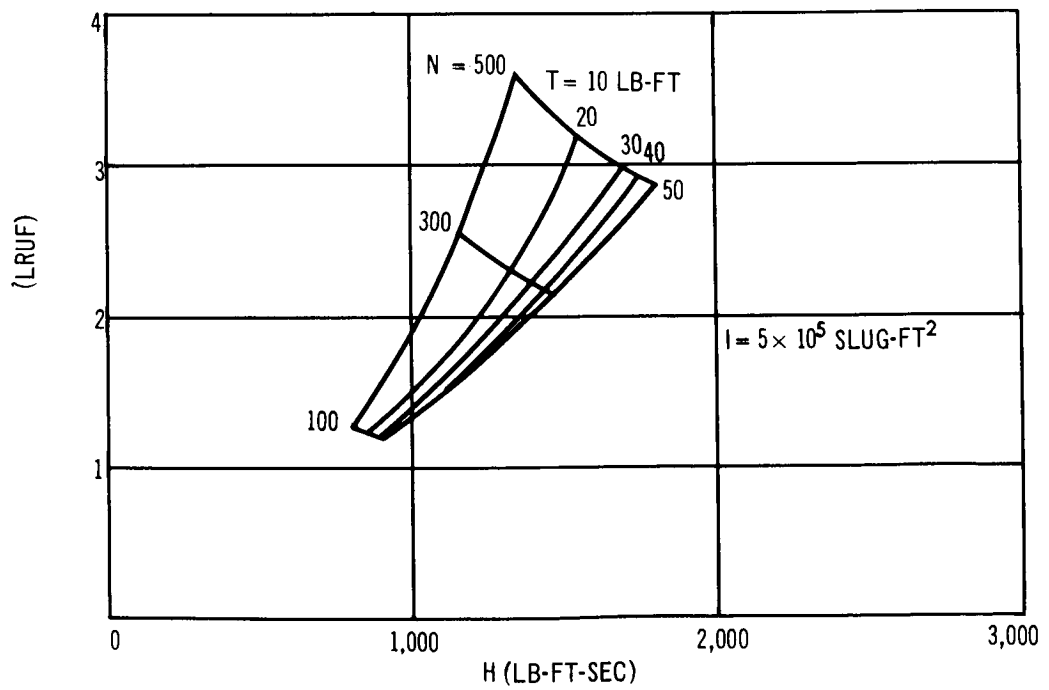
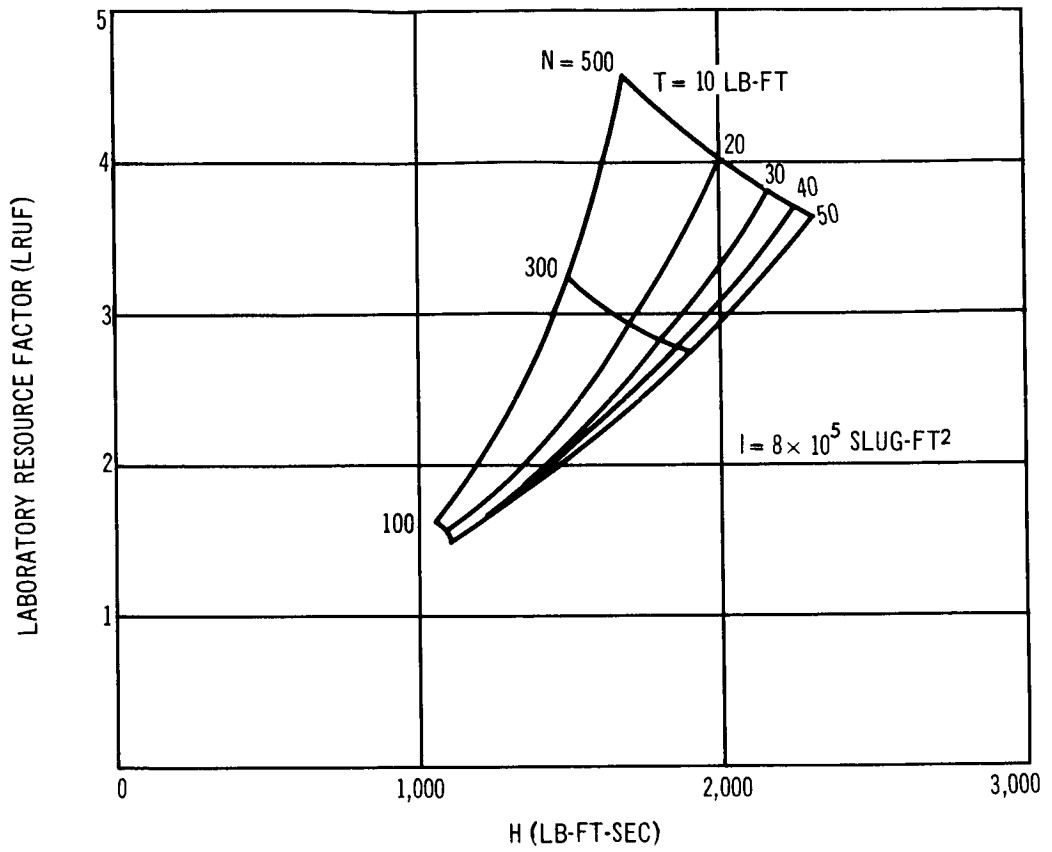


Figure A-42. Resource Usage for CmG Roll Maneuvers

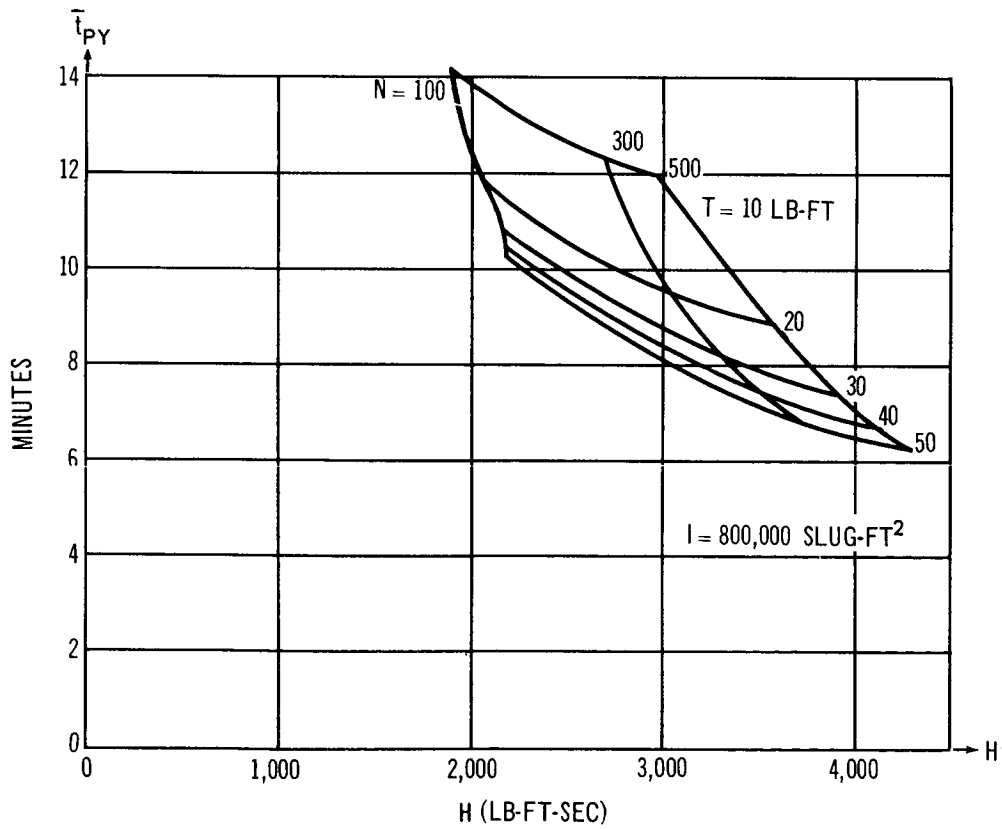
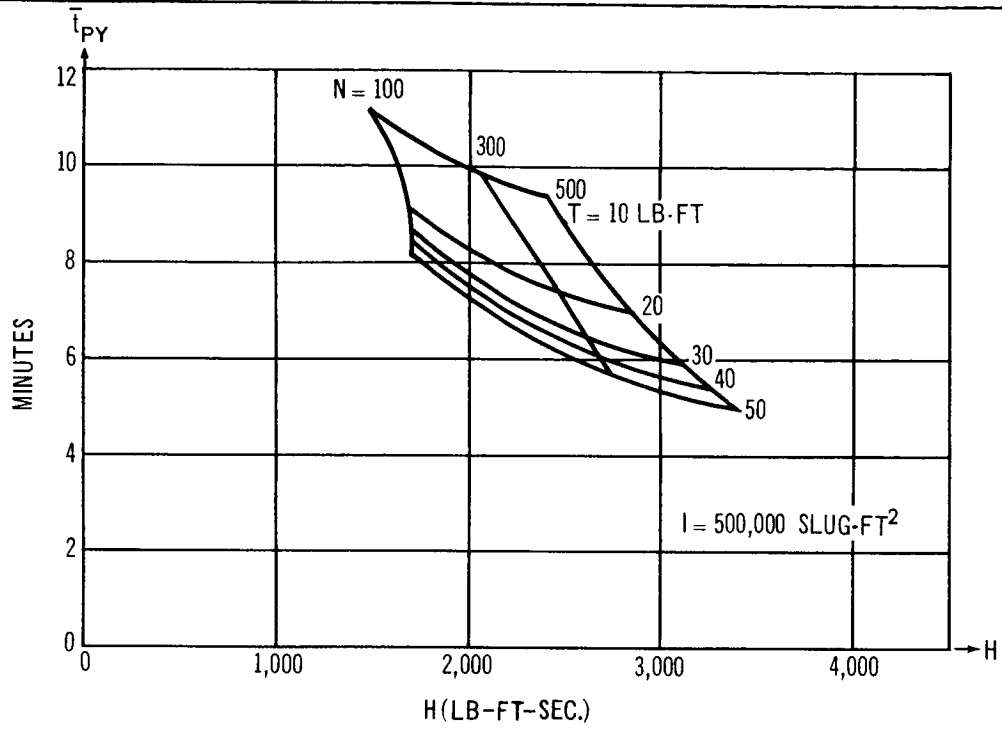


Figure A-43. Expected Time Per CMG Pitch-Yaw Maneuver

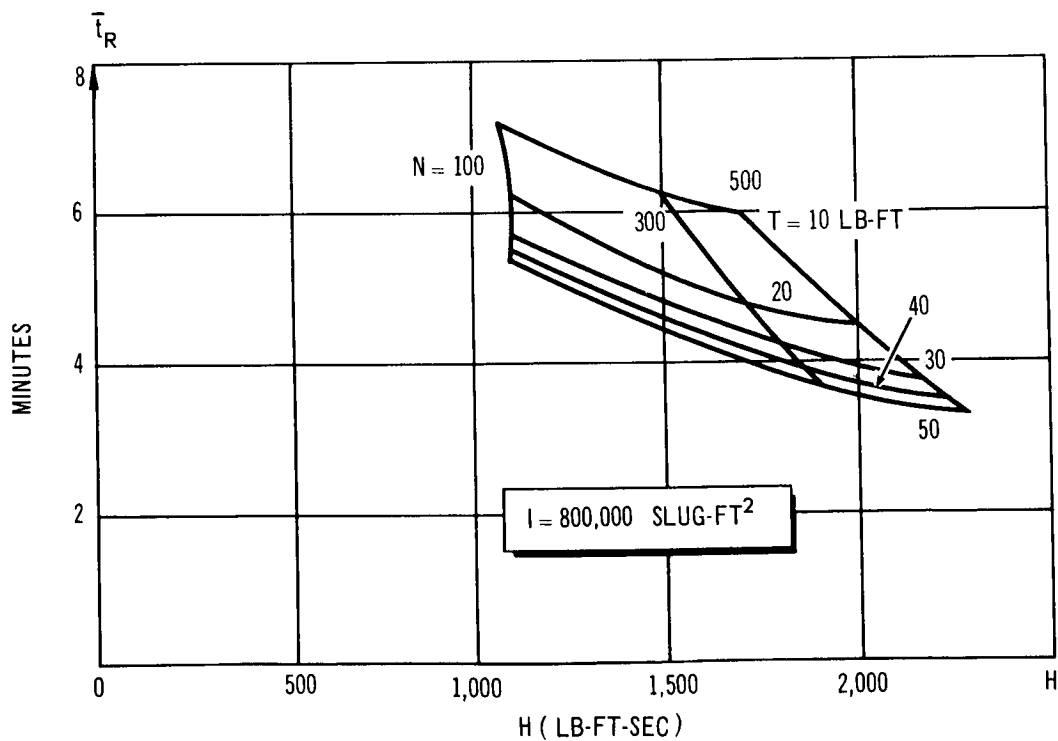
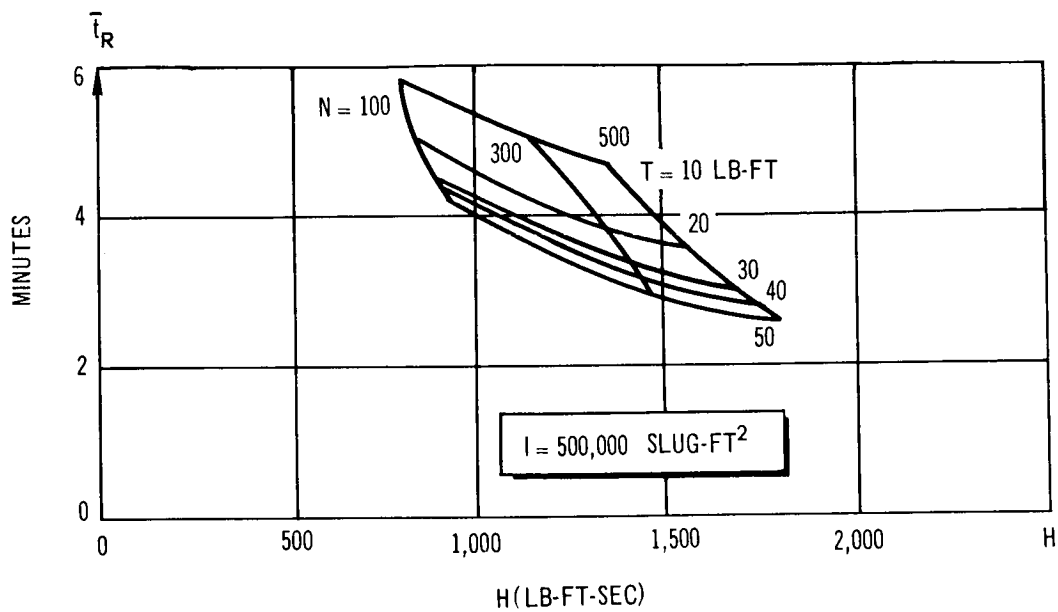


Figure A-44. Expected Time Per CMG Roll Maneuver

value, since the rate of decrease in maneuver time per unit of available torque is increased, and tends toward a constant value in the neighborhood of 50 lb-ft. This is further illustrated in Figure A-45.

The average operational time costs for reaction jet actuation were similarly computed as functions of jet actuation parameters and the possible number of maneuvers in the operational life. However, because of the much higher torques used with jet actuation, the time required to reach an optimum maneuver rate is negligible compared with the maneuver time. Hence, average cost is a function of impulse only, and is practically independent of the torque. The CMG rate profile, illustrated in Figure A-46, is shown to be either a trapezoid or a triangle, depending on whether torque reversal has been applied after or before the limiting angular momentum has been reached. For all practical purposes the jet profiles will be rectangular pulses; the acceleration times will be very small compared to the coast intervals for virtually the entire range of maneuver angles. These assumptions about the jet profiles ignore dynamic transients, which is justified when the required assumptions in modeling the maneuver statistics is considered.

The average operational time costs for jet actuation depend only on the available angular momentum,  $H$ , and the number of maneuvers,  $N$ . To develop data for comparing CMG and jet actuation, these costs were minimized with respect to  $H$ , and a linear relationship between cost and time and between propellant weight and angular momentum was assumed.

As indicated in Figures A-41 and A-42, the optimized angular momentum for the CMG is dependent on  $N$  and  $T$ , as well as  $I$ , the vehicle inertia. Figure A-47 compares the minimized costs for the jet and CMG actuation, with the CMG torque set at 50 lb-ft.

The results of this study indicate that, for a total of 100 pitch and yaw maneuvers, the optimum angular momentum and torque for the DG CMG using the minimum cost criteria, are 2,200 lb-ft-sec and 50 lb-ft (25 lb-ft/torque), respectively. The total angular momentum for the DG CMG is the maneuver requirement plus the disturbance requirement, or  $2,200/2 + 910/2 \sin 60^\circ = 1,625$  lb-ft-sec per gyro. The comparison of costs of the pitch-yaw

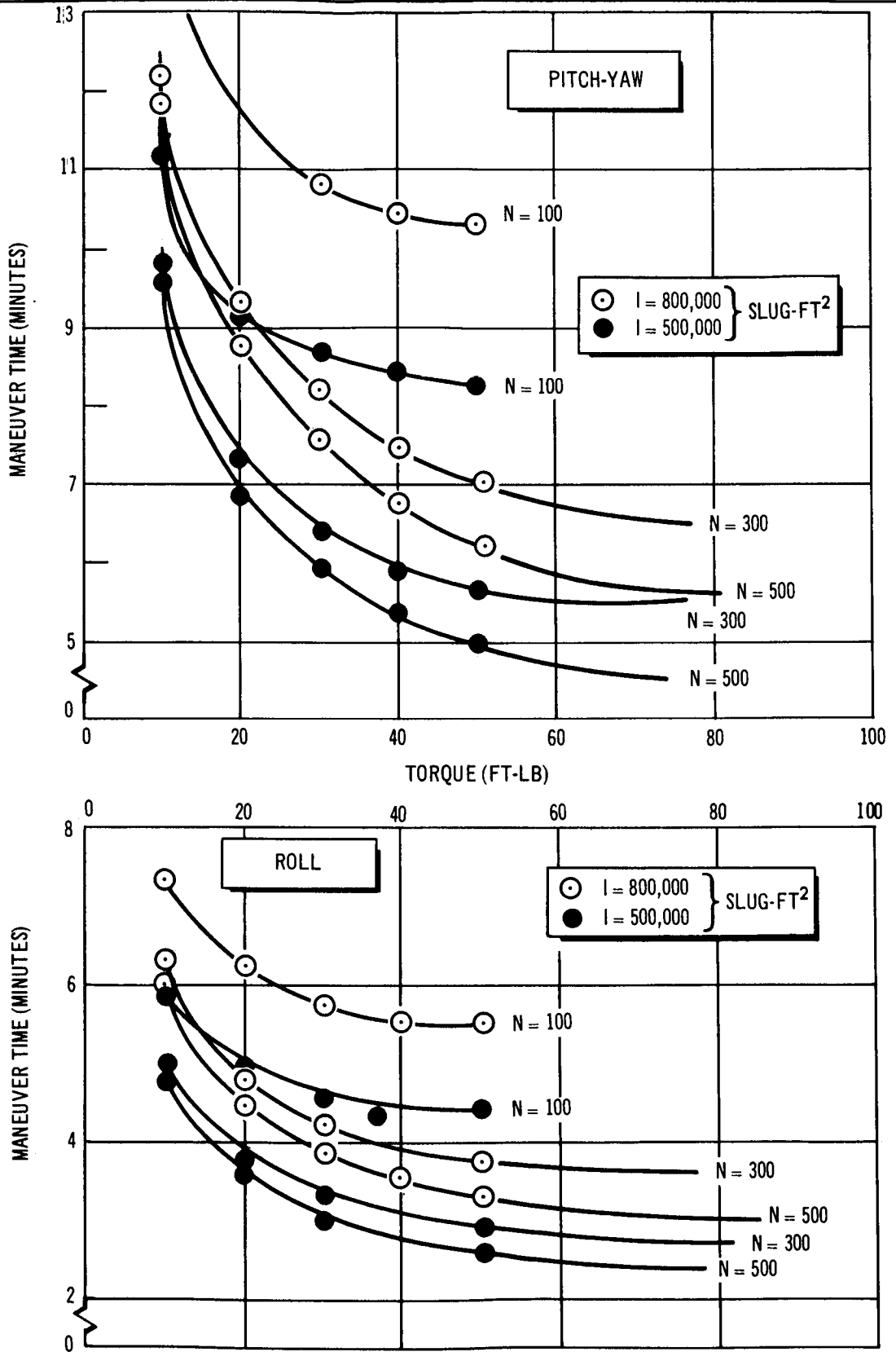


Figure A-45. Time for Minimum Cost Maneuver as a Function of Torque



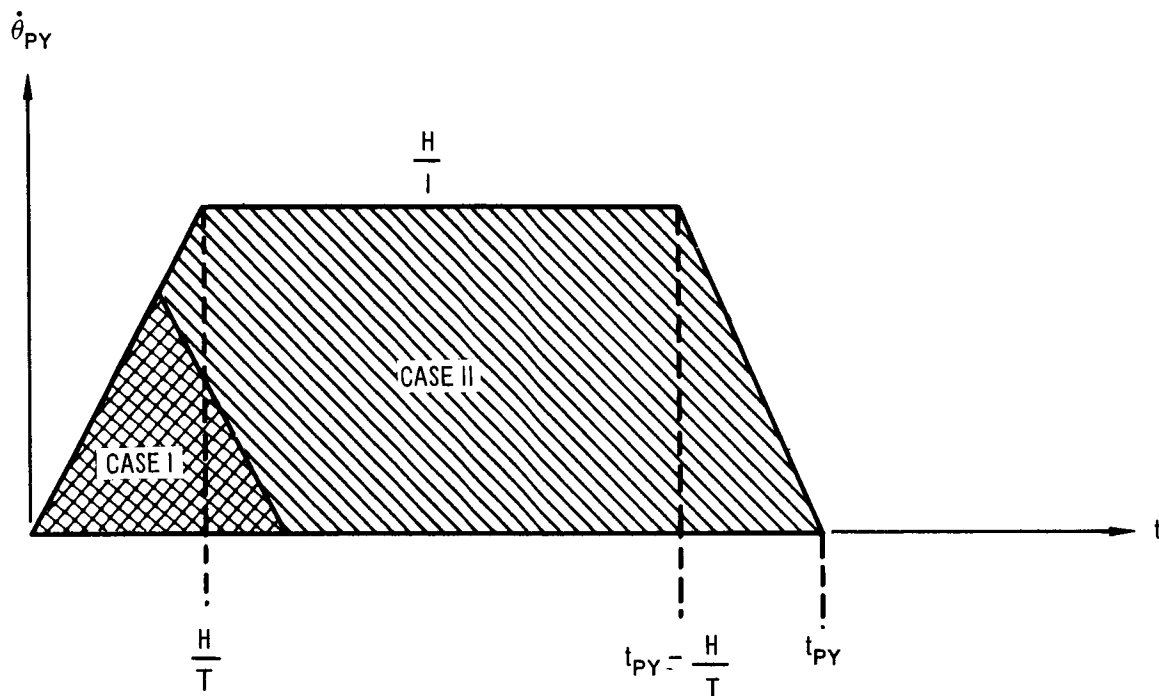


Figure A-46. Two Cases of Angular Rate Profiles

maneuver performed with CMG and with jets indicates that for more than 75 pitch-yaw maneuvers, the CMG costs less.

The angular momentum sizing for the SG CMG of the roll axis is determined from the centrifuge requirement and the external disturbances. The maneuvering capability is determined by assuming the centrifuge will not be in operation during the roll maneuver. The SG CMG are sized at 1,790 lb-ft-sec per gyro with a 25 lb-ft capacity per torquer. The comparison of costs of the roll maneuver performed with CMG and with jets indicates that for more than 275 roll maneuvers, the CMG cost less.

### A. 3. 2 Attitude Maneuver Statistical Models

Pitch and yaw, and roll maneuvers are discussed in the following subsections.

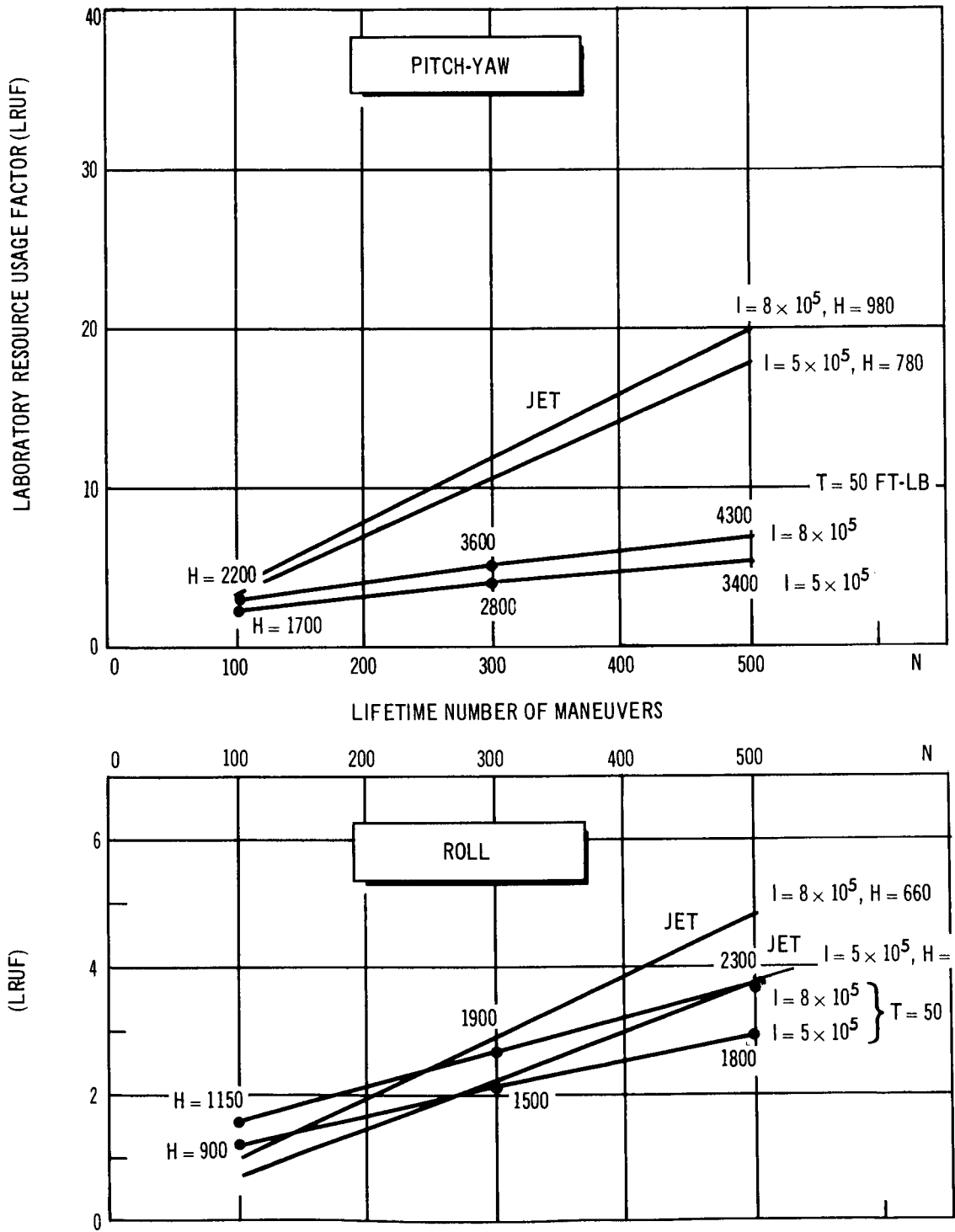


Figure A-47. CMG and Jet Actuation Usage Factor Comparison

### A. 3. 2. 1 Pitch and Yaw Maneuvers

Pitch and yaw rotations of the vehicle, as provided by two DG CMG, are considered to be combined into one rotation,  $\theta_{py}$ , about some resultant axis, which will take the vehicle from any pointing direction to any other pointing direction. If these pointing directions are equally probable throughout a unit sphere, then the probability of a vehicle rotation with the limits,  $\theta_{py}$  and  $\theta_{py} + d\theta_{py}$ , is  $dA/A$ , where  $dA$  is the area of the spherical zone subtended by the central angles,  $\theta_{py}$  and  $\theta_{py} + d\theta_{py}$ , and  $A$  is the area of a unit sphere. In terms of the probability density function,

$$p_1(\theta_{py}) d\theta_{py} = \frac{dA}{A} = \frac{\pi \sin \theta_{py}}{2} d\theta_{py}$$

or

$$p_1(\theta_{py}) = \begin{cases} \frac{1}{2} \sin \theta_{py} & , 0 \leq \theta_{py} \leq \pi \\ 0 & , \text{for } \theta_{py} \text{ elsewhere} \end{cases} \quad (\text{A-60})$$

It is noted that, if the rotations are performed about resultant axes to exclude superfluous rotation, the magnitude will be bounded by 0 and  $\pi$  radians. If in addition it is recognized that the probability density in time for the pitch-yaw rotation,  $p_2(t_{py})$ , is required, and for which only positive maneuver times are admissible, then Equation A-60, which excludes negative rotations, will correctly map the time probability density.

The mapping constraint is provided by a model of angular rate as a function of time. Two cases must be considered, as shown in Figure A-46. Case 1 specifies a maneuver angle,  $\theta_{py}$ , small enough so that the CMG spends the first half of the maneuver time accelerating, and the second half decelerating the vehicle. Neglecting dynamic details, the vehicle rate profile is a triangle with an area equal to the maneuver angle. In terms of maneuver time,  $t_{py}$ , vehicle inertia,  $I$ , and control torque,  $T$  (assumed equal to delivered torque),

$$\theta_{py} = \frac{T}{4I} t_{py}^2 \quad (\text{Case 1}) \quad (\text{A-61})$$

Which is the case for  $t_{py} \leq 2H/T$  or  $\pi \leq H^2/IT$ .

Case 2 is, of course, where  $\theta_{py}$  is large enough so that the accelerating and decelerating periods are separated by a coasting period in which the vehicle angular rate is  $H/I$ . The vehicle rate profile is then a trapezoid, from which it is easily shown that

$$\theta_{py} = \frac{H}{I} \left( t_{py} - \frac{H}{T} \right) \quad (\text{Case 2}) \quad (\text{A-62})$$

$$\text{for } t_{py} \geq \frac{2H}{T} \text{ or } \pi \geq \frac{H^2}{IT}$$

Using the mapping theorem for a single valued functional relationship

$$p_2(t_{py}) = p_1 \left\{ \theta_{py}(t_{py}) \right\} \left| \frac{d\theta_{py}}{dt_{py}}(t_{py}) \right| \quad (\text{A-63})$$

The probability density in pitch-yaw maneuver time for the two cases is then

$$p_2(t_{py}) = \begin{cases} 0, & \text{for } t_{py} \leq 0 \\ \frac{T}{4I} \sin \left[ \frac{T}{4I} t_{py}^2 \right] t_{py}, & 0 \leq t_{py} \leq \sqrt{\frac{4\pi I}{T}} \\ 0, & t_{py} \geq \sqrt{\frac{4\pi I}{T}} \end{cases} \quad \text{Case 1} \left( \pi \leq \frac{H^2}{IT} \right) \quad (\text{A-64a})$$

$$p_2(t_{py}) = \begin{cases} 0, & \text{for } t_{py} \leq 0 \\ \frac{T}{4I} \sin \left[ \frac{T}{4I} t_{py}^2 \right] t_{py}, & 0 \leq t_{py} \leq \frac{2H}{T} \\ \frac{H}{2I} \sin \left[ \frac{H}{T} \left( t_{py} - \frac{H}{T} \right) \right], & \frac{2H}{T} \leq t_{py} \leq \frac{H}{T} + \pi \frac{I}{H} \\ 0, & t_{py} \geq \frac{H}{T} + \pi \frac{I}{H} \end{cases} \quad \text{Case 2} \left( \pi \geq \frac{H^2}{IT} \right) \quad (\text{A-64b})$$

### A. 3. 2. 2 Roll Maneuvers

Roll maneuvers away from belly-down orientation are provided by two SG CMG. It is assumed that each roll rotation, the purpose of which is to support the aiming of instruments at Earth targets, is followed by an equal and opposite rotation to return the vehicle to the belly-down orientation before initiating the next rotation. Also, the limits of these rotations are  $\pm\bar{R} = \pm 75^\circ = \pm 1.31$  radians. Without more detailed information it is plausible to assume a roll probability density function which is an isosceles triangle, with apex at  $R = 0^\circ$ , and cutoffs at  $\pm\bar{R}$ . This simply reflects the assumption that the relative frequency of Earth targets decreases proportionally with the roll angle away from nadir. However, for the purpose of obtaining the roll time probability density, negative roll angles are excluded and, from the symmetry of the physical roll statistics, the mathematical roll model assumed is:

$$p_3(R) = \begin{cases} 0, & R \leq 0 \\ \frac{2}{\bar{R}} \left( 1 - \frac{R}{\bar{R}} \right), & 0 \leq R \leq \bar{R} \\ 0, & R \geq \bar{R} \end{cases} \quad (\text{A-65})$$

This is a right triangle, with apex at  $R = 0$ , and cutoff at  $R = \bar{R}$ .

By the same arguments used for the pitch-yaw maneuver, two cases are considered:

$$R = \frac{T}{4I} t_r^2 \quad \text{Case 1} \left( \bar{R} \leq \frac{H^2}{IT} \right) \quad (\text{A-66a})$$

$$R = \frac{H}{I} \left( t_r - \frac{H}{T} \right) \quad \text{Case 2} \left( \bar{R} \geq \frac{H^2}{IT} \right) \quad (\text{A-66b})$$

By the use of the mapping theorem in Equation (A-63), the probability density in the time of the roll maneuver,  $t_r$ , is then

$$p_4(t_r) = \begin{cases} 0, & \text{for } t_r < 0 \\ \frac{T}{\bar{R}I} \left( 1 - \frac{T}{4\bar{R}} t_r^2 \right) t_r, & 0 < t_r < \sqrt{\frac{4\bar{R}I}{T}} \\ 0, & t_r > \sqrt{\frac{4\bar{R}I}{T}} \end{cases}$$

Case 1  $\left( \bar{R} \leq \frac{H^2}{IT} \right)$  (A-67a)

$$p_4(t_r) = \begin{cases} 0, & \text{for } t_r < 0 \\ \frac{T}{\bar{R}I} \left( 1 - \frac{T}{4\bar{R}} t_r^2 \right) t_r, & 0 < t_r < \frac{2H}{T} \\ \frac{2H}{\bar{R}I} \left[ 1 + \frac{H}{\bar{R}I} \left( \frac{H}{T} - t_r \right) \right], & \frac{2H}{T} < t_r < \frac{H}{T} + \bar{R} \frac{I}{H} \\ 0, & t_r > \frac{H}{T} + \bar{R} \frac{I}{H} \end{cases}$$

Case 2  $\left( \bar{R} \geq \frac{H^2}{IT} \right)$  (A-67b)

### A. 3. 3 CMG Averages for the Two Statistical Models

Since the cost in laboratory operational time is assumed to be proportional to maneuver time, the average cost per maneuver is proportional to the average time per maneuver. Hence, if  $k_1$  is the cost penalty (in dollars) per unit operational time,  $\bar{t}_{py}$  and  $\bar{t}_r$  are the average times per maneuver for the pitch-yaw and roll maneuvers, and  $N$  is the number of maneuvers performed during the laboratory lifetime, then the average lifetime costs of these maneuvers are  $Nk_1 \bar{t}_{py}$  and  $Nk_1 \bar{t}_r$ .

Also, the cost associated with the angular momentum requirement must be added. Design experience indicates that, above a certain value, CMG equipment weight increases roughly linearly with available angular momentum, and in turn that the cost attached to this weight increases linearly. The cost attached to available angular momentum is therefore approximately linear. Evaluations for the CMG angular momentum constant,  $k_2$ , as well as the operational time constant,  $k_1$ , are given in Subsection A. 4. 5. In terms of CMG parameters, the total expected costs for the pitch-yaw and the roll maneuvers are

$$\left. \begin{aligned} \bar{C}_{py} &= Nk_1 \bar{t}_{py} (H, T, I) + k_2 H \\ \bar{C}_r &= Nk_1 \bar{t}_r (H, T, I) + k_2 H \end{aligned} \right\} \quad (A-68)$$

It should be noted that while the proposed pitch-yaw actuation uses two double-gimbaled CMG and the roll actuation uses two single-gimbaled SG CMG, the angular momentum cost constants indicated in Equation (A-68) for the two types of maneuvers are the same. This cost accounting shows that only those costs above CMG use (to cope with internal and external disturbances) are chargeable to maneuvers. Design studies indicate that for a given angular momentum, the DG CMG weighs about 30 lb more than the SG CMG, and weights for both increase nearly linearly and at the same slope for spin angular momentum beyond 1, 000 lb-ft-sec. The difference in weights would be reflected as a difference in CMG stabilization costs, while, because of equal slopes for the double- and single-gimbal versions, the weight cost increments chargeable to the maneuvers for the two versions would be the same.

The average time per maneuver is the first moment of the probability density

$$\bar{t} = \int_0^{\infty} t p(t) dt \quad (A-69)$$

Substituting Equation (A-69) into Equations (A-64a), (A-64b), (A-67a), and (A-67b),

$$\begin{aligned} \bar{t}_{py} \text{ (minutes)} &= \frac{2\pi^2}{60} \sqrt{\frac{\pi I}{T}} \left\{ \frac{1}{5 \times 1!} - \frac{\pi^2}{9 \times 3!} + \frac{\pi^4}{13 \times 5!} - \frac{\pi^6}{17 \times 7!} + \dots \right\} \\ &= \frac{2.393}{60} \sqrt{\frac{I}{T}} \\ &\quad \text{Case 1} \left( \pi \leq \frac{H^2}{IT} \right) \end{aligned} \tag{A-70a}$$

$$\begin{aligned} \bar{t}_{py} &= \frac{2H^5}{60I^2 T^3} \left\{ \frac{1}{5 \times 1!} - \frac{1}{9 \times 3!} \left( \frac{H^2}{IT} \right)^2 + \frac{1}{13 \times 5!} \left( \frac{H^2}{IT} \right)^4 \right. \\ &\quad \left. - \frac{1}{17 \times 7!} \left( \frac{H^2}{IT} \right)^6 + \dots \right\} \\ &\quad + \frac{1}{60 \times 2} \left\{ \frac{I}{H} \left[ \pi - \sin \left( \frac{H^2}{IT} \right) \right] + \frac{H}{T} \left[ 1 + 2 \cos \left( \frac{H^2}{IT} \right) \right] \right\} \\ &\quad \text{Case 2} \left( \pi \geq \frac{H^2}{IT} \right) \end{aligned} \tag{A-70b}$$

$$\bar{t}_r \text{ (minutes)} = \frac{1}{60} \times \frac{16}{15} \sqrt{\frac{\bar{R}I}{T}}$$

$$\text{Case 1} \left( \bar{R} \leq \frac{H^2}{IT} \right) \tag{A-71a}$$

$$\bar{t}_r = \frac{1}{60} \frac{H}{T} \left[ \frac{1}{15} \left( \frac{H^2}{\bar{R}IT} \right)^2 - \frac{1}{3} \left( \frac{H^2}{\bar{R}IT} \right) + 1 + \frac{1}{3} \left( \frac{\bar{R}IT}{H^2} \right) \right]$$

$$\text{Case 2} \left( \bar{R} \geq \frac{H^2}{IT} \right) \tag{A-71b}$$

The CMG average costs for the two cases applied to both pitch-yaw and roll maneuvers were obtained by substituting the maneuver time averages into



Equation (A-68) and programming the combined formulations into a computer. Average costs for pitch-yaw and roll were thus tabulated first as functions of four independent variables (N, H, T, I). Average minimum costs were then derived by adjusting H for a given N, T, and I, the results of which are indicated in Figures A-41 and A-42.

#### A. 3. 4. Jet Averages for the Two Statistical Models

As previously stated, it is assumed that the reaction jet torque and available angular momentum result in a vehicle angular rate profile which is practically rectangular, as would be the case for opposite torque impulses at the beginning and end of the maneuver. In this case the probability densities in pitch-yaw, and roll maneuver times are

$$P_{2j}(t_{py}) = \begin{cases} 0, & \text{for } t_{py} \leq 0 \\ \frac{H}{2I} \sin \left[ \frac{H}{T} t_{py} \right], & 0 \leq t_{py} \leq \pi \frac{I}{H} \\ 0, & t_{py} \geq \pi \frac{I}{H} \end{cases} \quad (\text{A-72})$$

$$P_{4j}(t_r) = \begin{cases} 0, & \text{for } t_r \leq 0 \\ \frac{2H}{\bar{R}I} \left( 1 - \frac{Ht_r}{\bar{R}I} \right), & 0 \leq t_r \leq \frac{\bar{R}I}{H} \\ 0, & t_r \geq \frac{\bar{R}I}{H} \end{cases} \quad (\text{A-73})$$

The time averages per maneuver, using Equations (A-69), (A-72), and (A-73), are for pitch-yaw and roll

$$\bar{t}_{pyj} = \frac{\pi I}{2H} \quad (\text{A-74a})$$

$$\bar{t}_{rj} = \frac{\bar{R}I}{3H} \quad (\text{A-74b})$$

The average laboratory lifetime costs for the jet actuated maneuvers are

$$\bar{C}_{pyj} = N \left[ k_1 \bar{t}_{pyj} + k_{2py} H \right] \quad (A-75a)$$

$$\bar{C}_{rj} = N \left[ k_1 \bar{t}_{rj} + k_{2r} H \right] \quad (A-75b)$$

The accumulation of fuel cost as well as time cost for the laboratory life-time is reflected by the lifetime number of maneuvers,  $N$ , factoring into both kinds of costs. The two different angular momentum constants reflect the different torque lever arms for pitch-yaw and roll.

Combining Equations (A-74) and (A-75) and differentiating with respect to  $H$  results in the following optimization constraints:

$$\left. \begin{aligned} \hat{H}_{py} &= \sqrt{\frac{\pi k_1 I}{2k_{2py}}} \\ \hat{H}_r &= \sqrt{\frac{\pi k_1 I}{2k_{2r}}} \end{aligned} \right\} \quad (A-76a)$$

$$\left. \begin{aligned} \frac{\Delta}{C}_{pyj} &= N \sqrt{2\pi k_1 k_{2py} I} \\ \frac{\Delta}{C}_{rj} &= N \sqrt{2\pi k_1 k_{2r} I} \end{aligned} \right\} \quad (A-76b)$$

$$\left. \begin{aligned} \frac{\Delta}{t}_{pyj} &= \sqrt{\frac{\pi k_{2py} I}{2k_1}} \\ \frac{\Delta}{t}_{rj} &= \sqrt{\frac{\pi k_{2r} I}{2k_1}} \end{aligned} \right\} \quad (A-76c)$$

Numerical results for Equation (A-76b) are plotted as the straight lines in Figure A-47 for the two inertias.

### A. 3.5 Deterministic Optimum Jet Maneuver Rates

A single-axis attitude maneuver which uses rate-limiting consists of a thrust-coast-thrust sequence, provided external disturbances have a negligible effect over the maneuver interval. The cost of this maneuver is expressed in terms of vehicle resources, weight of propellant expended, and crew time. For any given maneuver, this cost is minimized with respect to the maneuver rate. Hence, the optimum maneuver rate for any single-axis attitude maneuver which uses jets can be determined.

The optimum maneuver rate for any given attitude maneuver is determined as follows: the total firing time,  $t_f$  (acceleration-deceleration), with zero initial rate is

$$t_f = \frac{2 I \omega_{LIM}}{TL} \quad (A-77)$$

where  $\omega_{LIM}$  = maneuver rate, and

Parameter	Case 1	Case 2
I (moment of inertia)	$0.41 \times 10^6 \text{ slug-ft}^2$	$0.71 \times 10^6 \text{ slug-ft}^2$
T (jet thrust)	100 lb	200 lb
L (jet lever arm)	8 ft	8 ft

The total maneuver time,  $t_m$ , is obtained by adding the coast time and firing time.

$$t_m = \frac{I \omega_{LIM}}{TL} + \frac{\theta_T}{\omega_{LIM}} \quad (A-78)$$

with  $\theta_T$  being the total maneuver angle,

The propellant consumption,  $W_p$ , in weight is obtained from Equation (A-77)

$$W_p = \frac{T t_f}{\sigma} = \frac{2 I \omega_{LIM}}{L \sigma} \quad (A-79)$$

where  $\sigma$  is the fuel specific impulse

The cost of a given maneuver is now expressed in terms of the vehicle resources, weight, and crew time. If  $k_1$  is the cost per pound of fuel in orbit and  $k_2$  is the cost per second of available crew time, the total maneuver cost,  $C_m$ , is given as

$$C_m = k_1 W_p + k_2 t_f = k_1 \frac{2 I \omega_{LIM}}{L \sigma} + k_2 \left( \frac{I \omega_{LIM}}{T L} + \frac{\theta_T}{\omega_{LIM}} \right) \quad (A-80)$$

By differentiating Equation (A-80) with respect to the maneuver rate,  $\omega_{LIM}$ , and setting it equal to zero, the optimum maneuver rate is obtained as

$$\omega_{LIM} = \left( \frac{k_2 \theta_T T L \sigma}{2 k_1 T I + k_2 I \sigma} \right)^{1/2} \quad (A-81)$$

Figure A-48 is a plot of the LRUF as a function of maneuver rate for a one radian attitude maneuver. The LRUF constant is essentially a ratio between the crew time and weight. These are given as  $k_1 = 1$  (LRUF/lb) and  $k_2 = 3.3$  (LRUF/sec). The two cases shown on the plot are for two different body inertias. Case 1 is for  $I = 0.41 \times 10^6$  slug-ft<sup>2</sup> and Case 2 is for  $I = 0.71 \times 10^6$  slug-ft<sup>2</sup>. The  $\sigma$  used for the propellant is 250 sec. Note that a rate higher than optimum yields less cost increase per unit error than does a rate lower than optimum.

### A. 3.6 Numerical Results and Conclusions

The operational time constant,  $k_1$ , was evaluated as \$1,050/min. following the estimate given in Douglas Report SM-46086.

The CMG angular momentum constant,  $k_2$ , was evaluated as follows:

$$k_2 H = 2k_w \Delta W \quad (A-82a)$$

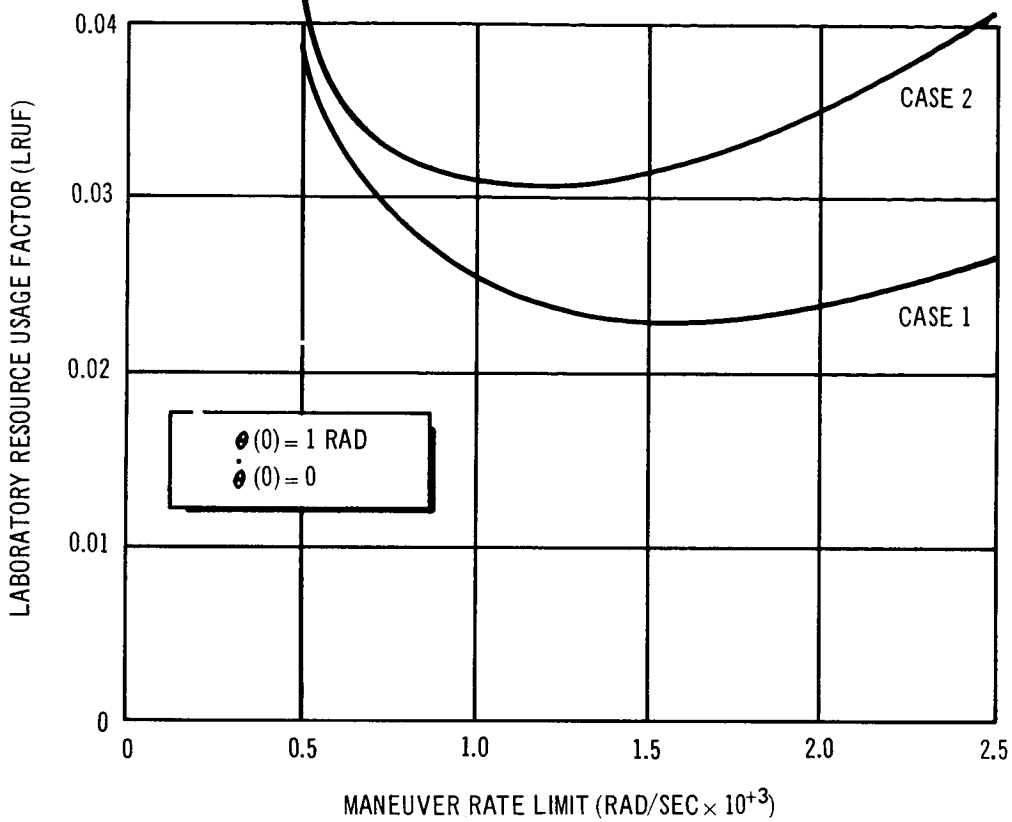


Figure A-48. Laboratory Resource Usage Factor as a Function of Jet Maneuver Rate

with the right side expressing cost in terms of weight increment,  $\Delta W$ , for one CMG. With  $\pm 60^\circ$  as the limits in gimbal angle excursion, each of the CMG with increased spin momentum,  $\Delta H_s$ , will increase its excursion range in available angular momentum,  $H/2$  by the following:

$$\frac{H}{2} = \cos 30^\circ \Delta H_s \quad (\text{A-82b})$$

hence

$$k_2 = \frac{k_w}{\cos 30^\circ} \frac{\Delta W}{\Delta H_s} \quad (\text{A-82c})$$

From Douglas Report SM-46068, with the following cost:

$$k_w = \$19,000/\text{lb}$$

$$\frac{\Delta W}{\Delta H_s} = \frac{0.038 \text{ lb}}{\text{lb-ft-sec}}$$

which yields

$$k_2 = \$836/\text{ft-lb-sec}$$

The following illustrates the evaluation of the jet angular momentum constants. Allowing for the requirement that the jets decelerate as well as accelerate the vehicle for each maneuver in which a coasting angular rate,  $H/I$ , is achieved, the fuel weight required,  $\Delta W_p$ , is

$$\Delta W_p = \frac{2H}{L\sigma} \quad (\text{A-83a})$$

where  $\sigma$  is the fuel specific impulse and  $L$  is the lever arm of the thrust impulse. The weight cost for the maneuver is  $k_w \times \Delta W_p$ . By definition

$$k_{2j} H = k_w \Delta W_p \quad (\text{A-83b})$$

hence

$$k_{2j} = \frac{2k_w}{L\sigma} \quad (\text{A-83c})$$

For pitch-yaw,

$$L_{py} = 8 \text{ ft}$$

For roll,

$$L_r = 10 \text{ ft}$$

The fuel specific impulse,

$$\sigma = 270 \text{ sec.}$$

The jet angular momentum cost constants for the two classes of maneuvers are the following:

$$k_{2py} = \frac{2k_w}{L_{py}\sigma} = \$17.50/\text{lb-ft-sec} \quad (\text{A-84})$$

$$k_{2r} = \frac{2k_w}{L_r\sigma} = \$14.00/\text{lb-ft-sec} \quad (\text{A-85})$$

With all constants evaluated, optimal evaluations for angular moment were obtained for the CMG and jet operations. For the CMG, the optimal H depends on N, T, and I. For the jet, optimal H depends only on I.

The recommended CMG parameters for the Phase IIb baseline are as follows:

DG CMG (pitch-yaw axes)--1,625 lb-ft-sec/gyro.

SG CMG (roll axes)--1,790 lb-ft-sec/gyro.

Torquer capacity for both sets of gyros--25 lb-ft/gimbal.

The optimized costs for jet and CMG operation are shown in Figure A-47. The CMG cost curves in this illustration correspond to the lowest cost curves in Figures A-41 and A-42 (which contain the points A, B, and C at torque equal to 50 lb-ft). The indicated values of optimal H are within 100 lb-ft-sec of theoretical values. Crossovers of CMG and jet cost curves for both inertias occur at about 275 roll maneuvers, and for the pitch-yaw maneuvers, the crossovers (not indicated) are at about 75.

The hypothetical model for pitch-yaw limits rotations to 180°, while roll rotations are limited to 75°. For the distributions assumed, the average pitch-yaw rotation is 90° while for roll the average is 25°. The much greater divergence of the two costs for pitch-yaw as N increases reflects its much greater average angular rotation.

From a resource usage point of view, it appears that CMG actuation for maneuver requirements is favored over jets for missions requiring more than 275 roll maneuvers (aimed at Earth target surveillance) and for

missions requiring more than about 75 large angle rotations (aimed at astronomical objects). However, since the roll axis CMG are sized for centrifuge control, use of these CMG for maneuvering when the centrifuge is not operating is preferred over using the RCS jets.

#### A.4 MANUAL CONTROL STUDIES

Analog simulation, together with machine-integrated display and operator control devices, were the analytical tools used to study the manual control of the MORL. The study areas included examination of critical mission events (Earth tracking) and of maneuvers using reaction jets and momentum storage devices. Only normal control situations were considered; emergency control operation was beyond the study. The three control philosophies studied were: (1) acceleration command, (2) rate command, and (3) command of a fixed pulse width jet firing.

##### A.4.1 Introduction

Various manual control options were evaluated in the light of the response time necessary to achieve a given result (defined in terms of angle and rate accuracy), the propellant consumed, and the number of reaction jet actuations needed. In general, the studies indicate that for response rates on the order of  $5.0^\circ$  to  $0.5^\circ$  per sec, response times, propellant consumption, and jet actuations are comparable for the various controller methods of operation, various displays, and for both 1-man and 2-man control. The primary exceptions are that fixed pulse width control (where the pulse width is set at either 1.0 or 2.0 sec) produces excessive response times for the 3-axis maneuvers considered, and that rate command operation yields minimum propellant consumption. The former study result was primarily from the fact that the minimum impulse chosen for the system was large. If very narrow pulse widths were used, a continual sequence of pulse width commands would be necessary for a minimum time maneuver, thus significantly increasing the number of reaction jet actuations. For a minimum propellant maneuver, a time period long with respect to the minimum time (but short with respect to the period associated with external disturbances) fixed pulse width command appeared to have a distinct advantage and should be given further consideration in future investigations.



The results also indicated that, as the control objectives are lowered to 0.5° and 0.05° per sec (the ratio of angular error to rate error was arbitrarily maintained at 10), 2-man control has a distinct performance and fatigue factor advantage over 1-man control, with the rate error limits being the more difficult to satisfy. In addition, operator fatigue for the 0.5° and 0.05°/sec end objective was appreciably less when rate commands were used in conjunction with the all-attitude display. Rate command operation also exhibited faster response and less fuel consumption than the on/off or fixed pulse width operation, but tended to result in more jet actuations. The latter could be minimized by the proper choice of control stick dead-band and a mechanical indication of zero.

#### A. 4. 2 Analog Simulation System Model Details

Details of the vehicle simulation, displays, and control mechanisms are presented below.

##### A. 4. 2. 1 Vehicle Model

The manual control simulation consisted of an analog computer simulation of the vehicle dynamics with meter and oscilloscope displays to one or two operators who activated the MORL reaction jets by means of stick or pushbutton controls.

The rotational equations of motion used in the MORL mathematical simulation were

$$\dot{\omega}_x = \frac{(I_y - I_z)}{I_x} \omega_y \omega_z + \frac{T_{jx}}{I_x}, \quad T_{jx} = F_x l_x \quad (A-86)$$

$$\dot{\omega}_y = \frac{(I_z - I_x)}{I_y} \omega_x \omega_z + \frac{T_{jy}}{I_y}, \quad T_{jy} = F_y l_y \quad (A-87)$$

$$\dot{\omega}_z = \frac{(I_x - I_y)}{I_z} \omega_x \omega_y + \frac{T_{jz}}{I_z}, \quad T_{jz} = F_z l_z \quad (A-88)$$

where  $F_x$ ,  $F_y$ ,  $F_z$  are the thrusts associated with on/off reaction jets.

The Euler angle equations were

$$\dot{\phi} = \omega_x + \dot{\psi} \sin \theta \quad (\text{A-89})$$

$$\dot{\theta} = \omega_y \cos \phi - \omega_z \sin \phi \quad (\text{A-90})$$

$$\dot{\psi} = \omega_z \cos \phi \sec \theta + \omega_y \sin \phi \sec \theta \quad (\text{A-91})$$

The parameters used in the simulation to represent MORL vehicle parameters were

$$I_x = 0.41 \times 10^6 \text{ slugs-ft}^2$$

$$I_y = 0.71 \times 10^6 \text{ slug-ft}^2$$

$$I_z = 0.50 \times 10^6 \text{ slug-ft}^2$$

$$l_x = 8 \text{ ft}$$

$$l_y = 8 \text{ ft}$$

$$l_z = 8 \text{ ft}$$

$$F_x = 100 \text{ lb}$$

$$F_y = F_z = 200 \text{ lb}$$

The following notation applies to the above equations:

$I_i$  = moment of inertia about the principal  $i^{\text{th}}$  axis

$\omega_i$  = body rate about the  $i^{\text{th}}$  axis

$T_{ji}$  = torque about the  $i^{\text{th}}$  axis due to jet thrust

$F_i$  = total thrust level of the jets producing torque about the  $i^{\text{th}}$  axis

$l_i$  = moment arm of the jets producing torque about the  $i^{\text{th}}$  axis

$\phi, \theta, \psi$  = standard Euler angles

$x, y, z$  = principal body axes

#### A. 4. 2. 2 X-Y Representation

The initial display used in the manual control study consisted of a 30 x 30 in. dual pen plotter. Two-axis monitoring was achieved by viewing an 8 x 8 in. cross plot of  $\psi$  and  $\theta$ , and control was provided by on/off reaction jets actuated by a two-degree-of-freedom control stick. Consistent operation with this display and control stick was achieved in a very short period of time; however, for the smaller values of control objectives, the display did not have sufficient resolution, and limit cycling occurred. The scaling on the display was then doubled (16 x 16 in. cross plot of  $\psi$  and  $\theta$ ). Limit cycling was eliminated in the case of the smaller thresholds and control became easier with the expanded display.

Three-axis control was also attempted with a second pen to display the roll angle,  $\phi$ , as a function of time. This proved to be a difficult operation because the necessary pen separations required the operator to sight back and forth between pens with a severe degradation in concentration and, therefore, performance.

#### A. 4. 2. 3 Attitude Rate and Angle Meters

Individual displays of body rates and attitude were obtained with voltmeters mounted on a display board. Integration of these meters into the all-attitude display is shown in Figure A-49. The rate meters displayed a maximum reading of  $\pm 2^\circ / \text{sec}$ . The attitude meters were nonlinear in that  $\pm 5^\circ$  required 30% of the available indicator deflection; the total display capability was  $\pm 90^\circ$ . The rate displays presented the operator with sufficient angular rate resolution to ensure that the more accurate control objectives could be achieved without excessive limit cycling. Using this display and a control stick that was not spring-loaded, both two- and three-axis control were possible with relative ease. However, additional practice was required by the operator for him to become familiar with the nonlinearities of the display.

Both on/off and rate command operations were studied with this display. Either system allowed both two- and three-axis control, after sufficient practice.

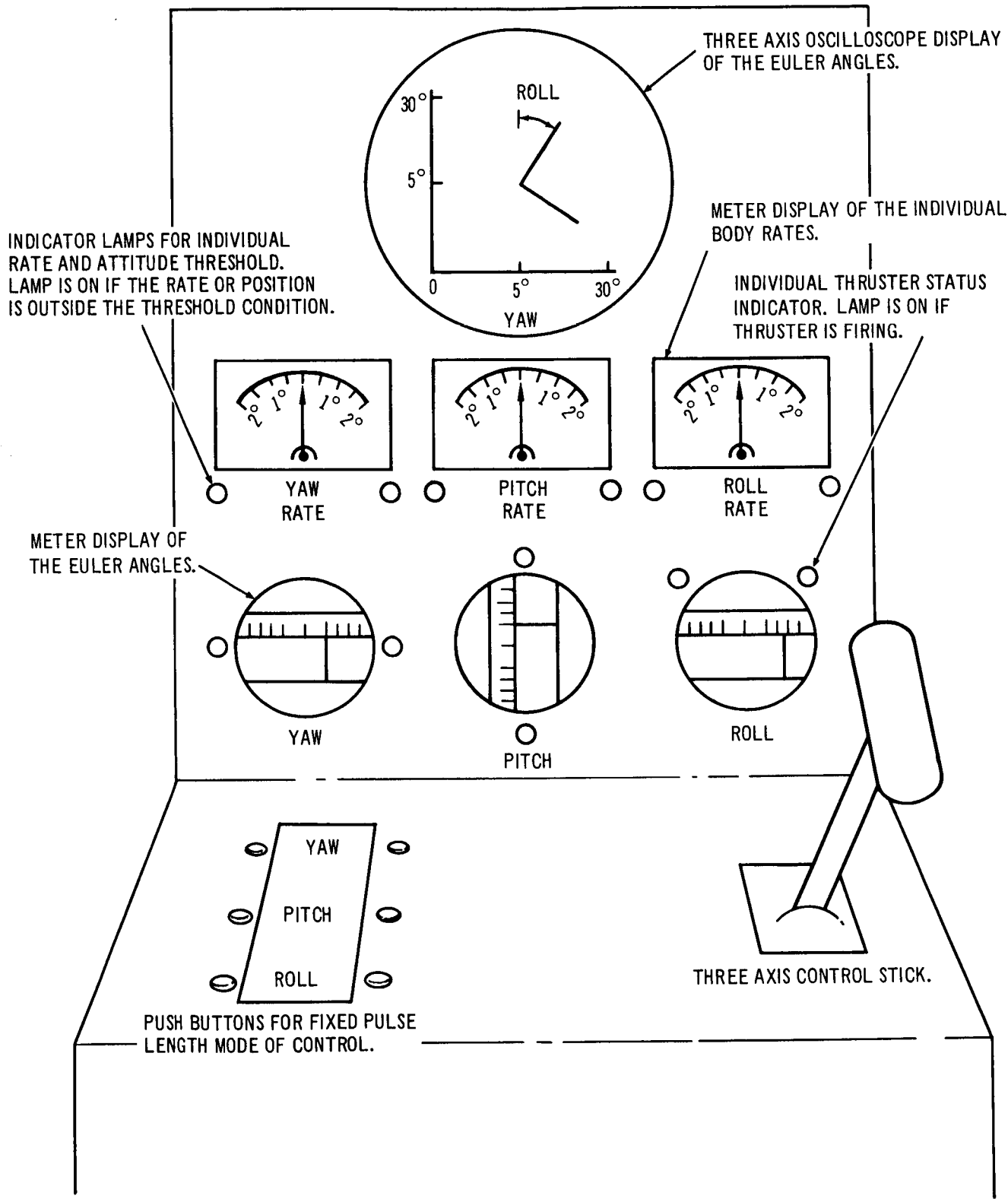


Figure A-49. MORL Control Simulator

The control stick used did not have a detent, and a zero rate command was sometimes difficult to detect. This difficulty increased as the accuracy of the control objective increased but can readily be eliminated with the addition of a small control stick dead-band and a mechanical indication of zero.

#### A. 4. 2. 4 All-Attitude Display Plus Rate Monitor

A 5-in. oscilloscope was the central presentation mechanism for the all-attitude display shown in Figure A-49. The angles  $\psi$  and  $\theta$  were proportional to the rotation of the monitored display axes. The operator had to align the displayed axes (as required by the control objective) with a fixed set of axes on the oscilloscope grid. Also included in this display were lights that indicated when the threshold conditions were satisfied as well as the on/off status of the reaction jets in each control channel. By having the three attitudes displayed on the oscilloscope, the operator could achieve greater concentration than with either of the previous displays. The inclusion of the threshold indicators also increased the ease of operation, since the operator no longer had to take time to determine which of the conditions remained to be satisfied near the end of a particular reorientation. As with the metered display, the attitude display was nonlinear with half of the total indicator deflection being equal to  $5^\circ$ .

Both on/off and rate command operations were investigated with the all-attitude display. In addition, pulses of fixed duration were commanded by pushbuttons mounted on the display. In this latter case, operator fatigue was significantly increased because of the number of commands required.

The conclusions reached are preliminary, and to a large extent intuitive, despite the large amount of simulation data obtained. To reach absolute conclusions, additional control and human factor considerations must be incorporated in the study. For example, in the case of one of the control operators, efficiency diminished noticeably during the latter part of the day, which in some cases required that data be taken only in the morning. This and similar human factors have not been fully considered in the simulation studies to date.

#### A. 4. 2. 5 The Two-Axis Control Stick as Compared to the Three-Axis Control Stick, with and without Artificial Feel

Two types of control sticks were used for the study. For the X-Y representation, a two-axis stick with a detent formed by spring action was used. For the scope and metered displays, the control stick had three-axis movement capabilities without detent. With the on/off control, the detent was advantageous, since the operator could rely on the stick to return to zero merely by releasing it. With the detent he could also apply short pulses by displacing the stick from zero a small amount, and then releasing it. In the case of the control stick without the detent, the operator had to monitor the thrust firing indicators to be sure he had the stick in the zero command position. For rate control, the stick with detent may not be as useful as the one without the detent. Here, the subject wanted to position the stick according to some corresponding rate and have it remain. The return springs of the stick with the detent require that the subject hold the control stick at the desired position. The stick without the detent will stay in any position until the operator repositions it.

#### A. 4. 3 Detailed Results and Conclusions of the Manual Control Study

Study results and conclusions are summarized below.

##### A. 4. 3. 1 Response Comparison

As previously noted, three types of controller operation were considered. Minimum time maneuvers were selected because they allow a direct and easy comparison of operator performance. Other comparisons (such as minimum fuel consumption within a specified time) are possible, but require a far more subtle assessment of manual dexterity. The rate command type of controller operation used rate commands proportional to stick deflection. The fixed pulse width controller used fixed-duration jet pulses initiated each time the control stick or pushbutton was deflected.

In comparing the various types of controller operation with the minimum time attitude maneuver, two operators were used and propellant consumption and response times were computed, based on the average of at least six

successive trials. In general, each set of trials was preceded by a brief training period so that the operator could become accustomed to the display and stick deflection characteristics.

The response time for a given trial was defined as the time to reach the desired control objective. The control objectives varied between  $5^\circ$  and  $0.5^\circ$  per sec, and  $0.5^\circ$  and  $0.05^\circ$  per sec. In every case, the control objectives were identical for each axis and the ratio of the angle objective to the rate objective was maintained at 10.

For all three-axis maneuvers, a control stick capable of two deflections and one rotation was used. This control stick was not spring-loaded (an advantage for rate command operation) and did not have any mechanical indication of zero so that monitoring was required to ensure that channels which had zero error did not receive any unintended commands. For two-man control about three axes, a second control stick for the roll channel was used. This control stick was spring-loaded, which gave the necessary artificial feel and eliminated any difficulty in centering the stick. This stick was awkward for three-axis control, however, since one channel was activated by a small thumb-actuated wheel set in the control stick. The three displays used were: (1) an X-Y plot of the pitch/yaw attitude angle trajectory plus an X-Y time history of roll angle, (2) a display in which both angles and body rates were displayed on meters, and (3) an all-attitude scope display in which the origin of an X-Y coordinate system traced the pitch/yaw attitude trajectory, and the rotation of the X-Y coordinate system was proportional to roll angle. In addition, the third display presented attitude angles and body rates on meters.

The detailed results of the comparison made between the various types of controller operation are shown in Figures A-50 through A-55 in terms of response times. Figure A-50 shows response time as a function of control objective for the on/off operation, the X-Y display, and for the various commands. Figure A-51 shows the same data for the metered display. As indicated by these results, the change in display had little effect, but the more accurate control objectives more than doubled response times in the three-axis case.

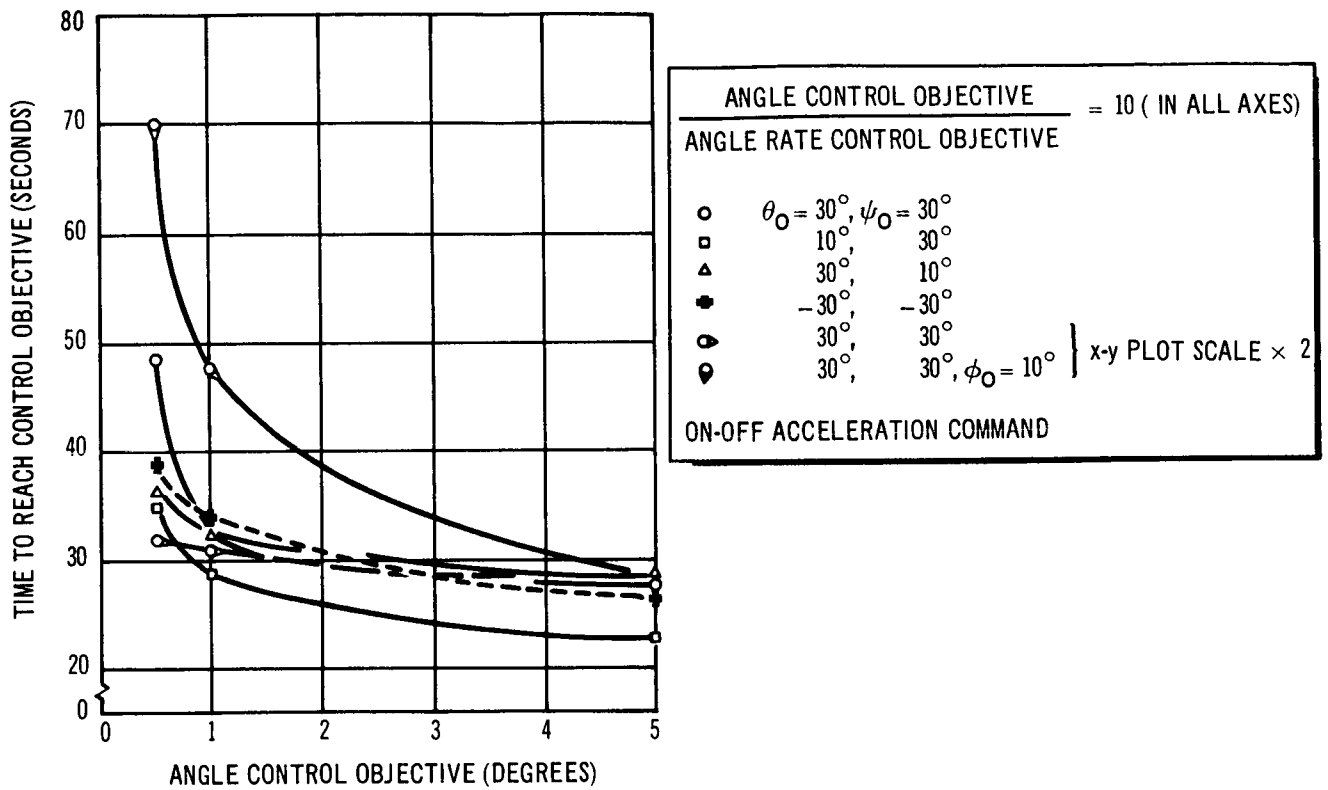


Figure A-50. Response Using Acceleration Command - x-y Display

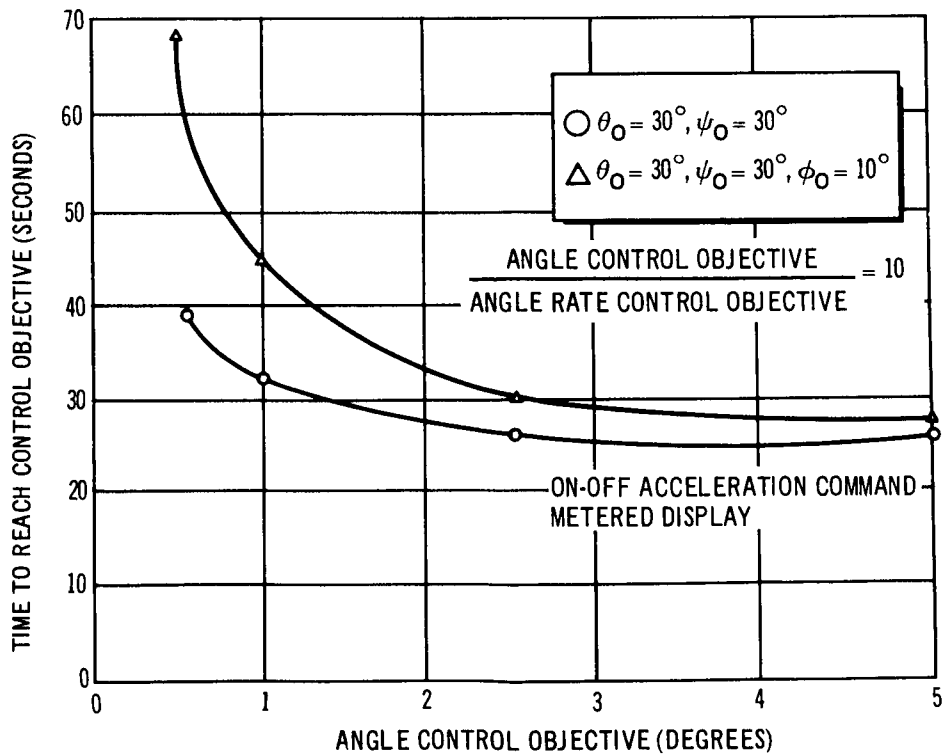


Figure A-51. Response Using Acceleration Command - Meter Display



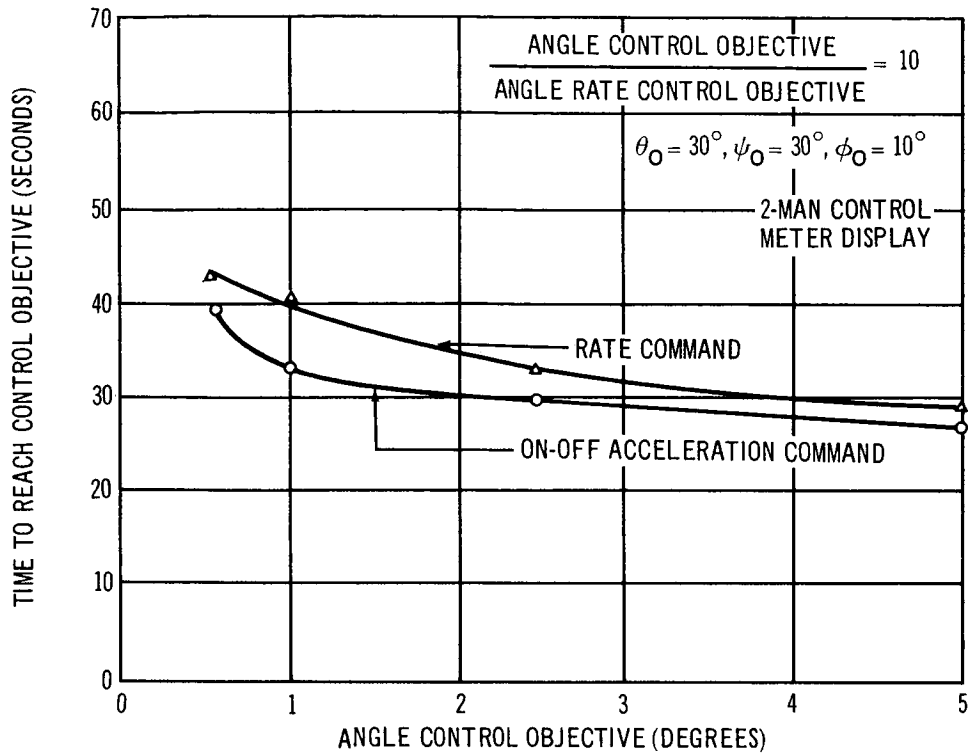


Figure A-52. Response Using Two-Man Control

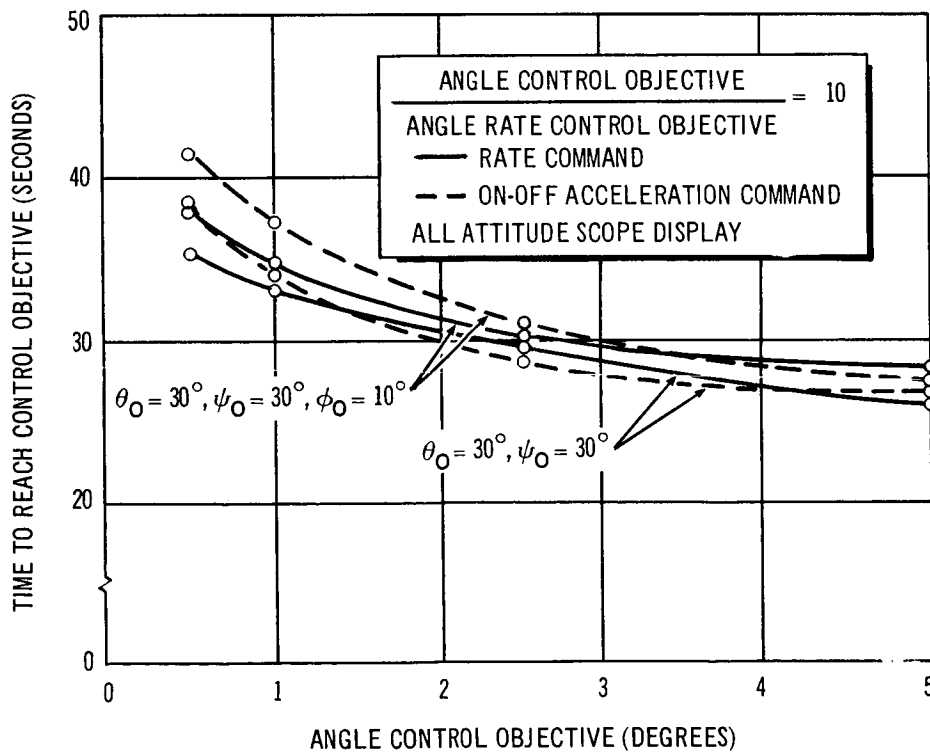


Figure A-53. Response Using All Attitude Display

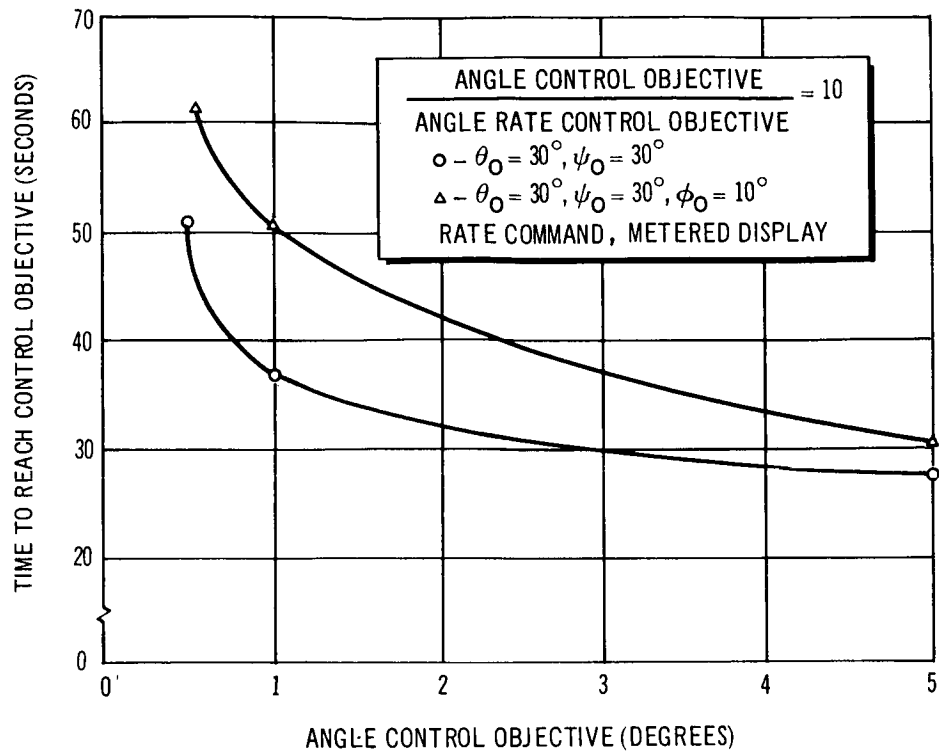


Figure A-54. Response Using Rate Command, Two-Man Control (3-Axis Maneuver)

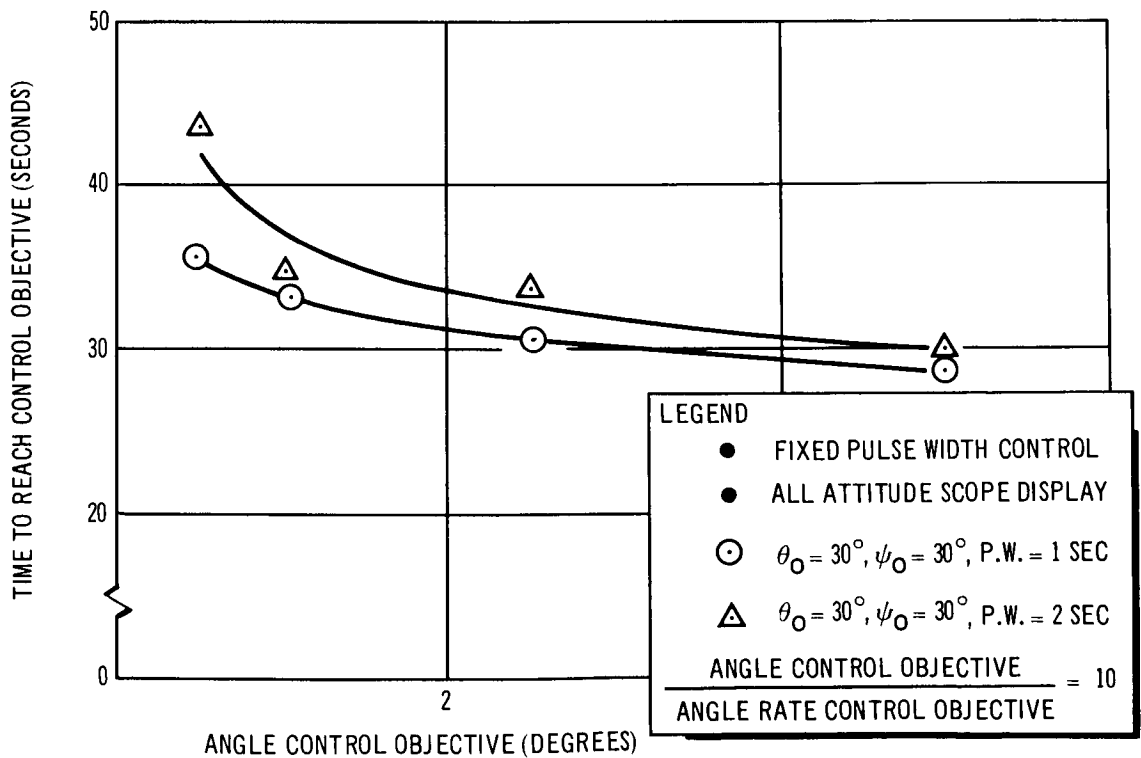


Figure A-55. Response Using Rate Command, Two-Man Control (2-Axis Maneuver)

In Figure A-52, the reduction in response time for on/off operation with two-man control for a three-axis maneuver is shown to be significant. It is also the only case where on/off operation had any advantage (however small) over rate command operation. However, two-man control produced less of an improvement when rate command operation was used, as seen from a comparison of Figures A-52 and A-54. As indicated in Figure A-53, rate command or on/off operation for a single operator three-axis maneuver using the all-attitude display resulted in a performance equivalent to that obtained with two-man control using the other displays.

In Figure A-55, the response times obtained with a fixed pulse width operation are shown for two-axis maneuvers only. For three-axis maneuvers, response times became excessive, primarily due to the selected pulse widths of 1.0 and 2.0 sec. These pulse widths were selected as a compromise between (1) very short pulse widths which require many actuations to achieve minimum time responses but are consistent with accurate control objectives, and (2) very long pulse widths which yield the desired body rates for minimum response time but are not consistent with accurate control objectives.

Based on the above results, it can be seen that rate command operation yielded a better response than on/off operation or fixed pulse width operation. In addition, the all-attitude display was selected, since it minimized operator fatigue and produced the best response achievable with each type of controller operation. It was also concluded that, with the all-attitude display, three-axis single operator maneuvers can be performed as well as two operator three-axis maneuvers which use the other displays.

#### A. 4. 3. 2 Propellant Consumption

Propellant consumption was determined for various types of controller operations, displays, and maneuvers and for both one- and two-man control. In general, the trends established for response times can be applied to propellant consumption with the single exception that the rate command system used significantly less propellant, independent of the type of maneuver or the control objective. This further enhances the desirability of using rate command operation as the primary manual control option. However, it is

emphasized that minimum time 3-axis attitude maneuvers are extremely costly in terms of propellant consumption (10 to 20 lb, depending on the control objective and the control option employed) and should be used only in emergency situations. This type of maneuver, however, provided a convenient yardstick for comparing control options and was used in the study for this purpose.

#### A. 4. 3. 3 Effect of the Control Objective

Control objectives ranged between  $5^\circ$  and  $0.5^\circ$  of angle and between  $0.5^\circ$  and  $0.05^\circ/\text{sec}$  in rate, with an angle-to-rate ratio of 10. In general, the rate objective appeared to be the more sensitive. This can be seen from the fact that for each second of firing about the Z axis, a body rate of approximately  $0.1^\circ/\text{sec}$  results. Therefore, to achieve a control objective of  $0.05^\circ/\text{sec}$  requires rapid operator response and inevitably results in a certain amount of limit cycling about this rate control objective. On the other hand, an angular accuracy of  $0.5^\circ$  requires only moderate operator response since approximately 3 sec of firing are required to produce this change in orientation (about the Z axis), assuming zero rate initially.

#### A. 4. 3. 4 Conclusions

These studies resulted in the following conclusions:

1. The one-man and two-man control studies exhibited comparable response times for control objectives on the order of  $5.0^\circ$  in attitude, and  $0.5^\circ/\text{sec}$  attitude change rate.
2. With the metered display, 2-man control yielded a 33% reduction in time response, produced appreciably less operator fatigue, and used less fuel and jet actuations than 2-man control (3-axis maneuver) for end objectives on the order of  $0.5^\circ$  and  $0.05^\circ/\text{sec}$ .
3. Rate command operation in general yielded faster response (15% better for single operator, 3-axis control, using the all-attitude display) than on/off or fixed pulse width operation for end objectives of  $0.5^\circ$  and  $0.05^\circ/\text{sec}$ .
4. Single operator performance with rate command operation which used the all-attitude display was equivalent to two-man control using other displays.
5. Rate command and on/off operation yielded comparable performance for end objectives of  $5.0^\circ$  and  $0.5^\circ/\text{sec}$  in the case of 3-axis maneuvers.

6. The combination of rate command operation and the all-attitude display resulted in significantly less (30%) propellant consumption than on/off or fixed pulse width operation. However, propellant consumption for any minimum time maneuver is large and hence such maneuvers are reasonable only in emergency situations.
7. Fixed pulse width operation resulted in excessive maneuver time and propellant consumption for three-axis maneuvers.
8. The all-attitude display was easier to use on an intuitive basis, and provided the operator with a coordinated display which physically represented vehicle attitude motion. It improved performance as much as the addition of another operator to control roll motion.
9. A spring-loaded control stick with mechanical dead-band appeared best for on/off operation. A control stick not spring-loaded but with a dead-band and a mechanical indication for the zero position appears best for rate command operation.

#### A. 4. 4 Earth Tracking Maneuver by Manual Control of Reaction Jets

The manual control study of the Earth tracking maneuver included both single-axis and three-axis operation. In the three-axis case, the vehicle roll axis was automatically stabilized.

##### A. 4. 4. 1 General

Manual tracking maneuvers performed in pitch and yaw included the effects of inertial coupling. Reaction jets of both fixed and variable amplitude output were considered. Five types of control were evaluated:

1. On/Off Acceleration, Stick Control--On/off operation in which the propellant valve is controlled by control stick deflection.
2. On/Off Acceleration, Pushbutton--On/off operation in which the propellant valve is controlled by depressing a pushbutton.
3. Fixed Pulse Width, Pushbutton--On/off operation in which the propellant valve is set for a fixed-pulse width and is controlled by depressing a pushbutton.
4. Rate Command, Stick Control--Rate command operation with attitude rate proportional to stick deflection.
5. Proportional Acceleration, Stick Control--Full proportional control in which the reaction jet valve is actuated during the entire maneuver and the output level is proportional to stick deflection.

For each control option, the display consisted of the following:

1. An X-Y axis CRT display of the pitch and yaw angle errors.
2. A metered display of the yaw, pitch and roll body rates.
3. Neon lamps to indicate the firing status of the reaction jets.
4. Metered display of the yaw, pitch, and roll angles.

The various controller techniques were evaluated on the basis of tracking error and error rate, which resulted in the performance of an Earth-tracking maneuver while in a simulated 200-nmi circular orbit. Figure A-56 shows the desired rate profile for a target in the orbital plane.

#### A. 4. 4. 2 Comparison of Controller Modes

The following items compare tracking capabilities:

1. On/Off Acceleration, Stick Control--This method of control was found to be unsatisfactory with regard to accuracy. Since the threshold conditions imposed were strict, any delay by the operator in turning the control jets, either on or off, resulted in large attitude changes which were impossible to correct.
2. On/Off Acceleration, Pushbutton--This method proved to be the best when relatively low thrust levels were used. With the jet thrust lowered, the operator is better able to control the needed velocity increments and, also, the number of thrust actuations is reduced.
3. Fixed Pulse Width, Pushbutton--The use of various size, fixed-pulse-width, pushbutton-actuated reaction jets resulted in adequate performance but required a large number of operations for tracking and caused operator fatigue.

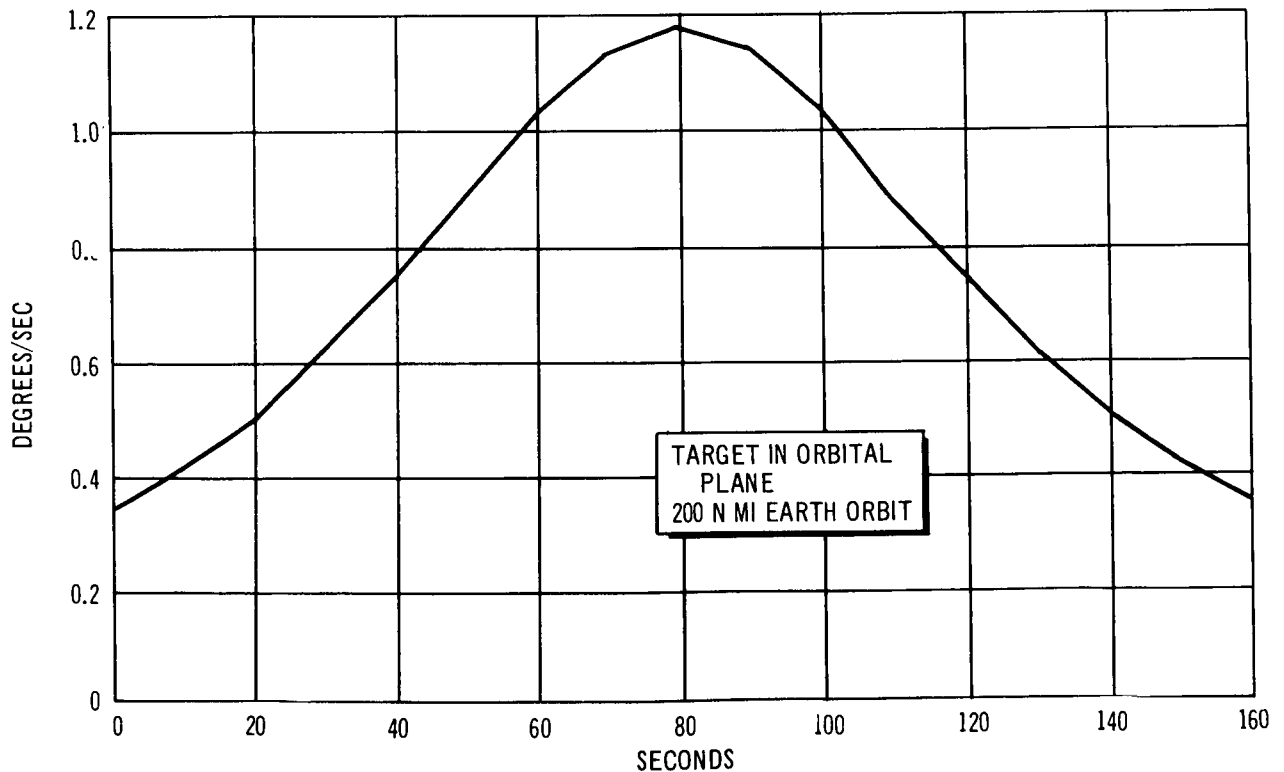


Figure A-56. Rate Profile for Earth-Tracking Maneuver

4. Rate Command, Stick Control--The rate feedback option, that proved best for the prior attitude reorientation study, does not allow for the low-velocity changes necessary for the tracking maneuver. For the selected mechanization, the control stick has a total deflection of  $\pm 60$  degrees and the stick length is 4 in. To be able to track the maximum rate of  $1.2^\circ/\text{sec}$  with a desired resolution of  $0.001^\circ/\text{sec}$ , the stick travel is then 0.0035 in. It is impossible for the operator this small stick movement.
5. Proportional Acceleration, Stick Control--The fully proportional jet control also lacks adequate control capability. If an appreciable rate differential builds up, the operator is required to increase the thruster level beyond the proper tracking level in order to null the error. After the correction, he must return the output to the correct level. This operation was found to be very difficult and tended to produce an oscillatory condition.

#### A. 4. 4. 3 Propellant Consumption

The propellant consumption was large (approximately 15 lb per tracking maneuver) and essentially independent of controller option since the net torque required is the same regardless of the threshold condition.

#### A. 4. 5 MORL Manual Attitude Control Using Control Moment Gyros

The MORL manual control simulation described in Section A. 4. 2 was used to investigate the use of control moment gyros for manual attitude maneuvers. In this investigation, both one-axis and two-axis capabilities were considered. In addition, various initial roll CMG gimbal angles and initial vehicle body rates were included to determine the effects of stored angular momentum on the attitude maneuver.

The use of control moment gyros for manual attitude maneuvers was considered for the yaw and pitch axes only. The roll channel was automatically stabilized and therefore had zero-rate and zero-position error at all times. Since the output torque from a gyro about the desired axis decreases as a function of the cosine of the gyro gimbal angle, gimbal deflection was limited to one radian. In addition, because of output torque limitations, the maximum double gimbal gyro command rate was limited to  $0.5^\circ/\text{sec}$ .

Displayed in Figure A-57 are strip recordings illustrating the response of the CMG gimbal and the vehicle dynamics for the small attitude maneuvers considered. These results show that the operator was able to converge steadily on the control objectives of  $0.5^\circ$  and  $0.05^\circ/\text{sec}$ , with initial condition

$$\theta_0 = \psi_0 = 5 \text{ DEGREES}$$

$$\dot{\theta}_0 = \dot{\psi}_0 = 0$$

$$a_1(0) = a_2(0) = 0$$

MANUEVER TIME  
= 130 SEC

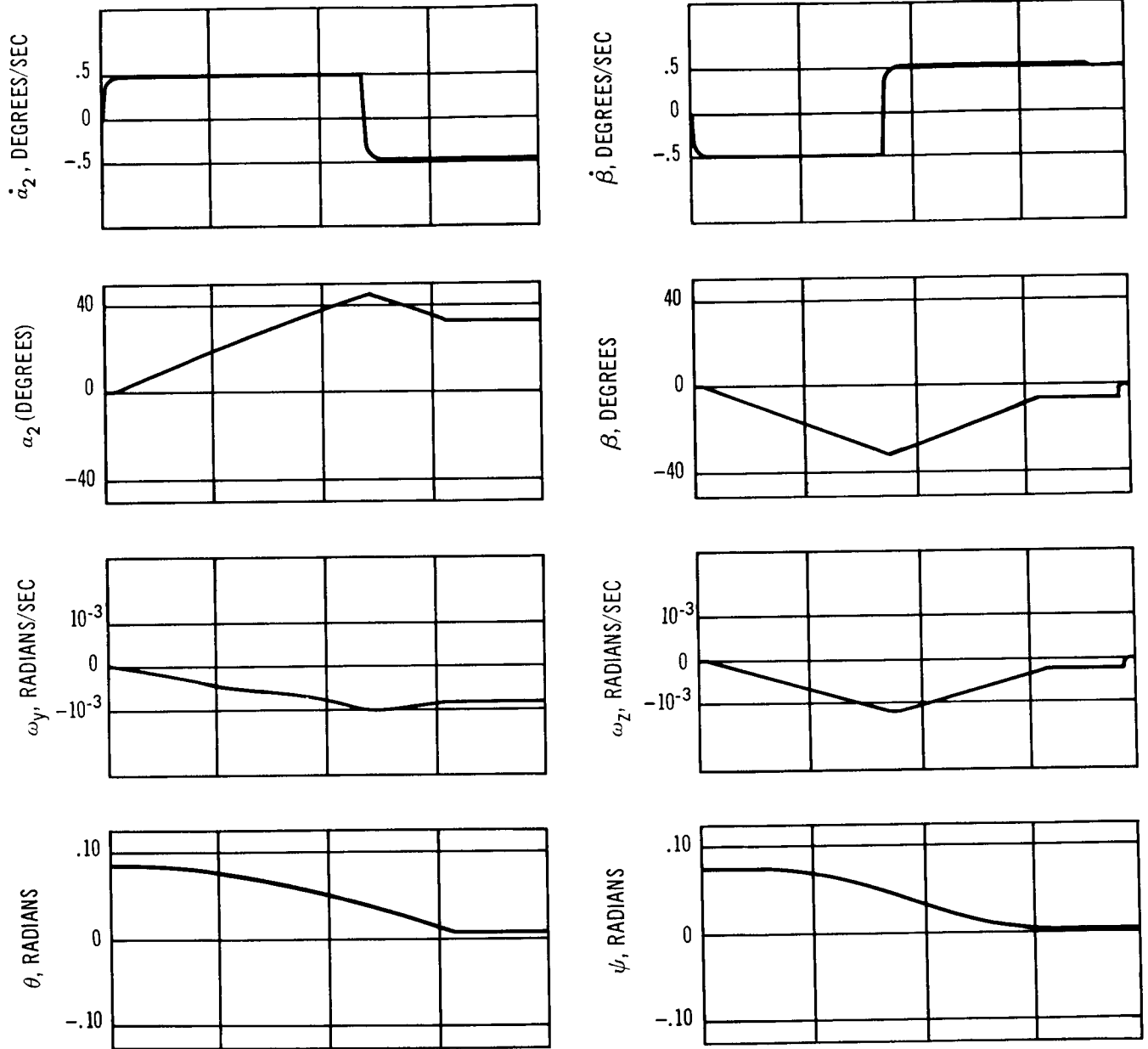


Figure A-57. Response to Small Attitude Errors Using CMG's



of  $0.5^\circ$  error in each axis and zeroed body rates. The time required to reach the control objective, 130 sec, was governed by the allowed CMG gimbal rate and the gimbal rate profiles  $\dot{\alpha}_2(t)$  and  $\dot{\beta}(t)$  show that the operator used the CMG in essentially an on/off control mode.

Figure A-58 defines the allowable initial body rate as a function of the initial CMG gimbal angle for each of the axes considered and for the baseline CMG parameters. It shows that, for the pitch channel, the behavior is approximately linear and  $-0.14^\circ/\text{sec}$  is the maximum rate which can be nulled before gimbal saturation occurs. The initial gyro angle for that condition was  $+45^\circ$ . Smaller initial angles (in a direction to decrease the total available gimbal deflection angle) result in a lesser capability to null initial rates. The yaw channel has a similar behavior, with  $-0.20^\circ/\text{sec}$  being the maximum permissible rate for an initial gyro angle of  $-45^\circ$ .

#### A. 4. 6 MORL Manual Control Philosophy

As part of the MORL Phase IIb effort, the manual control of the MORL vehicle has been considered and an overall manned control philosophy developed.

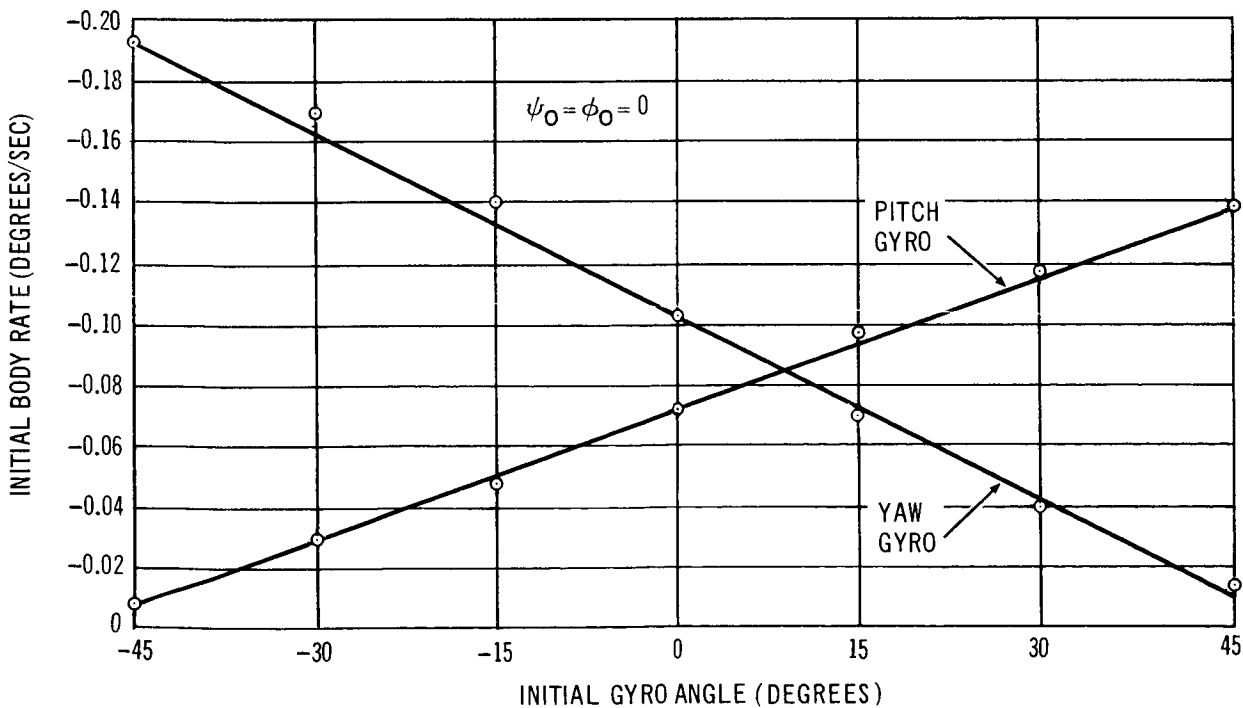


Figure A-58. Allowable Rate as a Function of Initial Gyro Angle Single-Axis Results

#### A. 4. 6. 1 Introduction

The possible control philosophies range from fully automatic to completely manual. The three specific manual control approaches considered in the study are as follows:

1. Completely automatic with manual override control for checkout and emergency.
2. Automatic only when necessary with manual control for checkout, emergency, and in all situations within man's capability.
3. Automatic most of the time with manual control for checkout, emergency, and in those situations where man in the loop significantly enhances either mission success, crew safety, or efficiency of operation. Manual participation is determined by control functions to be performed.

The completely automatic control philosophy can be reasonably used only for an extremely advanced space station technology applied in specific predetermined operational sequences. For the baseline MORL (in the context of current and anticipated level of technology of stability and control), with its broad range of experimental objectives, full-control automation is not only unnecessary but it can seriously degrade the probability of mission success. The other extreme, that of using man for all control functions within his capability without regard to mission success, crew safety, or operational efficiency, is equally undesirable from a cost effectiveness standpoint. For the MORL to have an acceptable cost effectiveness index, the crew time available for experimentation must be optimized. For this reason, the third manual control philosophy mentioned above was selected for detailed consideration. The results of this consideration are presented in detail in the following sections and draw extensively on the manual control studies presented in the previous sections.

#### A. 4. 6. 2 Control Modes and Control Options

To set the stage for a logical development of a manual control philosophy for the MORL vehicle, the following control modes are considered:

1. Mission control sequences (zero-g).
  - A. Long-term belly-down and inertial/celestial stabilization.
  - B. Attitude reorientation.
  - C. Critical mission events: rendezvous/orbit-keeping.

2. Experimental control sequences (zero-g).
  - A. Long-term stabilization (belly-down, inertial/celestial).
  - B. Attitude reorientation.

The control modes listed above are primarily associated with the manned MORL mission phases. In defining man's roll in these control modes, man's capability (based primarily on response, dexterity, and fatigue) to control short-period noncritical maneuvers, to provide long-term stabilization, and to provide both stabilization and control for short periods of time during critical mission phases, was considered. Various control options establishing the level of crew participation are listed below for this purpose.

1. Automatic--Automatic command and execution.
2. Semiautomatic--Preselected manual command, automatic execution.
3. Manual command--On-line manual command (rate control mode), automatic execution.
4. Manual control--Manual command (acceleration control mode), manual execution.

Figure A-59 is a block diagram indicating where man is in the control loop. Detailed descriptions of the control options are given as follows:

1. Automatic command (A)--The crew performs only a monitoring function in this control option, with completely automatic control commands and execution.
2. Semiautomatic command (SA)--In this control option, manual commands are preselected and automatically executed.
3. Manual command (MC)--In this control option, automatic commands generated by the control command computer are replaced by manual commands generated in an on-line manner. The execution of these commands is performed automatically by the attitude control system. The actuator selection logic determining momentum dump remains operative.
4. Manual control (C)--In this control option, manual inputs are sent directly to the control actuators. The manual operator is responsible for determining when the commands have been executed, based on the available displays, and must select which actuator (RCS or CMG) to use.

With reference to the switches shown in Figure A-59, the matrix of switch positions shown in Table A-13 defines the above control options where

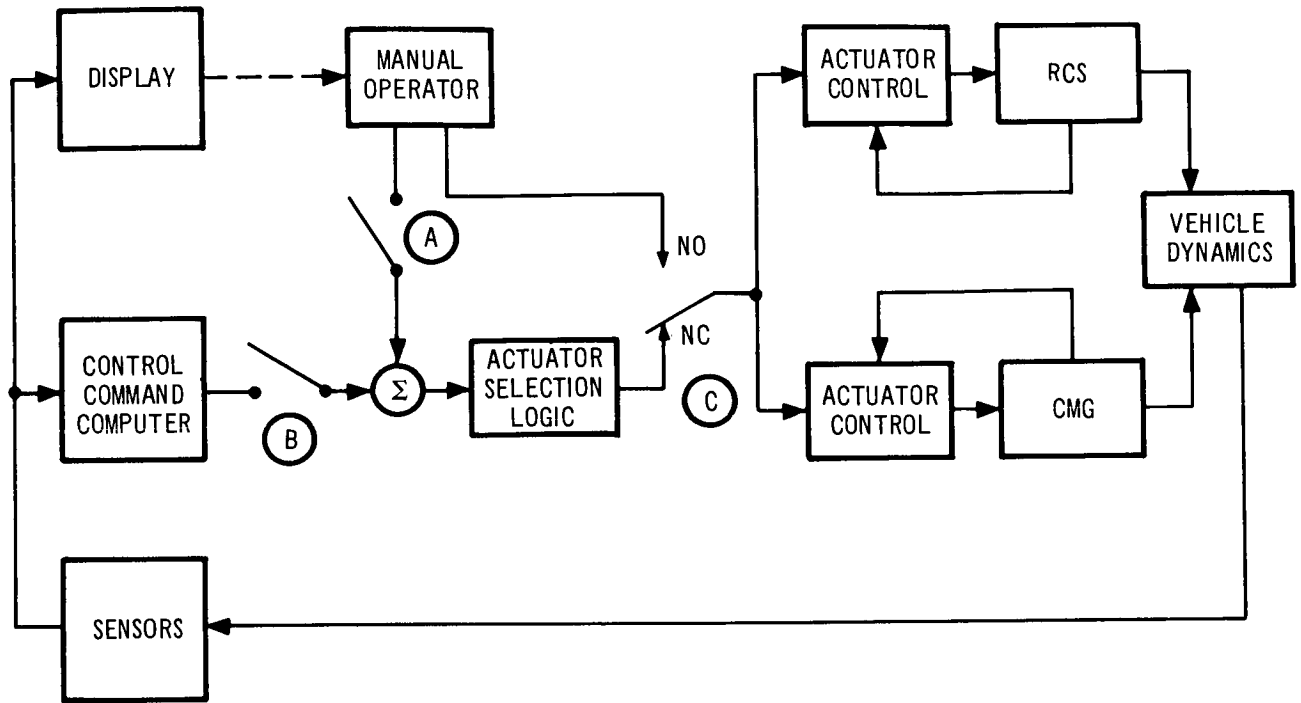


Figure A-59. Manual Control Options and Switching Logic

O means switch open, C means switch closed, NC means the normally closed position, and NO means the normally open position.

Table A-13

MATRIX OF SWITCH POSITIONS DEFINING CONTROL OPTIONS

Switch Designation	Control Options			
	A	SA	MC	C
A	O	C/O	C	O
B	C	C	O	O
C	NC	NC	NC	NC

In general, the following criteria will define the particular control option used at any given time.

1. For the automatic command options--This control option is the normal, long-term operating mode and is used for stabilization, with respect to a long-term attitude reference, and for routine short-period control functions unless the crew exercises one of the options described below.
2. For the semiautomatic--This control option is used by the crew to adjust the mission profile based on contingencies detectable by the crew. The automatic system executes preselected manual commands.
3. For the manual command option--This control option is used when the desired attitude profile adjustment is beyond the capability of the automatic system, either because of a malfunction in the computers or because of significant changes required in the mission profile. The manual command option may also be used as a backup to all manual control if the latter is the primary mode and crew time is in critically short supply.
4. For the manual control option--This control option is used when it is necessary to directly control the actuation of appropriate control forces. It is anticipated that this option would be used in case of serious malfunctions in the control loop (for example, sensor failure or other emergency situations) or during critical mission phases where manual control will increase mission-success probability, crew safety, or operational efficiency.

The above discussion of the possible control options, together with the various control modes, are used to define an approach to MORL manual control. In this definition, the importance of man in the loop is not de-emphasized; rather, man is used in the loop to maximize crew safety and to increase mission-success probability through control redundancy.

#### A. 4. 6. 3 Specific Control Options as a Function of Control Mode

To select specific control options for each possible control mode, two control states, normal and emergency, are defined together with a system of priorities which rank all the reasonable control options for a given control mode on the basis of percent of utilization. The complete array of control modes and control options is summarized in Table A-14. The requirements are derived primarily by applying an appropriate scale factor to the MORL baseline requirements. A brief description of each control mode/control option is given below.

1. Long term stabilization. The following paragraphs describe priorities and modes of stabilization control.

Table A-14  
MISSION SEQUENCES CONTROL (ZERO-G)

Control Mode	Control State	Priority	Control Option	Angle Error (deg)	Performance Rate Error (deg/sec)	Requirement Max. Stewing Rate (deg/sec)	Remarks
Long-term stabilization	Normal	2	Semiautomatic	±0.5	±0.1 (±0.01)*		Fulltime crew monitoring-periodic preselected manual adjustments
	Emergency	1	Fully automatic	±0.5	±0.1 (±0.01)		Long-term unattended operation
		1	Manual command	±5.0	±0.15 (±0.15)		Initiated for minor short-term malfunction
		2	Manual control	±5.0	±0.15 (±0.15)		Initiated for major short-term malfunction
Attitude reorientation	Normal	1	Semiautomatic	±0.5	±0.05	5.0 (0.2)**	Commands are preselected and automatically executed
	Emergency	2	Manual command (rate command operation)	±0.5	±0.15	5.0 (0.2)	Coarse control manually followed by fully automatic stabilization to a selected reference
Critical mission events	Emergency	1	Manual command	±0.5	±0.15	5.0 (0.2)	For use in case of malfunction
		2	Manual control (on off operation)	±0.5	±0.15	5.0 (0.2)	For use in case of equipment malfunction to continue short-duration mission objectives
	Normal orbit keeping	1	Automatic	±5.0	±0.1		Consistent with the normal long-term stabilization control mode, for standard orbit keeping maneuver
	Normal rendezvous	2	Manual command	±5.0	±0.1		To be used if nonstandard orbit keeping maneuver is performed
Long-time stabilization	Emergency orbit-keeping	1	Semiautomatic manual command	±0.5	±0.05	±0.15 (0.2)	Semiautomatic maintained until MORL/ferry line-of-sight orientation is initiated, manual control about two axes only with automatic rate stabilization about the third axis and equipment proficiency
		1	Manual control	±5.0	±0.1		Verify new rendezvous techniques
	Normal	1	Semiautomatic	Determined by experiment			To be used only if malfunction can be corrected and mission continued
	2	Manual command	Determined by experiment				As required by experiment
Attitude reorientation	Emergency	1	Manual command	Determined by experiment			Experiments not performed during emergency status
	Normal	2	Semiautomatic	Determined by experiment			Coarse control followed by automatic stabilization to desired reference
							Used to conserve crew time during experiment

\*Requirement in parentheses indicates long-term average.  
\*\*Requirement in parentheses is nominal value obtained with CMGs. Higher values require the RCS gas jets.

99226

- A. Normal, priority No. 1, fully automatic. A fully automatic long term stabilization mode is provided as a No. 1 priority control option to minimize crew fatigue and allow unattended operation over long periods of time.
  - B. Normal, priority No. 2, semiautomatic. The semiautomatic mode is provided so that preselected operator commands can be automatically executed. In this manner maximum mission flexibility is retained automatically, yet the mission can be controlled at the option of the operator.
  - C. Emergency, priority No. 1, manual command. Multiple emergency control procedures have been defined to maintain a balance between the severity of the emergency and the corrective control procedure. In a sense, overcontrol in an emergency may only worsen the situation. Therefore, priority assignments have been made in case of an emergency for each control mode. A No. 1 priority assignment has been selected for the manual command option to cover relatively minor short-term malfunctions in the sensors or control-command computer. Normal control options would be initiated as soon as the situation was consistent with any given normal option (not necessarily the desired option) and the desired option would be resumed as soon as possible.
  - D. Emergency, priority No. 2, manual control. The manual control option was assigned a No. 2 priority. This emergency option would be used only in case of a major short-term malfunction, such as the failure of one actuator or a power loss to a major equipment module. In all of these emergency options, it is assumed that sufficient display data will be available to the crew so that the severity of a given emergency can be determined quickly, and an emergency control option can be selected.
2. Attitude Reorientation. The following paragraphs describe priorities and modes of attitude reorientation.
- A. Normal, priority No. 1, semiautomatic. For short period attitude maneuvers, a semiautomatic control option is provided. This option allows the desired maneuver to be preselected by the control operator. Automatic execution of the maneuver is also initiated by the operator, which yields maximum operational flexibility.
  - B. Normal, priority No. 2, manual command. A backup manual command option for short period attitude maneuvers is provided when the desired maneuver corresponding to a specific mission objective cannot be preselected. The use of man in the loop for many maneuvers ensures flexibility and reliability in the accomplishment of mission objectives and obviates the necessity for automatic control sequences for every mission contingency.

- C. Emergency, priority No. 1, manual command (rate command operation). The manual command control option is regarded as the No. 1 priority emergency option for the normal semi-automatic mode in case of emergencies of moderate severity.
  - D. Emergency, priority No. 2, manual control. Manual control can be considered an emergency control option to replace the normal No. 2 priority control option in case of equipment malfunction. The severity of the emergency is, in general, greater for this case than that for the No.1 priority option.
3. Critical mission events. The following paragraphs describe priorities and modes of critical mission events.
- A. Normal, orbit keeping priority No. 1, automatic. The No. 1 priority control option is automatic since stabilization in the belly-down mode is required for 1 to 2 hours to complete the orbit-keeping maneuver. This selection is consistent with the normal No. 1 priority option for the mode described in Item 1, and minimizes crew time. This control option would be used for all standard (that is, circularization) orbit-keeping maneuvers.
  - B. Normal, orbit keeping priority No. 2, manual command. In case of a nonstandard orbit-keeping maneuver, such as the maintenance or attainment of an eccentric orbit, manual command is recommended because of its inherent flexibility and reliability and because of the noncritical aspects of the performance requirement.
  - C. Normal, rendezvous, priority No. 1, semiautomatic/manual command. For the rendezvous maneuver, a combination of semiautomatic and manual command has been selected. This combination of control options uses the best of man and machine. Semiautomatic control is used at relatively long laboratory/ferry ranges while the MORL vehicle is in the belly-down orientation.  
  
At shorter ranges it may be desirable to maneuver the laboratory so that the docking axis tracks the logistic spacecraft in line-of-sight. If this is required, the manual command option should be used to take advantage of man as an optical alignment sensor. In this option, automatic rate stabilization is maintained about the axis perpendicular to the docking surface and manual command is maintained about the remaining two mutually perpendicular body axes.
  - D. Normal, rendezvous, priority No. 2, semiautomatic/semiautomatic. If automatic rendezvous techniques are used, an automatic control option may be provided throughout the rendezvous maneuver. Close status monitoring would be maintained to ensure safe accomplishment of the procedure.



- E. Emergency, orbit keeping, priority No. 1, manual control. A manual control option for orbit-keeping is used if the assessment of the emergency status indicates that the situation can be remedied and the mission continued.
4. Long-term stabilization, normal. The specific control options required for stabilization in an experimental mode are a function of the experiment. It is anticipated, however, that the semi-automatic and manual command options will satisfy most of the normal operational requirements. No emergency control options are defined.
  5. Attitude reorientation, normal. Manual command and semiautomatic control options are provided for the attitude maneuvers required by the MORL experiments. The specific performance requirements are a function of the experiments and must be defined on an individual basis.

#### A. 4. 6. 4 Conclusions

The MORL manual control philosophy is summarized in Table A-14. Man's capability is used when required to increase the probability of mission success or to ensure crew safety. The various control options provide a large measure of control redundancy and, hence, also contribute to the mission probability of success.

## Appendix B SYSTEM IMPLEMENTATION

This section describes the hardware of the Stabilization and Control System (SCS). The system has been developed from examination of mission requirements, improvement studies, and tradeoff analyses. Where possible, existing equipment has been specified, and new equipment will be developed only where necessary to meet design requirements or where sufficient improvement will warrant the expense.

The system is described in the following terms:

- Function requirements in each operational mode.
- Operating procedures.
- Equipment selection.
- Component specification.

Use of Apollo components has been emphasized and this standardization has simplified the changeover from a solar power system to a Brayton Cycle Power system. This also allows deletion of the roll solar mode of control and eliminates the need for sun sensors as well as the complex sequencing procedure for mode updating.

### B.1 SCS EQUIPMENT SELECTION

During the course of the Phase IIB program effort, the MORL SCS equipment selection has been re-evaluated to take fullest advantage of Apollo and other available equipment. The control electronics have been rearranged to obtain a better functional grouping and the roll solar sensing elements have been eliminated.

The work accomplished reflects continued emphasis of on-board maintenance as an important criterion for functional grouping of electronics and for the use of available equipment.

In surveying the Apollo SCS, it has been determined that Block I equipment generally meets the MORL on-board maintenance requirement. The equipment reflects a modular design with easily replaceable subassemblies and carries provision for on-board troubleshooting. Block I was, in fact, developed for easy maintenance. Block II, the current design, employs hermetic seals, potting, and hardwired subassemblies to overcome an anticipated high humidity environment. Thus, Block II components, to be applicable to MORL, must be those for which complete replacement can be justified in terms of life, spares provisioning, basic weight and equipment, and in skill necessary for on-board repair.

In terms of direct applicability, the following selections and recommendations are made:

1. The Block I three-axis attitude gyro and accelerometer package, Type DGG 245C, is directly applicable to the MORL SCS system. It will replace the previously specified inertial rate integrating gyros (IRIG) and additionally, will provide longitudinal acceleration sensing for the orbit-keeping functions. As Block I, it meets the present MORL maintenance criteria.
2. The Block I three-axis rotational controller, Type DCG 146G, is applicable and was carried on the previous MORL equipment list. The unit provides the necessary interlocking and command functions required by the MORL SCS. Its force-command operation may relegate this device to a backup role in the future since present maneuvering trends favor extremely slow (fuel-efficient) changes and a hand-operated force-stick may be tiring to the operator.
3. The flight director attitude indicator (FDAI) of Block I or II is applicable and is specified for use in the MORL system. Block II represents a ruggedized version of the Block I device and a final choice will hinge upon the results of detailed maintenance studies.
4. The Block I velocity change indicator, type DCG 148G, as employed on Apollo, provides all of the functions required by the MORL SCS system and, in addition, provides an ullage command. Since ullage thrust is not required for MORL orbit-keeping propulsion, only subassemblies of this device are deemed directly applicable.
5. The Block I electronic control amplifiers provide many of the functions required by the MORL SCS. Their direct applicability as complete assemblies is marginal. Insofar as MORL electronics are concerned, the use of modular subassemblies of these packages appears more probable. A final decision requires additional depth in MORL system design, the selection of the basic electronics technology to be employed, the establishment of firm packaging concepts, and detailed maintenance and spares provisioning requirements.

## B.2 MORL EQUIPMENT COMPLEMENT

The revised MORL equipment complement is presented in Table B-1. This table summarizes power, weight, size, and other pertinent characteristics of the required equipment. The subsequent pages briefly describe each major component of the system and its general properties to better establish the relationships between these components, and the system and its operation. The rotating mode equipment is also shown at the end of Table B-1. Although not actively studied for this phase of effort, it is included for completeness.

### B.2.1 Horizon Sensor

The four-head horizon sensor concept shown in Figure B-1 is a packaging variation of the Advanced Orbiting Geophysical Observatory (AOGO) scanning heads. This arrangement allows ease of removal of the individual heads from within the spacecraft for repair or replacement. The horizon sensor, an edge tracker, has the following performance properties.

- |   |   |
|---|---|
| 1. Field of View  | Scan $\pm 47^\circ$<br>Track $\pm 2^\circ$  |
| 2. Accuracy in detecting thermal horizon including anomalies but excluding oblateness | $\pm 0.1^\circ (3\sigma)$   |
| 3. Linearity  | $0.1^\circ$ up to $1^\circ$ and 10% of actual value from $1^\circ$ to $10^\circ$ of vehicle offset. |
| 4. Sensor null accuracy   | $0.05^\circ$ .  |
| 5. Time constant  | 0.1 sec.  |

### B.2.2 Attitude Gyro and Accelerometer

The MORL control system in its various modes of operation requires three-axis attitude, three-axis rate and a velocity measurement for orbit-keeping. The Apollo attitude gyro and accelerometer package illustrated in Figure B-2 provides this capability and is specified.

Table B-1 (page 1 of 3)  
EQUIPMENT LIST

Equipment Nomenclature	Quantity Employed	Function	Volume cu ft (each)	Weight lb (each)	Power (each) ac (W) dc (W)
Attitude gyro and accelerometer package (AGAP)	2	Provide attitude and rate sensing and acceleration sensing for orbit-keeping	0.190	13.7	7.9 57.6
Single gimbal triad (inertial platforms)	1	Provide an inertial reference for precision experiments	0.147	11.6	17.0 70.0
Star tracker	2	Provide inertial reference updating and celestial tracking	0.67	25.0	- 7.8
Horizon scanner	2	Provide a local vertical reference for accomplishing pitch and roll control	0.15	10.0	- 3.0
Sensor electronics assembly (SEA)	1	Accommodate control electronics for horizon sensing, Earth acquisition, and star tracking	1.12	41.8	1.1 40.0
IRIG control electronics (ICE)	1	Provide AGAP control electronics and FDAI display conditioning	0.845	33.8	8.0 33.4
Reaction control amplifier (RCA)	1	Provide valve drive power, control logic and signal processing	0.570	26.2	3.0 74.0
Logic and processing electronics (LPE)	1	Provide gyrocompassing control actuator and signal selection and FDAI coupling	1.190	42.6	22.8 12.1
CMG control electronics (CCE)	1	Provide CMG synchronization, control and desaturation electronics, wheel drive and monitoring	0.37	10.5	- 12.0

Table B-1 (page 2 of 3)

Equipment Nomenclature	Quantity Employed	Function	Volume cu ft (each)	Weight lb (each)	Power (each)	
					ac (W)	dc (W)
Regulated power supply	2	Supply regulated power for electronics	0.2	10.0	20.0	10.0
Attitude reference computer (ARC)	1	Provide the updated inertial reference and euler angle computations	0.174	10.0	1.0	27.0
Double gimbal control moment gyro (DG CMG)	2	Provide control about the vehicle pitch and yaw axes	11.24	168.0	30.0	11.0
Single gimbal control moment gyro (SG CMG)	2	Provide control about the vehicle roll axis	10.08	146.0	29.0	5.5
CMG control panel	1	Provide energizing, caging and operating controls for the CMG subsystem	0.161	3.0	-	-
Orbit-keeping control panel	1	Provide $\Delta V$ selection and orbit-keeping commands	0.045	1.7	-	3.0
Inertial reference command panel	1	Provide means for initiating precision attitude maneuvers	0.10	3.0	-	20.0
SCS mode select panel	1	Provide basic mode selection for the SCS system	0.045	1.6	-	2.0
Dual star tracker control panel	1	Provide basic operating controls for two separate star trackers	0.085	1.5	-	0.4
Horizon scanner control panel	1	Provide basic operating controls for two separate horizon scanners	0.026	0.8	-	0.4
Flight director attitude indicator (FDAI)	1	Provide display of vehicle attitude and body rates	0.187	8.75	-	4.0

Table B-1 (page 3 of 3)

Equipment Nomenclature	Quantity Employed	Function	Volume cu ft (each)	Weight lb (each)	Power (each) ac dc (W) (W)
Rotational controller	1	Provide manual rate and acceleration commands	0.029	4.9	- -
Miscellaneous switching and displays	-	Secondary controls	0.10	5.0	- 10.0
ARB alignment equipment	1	Optical alignment of precision sensing equipment	0.28	74.0	- 22.5
Totals (Zero g)			27.914	631.95	See Note
Single degree of freedom platform	1	Attitude sensing and orbit-keeping firing control	0.2	10.0	5.0 40.0
Single axis horizon detector	1	Horizon detection during rotating mode	0.002	1.0	- 3.0
Three-axis rate gyro package	1	Sense body rates	0.003	1.5	10.5 -
Accelerometer	1	Artificial-g sensor	0.001	0.5	1.5 -
Rotating mode control electronics	1	Provide spin control and logic, thrusting command and sensing electronics	0.44	10.0	- 27.0
Total (artificial-g mode)			0.646	23.0	See Note
Subsystem totals (zero g plus artificial g)			28.560	654.95	See Note

Note: System power requirements are a function of operating mode. This information is called out in the SCS power profile.

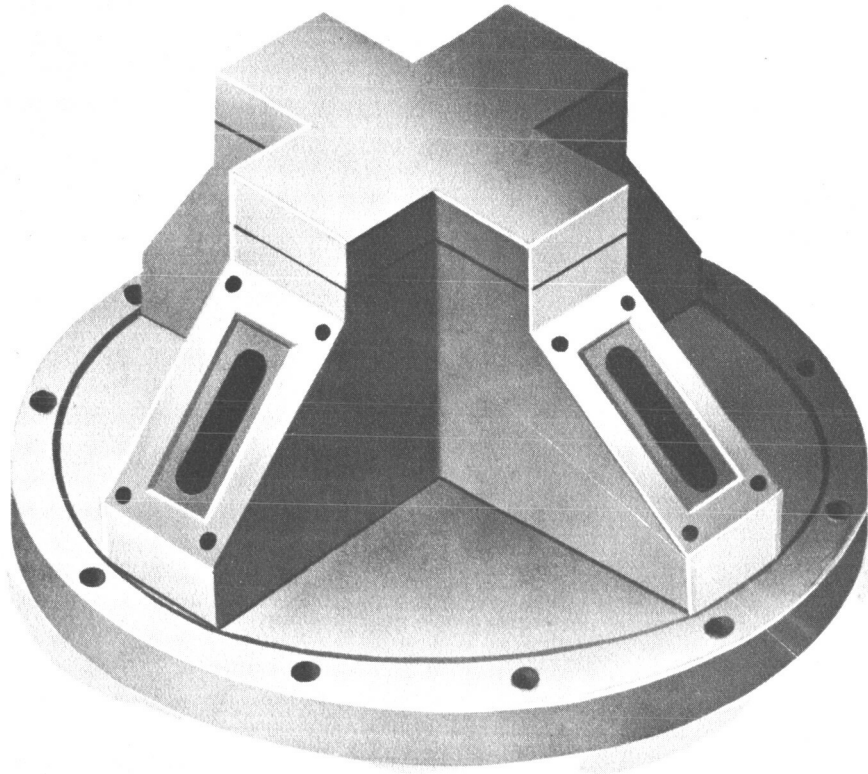


Figure B-1. Four-Quadrant Horizon Scanner

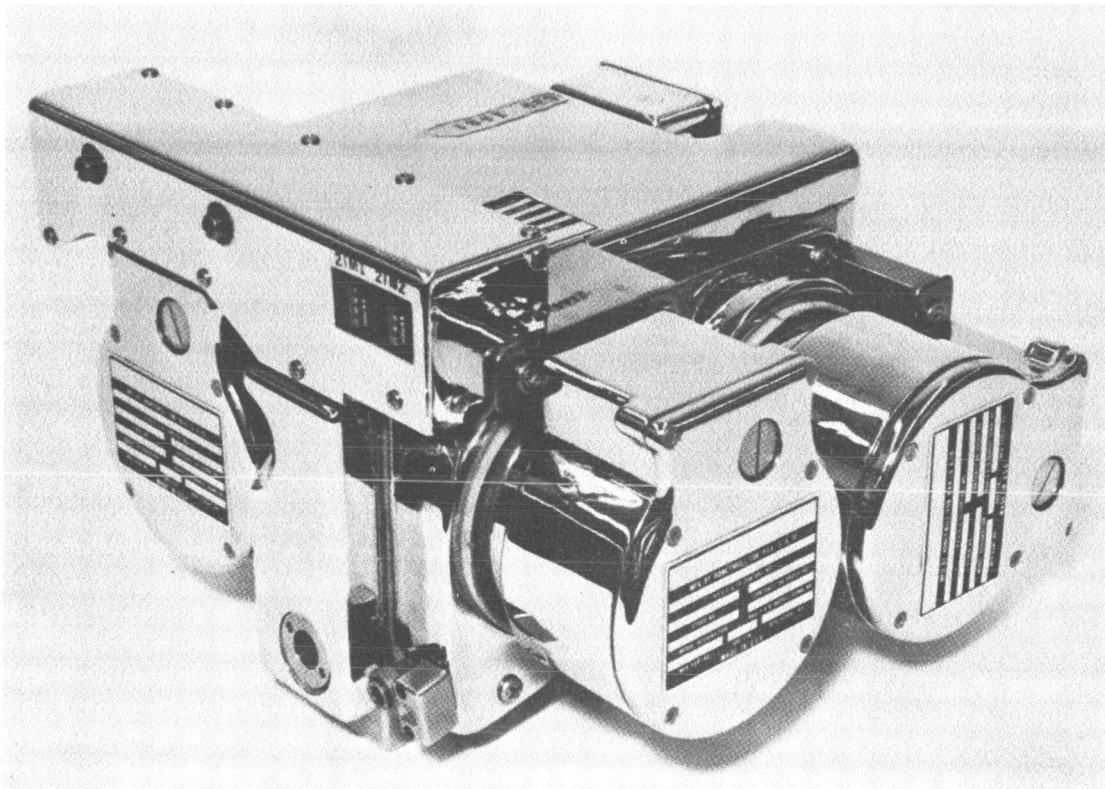


Figure B-2. Attitude Gyro and Accelerometer Package



The package contains three IRIG and an integrating accelerometer having the following performance characteristics:

Gyro	GG 248
1. Angular momentum	$1 \times 10^5 \text{ gm-cm}^2/\text{sec.}$
2. Input angular freedom	$\pm 20^\circ$ .
3. Gravity insensitive drift	$0.1^\circ/\text{hour.}$
4. Threshold	$< 0.01^\circ/\text{hour.}$

Accelerometer	DGG 177
1. Pendulosity	$2.86 \text{ gm-cm.}$
2. Pendulum freedom	$\pm 0.23^\circ$
3. Threshold	$< 1 \times 10^{-5} \text{ g}$

### B.2.3 Inertial Reference System

The inertial reference system most applicable to the MORL mission consists of three single-axis platforms. This mechanization keeps computer requirements to a minimum. The three-axis package depicted in Figure B-3 allows individual platform replacement for ease of system maintenance.

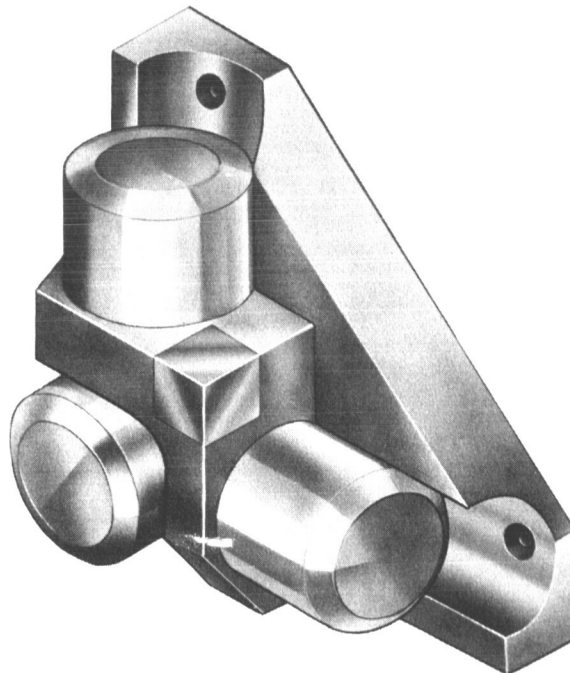


Figure B-3. Single Gimbal Triad

The inertial reference system provides the following general performance in keeping with experimental requirements:

1. Maximum input angular freedom 360°
2. Maximum input rate 480°/hour
3. Position accuracy  $\pm 0.1^\circ$ /hour
4. Threshold 0.01°
5. Resolution (readout) 0.01°
6. Random drift rate  $< 0.01^\circ$ /hour

#### B.2.4 Star Tracker

The OAO star tracker has been selected as the basic reference for direct precision pointing and for updating the inertial reference system. The tracker consists of a tracking telescope mounted on a two-gimbal set providing  $\pm 60^\circ$  of angular freedom in each axis. Dc torquers attached to the gimbals are used to position the telescope in response to computer commands and to accomplish star tracking. Precision gimbal readout is provided through the use of optical encoders. This device, more fully described in Section A.3.2, is illustrated in Figure B-4.

1. Gimbal range  $\pm 60^\circ$  each axis
2. Field of view  $\pm 1^\circ$  each axis
3. Star recognition
  - A. Accuracy 2.0 magnitude or brighter
  - B. Command mode 60 arc sec
  - C. Track mode 30 arc sec
4. Tracking rate  $0.5^\circ$ /sec

#### B.2.5 SCS Electronics

The MORL SCS electronics is contained in a series of packages as listed below:

1. Sensor electronics assembly (SEA).
2. IRIG control electronics (ICE).
3. Reaction control amplifier (RCA).
4. Logic and processing electronics (LPE).
5. CMG control electronics (CCE).

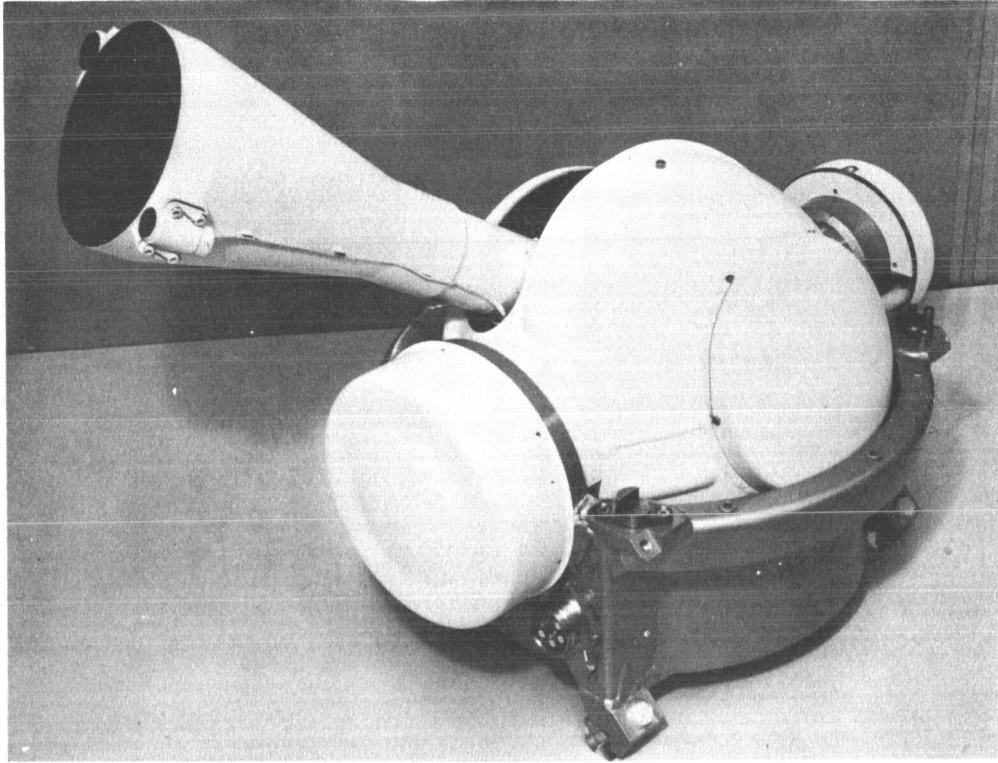


Figure B-4. Star Tracker

6. Attitude reference computer (ARC).
7. Regulated power supply (RPS).

The general contents of these packages are tabulated on the SCS equipment list Table B-1.

Although the above units are not designed in detail, these assemblies will conform to a cold-plate rack-mount configuration, will provide a gasket seal for environmental protection, and will provide built-in test and maintenance features. Thus, the external package will be as shown in Figure B-5. Its lower surface will be smooth for positive contact with the MORL rack provided cold plate.

The locking handle uses cam action to retain the package in its drawer and force the lower surface of the package to contact the cold-plate surface. When a maintenance action is required, lifting the handle will release the locking mechanism allowing the unit to be withdrawn on drawer slides. The cover is removed by releasing the side latches.

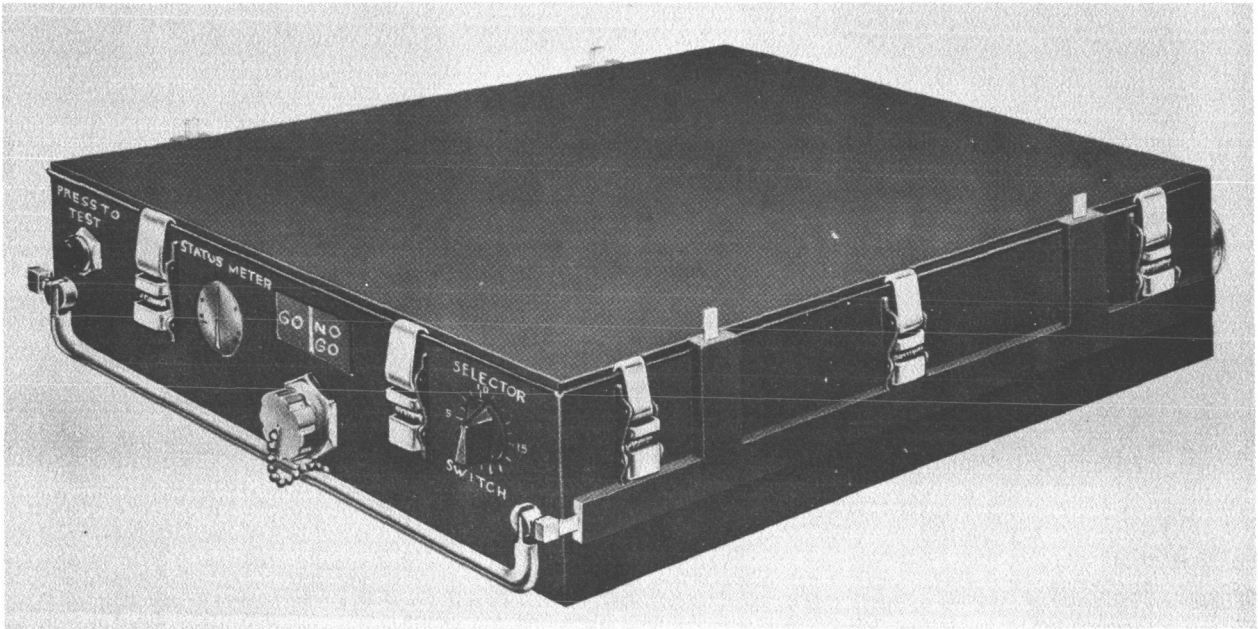


Figure B-5. Electronics Assembly

---

The electronics in the package uses present level of technology microminiature flat packs and discrete high-reliability parts arranged in functional plug-in modules to form the specific circuitry for the various electronics assemblies. In the detailed design of the electronics, every effort will be made to use common module types to minimize spares provisioning. In the concept shown, the built-in test equipment, shown on the front face of the package, consists of a press-to-test button, a center reading meter, a go/no-go light, and a test selector switch. Test procedures and circuitry will vary with the specific unit function, but in all cases will determine the functional status of each replaceable module.

#### B. 2. 6 Rotational Maneuvering Controller

The MORL maneuvering controller is the Apollo rotational maneuvering stick shown in Figure B-6. The unit provides the necessary detent, command, and emergency switching functions required by the MORL SCS.

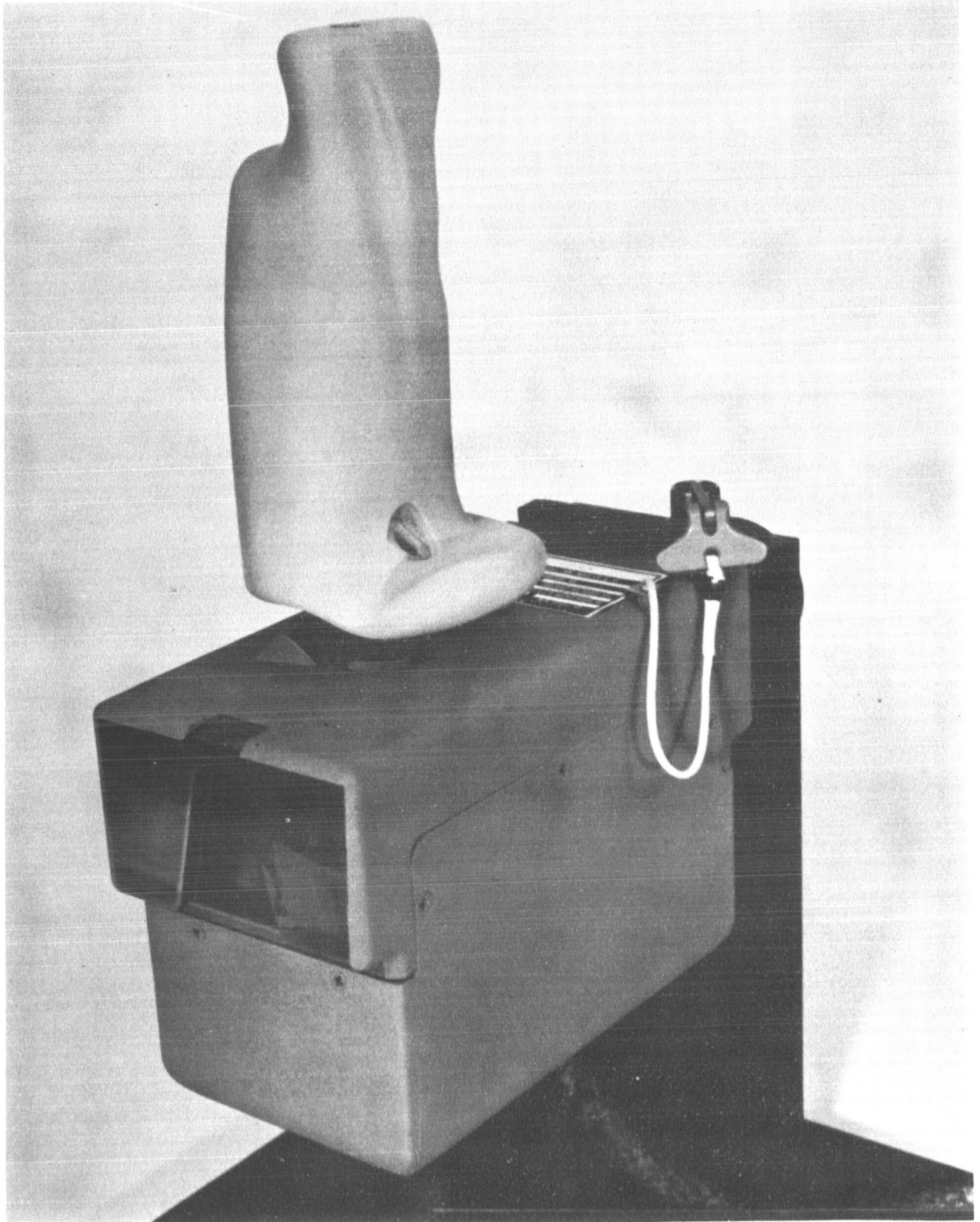


Figure B-6. Three-Axis Control Stick

This controller has the following characteristics:

- |                            |  |
|----------------------------|--|
| 1. Type                    | Three-axis maneuvering force stick.  |
| 2. Command                 | Pitch and roll via direct deflection<br>yaw via rotation.  |
| 3. Detent switches         | Operation at 0.15 arc-in. deflection<br>and 2° in rotation.  |
| 4. Proportional commands   | 0.3 to 6Vac, 400 cps, reversible<br>over deflection range of 0.15 to<br>0.75 arc-in. and 2° to 16° in<br>rotation. |
| 5. Direct control switches | Closure at 0.60 arc-in. and 13° of<br>rotation.  |

#### B. 2. 7 Double Gimbal Control Moment Gyro

The MORL control system employs two double-gimbal control moment gyros for the development of proportional torque about the pitch and yaw axes.

This device is depicted in Figure B-7. These gyros provide the following performance capability:

- |                     |                 |
|---------------------|-----------------|
| 1. Gimbal freedom   | ±60°            |
| 2. Angular momentum | 1,625 lb-ft-sec |
| 3. Rated torque     | 25 lb-ft        |

#### B. 2. 8 Single-Gimbal Control Moment Gyro

Two single-gimbal control moment gyros are employed on MORL for the development of torque about the roll axis.

These gyros provide the following performance capability:

- |                     |                 |
|---------------------|-----------------|
| 1. Gimbal freedom   | ±60°            |
| 2. Angular momentum | 1,790 lb-ft-sec |
| 3. Rated            | 25 lb-ft        |

#### B. 2. 9 Flight Director Attitude Indicator

The Apollo flight director attitude indicator (FDAI), illustrated in Figure B-8, has been specified for use in the MORL SCS.

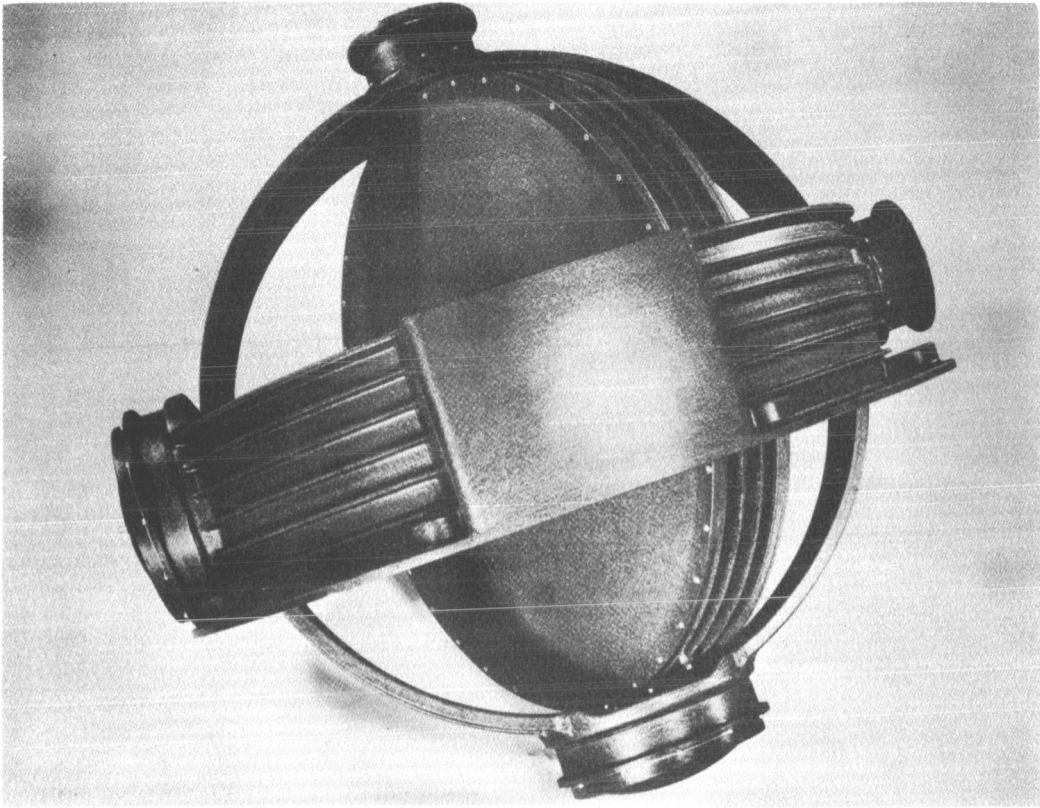


Figure B-7. Double Gimbal Control Moment Gyro

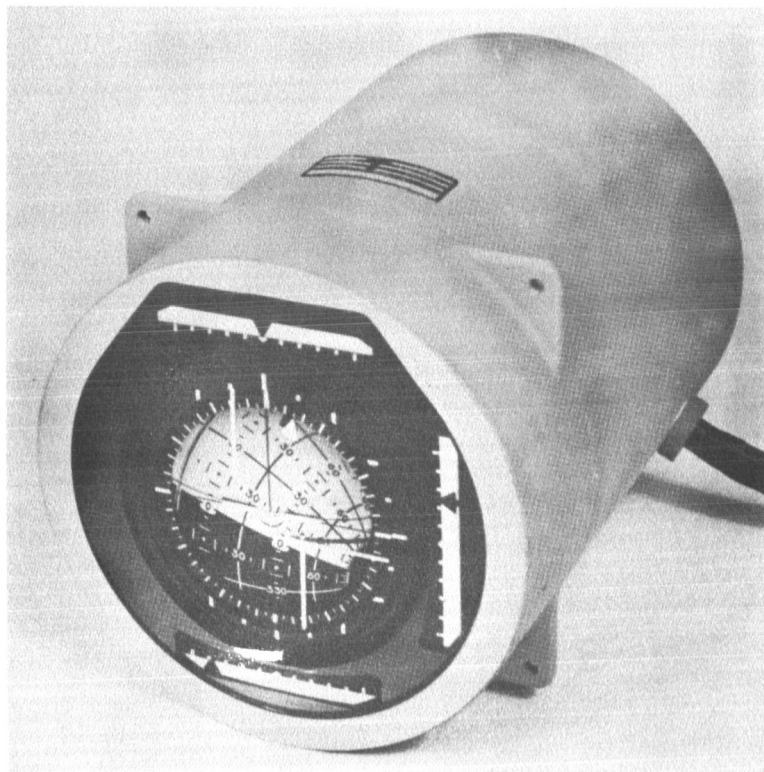


Figure B-8. Flight Director Attitude Indicator

The unit uses a 4-in. ball presentation of attitude which can follow maneuvers through 360°. In addition, the unit shows three axis rates and maneuvering commands with needles and bars around the periphery of the ball.

#### B.2.10 Control Panels

The control panels for the operation and monitoring of the MORL SCS have been arranged to provide a rapid appraisal of system status through functional grouping. Thus, individual panels are provided for mode selection and the control of the various subsystems within the SCS. Each panel is proportioned in accordance with aircraft design standards and is mounted with typical Zeus fasteners. The individual panel approach allows units to be easily removed for maintenance and repair during the mission. Although not illuminated, the panels will accommodate conventional edge lighting or electroluminescence for a small power penalty. Separate panels are provided as follows.

##### B.2.10.1 SCS Mode Selection Panel

This panel consists of two three-solenoid-held position toggle switches for mode selection. Holding power for each of these switches is 0.1 amp at 28 Vdc; however, only one selection at a time is possible because of interlocking within the system. A three-position manual rotary selector is provided for IRS update selection and a two-position manual toggle is provided for actuator choice. An update indicator light is also provided on this panel.

##### B.2.10.2 Inertial Reference Command Panel

The inertial reference command panel consists of six servoed digital counters providing polarity readout and five digits. Manual-input thumbwheels are used to adjust three of the counters for command insertion, and a command execute push-button is used to initiate control action. The panel elements are arranged for the rapid appraisal of existing attitude and that commanded for the vehicle body axes.



### B. 2. 10. 3 Orbit-Keeping Control Panel

The orbit-keeping control provides the necessary command and monitoring functions for an orbit-keeping operation. The control unit incorporates a four-digit servoed counter which is electrically commanded by a wobble type  $\Delta V$  switch. Two read-in speeds are available. A three-position selector is provided and is solenoid-held in the preselect position only. A thrust initiation function is provided by a momentary contact, normally-open push-button switch.

### B. 2. 10. 4 CMG Control Panel

This panel provides all necessary controls and monitors for the operation of the MORL CMG. The panel is equipped with three dual movement instruments calibrated in degrees of authority. Their dual arrangement allows rapid determination of balance while their close packaging ensures ease of surveillance.

Three unload push-buttons are provided in close association with each indicator to complete the command display portion of the panel. The remaining controls are used to energize cage/uncage, and monitor the gyros. Two three-position rotary selectors are provided with each controlling an operational pair of gyros. This combination prevents the inadvertent operation of single units which would result in unwanted stored momentum along one axis.

Four miniature ammeters and eight indicator lights indicate CMG operational status. Each of the four CMG is monitored for power consumption, common failure modes, and operating speed.

### B. 2. 10. 5 Star Tracker Control Panel

Controls for the two star trackers employed in the MORL system are provided on a dual panel. Each tracker is provided with separate controls consisting of a manually operated toggle switch for application of power, a manual three-position rotary selector for choosing each of the tracker's three modes of operation and three indicator light capsules as performance monitors.

#### B. 2. 10. 6 Horizon Scanner Control Panel

The MORL SCS provides dual horizon scanning subsystems. The horizon scanner control panel is a dual unit on which each subsystem's controls are mounted. Each subsystem is provided with a manually operated toggle switch (power) and two indicator light capsules for the display of horizon scanner status (search and track).

### B. 3 MODE MECHANIZATION

The MORL SCS is designed to accommodate all phases of the laboratory mission. In this capacity the SCS is required to provide control during orbit injection and the ensuing unmanned period of operation. During this period where maintenance is impossible, system simplicity and element redundancy provide the necessary reliability. After initial boarding, the control system must provide economical long-term control, and for by many of the experiments it must provide high-accuracy long-term stabilization. The diverse requirements of long maintenance-free life, high accuracy, and minimum expenditure of storable propellants all tend to complicate mechanization and the operating procedure. Hence, the various modes will be seen to require considerable equipment energization and manual selection prior to mode entry. This has been done to allow use of simple sensors for the long-term, more complex precision sensors for experiments, and in all cases, to extend the life of the equipment during its standby periods.

The block diagram of the SCS system in its entirety is illustrated in Figure B-9. This diagram shows the redundant application of functions for the unmanned modes and the signal flow and elementary switching for the remaining modes of operation.

Subsequent sections will present the elements of this diagram as they pertain to each of the operating modes.

#### B. 3. 1 Orbit Injection and Unmanned Control

Figure B-10 illustrates the progression of events occurring in the control system from activation at booster second stage burnout to final stabilization prior to boarding.

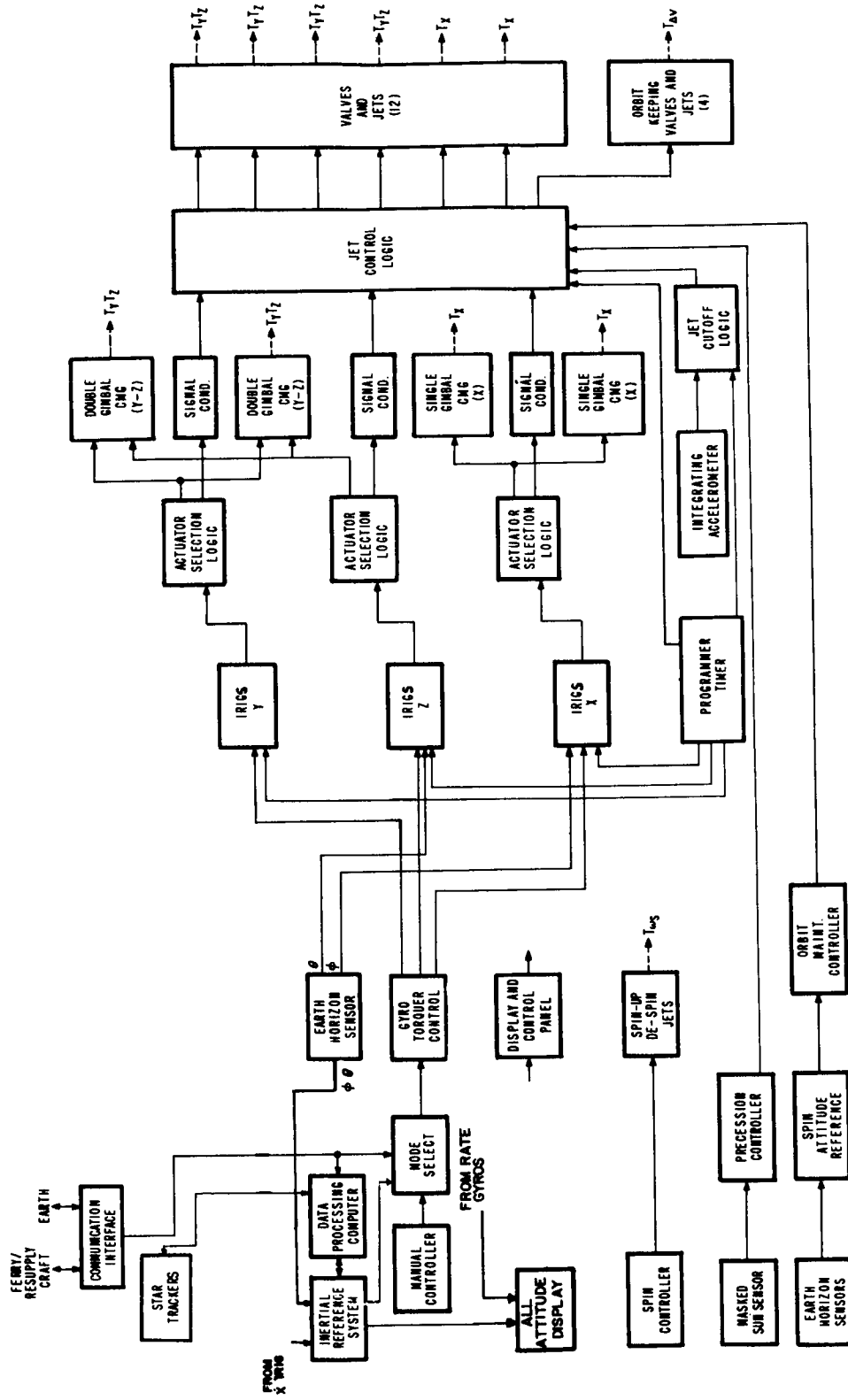


Figure B-9. Stabilization and Control System Block Diagram

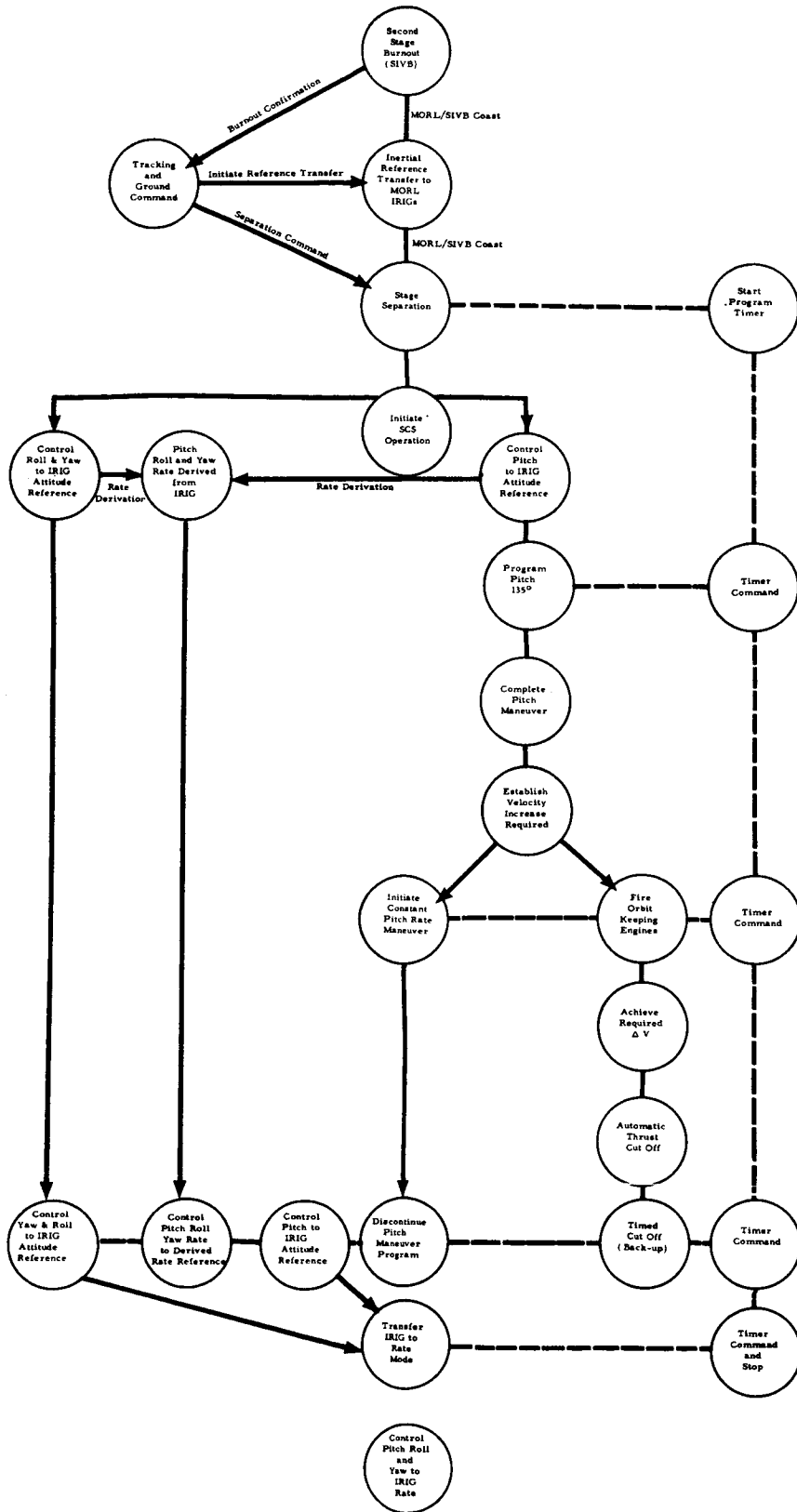


Figure B-10. MORL Control System, Mode Transition Diagram, Orbit Injection and Unmanned Stabilization

At burnout of the Saturn, the MORL orientation is available from the Saturn guidance system. At this time reference transfer to the MORL attitude reference is effected either through ground command or through programming initiated by thrust cut-off. When the attitude data are transferred, separation is accomplished and the MORL SCS maintains the reference attitude. Since both IRIG are operating as a redundant pair, rate is derived in the SCS electronics. At the proper time, controlled by an event timer, a pitch maneuver is initiated as part of the orbit circularization program. Having accomplished the maneuver, the program continues by firing the orbit-keeping thrusters and simultaneously initiating a constant pitch rate maneuver. Having achieved the necessary  $\Delta V$ , the system automatically cuts off thrust. If the automatic cut off fails, the programmer will effect cut off. At this point, maneuvering ceases and the system is switched to a rate stabilization mode. This mode has been chosen for both its simplicity and fuel economy, and the mode continues in effect till after boarding has been completed.

### B. 3.2 Belly Down

The laboratory, controlled to minimize rate errors only, is boarded after rendezvous. After boarding (Figure B-11), equipment is activated and checked out, and the mode established to preselect a belly-down attitude, the horizon hold mode. A manual maneuver must be accomplished to acquire the Earth's horizon after which the SCS will track the horizon. The system will now control to a two axis (roll and yaw) horizon reference and use the IRIG in its rate mode for rate information and to provide a yaw axis gyrocompassing signal. The initial activation procedure is completed when the CMG have reached speed and are tied into the system for long-term control.

### B. 3.3 Experimental/Inertial Mode

Since the belly-down, or horizon hold, mode is the long-term mode of operation of the laboratory, Figure B-12 shows that the experimental/inertial mode is entered from this condition. This mode requires the use of the IRS and the star trackers for reference updating. The transition to this mode

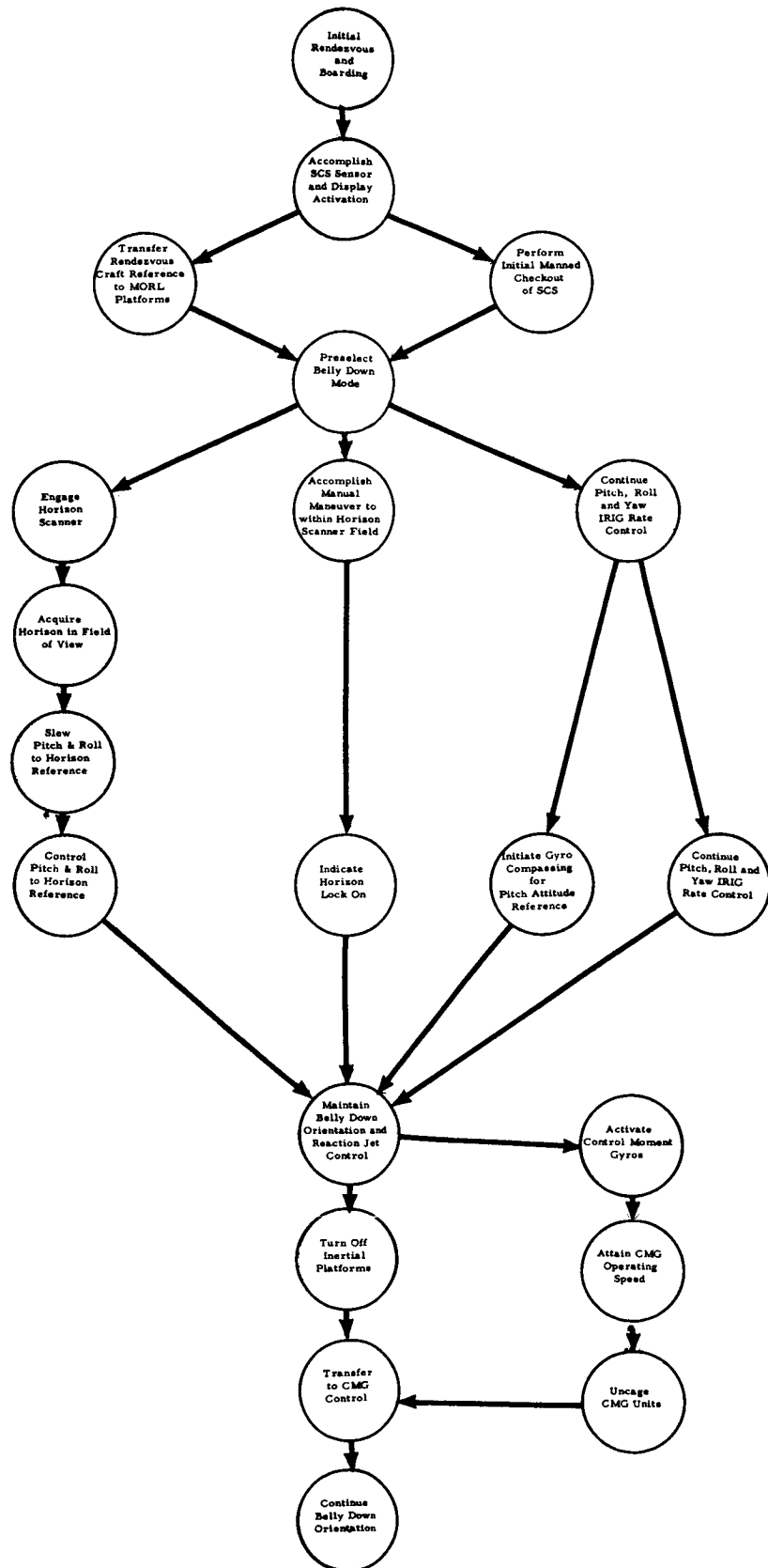


Figure B-11. MORL Control System, Mode Transition Diagram, Belly-Down Mode

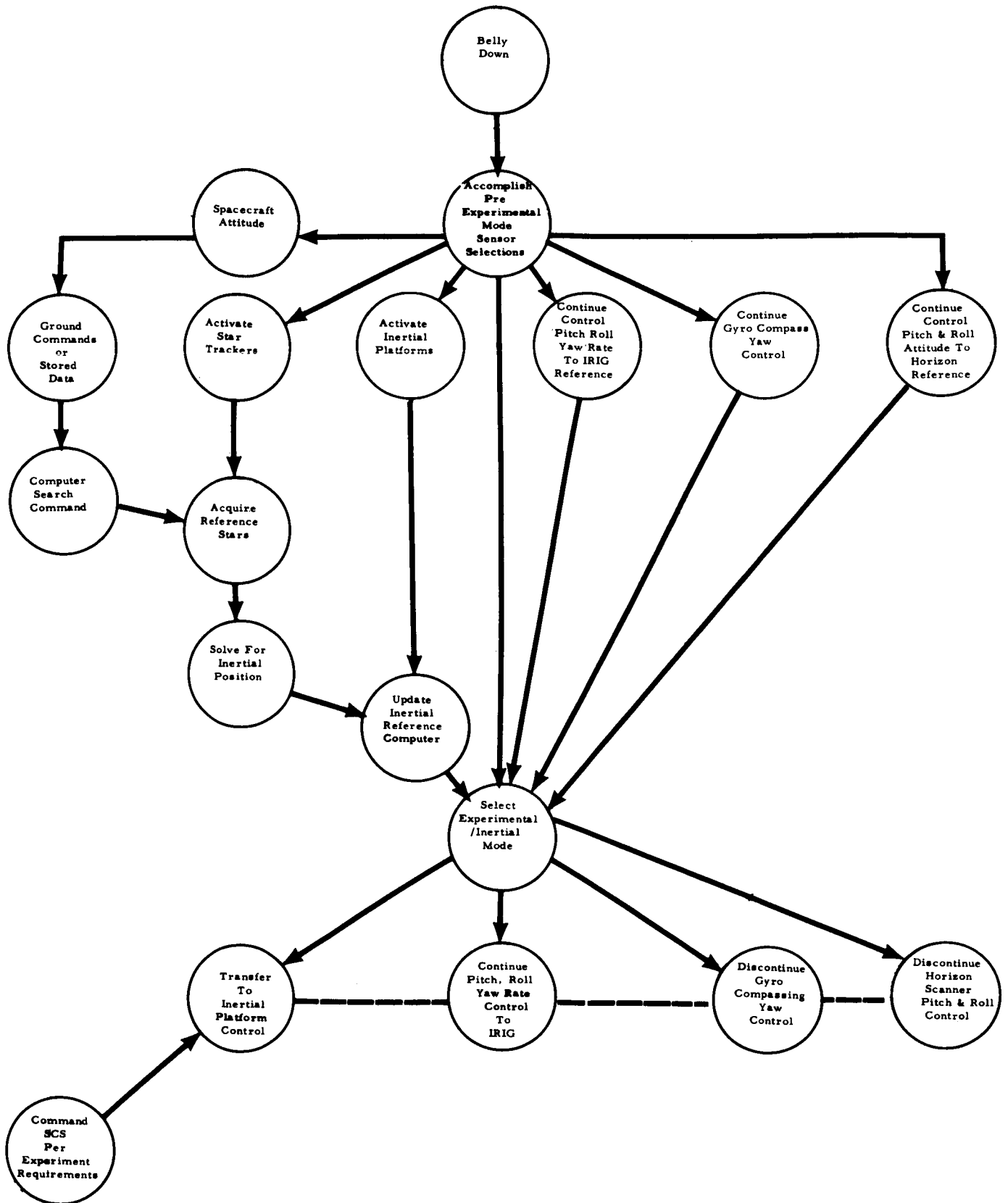


Figure B-12. MORL Control System, Mode Transition Diagram, Experimental/Inertial Mode

shows a continuation of belly down with its horizon and gyrocompass attitude reference until the inertial reference has been updated.

Inertial control during transition to the experimental/inertial mode requires the system to continue using the IRIG in their rate mode and vehicle attitude controlled to the inertial reference.

#### B. 3.4 Rendezvous

Rendezvous, shown in Figure B-13, is identical to the experimental/inertial mode except that the updating process for the inertial reference uses the horizon scanner. Provision is made for caging the CMG and using jet reaction control for required maneuvers.

The foregoing discussions and diagrams described the system in a time sequence of events. Figures B-14 through B-17 illustrate the functional relationship between command flow and the units comprising the system.

### B. 4 MORL SYSTEM OPERATING PROCEDURE

This subsection discusses the operating procedures of the MORL system.

#### B. 4.1 Basic Philosophy

The system operating procedure and its implementation with necessary controls and displays are based on the revised modes of operation. As far as possible the procedure combines the common elements of the necessary operating orientations and modes into single manual selections. Specific variations are added as required. The common elements of control, based on the desired operational modes, are graphically illustrated in Table B-2. It may be seen, for example, that rendezvous represents a method of updating the inertial reference, as does the experimental mode. Hence, the previously described orientation nomenclature as belly down, rendezvous, and experimental/inertial have been eliminated and replaced by terminology more descriptive of the SCS function.



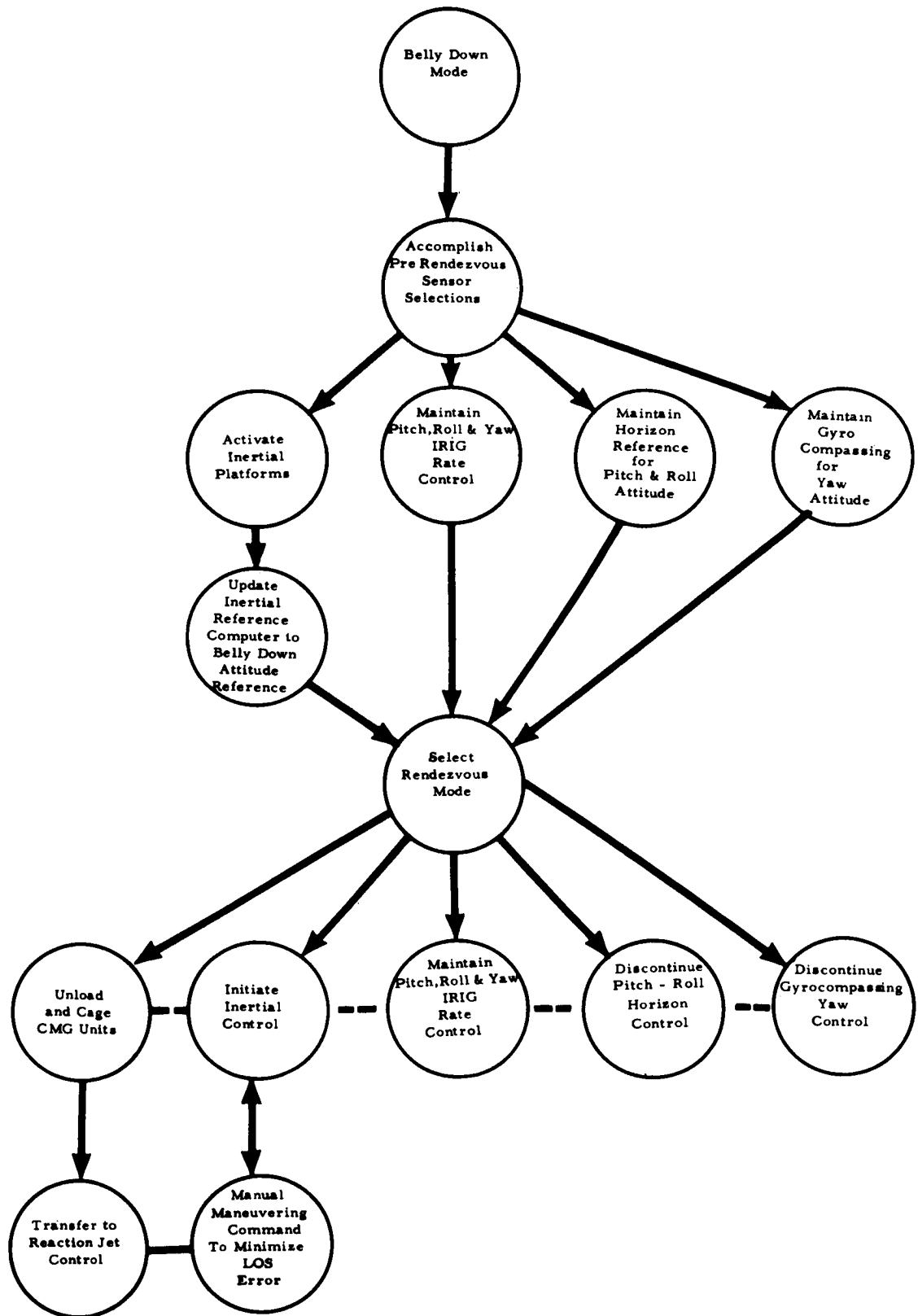


Figure B-13. MORL Control System, Mode Transition Diagram, Rendezvous Mode

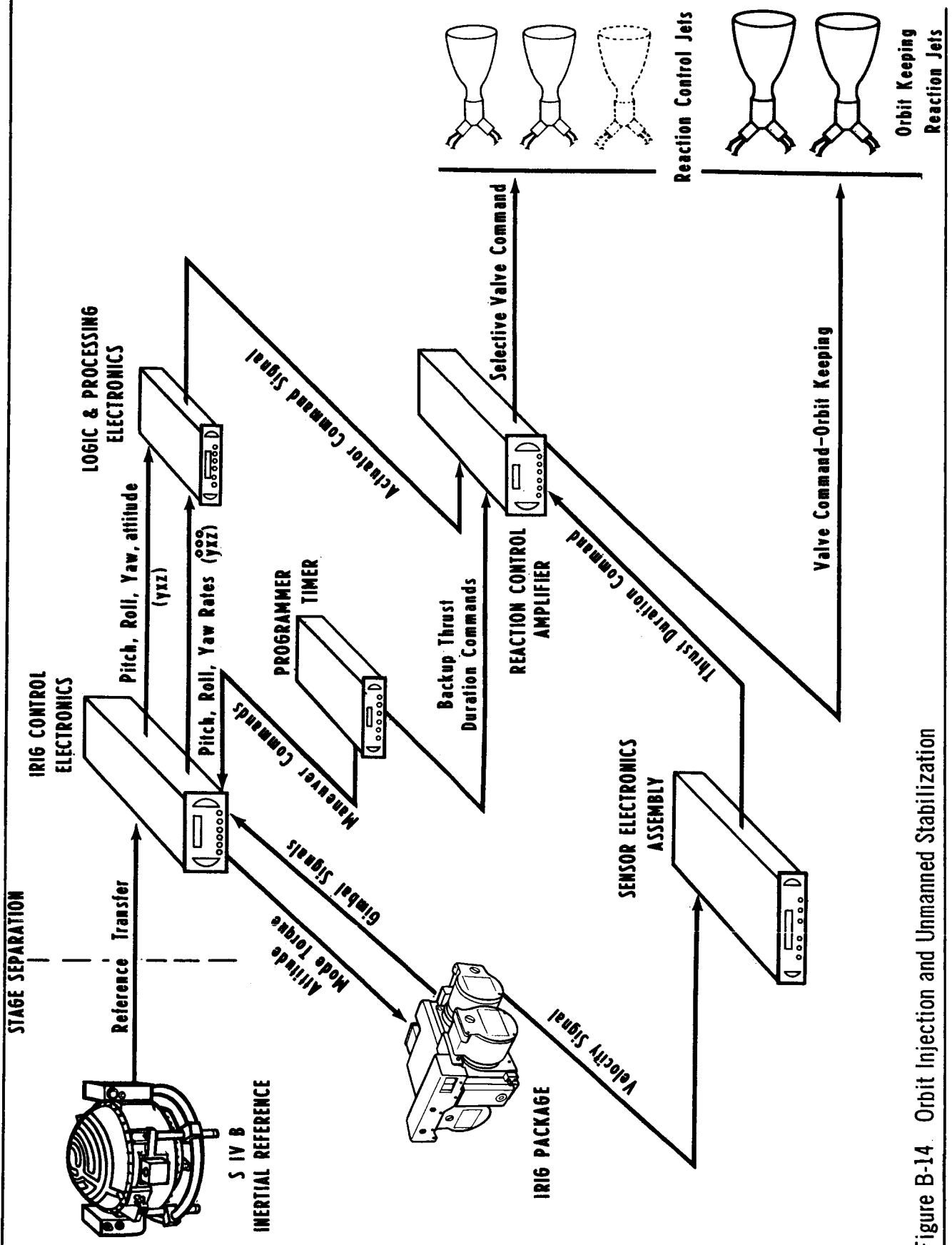


Figure B-14. Orbit Injection and Unmanned Stabilization

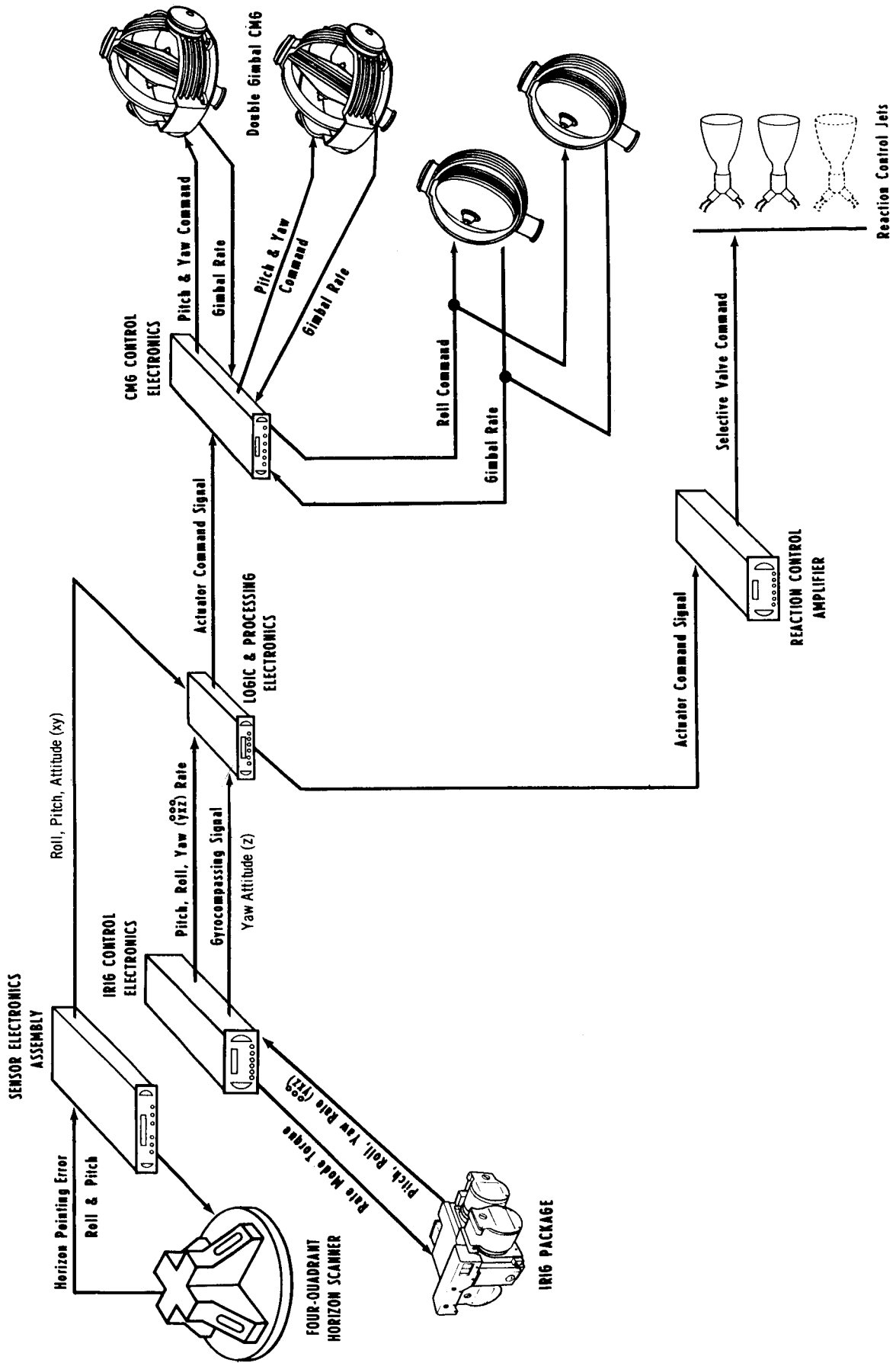


Figure B-15. Belly Down

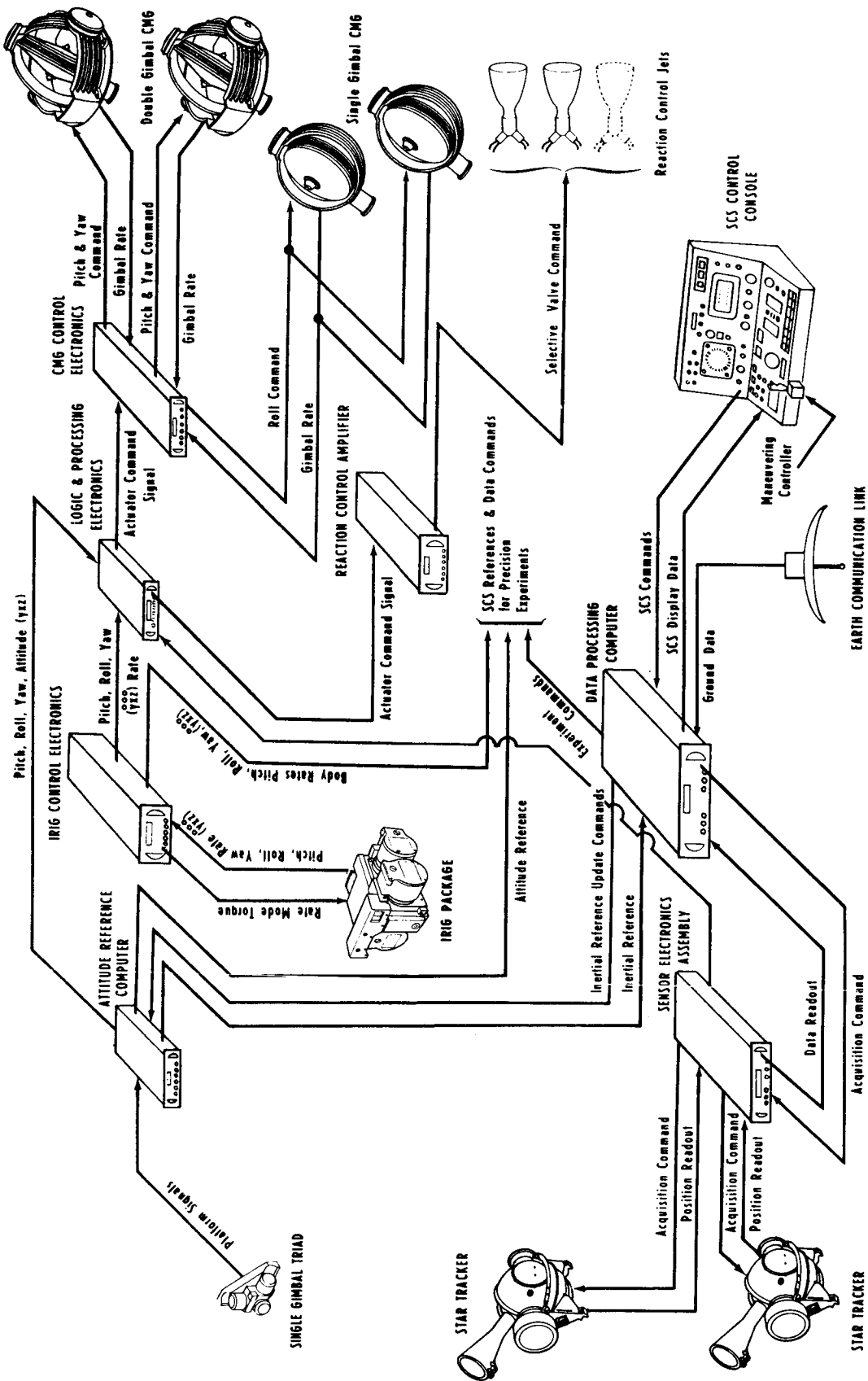


Figure B-16. Inertial Orientation

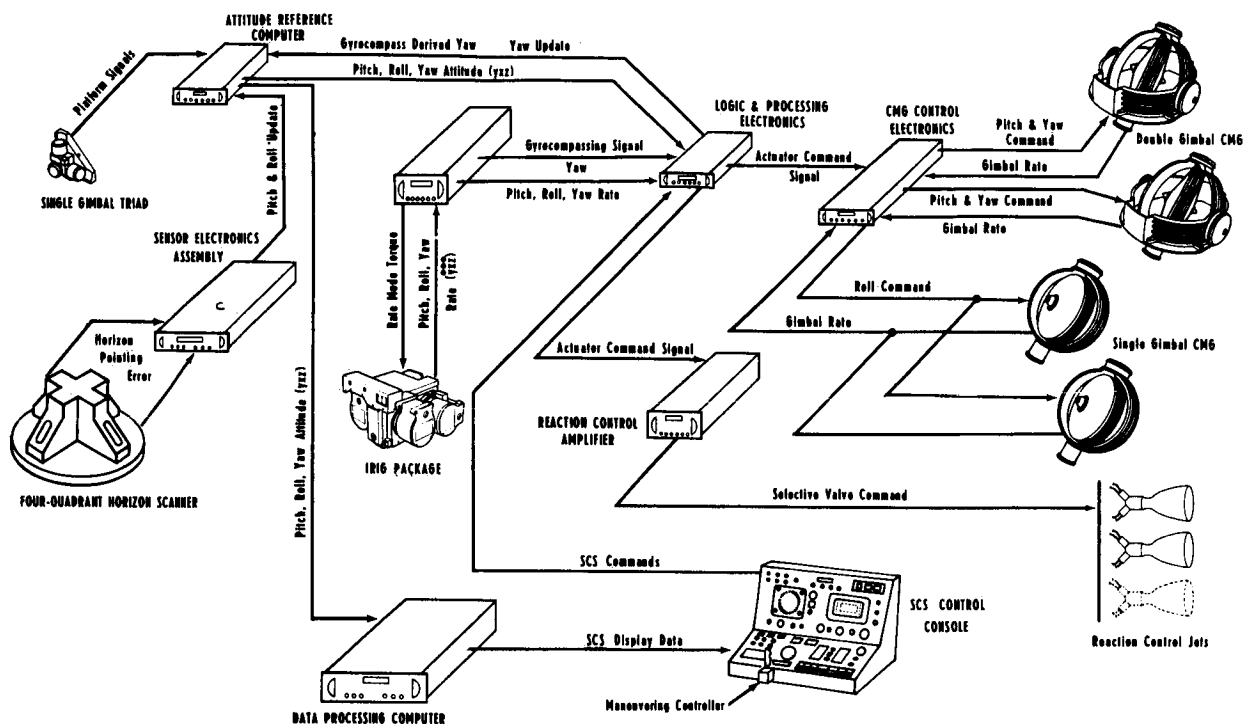


Figure B-17. Rendezvous

The underlying philosophy for the selection, sequencing command, and display mechanization for the SCS (which will be subsequently described) has been tabulated as follows:

1. The system will provide for individual selection of sensors, actuators, control channels, and instrumentation.
2. The system will provide monitoring of each separate control or display element for operability.
3. The system will require that individual element selection and their proper operation be indicated prior to selection of their using mode.
4. Conflicting modes shall be interlocked.
5. For fuel and power economy, normal maneuvering will be at a slow rate. Where possible, maneuvers will be accomplished through preselected automatic means to conserve crew time and reduce operator fatigue.
6. Command and execution of command shall be displayed.
7. Mode of operation and its effectiveness shall be continuously displayed or otherwise indicated.

8. Vehicle attitude shall be displayed in the most appropriate reference frame.
9. A single warning and a single corrective action shall be required in the event of a serious system malfunction.
10. When provided, manual maneuvering shall be logical in input motion, and command capability shall be within the range of the primary attitude reference employed.
11. At least one backup shall be instantly available for each automatic mode of operation.
12. The primary SCS controls and display shall be arranged for rapid assessment of system status, the initiation of commands, and the indication of system failure. Individual element controls and monitors shall retain a secondary status and be in a secondary location.

The following sections describe the system operation using this philosophy and depict the required controls.

#### B. 4. 2 System Operation

Upon boarding, the crew will find the SCS operating in a rate mode with redundant sensors and electronics. Jet reaction control will be in effect at this time. Since MORL in its unmanned condition will be controlled to rate only, the vehicle may be in any attitude. Thus, after initially checking out the controls and energizing the primary horizon scanner and selecting horizon hold, the crew will perform a manual maneuver to the near belly-down position. This will be accomplished as soon after boarding as practical to attain the vehicle's preferred minimum drag attitude.

The SCS manual controller will be operated to maneuver the vehicle and its body-fixed horizon scanner to within about  $10^\circ$  of the Earth's horizon. At this point the horizon scanner error signals will be used to command the vehicle to belly down, and gyrocompassing signals will command the vehicle to orient its longitudinal axis to coincide with the orbital plane.

At this time the CMG will be energized at the CMG control panel. When the panel display indicates all units have reached operating speed, their mode control selectors will be rotated to the operate position (to uncage the gyros). To use the gyros for SCS control the operator will throw the actuator selector

on the SCS control panel from reaction control to the CMG position. The system will then be operating in its long-term mode, (belly-down). Attitude will be stabilized to the horizon with the CMG providing the operating torque.

From the two panels, the SCS mode selection panel and the inertial reference panel, three SCS inertial/experimental modes can be selected. The selections are: (1) inertial hold, (2) celestial hold, and (3) pre-sel command.

#### B.4.2.1 Inertial Hold Selector

For inertial orientation, the inertial hold selector will be operated after the IRS has been energized. The system will automatically stabilize the laboratory to the reference existing at time it is engaged. The inertial reference command unit and the FDAI will indicate zero at that time. To establish a predetermined frame of reference, either the laboratory horizon scanners or the star trackers may be used to update the inertial system. The inertial reference computer will be updated (with corresponding adjustments in the attitude presentation being made automatically) after power has been applied and the selector has been switched to either horizon or celestial.

#### B.4.2.2 Pre-Sel Command Selector

Precision maneuvers to  $0.002^\circ$  indicated steps may be commanded with the preselect command counters of the inertial reference command unit. To operate, the new attitude is dialed into the device beside the present attitude presentation. The subsequent operation of the command execute push button will initiate an automatic maneuver to establish the new attitude. When the maneuver has been completed, both the acquired attitude and the command readings will coincide. Subsequently, if a manual maneuver is performed, the command display will repeat the attitude presentation after the detent switches on the rotational maneuvering controller have been operated. Maneuvering progress may be monitored on the inertial reference command unit and the FDAI.

To accomplish precision Earth-oriented experiments, orbital hold may be selected. Again, this requires that the IRS be in operation. In operation,

both manual and preselected commands are set as previously described. The principal difference is the addition of an orbital rate bias to constantly update the inertial reference computer to the geo-vertical.

#### B.4.2.3 Celestial Hold Selector

The third selection for precision experiments is celestial hold in which the system continually alters laboratory attitude to maintain a line-of-sight to a particular point in the celestial sphere. In this mode, the star trackers will provide the basic reference. Since manual and preselected inertial reference commands are inconsistent with this mode of operation, these maneuvering devices will be rendered inoperative.

Rendezvous orientation will be accomplished in the orbital hold mode, which will provide sufficient attitude accuracy through use of the IRS and an horizon update. Hence, the rendezvous capability is achieved by selecting orbital hold and horizon update with a prior energization of the horizon scanner reference. In this mode, as the vehicles approach each other, it may be desirable to unload and cage the momentum system and use jet reaction control alone. If so, the unload and cage operation will be accomplished with the CMG control panel and then the RCS actuation on the primary SCS controls.

During system operation manual maneuvering may be accomplished as follows:

1. Proportional rate all-attitude maneuvering during inertial and orbital hold.
2. Acceleration maneuvering through direct jet control at any time.

Since operation via direct jet reaction control is considered a backup mode, operation in this manner will drop out all previous selections and when the maneuver is completed the system will provide rate stabilization only.

### B.5 CONTROLS AND DISPLAYS

The following paragraphs discuss controls and displays.



### B. 5.1 SCS Mode Selection Panel

The SCS mode selector (shown in Figure B-18) represents part of the primary display and control panel. This selector provides only the basic selection functions (in keeping with established philosophy).

The panel employs two three-position solenoid-held toggle switches for mode selection. With both selectors in the off position the system is in a rate stabilization mode (the basic mode).

Because of solenoid interlock, horizon hold can be selected only if the horizon scanner has been previously turned on and has acquired the horizon (within its 45° acquisition range). The belly-down orientation is thus satisfied. The down position of this selector is similarly interlocked and held by a solenoid to give an immediate and positive indication that the selection

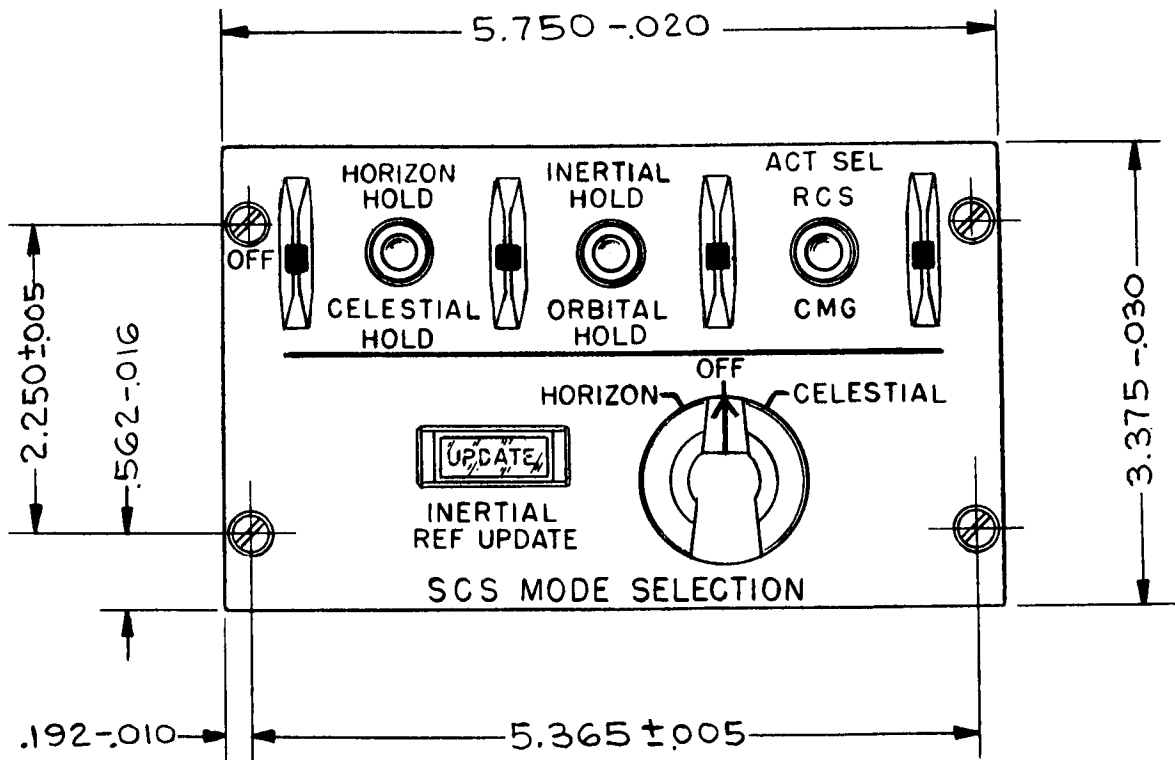


Figure B-18. SCS Mode Selection Control Panel

is effective. In this position the star tracker must be on and its computer must be providing a track signal. The selector allows the star tracker to maintain a celestial track.

The second selector, when in the inertial hold position, will cause the first selector to drop out (through the interlocking of incompatible modes). This inertial hold selector requires that the inertial reference be operating before it is engaged. As the marking implies, the vehicle will hold to the inertial reference. The other position of this selector, orbital hold, will cause the system to hold a precise orbital attitude with the inertial reference and a programmed orbital rate, and with the horizon scanner or star trackers providing an update. This second selector satisfies the experimental/inertial and rendezvous conditions.

The three-position rotary switch enables the operator to choose the means of inertial reference updating for the inertial or orbital hold modes. The switch is manually operated and requires that the updating reference has been turned on and is tracking. Update is indicated by the update light.

The two-position switch on the extreme right allows a selection of the jet reaction control system or the CMG as torque-producing elements. The switch is normally in the CMG mode (down position). Jet reaction control alone is provided primarily to satisfy the requirement for high rate maneuvering where CMG control might be inappropriate.

#### B. 5.2 Inertial Reference Command Panel

This panel, a part of the SCS primary controls and display, is a functional grouping of digital counter mechanisms. The panel provides a continued indication of vehicle attitude to  $0.01^\circ$  with a vernier on the last digit allowing  $0.002^\circ$  increments to be read (Figure B-19). The attitude mechanism is slaved to the IRS, and its zero position is based on a reference frame provided by the updating sensor (celestial or horizon). Three individual counters provide pitch, roll, and yaw attitude readings and are mounted beside identical counters which are used for preselecting attitude commands.

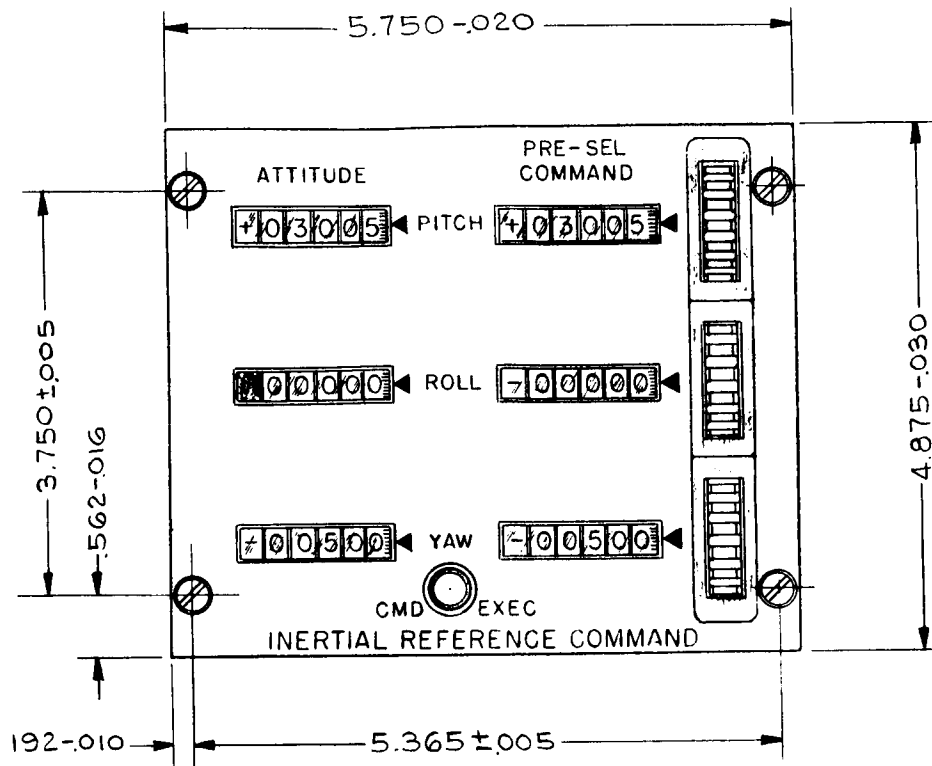


Figure B-19, Inertial Reference Command Control Panel

Commands in degrees of total attitude from the reference frame are dialed with the appropriate thumbwheel. Maneuver initiation is accomplished by momentarily depressing the command execute button. The presentation of vehicle attitude compared with command allows the operator to monitor progress of the maneuver. Residual errors will be evident by long-term discrepancies in the adjacent readings. In keeping with the interlocking and display philosophy, both attitude and command counters will remain at zero if the IRS is inoperative.

### B. 5. 3 Manual Commands

Manual commands may be input to the SCS with the rotational controller (Figure B-6). The controller, a stick, is identical to the one to be used on Apollo, and provides force-proportional control in three axes. When the control stick is moved out of detent position, switches will be actuated which will provide input for system interlocking. The force-proportional

region will allow the operator to initiate proportional rate commands to the SCS. Upon release, the stick's spring system will return it to detent, which will allow the system to return to fully automatic stabilization. As an emergency provision, stick deflection beyond the proportional region engages an additional set of switches. These switches apply dc power to the jet reaction control valves which will completely bypass this system's logic and amplifier circuits.

#### B. 5.4 Orbit-Keeping Control Panel

The third of the primary SCS control and displays is the orbit-keeping control panel (Figure B-20). This device is identical to the Apollo  $\Delta V$  display except that the ullage control has been deleted.

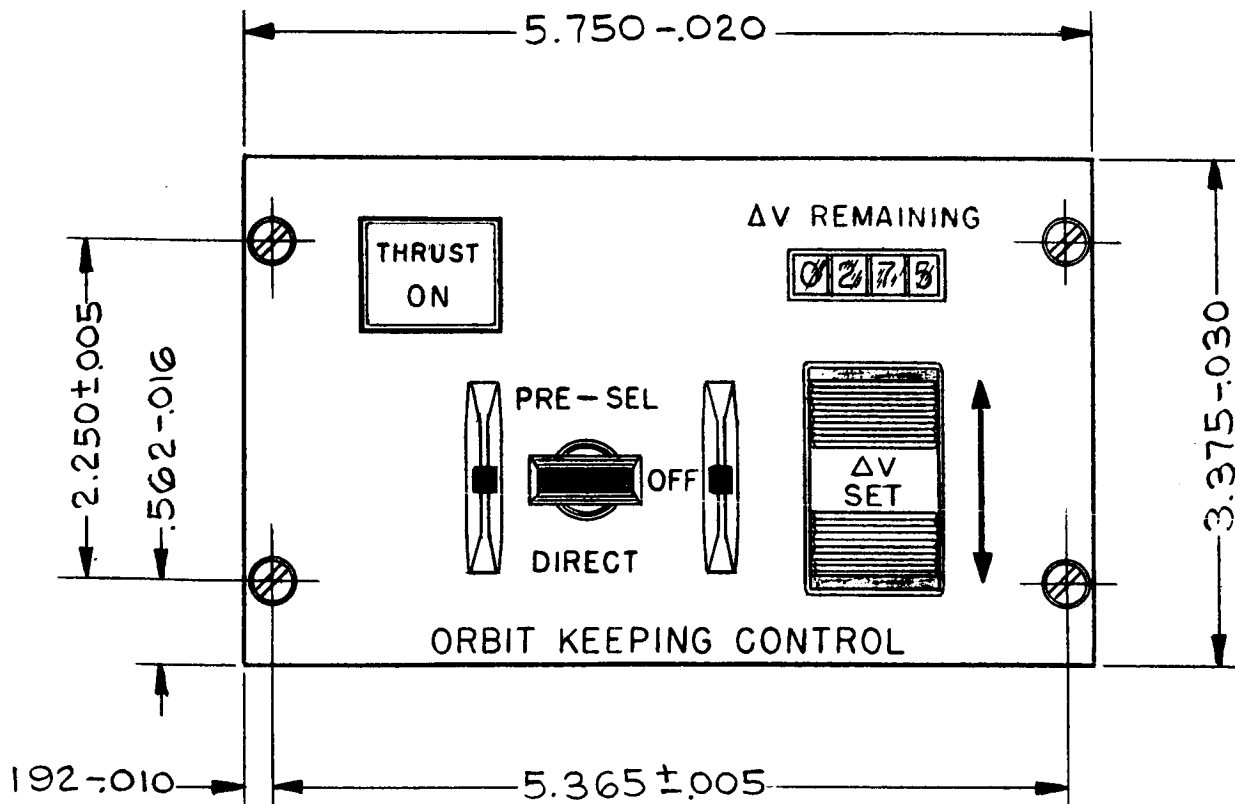


Figure B-20. Orbit Keeping Control Panel

The orbit-keeping control consists of a momentary contact thrust switch, a three-position toggle switch (solenoid held in preselect only), a  $\Delta V$  set button, and a servoed digital counter. The unit provides all necessary controls for automatic or manual orbit keeping. The solenoid-held preselect switch may be engaged only after certain prerequisites have been satisfied. The system must be engaged in the horizon hold mode and the manual maneuvering controller must be in detent. With orbit keeping preselected, the required  $\Delta V$  may be preset into the automatic system by operating the  $\Delta V$  set control. Two speeds of command insertion are possible by varying pressure on the wobble control.

The digital counter will register the required  $\Delta V$  and then thrust may be initiated by momentarily depressing the thrust on button. Thrust cutoff will be automatic when the  $\Delta V$  remaining display reaches zero. Upon cutoff, the preselect switch will drop to off which will reinstate all modal selection and command functions of the SCS. As a backup mode, the three-position selector can be manually placed in direct which will cut out the SCS maneuvering capability and will allow orbit-keeping thrust to be applied as long as the thrust on switch is depressed.

#### B. 5. 5 Failure Warning

A three-capsule warning light assembly will be on the primary control and display panel. The three capsules will be marked pitch, roll and yaw. In operation, a malfunction which renders the SCS inoperative will cause all three capsules to light. They will remain lighted until power is removed from the system. In addition, the capsules will be interlocked with the individual channel disable switches which will indicate that a particular channel has been disconnected, either arbitrarily or to allow continued operation in the face of a single-channel malfunction. These indicators have not been packaged because they should be grouped with other primary warning indicators.

### B. 5. 6 Flight Director Attitude Indicator

The flight director attitude indicator (see Figure B-8) is a slaved three-axis indicator used to display laboratory rate, attitude and attitude commands to the SCS operator.

Within its 2° visual accuracy it will display pitch, roll, and yaw attitude about the selected SCS frame of reference.

In the horizon hold and celestial hold mode the zero-attitude indicator will serve as a monitor of mode performance. The rate needles will similarly read zero. In the inertial hold and orbital hold modes, the attitude ball will indicate laboratory attitude as sensed by the IRS. The rate needles will display the vehicle rates of preselected or manually controlled maneuvers.

As both preselected and manual commands are being executed, their progress can be monitored with the command bars which are on the FDAI.

The indicator subsystem, as presently conceived, allows the manual selection of several command bar sensitivities, which will be provided on the primary SCS control and display panel in the form of a simple rotary selector.

The instrument, connected to the SCS, will serve primarily as a situation monitor. It will provide a base reference for coarse maneuvers with the manual rotation controller only when the IRS is operating.

### B. 5. 7 Secondary Controls

The following control panels, although an important part of overall SCS operation, are considered secondary in that the control and monitoring functions they provide are indirectly related or are prerequisites to mode selection. Through the interlocking of primary and secondary controls, the system prevents the engagement of any mode in which these devices are required, if they are inoperable because of malfunction or a failure to be energized.

### B. 5. 8 Control Moment Gyro Controls

The control moment gyro is a limited-momentum storage device and it requires unloading through reaction jet operation.

The control panel for monitoring gyro performance and controlling gyro operation is shown in Figure B-21. The three horizontal-scale dual indicators have been arranged to indicate gimbal authority by control axis rather than by unit to allow a rapid appraisal of remaining authority.

The use of dual indicators allows CMG balance to be evaluated at a glance, and through separate biasing techniques, permits ready alignment. Although unloading is normally an automatic function, separate unload push buttons are provided for each axis for manual unloading.

Individual mechanism controls and the safety and performance monitors are located on the lower half of this secondary panel. Only two identical rotary selector switches are provided for the four gyro units because of their interrelated operation. The three-position rotary switches apply power and cage the units in the second position. When operating speed has been reached the individual operate speed lights will come on, at which time the operator will turn the selectors to on.

The CMG is the normal means of actuation of the MORL SCS, and if the actuator selector on the primary panel is down, CMG control is engaged.

A study of the failure modes of the CMG indicates that monitoring bearing temperature, vibration, speed, and power will adequately monitor the condition of the unit. Hence, the panel failure lights indicate deviations in temperature, vibration and speed. The meter for each unit directly indicates power consumption, and indirectly monitors speed, friction, windage, and bearing load because all are reflected in wheel power.

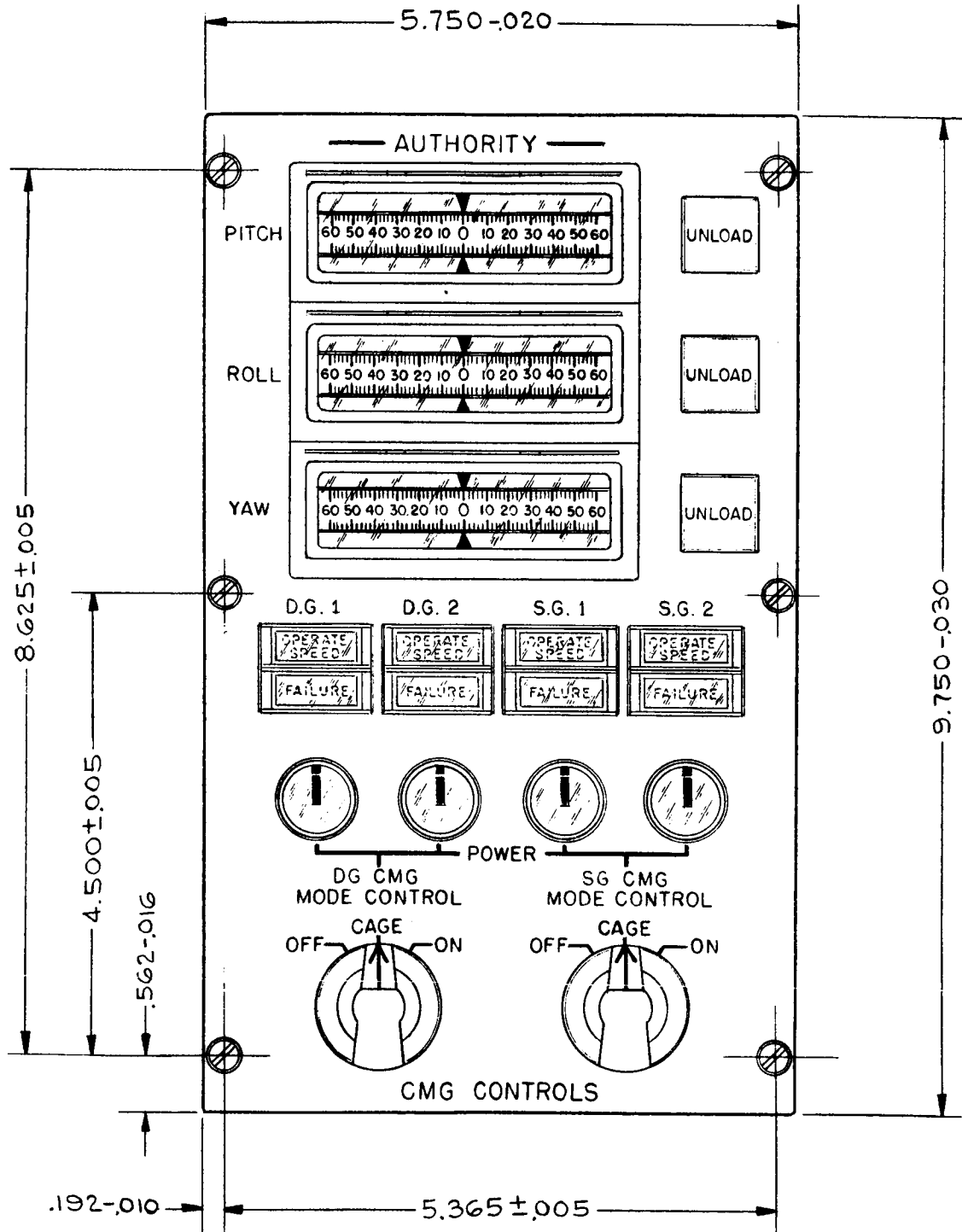


Figure B-21. CMG Control Panel



### B. 5. 9 Star Tracker Control Panel

The star tracker control panel for the dual trackers employed on MORL is shown in Figure B-22. Identical functions are provided on each half of the panel, and two-position switches are provided for energizing each tracker. Three-position rotary selectors provide mode selection. In the automatic position, with a computer star fix, the tracker will automatically sequence from field presence and capture to the final tracking mode. During this automatic sequencing the panel lights will indicate the progression of sequencing from presence to track and thus provide continuous monitoring of operation. By selecting manual command and then track the acquisition process can be accomplished manually. The indicator lights will again indicate the system status by signalling the completion of the selected function.

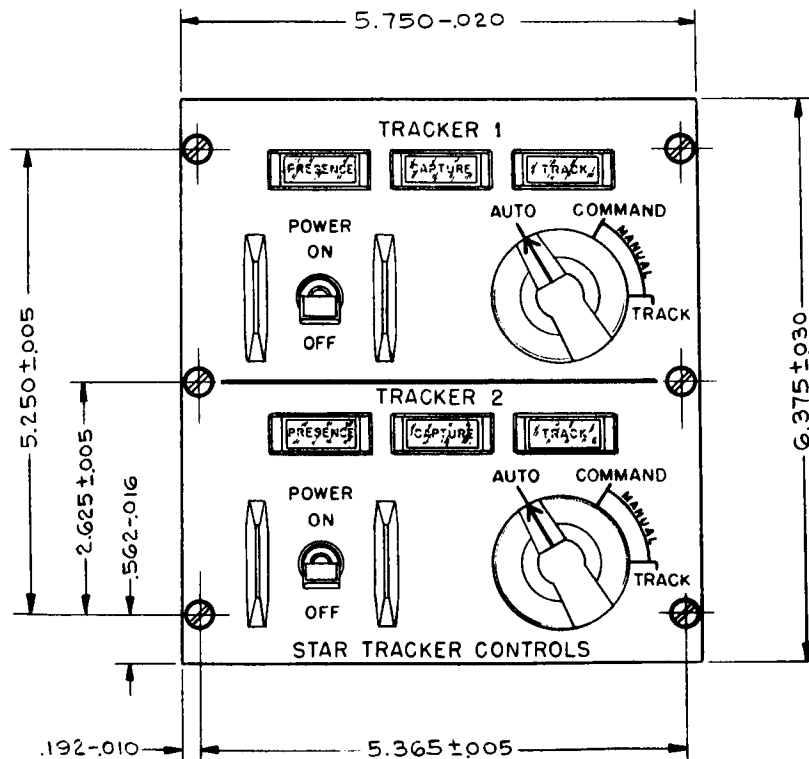


Figure B-22. Star Tracker Control Panel

The star tracker controls are considered secondary to SCS mode selection and should occupy a secondary position. Through appropriate tracker/monitoring and interlocking with the SCS system, selection of tracker modes will be prevented unless they are operating satisfactorily.

B. 5.10 Horizon Scanner Control

The horizon scanner control panel shown in Figure B-23 provides the basic control and visual monitoring functions for the SCS primary and secondary horizon scanners. Two-position toggle switches are provided for power to the scanners. The scanners are automatic in operation once the spacecraft has pointed the detector heads to within 45° of the horizon (acquisition range), and hence, mode selections are not required. To provide a visual display of performance, internal monitoring will sequentially light the indicators as the search/track process is accomplished.

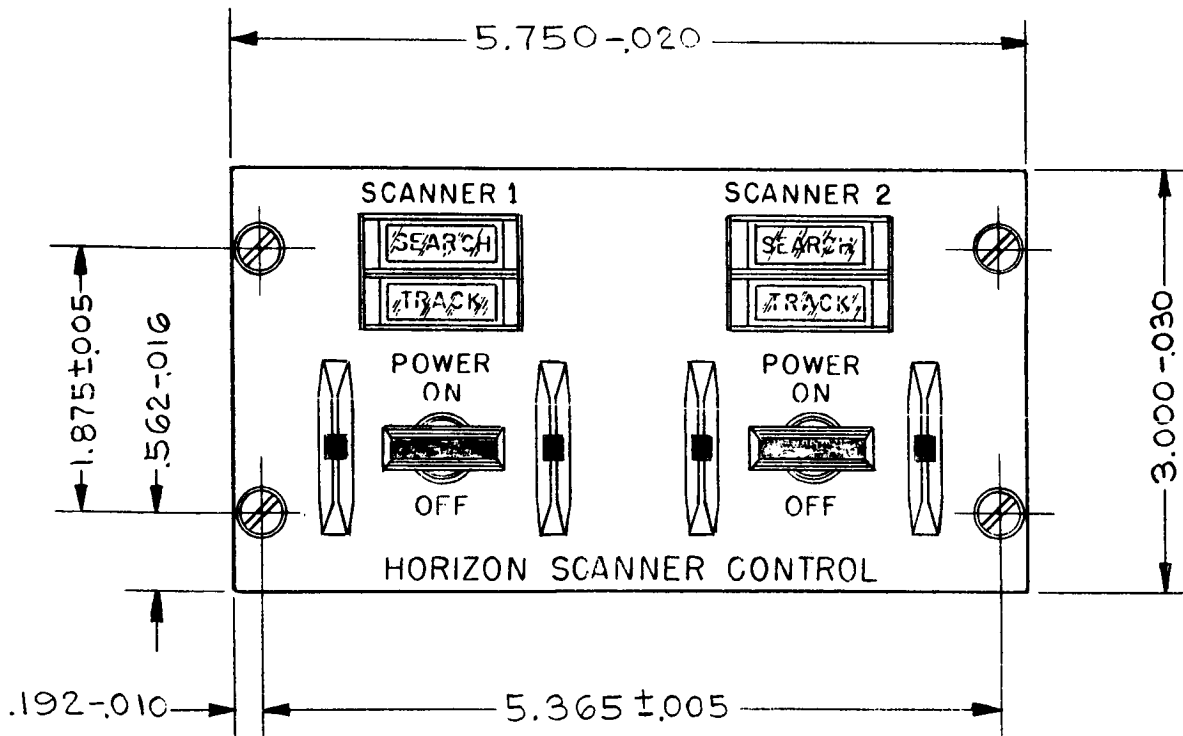


Figure B-23. Horizon Scanner Control Panel

The Internal monitoring with its search and track signals is used as part of the SCS mode selection interlocking which allows this panel to occupy a secondary position on the control and display panel.

#### B. 5. 11 Additional Controls

Although not illustrated, a small group of additional switches are required to give the SCS a flexibility not possible with the basic mode selector. Functions provided by these switches will be as follows:

1. Primary power to the SCS to implement the basic rate stabilization mode and the jet reaction control system.
2. Three-channel disable switches which allow the operator to disable individual channels if a malfunction occurs in a single channel, or to decrease fuel consumption if necessary.
3. Two switches are provided to transfer the redundant attitude gyro and accelerometer package into the system and to select either the primary or secondary horizon scanner.

## Appendix C

### SENSORS

The MORL stabilization and control system (SCS) as presently implemented employs two star trackers, two horizon sensors, two gyro and accelerometer packages, and a triad of single-axis platforms as its sensor complement. Recent orientation changes have eliminated the need for the sun sensors and solar detectors which were previously included in the sensor complement.

The following pages describe these sensors in the light of present system requirements, the performance improvements accrued through an advancing level of technology, and present maintenance and alignment criteria.

#### C. 1 STAR TRACKER

The MORL star tracker subsystem shown in Figure C-1 is made up of two mechanical assemblies that contain the telescopes and mounting gimbals, two electronics assemblies to provide gimbal control and analog signal processing, an interface unit to provide the digital/analog interface between the electronic assemblies and the data process computer, and a dual control panel.

This dual tracker subsystem has the following physical properties.

Total Weight	82.5 lb
Power (W)	ac      dc
Avg	1.1    39.3
Peak	1.1    44.7
Size	2.136 cu ft
Reliability	72.66 ppmh

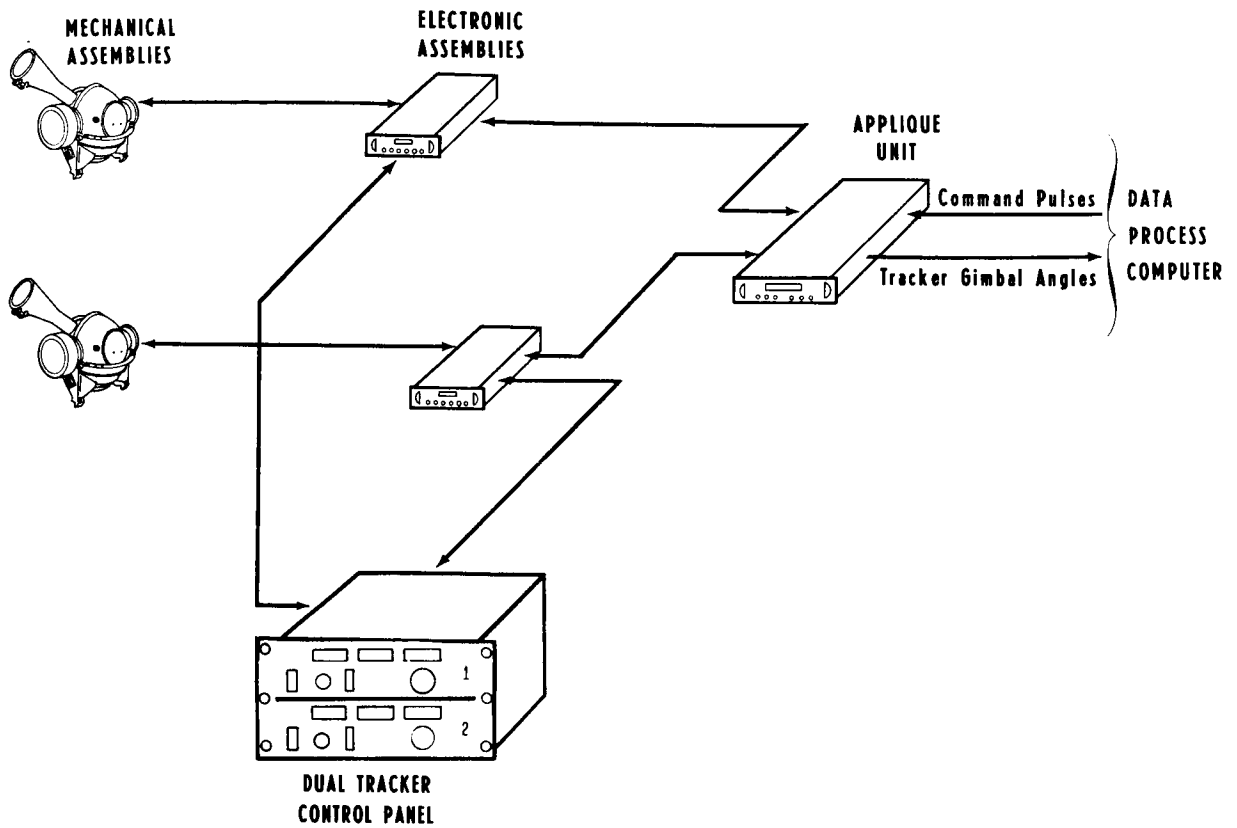


Figure C-1. MORL Star Tracker Subsystem

The performance and physical characteristics of the two independent sub-systems may be summarized as follows:

Star tracker subsystem--One mechanical assembly, one electrical assembly, and one control panel

Weight	38.8 lb	
Power (W)	ac	dc
Avg	0.55	11.1
Peak	0.55	13.9
Size	1.02 cu ft	
Reliability (Minuteman parts)	33.13 ppmh	
Operating life	12,000 hours	

Gimbal range	$\pm 60^\circ$ each axis
Field of view	$\pm 1^\circ$ each axis
Star recognition	2.0 magnitude or brighter
Star exclusion	3.0 magnitude or dimmer
Solar discrimination	
Track within	$30^\circ$ of sun line
Earth discrimination	
Track within	$12^\circ$ of Earth
Accuracy	
Command mode	60 arc sec
Track mode	22 arc sec each axis
Threshold-track mode	1.0 arc sec
Threshold-command mode	11 arc sec
Tracking rate	$0.5^\circ/\text{sec}$
Tracking acceleration	$0.045^\circ/\text{sec}^2$
Bandpass	1 cps

Two star trackers are normally used to update the inertial reference computer prior to operation of the selected precision pointing experiment. For long-term celestial-oriented experiments, which might require continuous open-loop pointing, inertial reference system gyro drift could contribute excessive error. In these cases the star trackers can be used, in conjunction with the data process computer (DPC), to directly control the vehicle on experiment. In the following discussion, the operation of one of the two star trackers is described.

A mechanization diagram of the star tracker subsystem is shown in Figure C-2, and referral to this illustration will prove helpful in understanding the operation of the various components.

Once mechanical alignment with the inertial reference system has been established, the tracker's mode control switches are positioned to command. The DPC then transmits digital inner and outer gimbal angle commands which are based on assumed (coarse) attitude information and orbit position. This information is transmitted to the trackers serially as an 18-bit binary

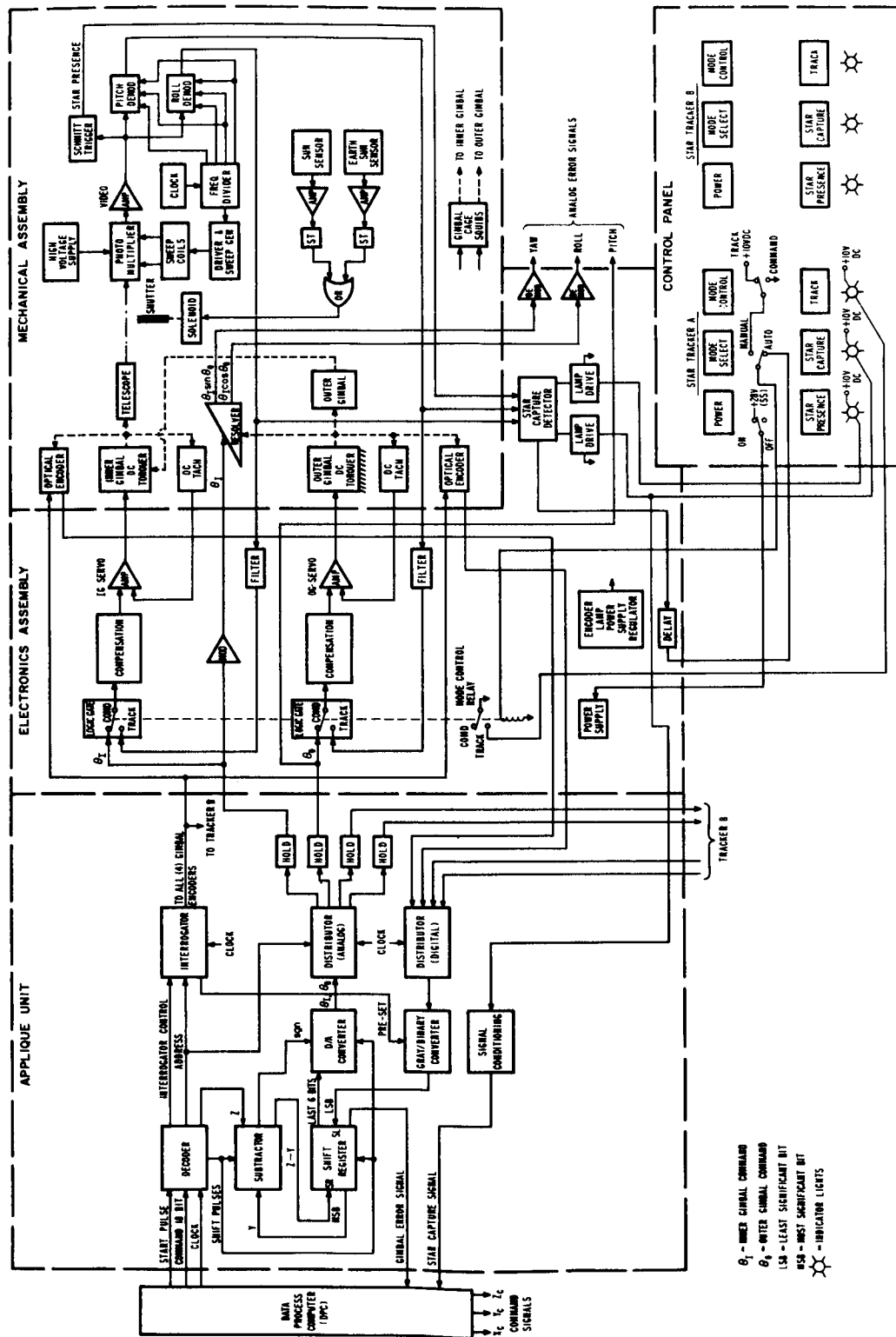


Figure C-2. Star Tracker Mechanization Diagram

word with 1 synchronization bit, 2 address bits, and 15 data bits. An alert pulse, time-phased with the command word synchronous bit, and 50-kc clock pulses are also required from the DPC.

The commanded gimbal angle optical encoders are sampled by the interrogator, and their outputs are returned to the shift register by way of the digital distributor and the gray-to-binary code converter. The gimbal command,  $z$ , and the gimbal angle,  $y$ , are then subtracted and the difference, transformed to analog error data by the D/A converter, is transmitted to the proper gimbal servo via the analog distributor. The hold circuits provided for each gimbal allow the DPC to multiplex between the two trackers (four gimbals) and other equipment. Zero-order holds of 50 msec can be readily accommodated by the present star tracker design.

The analog error command signal slews the respective gimbals at the maximum rate until the difference between gimbal command and gimbal position,  $z-y$ , is less than the last six significant bits. At this time, the servo goes into the linear operating region. When the gimbal error signal has been reduced to zero, the tracker's inner and outer gimbals have reached the commanded position and the selected guide star should be within the telescope's  $1^\circ$  field of view. If the guide star is not within the field of view, the initial assumed position was considerably in error or the gimbal angle computation was inaccurate; a star search must be initiated. If the guide star is in the field of view, star presence will be indicated on the control panel. Depending on the preselected position of the mode select switch, the tracker will either be automatically or manually switched to the track mode. A delay of approximately 0.25 sec is provided in the automatic mode to prevent switching to the track mode while slewing by large magnitude stars.

In the track mode, the telescope and its associated processing electronics control the gimbal positions. This is accomplished by sensing deviations of the star image from the telescope optical axis and supplying amplitude and polarity-sensitive dc signals, through proper filtering and compensation networks, to the inner and outer gimbal drives.



The gimbal encoders are continually sampled by the integrator and their outputs are returned to the shift register via the digital distributor and the gray-to-binary code converter. The subtracted gimbal error signals are then transmitted to the DPC. The DPC then generates roll, pitch, and yaw command signals ( $X_c$ ,  $Y_c$ , and  $Z_c$ ) which are used to supply vehicle actuator commands. These commands are processed through the SCS electronics to drive the vehicle until the star tracker gimbal angles coincide with the gimbal angles originally computed by the DPC. When the angles coincide (gimbal error signal goes to zero), the pitch and roll outputs of the photomultiplier demodulators go to null, the star image coincides with the telescope optical axis, and the vehicle axes are correctly positioned with respect to the desired set of inertial coordinates. A star-capture signal is generated as a result of the photomultiplier demodulator output going to null and this signal, in conjunction with a zero gimbal error signal, indicates update. The MORL IRS computer reference computation is then corrected and the single-gimbal platform gyros are switched into the control system to provide the inertial reference.

The preceding discussion described the operation of one star tracker in conjunction with the interface unit, the DPC, and the SCS. In normal operation, both star trackers would be employed to provide accurate three-axis information. Star tracker B would be mounted to the vehicle with its outer gimbal axis displaced  $90^\circ$  from the star tracker A outer gimbal. This allows direct reading of two of the vehicle tracker gimbal angles with only the third required to be computed from either one or both of the two trackers.

The star tracker has a pancake resolver, driven by the outer gimbal, which resolves the inner gimbal error command into coarse roll and yaw commands. These commands provide, along with the direct pitch axis error signal, three-axis analog error signals.

## C. 2 HORIZON SENSOR

The MORL horizon sensor subsystem consists of two four-quadrant sensor heads, their associated electronics packages, and a dual sensor control

panel. The dual nature of the subsystem is to provide full redundancy for local vertical sensing.

The dual system has the following physical characteristics:

Weight	29.6 lb
Average power	14.4 W
Size	0.758 cu ft

The horizon sensor subsystem, apart from packaging, is the same as the Advanced OGO (A-OGO) sensor system presently being developed by Advanced Technology Laboratories, Mountainview, California, for the NASA/Goddard Space Flight Center. Thus, the performance characteristics are identical with the A-OGO system and are as shown in Table C-1.

Table C-1 (page 1 of 3)  
 PERFORMANCE CHARACTERISTICS OF  
 A-OGO SENSOR SYSTEM

Parameter	Value
Altitude range	100 to 80,000 nmi
Performance requirements	<ol style="list-style-type: none"> <li>1. + pitch errors implies nose-up vehicle attitude.</li> <li>2. + roll errors implies cw rotation about roll axis as viewed from rear of vehicle.</li> </ol>
Control outputs	<p>Errors: 2,461 cps <math>\pm 0.05\%</math> suppressed carrier modulated voltage with zero <math>\pm 10^\circ</math> phase difference between the error signal and the reference carrier for + error signals, and <math>180 \pm 10^\circ</math> for - error signals. Reference carrier = 15 <math>\pm 2</math> V p-p 2,461-cps sinusoid.</p> <p>Position: 4 ac analog 2,461-cps suppressed carrier modulated voltages.</p>
TM outputs	Track/no-track one-zero indication.
Alarm outputs	<p>Track/no-track: Logical 1 (6 <math>\pm 1</math> Vdc) or logical zero (0 to +0.5 Vdc).</p> <p>Sun alarm: Sun presence = logical 1.</p>

Table C-1 (page 2 of 3)

Parameter	Value
Accuracy	2.5% maximum for roll and pitch (design goal)
Linearity range	$\geq 25^\circ$ roll and pitch.
Linearity requirement null offset	$0.1^\circ$ (3 sigma) at null altitude.
Total error	$0.15^\circ$ (3 sigma) over altitude range (design goal), $\pm 0.25^\circ$ at null (contractor requirement).
Scale factor	1. Control outputs = 0.4 V (rms)/deg. 2. TM outputs = 0.4 V (rms)/deg.
Output noise	$0.02^\circ$ (3 sigma).
Cross talk	Directly proportional to altitude.
Reproducibility	$0.1^\circ$ at null.
Operational range	$\pm 25^\circ$ in pitch and roll.
Open-loop gain	670 nominal.
System and response	2 to 4 cps (6 cps = design goal).
Dither frequency	15.1 cps.
Limiting values of output response	Not available.
Control outputs	For $\theta$ or $\phi \geq 25^\circ$ , then $E_{out} \leq 10.5$ V (rms) (2,461 cps).
Position outputs	For angular position of head $\leq 87.5^\circ$ or $\geq -2^\circ$ , then $E_{out} \leq 4.5$ V (rms).
Power	$\pm 20$ Vdc $\pm 1.5\%$ from $Z_{source} = 10$ ohms, $< 1\%$ ripple, 1.2 V (peak) transients, maximum power $\leq 12$ W.
Shock	45 g, 2.2 msec along thrust axis. (Design goal of 50 g for 2.2 msec, all axes). 22 g, 4.4 msec along transverse axes.
Acoustic noise	SPL of 145 dB overall from 51.5 to 9,500 cps as a design goal.
Vibration	1. Random: 20 to 2,000 cps, $0.1g^2/cps$ with a rolloff at 12 dB/octave above 1,000 cps for 8 min. in each axis. (Design goal of 12 min. /axis at same level.) 2. Sinusoidal: 3 min. in each axis.

Table C-1 (page 3 of 3)

Parameter	Value	
	Frequency Range	Level
	5 to 250 cps	3.5 g rms
	250 to 400 cps	6.5 g rms
	400 to 3,000 cps	13.0 g rms
Temperature	-35°F < T < +160°F as a design goal, -20°F < T < +140°F as a design requirement.	
Storage life	≥ 3 years.	
MTBF	256,000 hours based on three-tracker operation and 1 year.	
Equipment life requirements	≥ 3 years.	
Weight	Electronics package	4.5 lb
	Each head	4.0 lb (two required)
	Complete subsystem	12.5 lb

The A-OGO sensor operation utilizes four (or three) infrared search track units, which track points on the Earth's surface separated 90° in vehicle azimuth. This is accomplished by detection of the infrared energy in a narrow beam that is caused to oscillate (dither) sinusoidally about the horizon (Figure C-3). This beam is produced by a movable mirror (positor) and telescope. A tracking servo (Figure C-4) is intentionally made to oscillate at a controlled dither frequency (15 cps) and with a controlled amplitude (typically 3° peak to peak). This oscillation, manifested by the positor motion, causes the field of view of the telescope to continually cross and recross the horizon. If the horizon is centered in the oscillation field of view, the signal amplifier output will be symmetrical. The Schmitt trigger switches positive or negative, depending on whether the input voltage is positive or negative. Under these conditions, the trigger output will be positive for the same length of time that it is negative, resulting in a zero dc component in its output. If the horizon is displaced from the center of the positor oscillation, the Schmitt trigger will have a dc component. This signal is amplified by the positor drive amplifier and recenters the oscillation of the field of view on the horizon.

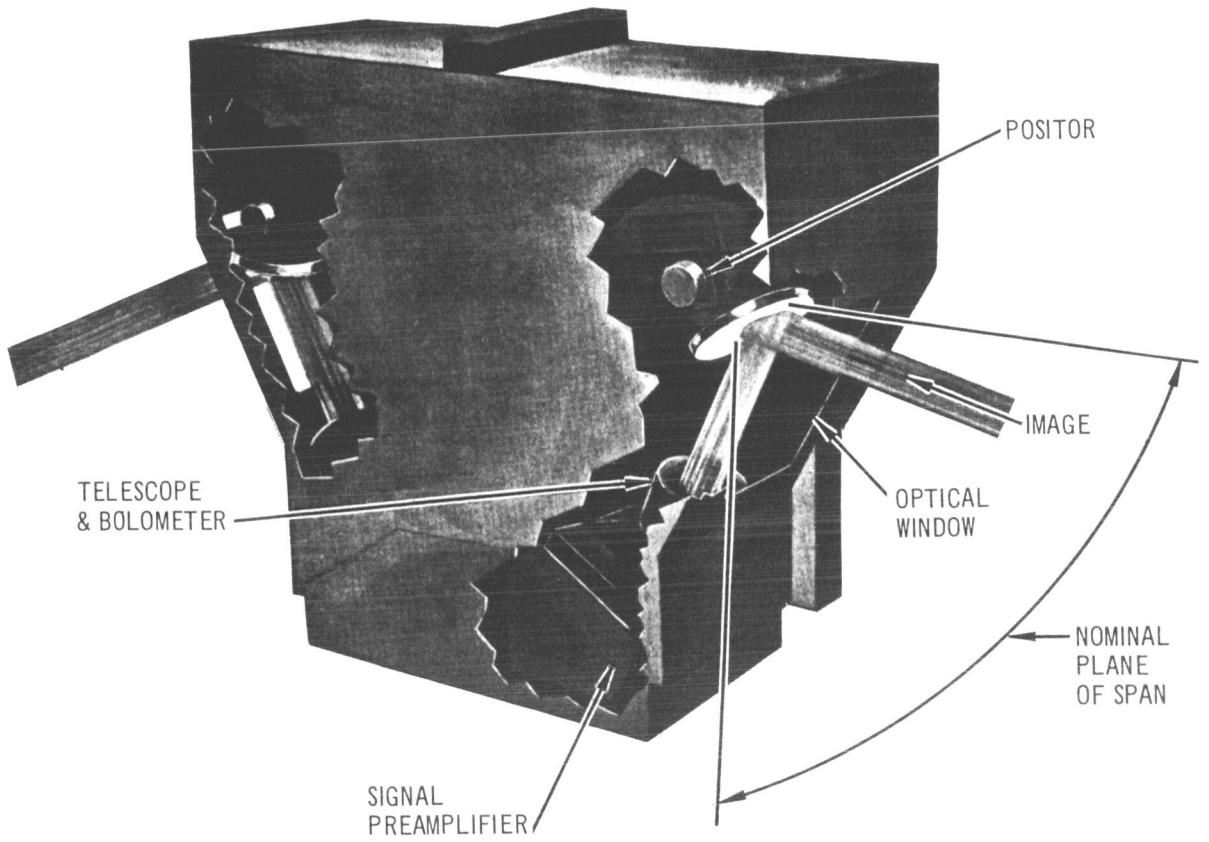


Figure C-3. OGO Dual Tracker Head

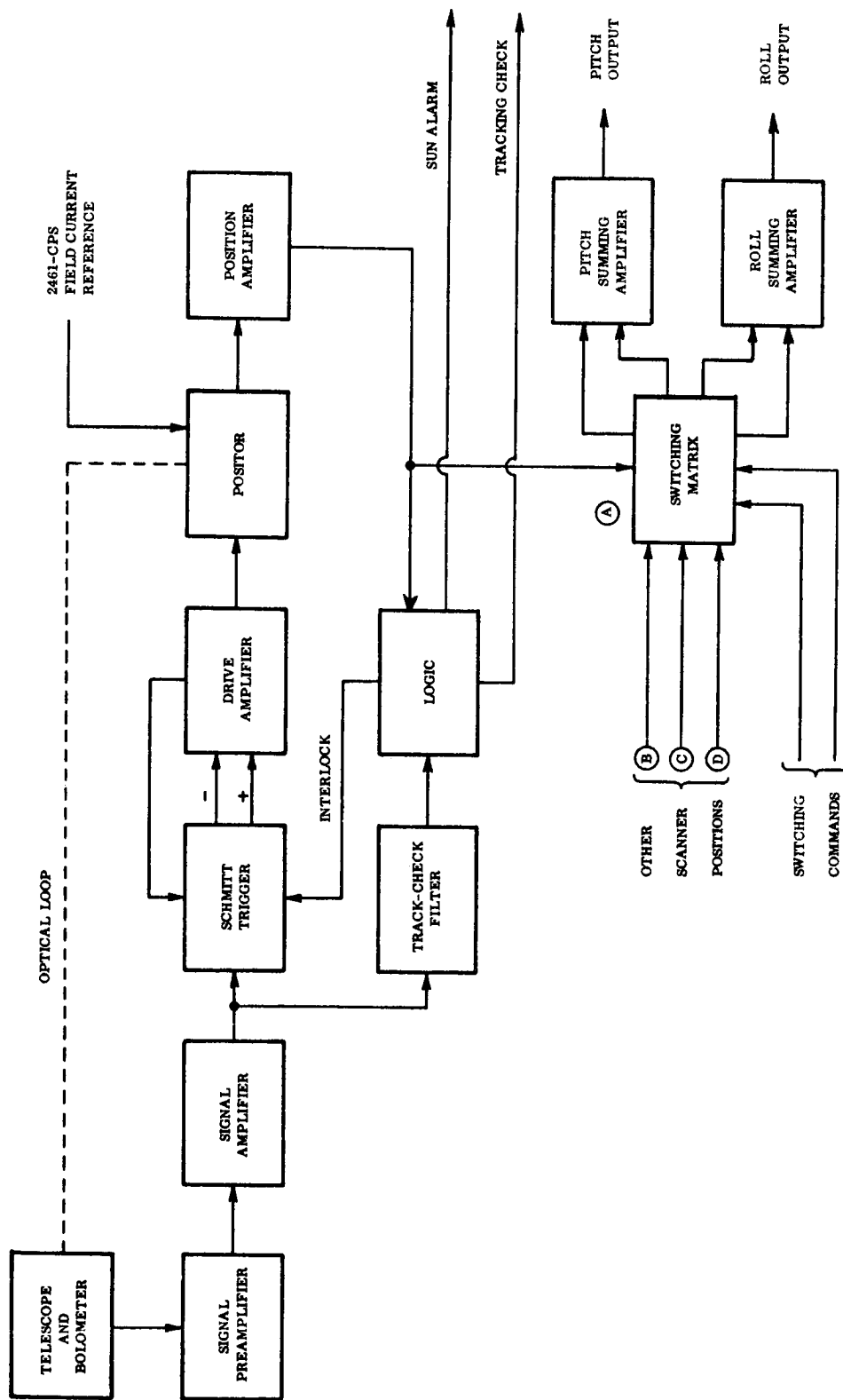


Figure C-4. Horizon Sensor Block Diagram

The trigger is designed so that, in the absence of an input signal, it will remain permanently in its last state. Means are provided to reverse this state when the positor reaches either limit of travel (typically  $\pm 45^\circ$ ); a search action will result. In this design, the state reversal to sweep Earthward is caused by breakdown of a Zener diode connected between the drive amplifier output and the Schmitt trigger input. The diode is set to conduct whenever the drive amplifier produces an output corresponding to slightly more than enough voltage to drive the positor to one extreme of its range. To sweep in the nominal upward direction (out of the Earth), an interlock reverses just after the full downward sweep, locking the Schmitt trigger output for the duration of the complete upward sweep. Regardless of the infrared gradients crossed during this sweep, the inputs to the Schmitt trigger will not affect the output. Upon completion of the upward sweep, the Zener diode clamps the Schmitt trigger input to the proper state, the interlock unlocks the Schmitt trigger output, and the downward sweep commences. Because the Schmitt trigger output is a square wave and the positor drive amplifier operates essentially as an integrator in the search mode, the resultant positor motion is nearly triangular during search.

The transition from the search mode to track mode is guaranteed by providing a delay in the positor reversal after the Schmitt trigger changes state, and by causing the initial crossing pulse to decay during this delay time.

The readout circuits include the redundant field current generator, individual position amplifiers for each tracker, a switching matrix, and two summing amplifiers. The field current generator supplies a 2,461-cps voltage to the field coils of all positors in series. This voltage, proportional to the positor angular position, is induced in the drive coils, amplified by the position amplifiers for each tracker, and combined as redundant pitch and roll outputs in the switching matrix and summing amplifiers.

Tracking check circuits are provided to furnish output signals to indicate if the trackers are actually tracking the Earth's horizon. During the search, the interlock circuits help prevent possible locking onto a gradient within

the Earth. This is accomplished by allowing lock-on only while the line of sight is searching in a downward direction. A sun alarm circuit furnishes a logical output signal that indicates when the sun is being tracked. Because only three of the four trackers are required for determination of the required pitch and roll information, the sensor is capable of operation if any one of the four trackers views the sun (or fails). This is brought about by routing the sun-alarm signal to the tracker logic circuitry. The three trackers to be used are thereby determined, and signals are sent to the switching matrix to eliminate the inoperative sensor and perform the required analog computations. In the case of a tracker failure, a track/no-track signal is sent from each tracker to the vehicle logic circuits, where the decision is made to eliminate the inoperative tracker and perform the required analog computations. It can be seen, therefore, that the system possesses an inherent three out of four redundancy characteristic.

### C. 3 ATTITUDE GYRO AND ACCELEROMETER ASSEMBLY

The MORL SCS employs the Honeywell DGG 245C attitude gyro and accelerometer assembly. This assembly was originally designed for and is in use in the Apollo SCS. The attitude gyro and accelerometer package contains three orthogonally mounted GG 248-type rate integrating gyros and a DGG 177-type hinged pendulous accelerometer. Each sensor has a thermally insulated shroud with an integral connector. These sensors may be readily replaced in a properly aligned position through the use of a quick-disconnect clamping mechanism operating against precision surfaces.

The complete package has the following physical characteristics:

Weight	13.7 lb
Power	7.9 W ac 57.6 W dc
Volume	0.19 cu ft



The GG 248 inertial rate integrating gyros (IRIG) contained within this unit exhibit the following physical and performance characteristics:

Angular momentum	$1 \times 10^5$ gm-cm <sup>2</sup> /sec
Gimbal freedom	$\pm 4.4^\circ$
Input angular freedom	$\pm 20^\circ$
Gain (H/D)	0.22
Operating temperature	170°F
Threshold	$< 0.01^\circ$ /hour
Gravity sensitive drift	0.06°/hour rms (1°/hour max.)
Gravity insensitive drift	0.09°/hour rms (1°/hour max.) (max. may be trimmed to 0.1°/hour)
Random drift	0.4°/hour

The DGG 177 pendulous accelerometer is a servo-rebalanced pendulous accelerometer with the following characteristics:

Pendulosity	2.86 gm-cm
Hinge axis damping coefficient	47,000 dcm-sec
Pendulum moment of inertia (hinge axis)	7.06 gm-cm <sup>2</sup>
Pendulum characteristic time	$150 \times 10^{-6}$ sec
Pendulum freedom	$\pm 0.23^\circ$
Operating temperature	170°F
Accelerometer current scale factor	13 ma/g
Pickoff sensitivity	50 V/rad
Threshold	$1 \times 10^{-5}$ g

The gyro and accelerometer assembly, as employed in the MORL system, provides three-axis attitude information during the orbit injection phase of the mission. Subsequent to injection, the package is used to provide vehicle body rates. The accelerometer provides the reference for thrust cutoff during the vehicle orbit-keeping operation.

Two identical assemblies are carried in the MORL SCS, providing redundancy during the unmanned mode of operation and a wired-in spare for the remainder of the mission.

#### C. 4 SINGLE-GIMBAL TRIAD

The requirement for an inertial reference system in the MORL SCS is satisfied by the single-gimbal triad (SGT) mechanization. The SGT consists of three single-axis platforms (SAP) mounted with their axes mutually perpendicular so as to form an orthogonal coordinate frame. Figure B-3 shows the SGT. The platform cylinders are modular in design so that they may be readily removed and replaced in the mounting. Furthermore, they are interchangeable, providing for economical maintenance in terms of required spares.

The SGT mounting is rigidly attached to the laboratory attitude reference base (ARB) structure and the axes of the three platforms are oriented to correspond with the laboratory pitch, yaw, and roll axes. Each platform contains an IRIG mounted on a single gimbal.

The gyro employed in the present application is the MIT-designed 18-PIRIG. In addition, each platform includes a gimbal torquer, an optical output shaft encoder, and the electronics required for gimbal torquing and output signal generation.

##### C. 4. 1 Single-Axis Platform

The SAP design is essentially a hybrid, combining those features of a fully gimbale platform and a strap-down inertial reference which is most useful to the MORL mission. The elimination of large gimbals and their associated pickoffs and torquers in a fully gimbale platform provides a considerable saving in weight, volume, and power. Since the attitude reference is not used for guidance or navigation, there is no need to mount accelerometers on a stable element, and the use of a single gimbal about each axis provides sufficient accuracy for experimental purposes.

Details of the electromechanical schematic and block diagrams which are used to describe SAP operations, are given in Appendix D. The input axis of the inertial rate integrating gyro is identical to the SAP gimbal axis. Vehicle rotation about the gimbal axis produces a gyro output displacement that is proportional to the input displacement. An error signal generated by the gyro pickoff is used to drive the gimbal torquer in such a way as to torque the gyro back to zero output displacement. The net effect is that the gyro and the gimbal shaft, to which it is attached, retain their original orientation in inertial space about the SAP axis while the vehicle rotates about the axis. The amount of this rotation is output by an optical incremental shaft encoder.

The incremental shaft encoder produces a pulse whenever the vehicle rotates through a certain small angle (approximately  $0.01^\circ$ ). The IRS computer updates its vehicle orientation output whenever a pulse is received. This permits small-angle approximations to be used throughout the computations.

#### C. 4. 2 Accuracy

The SGT has the following basic accuracies in its present configuration.

Resolution	$0.01^\circ$
Random drift	$< 0.01^\circ/\text{hour}$
Drift rate (between calibrations)	$0.08^\circ/\text{hour}$
Overall accuracy	$0.09^\circ/\text{hour}$

Furthermore, it has an all-attitude capability and can accommodate any combination of rates (about its three axes) up to  $0.1^\circ/\text{sec}$  absolute value while maintaining the above accuracies.

#### C. 5 ALIGNMENT OF SENSOR COMPONENTS

Mission objectives of the MORL require that the SCS reference sensors must be aligned to a common orthogonal frame. Capability must also be provided for aligning experiment sensors to the laboratory reference frame. To accomplish these objectives, a combination of mechanical and optical reference methods has been selected. The mechanical alignment provides an approximate common reference for the SCS and experiment sensors, and the optical alignment provides a precise reference.

### C. 5. 1 Mechanical Alignment

The structural frame of the laboratory furnishes the most appropriate alignment reference. Those portions of the SCS and associated systems which require only first-order alignment (from  $\pm 0.1^\circ$  to  $\pm 0.5^\circ$ ) will be referenced to it by rigid mounting and survey-type alignment to vehicle pitch, yaw, and roll axes. Components such as the CMG, attitude gyro, and accelerometer package can be referenced to the laboratory frame in this manner. The RCS is also aligned to this reference. Since the laboratory is operating in a zero-g environment at low turning rates, structural flexure and deformation should not be excessive and the vehicle structure can be considered a rigid body to a first approximation.

For those components of the SCS which require more precise alignment, an attitude reference base (ARB) is provided. The ARB is a rigid structural assembly on which the IRS, the star trackers, the horizon scanners, and alignment components are mounted. This base is located in the experiment bay of the laboratory with mounting pads provided between the ARB and the sensors to provide alignment to within  $0.1^\circ$ .

### C. 5. 2 Optical Alignment of SCS Sensors

The optical alignment equipments mounted on the ARB consist of two autocollimators and a periscope assembly. The optical alignment equipments permit precise alignment of the star tracker and the SGT inertial reference. The SGT frame is the fundamental precise reference frame for navigation and all experiments. One autocollimator and a periscope assembly are used to align the SGT and star trackers about the pitch and yaw axes; the setup is shown in Figure C-5. Polished optically flat faces on the SGT and trackers serve to reflect the light beams. Alignment about the vehicle roll axis requires a second autocollimator and additional optical equipment. The second autocollimator is mounted below and parallel with the first autocollimator as shown in Figure C-5. A second periscope is also mounted directly below the optical faces of the SGT and star trackers. Shutter mechanisms, similar to those used with the pitch-yaw autocollimator, are used to read each sensor alignment. Misalignments of the porro prisms about the

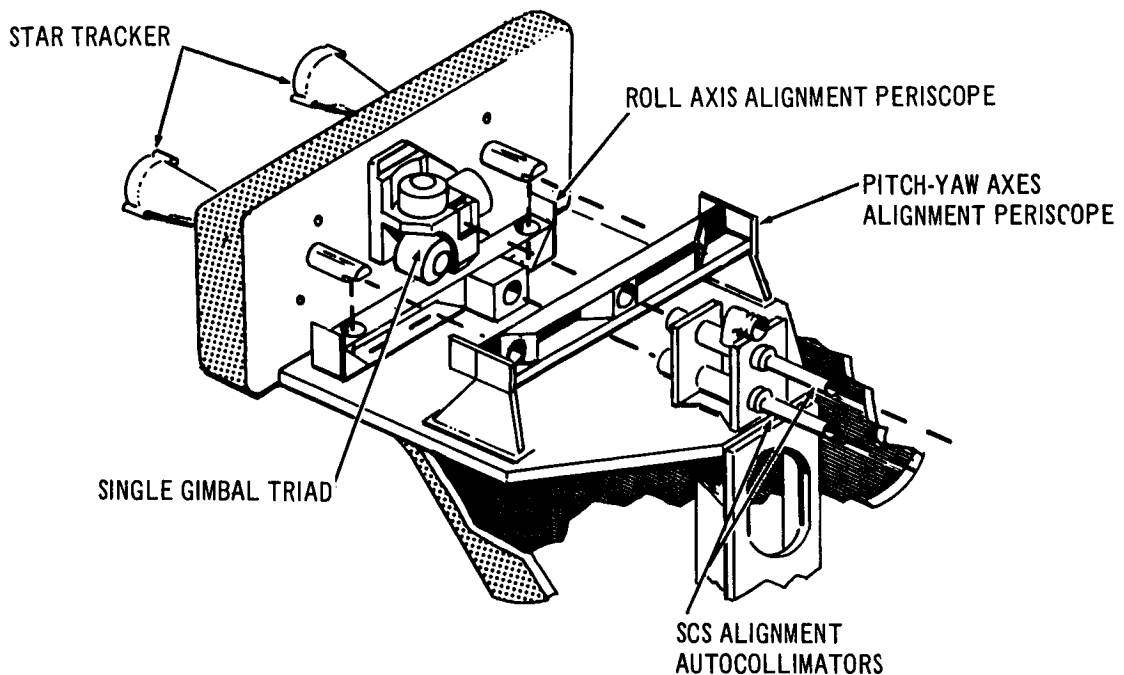


Figure C-5. Precise Sensor Alignment Configuration

periscope axis are not a source of error. Nevertheless, calibration may be checked using the same mirror as that described above. Alignment accuracies about all axes, using the above method, should be better than 10 arc sec.

In actual operation, the alignment is done computationally rather than physically because the mechanical mounting assures that all sensing elements will be oriented within the field of view of the autocollimator. The beam deviation made by each element is measured as an output in the form of an analog voltage. This voltage is fed to the DPC, as well as to the experiment and operational control panels, if required. Shutters and semiopaque prisms are employed to isolate each component for measurement. Porro prisms are used in the periscope for right-angle deflections of the light beam.

It is extremely important that these prisms do not rotate about the major periscope axis as a result of vibration or any other disturbance.

Misalignments such as these will cause errors in yaw axis alignment equivalent to the prism misalignment. Considering the environment in which the optical system is to be used, it is considered within the present level of technology to fabricate a periscope with the required stiffness, provided care is taken in the mechanical design to withstand the launch environment.

Calibration of periscope prism alignment can be most readily accomplished using an optically flat mirror of the same length as the periscope. The mirror is manually inserted between the periscope and the sensors. Alignment readings are then taken in the same manner as they would be for each sensor. Because the target surface should not show any misalignment, those misalignments which are read are caused by the periscope. Since the values of periscope deviation are known, corrections can thereafter be made in the computer. The mirror is then removed for normal operation.

Once the angular orientation between the SGT and star trackers has been established, it is not likely to change significantly unless maintenance is performed on the sensors or the vehicle is subjected to severe vibration or shock (for example, a large docking impact). In any case, sensor alignment should be checked before every series of precision experiments to obtain maximum scientific validity.

The ARB forms a portion of a larger mounting structure which provides a zero-load base to which experiment sensors may be attached permanently or temporarily. Optical alignment equipments are used to align the remotely located sensors relative to the attitude reference within the accuracy range of  $0.1^\circ$  to  $0.01^\circ$ . The configuration is shown in Figure C-6.

### C. 5.3 Alignment of the Experiment Sensors

Provision must be made for precise alignment of experimental equipment to the IRS coordinate frame. This involves the design of an optical path from the ARB to the experimental sensor mounting area.

The optical path is completed in two steps. The first step involves the setting up of two secondary alignment references at the upper level of the sensor mounting beam. Each secondary reference has an autocollimating

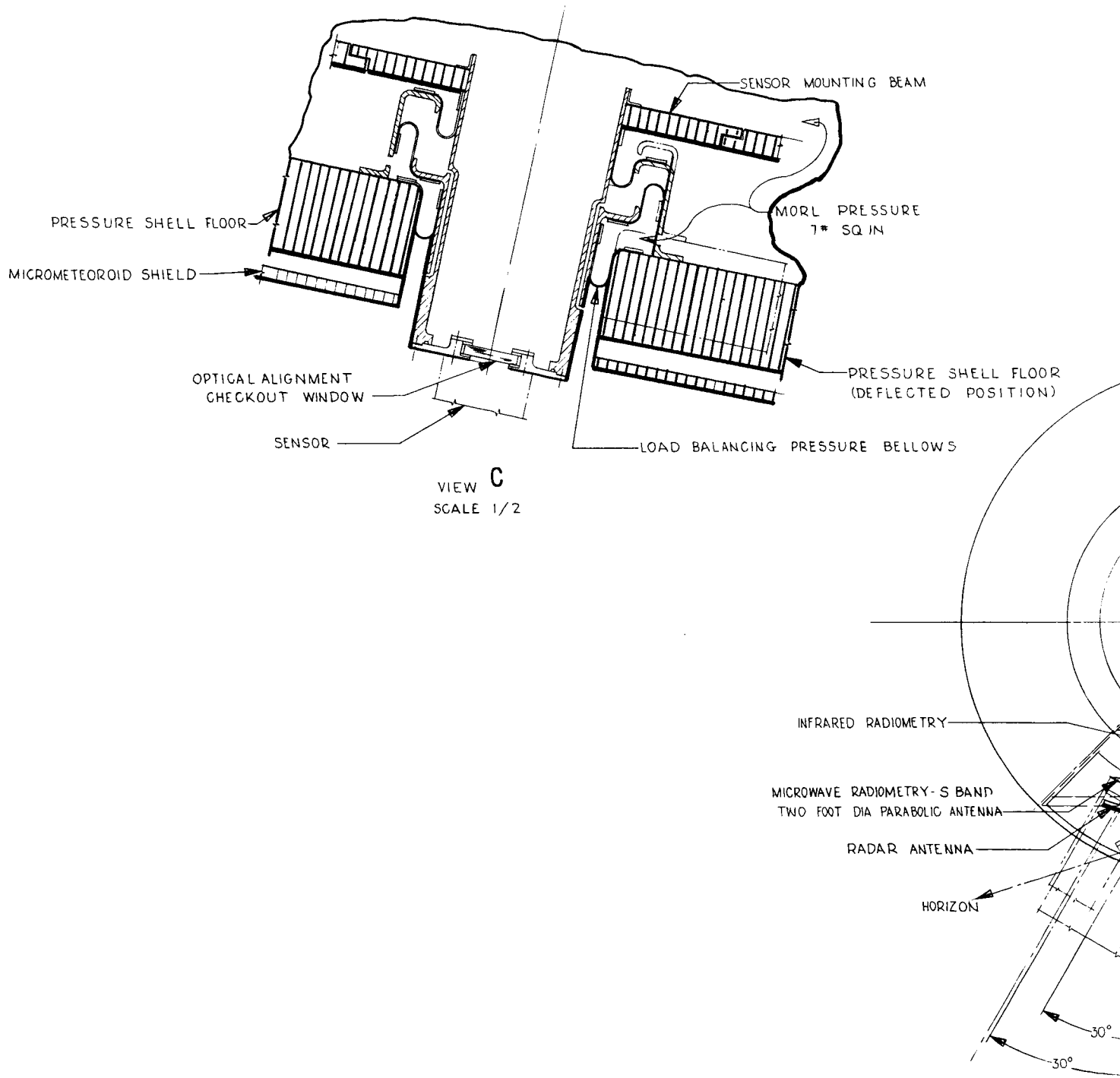
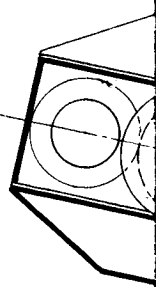
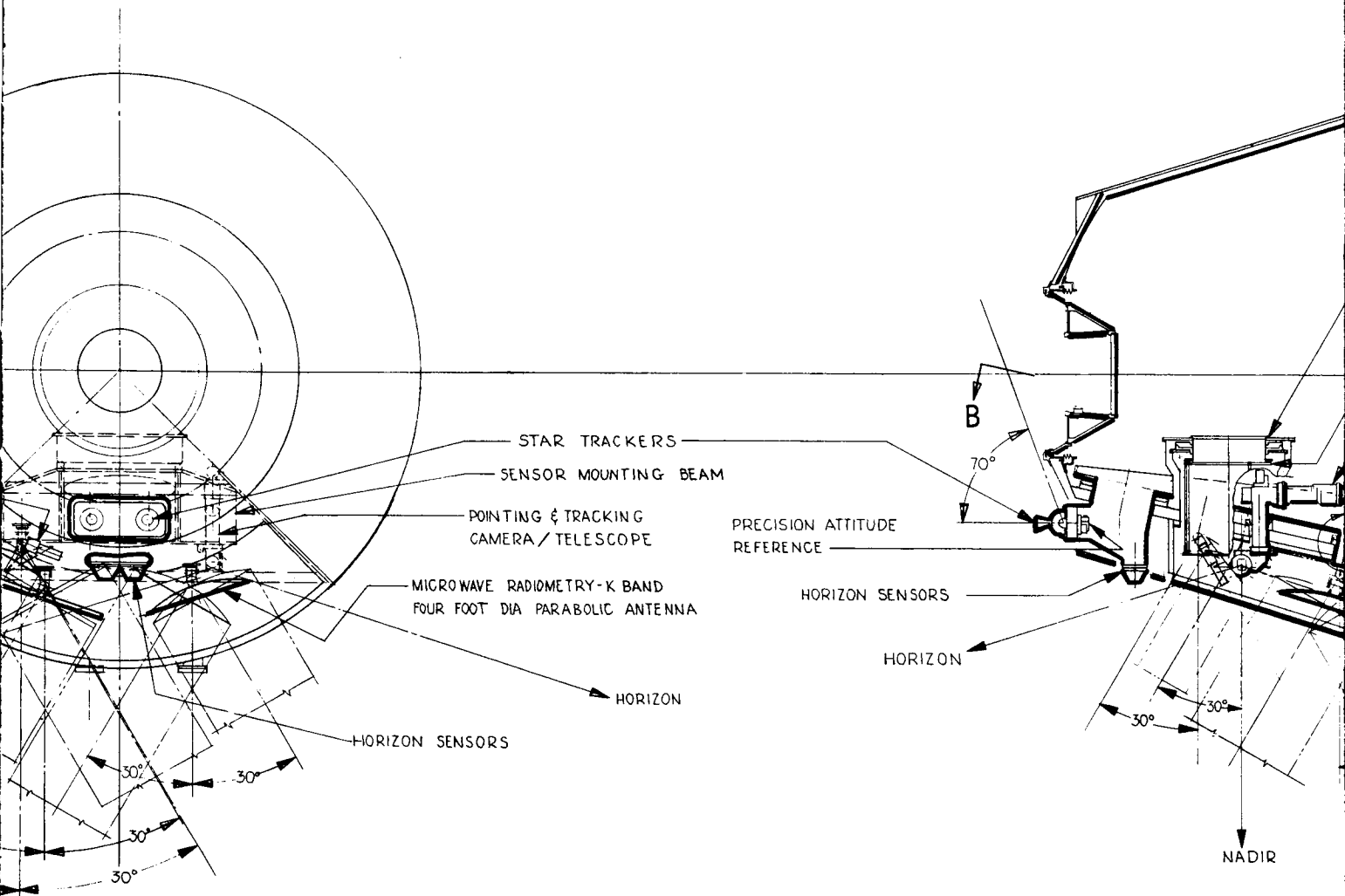


Figure C-6. MORL Experiment Bay

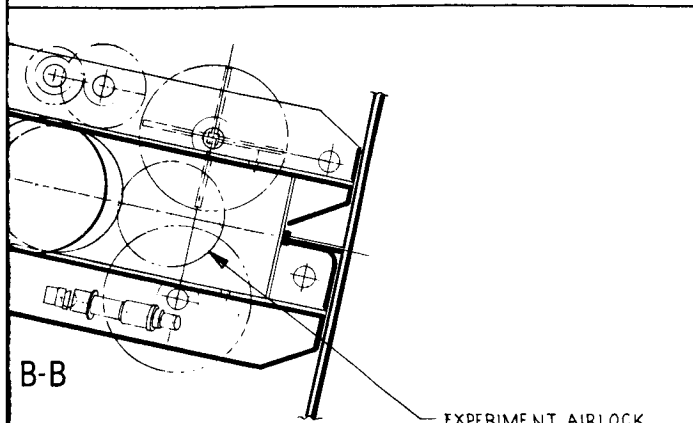


VIEW

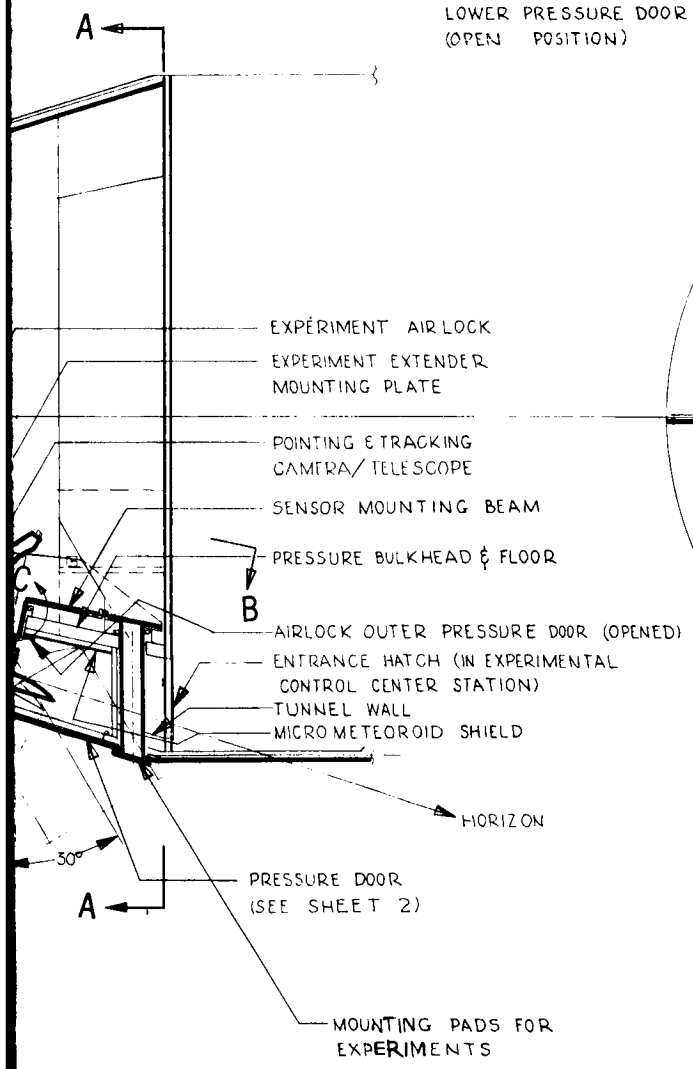


292-2

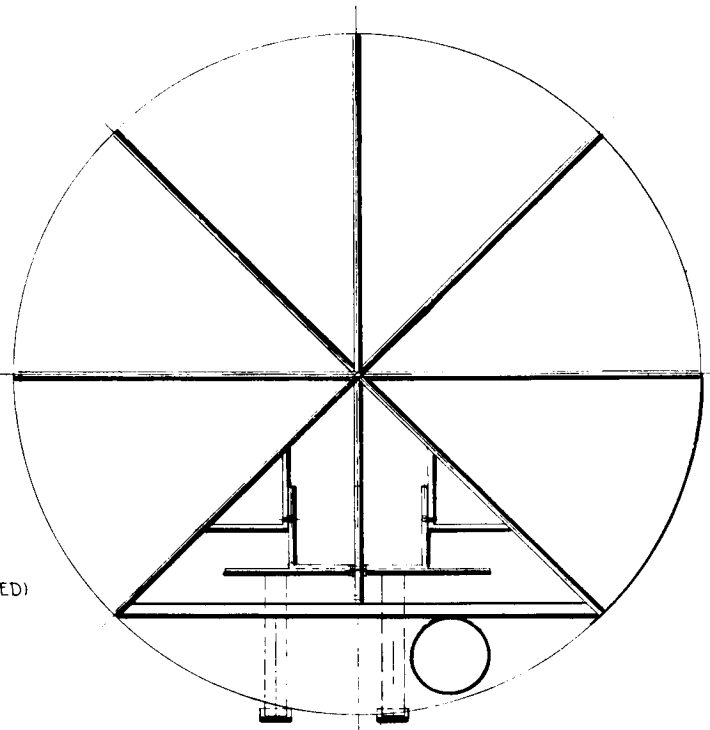




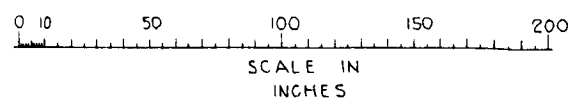
EXPERIMENT AIRLOCK  
LOWER PRESSURE DOOR  
(OPEN POSITION)



EXPERIMENT AIRLOCK  
EXPERIMENT EXTENDER  
MOUNTING PLATE  
POINTING & TRACKING  
CAMERA/ TELESCOPE  
SENSOR MOUNTING BEAM  
PRESSURE BULKHEAD & FLOOR  
AIRLOCK OUTER PRESSURE DOOR (OPENED)  
ENTRANCE HATCH (IN EXPERIMENTAL  
CONTROL CENTER STATION)  
TUNNEL WALL  
MICRO METEOROID SHIELD  
HORIZON  
PRESSURE DOOR  
(SEE SHEET 2)  
MOUNTING PADS FOR  
EXPERIMENTS



SECTION A-A



292-3

telescope and an optical target rigidly attached to each other and mounted on the sensor beam by means of an adjustable frame. Once adjusted, the frame is assumed to form a rigid body with the ARB.

The SGT has an optical target face perpendicular to the roll axis. This target face is a reflector and contains scribe marks parallel to the pitch and roll axes. A periscope is used to permit sighting of the SGT reference face from the secondary reference telescopes. The prisms in the periscope are rigidly aligned within 10 arc sec. The upper prism includes a beam splitter and a reflecting, scribed target to aid in aligning the telescopes. The lower prism contains scribe marks on its outer face to permit roll axis alignment of the periscope with respect to the SGT. Establishment of the secondary references requires: (1) the alignment of the periscope, and (2) the alignment of the telescopes to the reference targets on the periscope. A general method applies to these and the following cases of optical alignment.

Autocollimation establishes the perpendicularity of a line of sight to a target. Telescopic alignment to scribe marks establishes the orientation of the target plane about the line-of-sight axis. For sufficiently small angles, alignment may be computational rather than physical. It is assumed that the environment is such that, once alignment has been established for any mechanical element, it will not vary for the duration of an experiment. All optical alignment and experimental equipments can be mechanically aligned to within  $\pm 0.1^\circ$ , using precision pads on the sensor mounting beam, prior to optical fine alignment.

The optical targets that are rigidly attached to the telescopes consist of one or more 2-in. -square reflecting faces. They are oriented to the telescope axis and cross hairs such that, when the telescope is aligned to the SGT, they are perpendicular to the main sensor mounting beam plane and either perpendicular, or at a known angle, with respect to the yaw-roll plane. Each face is a reflector with scribe lines which are parallel and perpendicular to the sensor mounting plane. These targets may be considered as defining the vehicle coordinate frame, once they are aligned, provided a correction is made for the angle between the pitch-yaw plane and the sensor mounting beam plane ( $\approx 13^\circ$ ).

When a sensor is to be aligned, its gimbals are set to null. An optical target is mounted on the sensor nominally parallel to the sensor mounting beam plane, with scribe marks parallel and perpendicular to the pitch axis. Figure C-7 shows the arrangement for aligning a typical experimental sensor. A window in the pressure shell enables the target to be sighted from above. Provision is made on the sensor mounting beam for mounting a portable parallel autocollimating telescope, with its barrel pointed toward the nearest secondary reference target. A small periscope is permanently mounted to the front of this telescope. The periscope contains a beam splitter and a penta prism. The telescope is sighted and aligned (computationally) first to the secondary reference target, and then to the experiment sensor target. Scribe marks are used at the outputs of the penta prism to allow alignments about the lines of sight. Sensor misalignments can be determined directly by algebraic subtraction.

Autocollimation measurements are accurate within 10 arc sec at a 12-ft maximum sighting distance. Telescopic alignments about the line-of-sight axis are accurate to within 20 arc sec at a 12-ft sighting distance. Because there is only one long sight of up to 12 ft and two short sights of approximately 4 ft each involved, the maximum misalignment error is

$$20 \sqrt{1 + \frac{2}{9}} = 22 \text{ arc sec}$$

This is adequate, in conjunction with the star tracker accuracies of 20 arc sec, to ensure an experiment attitude fix of 30 arc sec, or  $0.01^\circ$ .

#### C. 5. 4 Weight, Power, and Volume

Table C-2 shows the equipment required for optical alignment along with the associated weight, power, and volume.

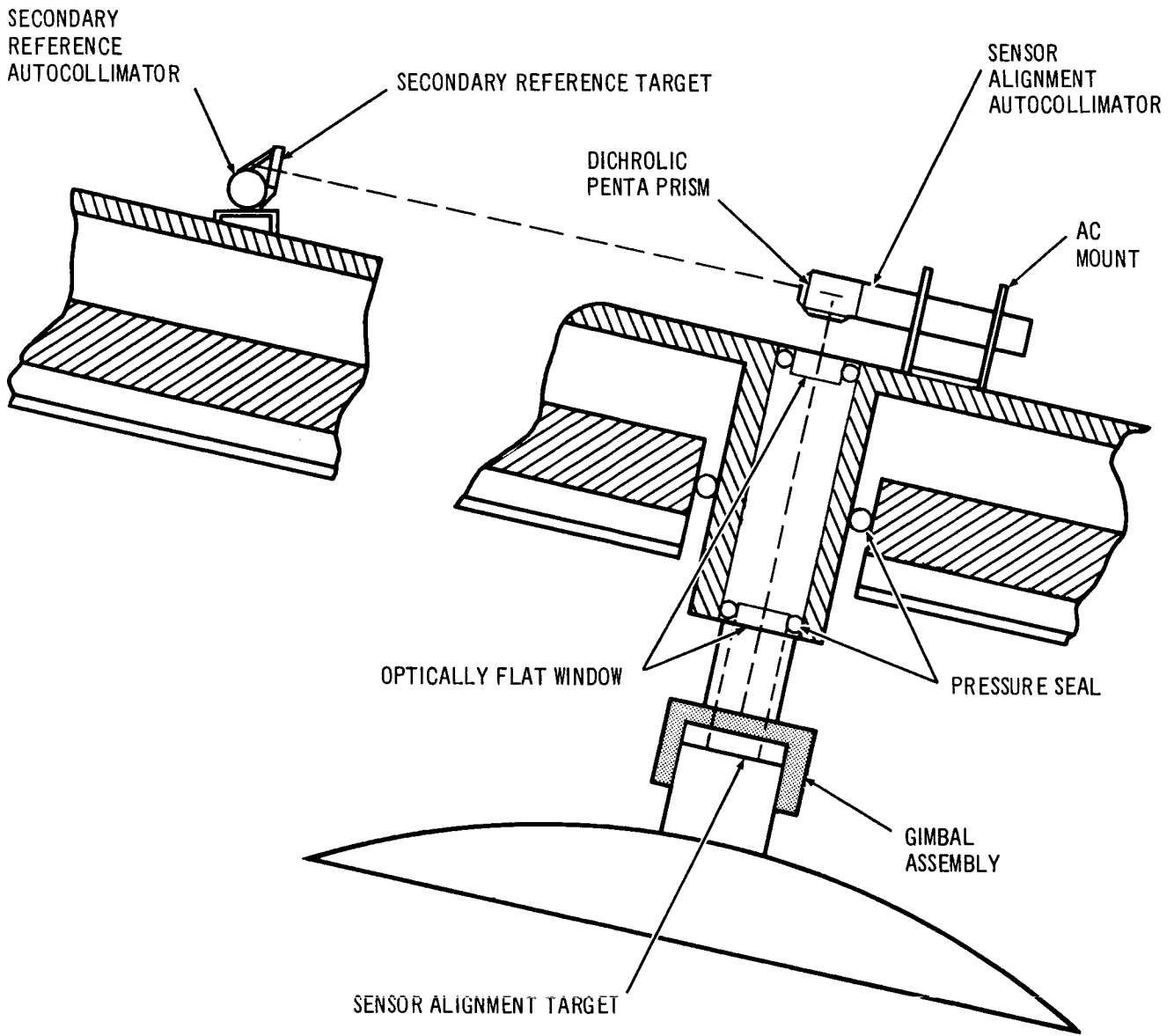


Figure C-7. Optical Alignment of Experiment Sensors, Side View

Table C-2  
OPTICAL ALIGNMENT EQUIPMENT

Description	Quantity	Total Weight (lb)	Total Power (W)	Total Volume (cu in.)
TA82* autocollimator	2	7.0	9.0	40
112636* Telescopic autocollimator	3	27.0	13.5	180
26-in. periscope	2	8.0		104
20-in. periscope	1	3.0		39
Fixed telescope mount	2	14.0		72
Portable telescope mount	1	7.0		36
Double autocollimator mount	1	6.0		27
Prism	4	2.0		16
Total		74.0	22.5	514

---

\*Equipment manufactured by Hilger and Watts, London, England

---

## Appendix D

### MORL INERTIAL REFERENCE SYSTEM COMPARISON STUDY

Three inertial systems are compared in this Appendix in terms of relative capability to provide an inertial reference for the laboratory. These are the single-gimbal triad (SGT), which is the present baseline system, the Gemini inertial measurement unit (IMU), and the gimbaless inertial reference unit (IRU) proposed for the Standardized Space Guidance System (SSGS) and Lunar Orbiter System.

Those systems capable of meeting MORL functional requirements and limitations have been established. The performance of each system is determined and compared to present laboratory specifications. It is also determined which system provides the best performance in terms of weight, power, and reliability.

For those systems which meet the basic requirements, a tradeoff evaluation is made based on the following criteria:

1. Performance.
2. Weight.
3. Power.
4. Volume.
5. Reliability.
6. Maintenance (crew time).
7. Spare parts (weight and volume).
8. Cost.

The tradeoff uses penalty factors established for the critical items above as a function of their relative impact on the MORL system. The systems are analyzed to determine the effect of potential modifications, and recommendations are made regarding the inclusion or omission of these system changes.

## D.1 INERTIAL REFERENCE SYSTEM--REQUIREMENTS

The MORL vehicle includes an inertial reference system (IRS) as an integral part of the stabilization and control system (SCS). The IRS is required to provide a stable attitude reference with all-attitude capability. It includes inertial sensors, electronics, star trackers, and a computer.

There are two basic modes of IRS operation, attitude reference in inertial space and attitude reference in rotating orbital space (belly-down orientation, for example). The specified requirements for attitude reference stability are the same for both modes. These specify that the attitude reference be held to within  $0.1^\circ$  of its initial orientation over a period of 1.0 hour and alignment to  $0.01^\circ$ , using star trackers. The initial orientation is normally provided by optical information and the orbital rate, if required, is provided by the data processing computer based on ground tracking data.

The IRS must have all-attitude capability in both modes of operation. This means that the laboratory must be capable of being maneuvered to any attitude while the IRS maintains the original attitude reference mechanically or computationally. The maneuvering can be controlled either manually or by means of error signals from the IRS. These error signals must provide capability to point the laboratory or its sensors in any direction in the celestial sphere or to any point on the Earth's surface. To provide information needed for manual control, the IRS must also produce signals which can be used to drive a flight director attitude indication (FDAI) display.

## D.2 CONFORMANCE OF BASELINE AND ALTERNATIVE IRS CONFIGURATIONS TO SYSTEM REQUIREMENTS

The following paragraphs discuss the conformance to system requirements of baseline and alternative IRS configurations.

### D.2.1 Single-Gimbal Triad

The present configuration of the Bendix concept utilizes three single-axis platforms (SAP) mounted in an orthogonal triad. Each SAP has an inertial rate integrating gyro (IRIG) mounted on a single gimbal. Figure D-1 represents schematically the electromechanical configuration of a SAP and its

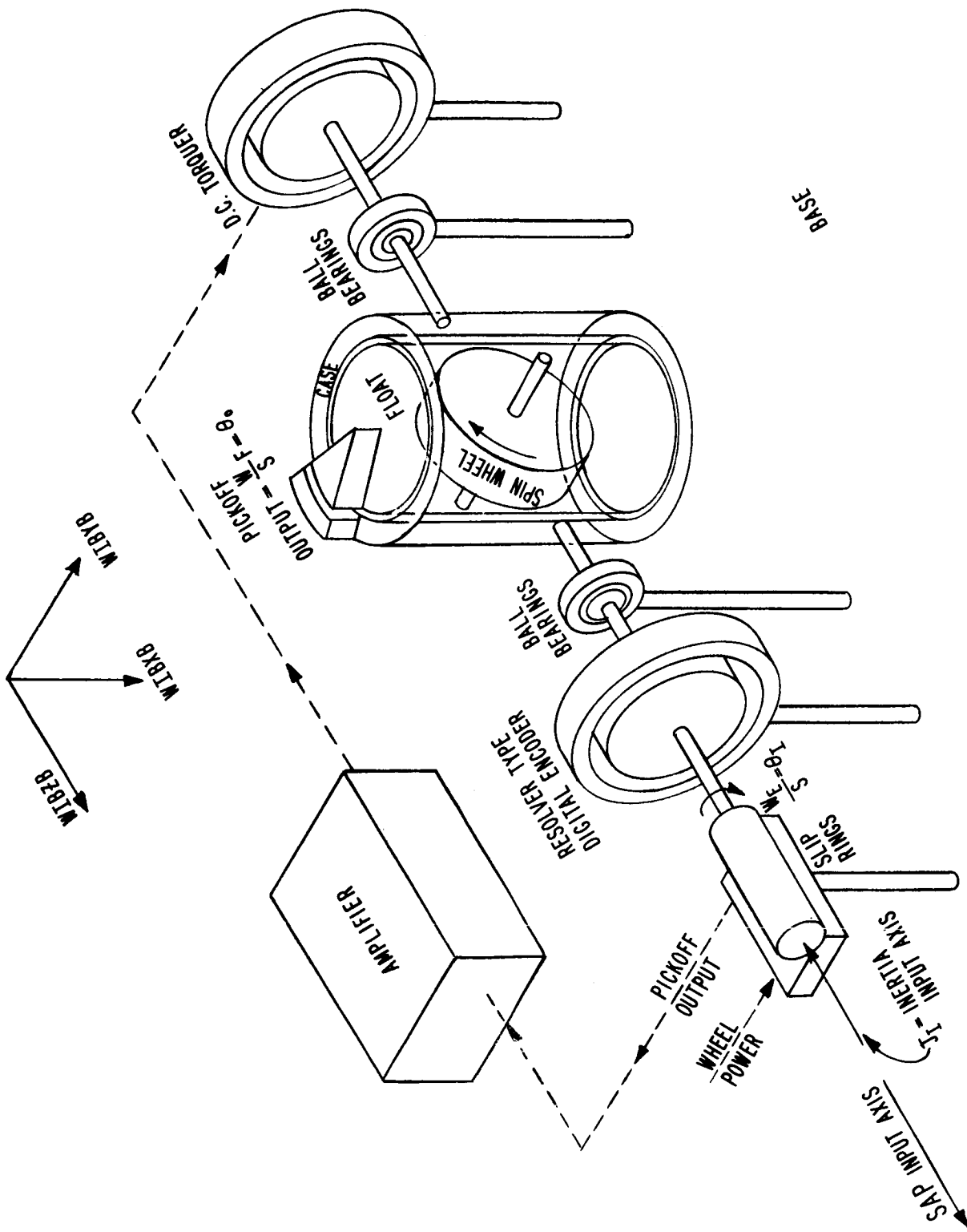


Figure D-1. Single Axis Platform



associated electronics. The particular IRIG selected for this application is the MIT Instrument Laboratory-designed 18-PIRIG. This gyro has a short-term random drift less than 0.01°/hour.

The output of each SAP is a digital-encoded signal proportional to the difference between the initial position of the inertially fixed gyro canister, with respect to the body-fixed reference frame, and the position at the instant of measurement. This provides a direct measure of the laboratory rotation about the SAP input axis. The latter coincides with one of the three major body axes. The measurement cycle time is sufficiently short to allow small-angle simplifications to be applied. The final position of one measurement becomes the initial position of the next measurement.

Changes in laboratory orientation are computed in a digital computer by use of direction cosines. The direction cosines can be converted to body Euler angles for attitude displays and maneuvering commands. They are also immediately useful in the orbital space mode for incorporating the orbital rate vector into the stabilization loop. Figures D-2 and D-3 show the block diagrams for the inertial space and orbital space stabilization modes, respectively. Figures D-4 and D-5 show the corresponding block diagrams for the attitude indicator display generation.

The accuracies associated with the SGT for each axis are as follows:

<u>Error Source</u>	<u>Degree/Hour</u>
Initial alignment	0.01
Rate cross-coupling	0.01
Encoder resolution	0.01
Gyro drift (maximum)	0.08
Computation	<u>0.04</u>
R. S. S.	0.09

Since these are worst-case error figures, the SGT is expected to provide adequate performance capability. Furthermore, the SGT is designed to have all-attitude capability. This is accomplished by using a computation frequency sufficiently high to allow small angle approximations to be employed

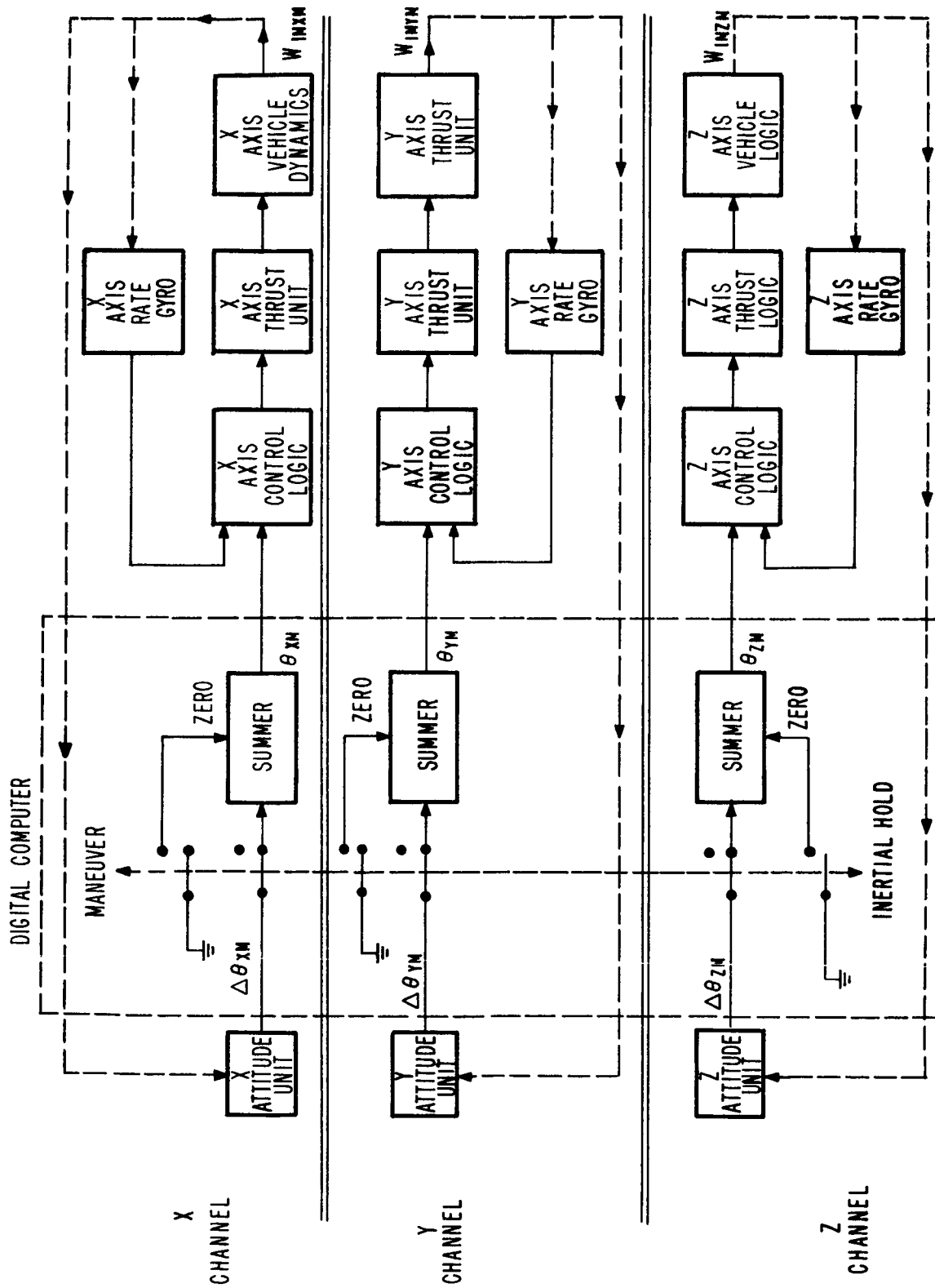


Figure D-2. Inertial Attitude Holding System

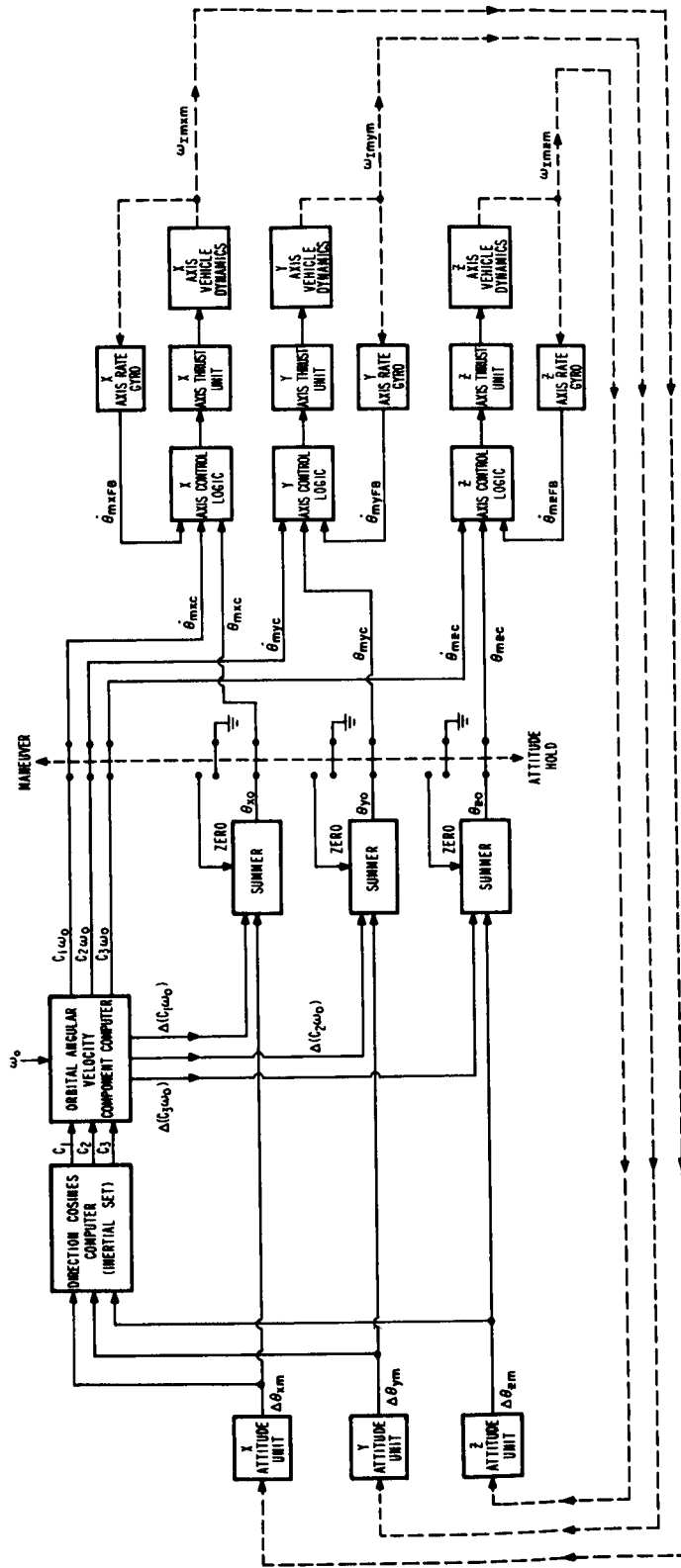


Figure D-3. Holding Attitude with Respect to Orbital Space

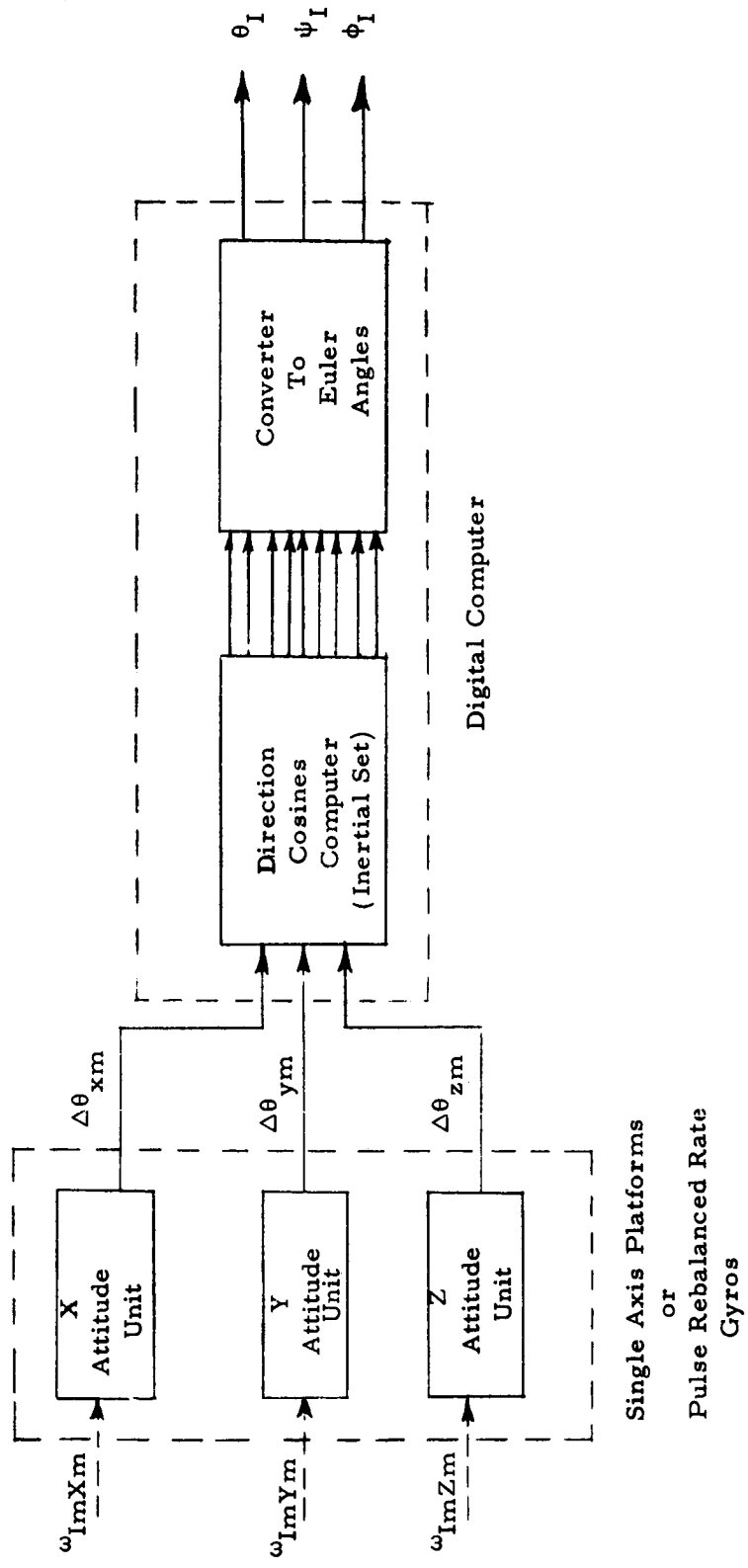


Figure D-4. Indication of Attitude with Respect to Inertial Space

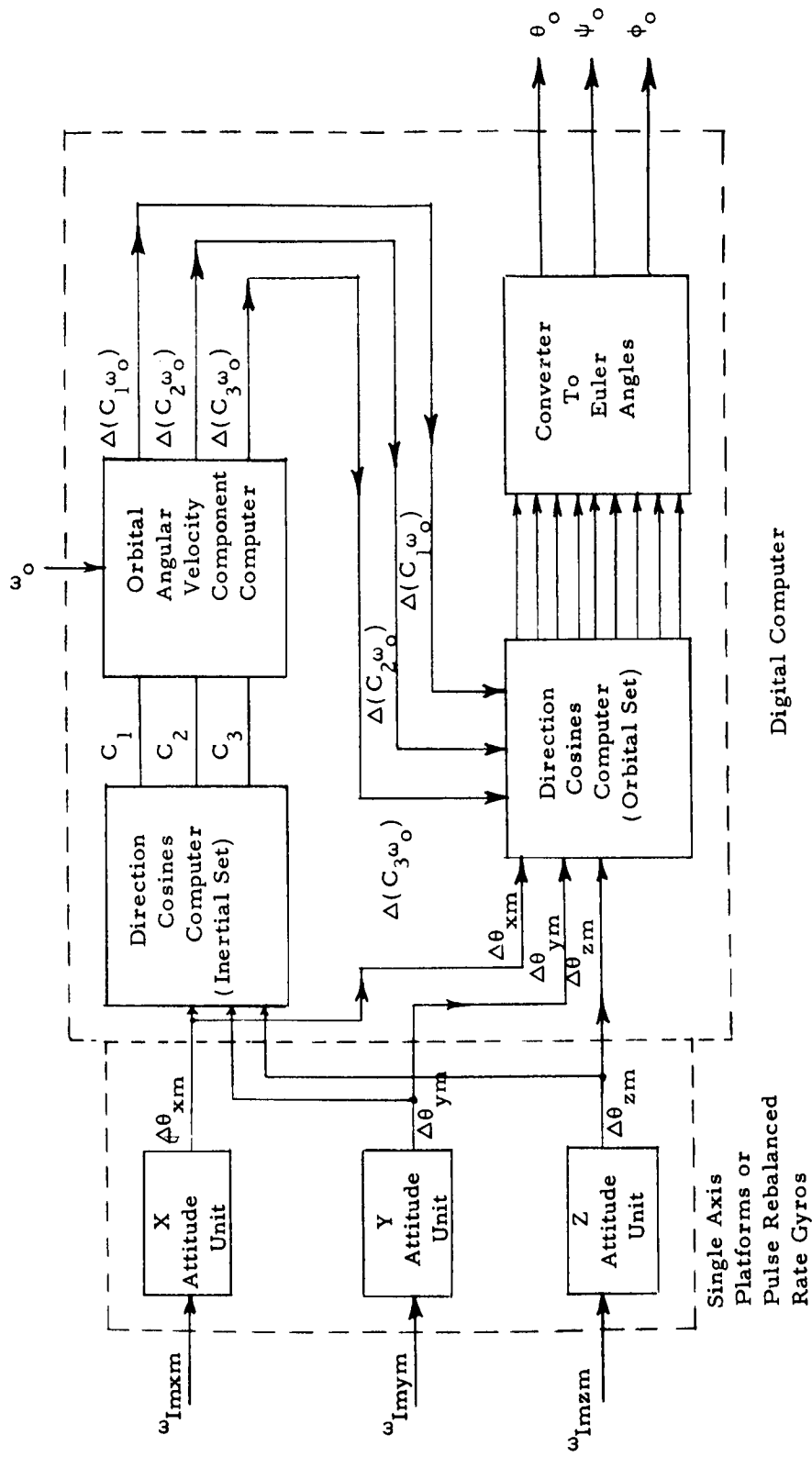


Figure D-5. Indication of Attitude with Respect to Orbital Space

with minimal cumulative error. Simulation of the computation scheme to be employed shows a total error of  $0.05^\circ$  for a full  $360^\circ$  rotation. The direction cosines method of computation provides a simple means of compensating for the effect of orbital rate when the system is operating in the inertial space mode. The product of the direction cosines and the orbital rate vector equals the instantaneous orbital rate about each of the body axes. This may be used either as an error signal to drive the attitude reference system (ARS), or as an additive (or subtractive) input to the attitude indicator display.

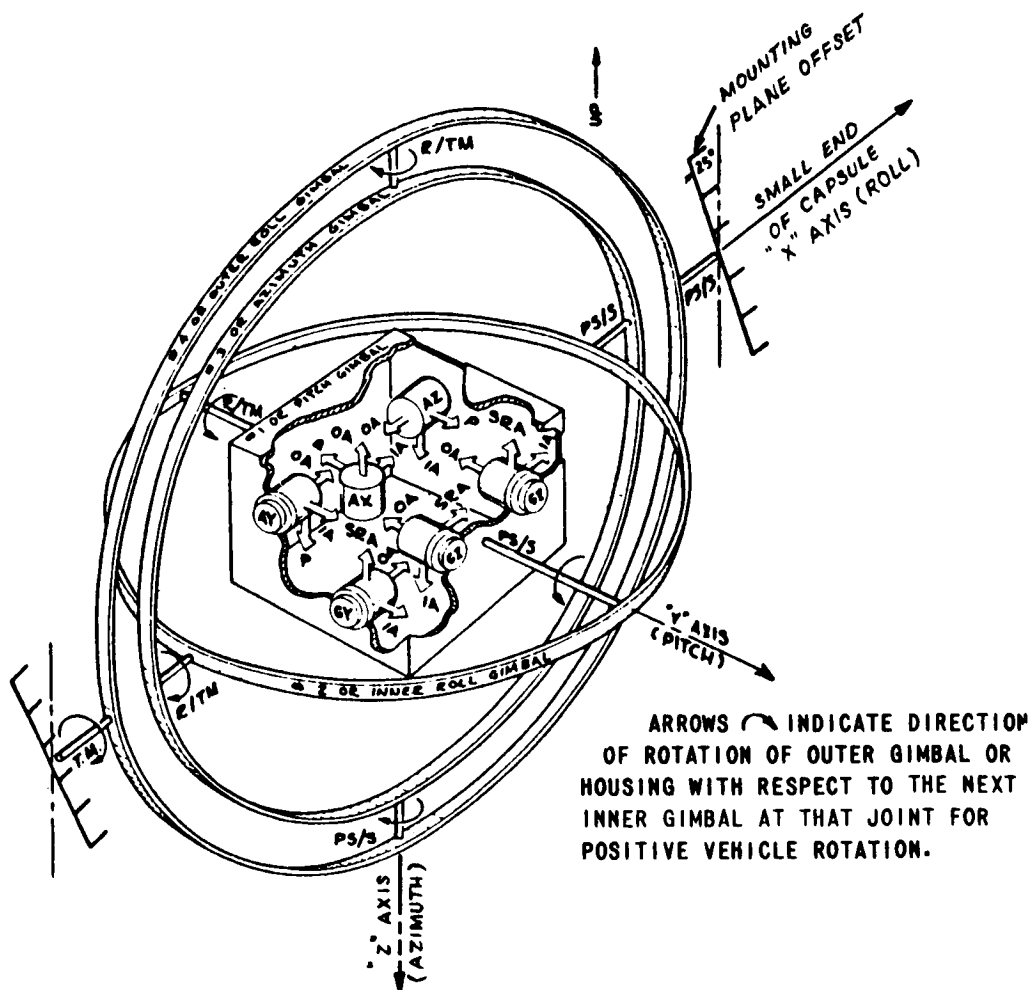
From the foregoing, it is clear that the SGT is capable of meeting baseline system requirements. Moreover, weight and power are compatible with a MORL vehicle.

#### D. 2. 2 Gemini Inertial Measurement Unit

The Gemini IMU is a four-gimbal platform used for guidance and navigation in the Gemini spacecraft. It is manufactured by Honeywell and uses three Honeywell GC 8001 gas bearing gyros as angular sensors. An IMU employed in a MORL application does not require the three linear accelerometers which are included in the complete platform configuration.

Figure D-6 shows schematically the electromechanical configuration of the IMU gimbal assembly. The stable member of the platform remains fixed in inertial space while the laboratory rotates about it. The amount and direction of the rotation is known from the angular position of the gimbal resolver pickoffs. Pickoff angles are processed in a digital computer to obtain the angular orientation of the laboratory with respect to the inertial reference. The angular orientation of the laboratory is expressed in terms of body Euler angles. These can be used to provide error signals to the ARS or to drive an FDAI display.

The stable member can be held fixed with respect to orbital space by first aligning to the orbital plane and local vertical and then torquing the Z gyro at orbital rate. The stable member will then be constantly aligned to local vertical and maneuvers may be performed about it with the same facility and accuracy as when it is aligned to a fixed inertial reference. Since the laboratory is continually turning with respect to inertial space when it remains



**LEGEND:**

- |                       |                          |                               |
|-----------------------|--------------------------|-------------------------------|
| P - PENDULUM          | GZ - AZIMUTH GYRO        | AY - ACROSS COURSE ACCEL.     |
| SRA - SPIN ROTOR AXIS | GY - PITCH GYRO          | TM - TORQUE MOTOR             |
| IA - INPUT AXIS       | AX - ALONG COURSE ACCEL. | R/TM - RESOLVER, TORQUE MOTOR |
| OA - OUTPUT AXIS      | AZ - VERTICAL ACCEL.     | PS/S - PHASE SHIFTER, SYNCHRO |
| GX - ROLL GYRO        |                          |                               |

Figure D-6 Gemini Gimbal and Inertial Component Orientation in Flight (Small End of Capsule Forward)

orbit-fixed, three integrators are required in the control system so that there will be no hang-off of the angle  $\theta_{zm}$ . That is, in the steady-state:  $\theta_{xm} = \theta_{ym} = \theta_{zm} = 0$  even though the vehicle is turning at a constant rate. The system is outlined in Figure D-7.

The basic limitation on platform accuracy in a zero-g environment is the drift stability of the gyros. The GC 8001 gyro has a maximum drift stability of  $0.1^\circ/\text{hour}$ , using digital compensation. In the present application, the accuracy of the gimbal resolver is also important. These have an overall accuracy of  $0.07^\circ$ . The two values quoted establish the effective accuracy of the IMU in an inertial space mode at  $0.12^\circ/\text{hour}$ . Taking into account compensated gyro torquer linearity, which is specified as  $\pm 0.04\%$ , the effective accuracy of the IMU in an orbital space mode is  $0.154^\circ/\text{hour}$ . From the standpoint of accuracy, these values show that the Gemini IMU is basically capable of meeting IRS functional requirements, provided worst-case components are upgraded.

#### D. 2. 3 Gimbaless Inertial Reference Unit (IRU)

The gimbaless IRU has been developed by Sperry Gyroscope for the Air Force SSGS and NASA Lunar Orbiter applications. It is essentially a refined strap-down attitude reference system employing three SYG-1000 gyros as angular rate sensors.

These gyros measure rates about the three principal body axes. The rates can then be integrated to body Euler angles in an analog computer to drive an attitude stabilization system. The gyro-measured rates can also be processed directly by means of a digital differential analyzer (DDA) to determine the change in laboratory orientation about an initial reference frame by successive small-angle steps. Depending on the laboratory rates being sensed, computer cycle times of 10 msec or less are required.

The IRU can also be operated open-loop (Figure D-8) to hold an inertial orientation. Any deviation from the initial orientation generates an error signal which is used to drive the attitude stabilization equipment. The only limitation on the accuracy of this mode of operation is the gyro drift. In the Lunar Orbiter configuration, the IRU is operated open-loop so that the gyro



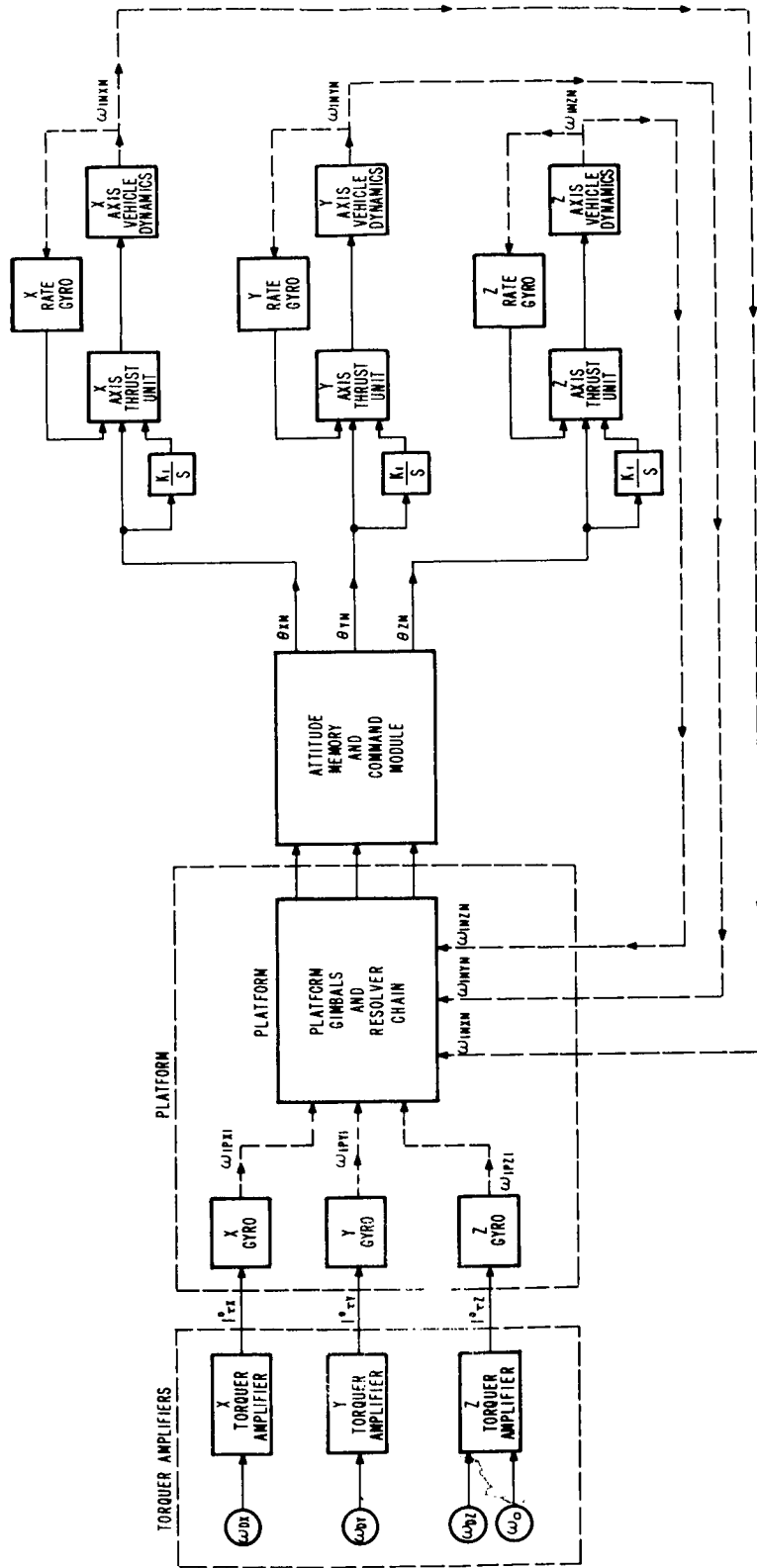


Figure D-7. Holding Attitude Mechanization with Respect to Orbital Space

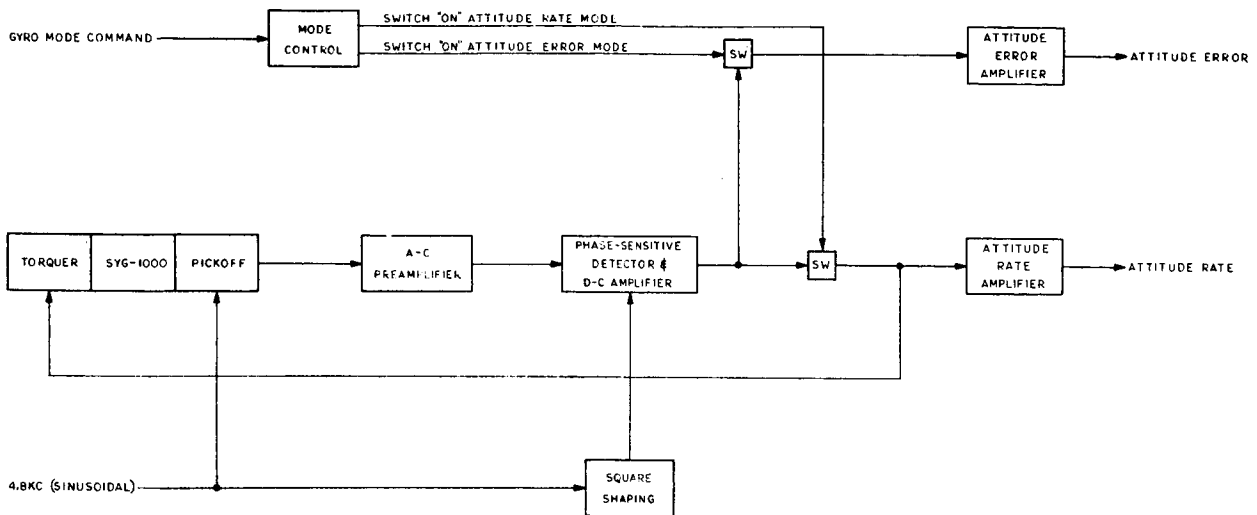


Figure D-8. Strap Down IRU Block Diagram

drift rate of  $0.3^\circ/\text{hour}$  determines the IRU accuracy. With properly selected gyros, there is no reason why this could not be reduced to  $0.1^\circ/\text{hour}$ . The IRU is capable of meeting MORL IRS accuracy requirements in an inertial space mode with no extensive maneuvering.

However, a problem arises when the use of the IRU in an orbital space mode is considered. The unit must be operated in a closed-loop rate mode since the open loop mode is limited to attitude changes of  $\pm 3^\circ$ . Although the gyro drift in rate mode can be limited to  $0.1^\circ/\text{hour}$ , torquer linearity and gyro pick-off null uncertainty play important roles. The effect of temperature changes on torquer null uncertainty and linearity is particularly critical. Any errors in either the torquer current or the gyro pickoff are essentially rate errors. For example, the pick-off null uncertainty specification of the SYG-1000 gyro is 1.0 mV or 3.0 mV maximum. The sensitivity of the pickoff is 5.7 mV/mrad, or  $0.1 \text{ V}/^\circ$ . For a transfer function between gyro pickoff and gyro input torquer of  $5 \text{ dyne-cm}/^\circ$ , the rate error resulting from a 3.0-mV pick-off null

uncertainty is 0.3°/hour. The overall accuracy of the IRU is approximately 0.5°/hour, including gyro drift and torquer current temperature-dependent errors. This is greater than the inaccuracy allowed for the IRS by system specification. It can be seen that improvement will be required in the IRU if it is to provide a feasible alternative to the present baseline IRS.

### D.3 SYSTEM COMPARISON TRADEOFF

The factors to be considered in tradeoffs are discussed in the following subsections.

#### D.3.1 Methodology

The baseline and alternative mechanizations for a MORL IRS are compared quantitatively for their relative contributions to mission success and efficiency by the following logic. Each type of mechanization enables some proportion of the entire complement of planned experiments to be performed without additional special attitude reference equipment. Each mechanization also makes a predictable demand on available MORL system resources in terms of weight, power, crew time, and so forth. An overall penalty factor for each mechanization is established by multiplying the inverse of the proportion of experiments which can be accommodated, and the proportional drain on available system resources. These penalty factors, when considered in conjunction with other nonquantifiable factors, provide a basis for determining the best potential mechanization.

The relative demand on available system resources is found by taking the ratio of IRS requirement to unassigned resources. Development and equipment costs may also be regarded as equivalent to the consumption of a resource, since the provision of physical resources is at some ultimate cost. To establish the equivalence more exactly, the following cost factors from Volume IX of the MORL Phase IIa final report are cited below.

Weight	\$ 19,000/lb
Power	\$ 21,000/W
Crew time	\$ 63,000/hour
Volume	\$155,000/cu ft

The unassigned resources available are as follows (from a sample problem calculated in Volume XV of the same report):

Unassigned weight	6,000 lb
Unassigned volume	4,000 cu ft
Unassigned crew time (per year)	1,500 hours
Unassigned electrical power	2,000 W

Thus, full utilization of all available resources would correspond to a total expenditure of \$870.5 million, or an average expenditure of approximately \$220 million for each available resource. For purposes of comparison, \$200 million is taken as the cost reference figure. Although this value is only an order of magnitude estimate, it is not unreasonable in view of the overall projected cost of the MORL, and it results in cost penalty factors which can be compared with the physical resource penalty factors.

### D. 3. 2 Inputs to Tradeoff

Table D-1 presents a summary of the inertial mode and orbital mode accuracies for the three systems described in Subsection D.2. The accuracies have been detailed both for the inertial space and orbital space modes, since this provides a method of relating them directly to experimental requirements.

Table D-1  
SYSTEM ACCURACIES (°/HOUR)

	Gemini IMU	SGT*	Strap-Down IRU
<b>Inertial Space</b>			
Hold	0.12	0.13	0.10
Maneuver	0.12	0.13	0.50
<b>Orbital Space</b>			
Hold	0.15	0.13	0.50
Maneuver	0.15	0.13	0.50

\*These values are based on an error analysis using 0.09° resolution encoders and are pessimistic, considering the use of an improved encoder of 0.01° resolution.

The requirements of each system in terms of laboratory resources are detailed in Table D-2. The weights and volumes shown include both the basic system and the spares necessary for the repair of any one system failure. It is assumed in this analysis that no system will fail more than once in any of the 3-month periods between laboratory resupply cycles.

Table D-2  
REQUIREMENTS OF ALTERNATIVE SYSTEM

	Gemini IMU	SGT	Strap-Down IRU
Weight (lb)	193.5	28.6	28.0
Power (W)	219	67.0	58.2
Volume (cu in.)	4,470	735	859
Crew time (hour/year) for maintenance	31	16	4

Crew time required for maintenance has been determined on the basis of the MTBF for each system, allowing an average time of 3 hours for each repair.

Figure 2-1 shows the experiment pointing accuracy requirements for the MORL SCS. Assuming that the SCS is required to hold vehicle attitude within the specified limits for a period of at least 20 min., for a linearly increasing error, the uncertainty associated with a 20-min. period will be, in degrees, 1/3 the error in degrees/hour. Therefore, Figure 2-1 provides a means of determining the proportion of experiments each IRS mechanization can accommodate.

Approximate values for the cost of the alternative systems are shown below. These costs are for further development, production, and factory testing of seven inertial systems.

<u>System</u>	<u>Cost</u>
Gemini IMU	\$3,000,000
SGT	600,000
Strap-down IRU	560,000

### D. 3. 3 Tradeoff Computations

The proportion of MORL experiments which can be accommodated by the various systems without additional equipment are listed below.

<u>System</u>	<u>Proportion Accommodated</u>
Gemini IMU	0.890
SGT	0.900
Strap-down IRU	0.660

These proportions have been computed from the data of Table D-1 and the experimental attitude-hold requirements which are summarized in Figure 2-1 and assume that an attitude must be held to the required accuracy for 20 min.

The resource penalty factors exclusive of cost for the various systems are computed from the data of Table D-2 and the unassigned resources of Subsection D. 3. 1. Table D-3 shows the results of these computations. Subsection D. 4 treats the computer requirements of each system. These have been included in the compilation of Table D-2.

Table D-3  
PHYSICAL RESOURCE PENALTY FACTORS

	Gemini IMU	SGT	Strap-Down IRU
Weight (lb)	0.0322	0.0048	0.0047
Power (W)	0.1095	0.0335	0.0291
Volume (cu in. )	0.0006	0.0001	0.0001
Crew time (hour/year) for maintenance	<u>0.0021</u>	<u>0.0011</u>	<u>0.0003</u>
Total	0.1444	0.0395	0.0342

The cost penalty factors for the inertial reference systems are computed from the system development and fabrication costs listed in Subsection D.3.2 and the estimated available funding in D. 3. 1. The following penalty factors result; as can be seen, they do not materially affect the outcome of the tradeoff.

<u>System</u>	<u>Cost Penalty Factor</u>
Gemini IMU	0.0015
SGT	0.003
Strap-down IRU	0.003

Adding the penalty factors found for each system, the following overall resource penalty factors are established:

<u>System</u>	<u>Resource Penalty Factor</u>
Gemini IMU	0.1459
SGT	0.398
Strap-down IRU	0.345

When each of these resource penalty factors is multiplied by the inverse of the proportion of experiments which can be accomplished with the particular system, the set of cost-effectiveness factors shown below is obtained.

<u>System</u>	<u>Cost Effectiveness</u>
Gemini IMU	0.1639
SGT	0.0443
Strap-down IRU	0.0523

The cost effectiveness values clearly establish the general superiority of the SGT and strap-down systems for the present application. The difference between the SGT and the strap-down IRU is not sufficient, in itself, to justify the selection of the SGT over the IRU. However, when considered as one factor, it tends to favor the selection of the SGT as the best potential system for the MORL application.

#### D. 3. 4 System Selection

In view of the results of the tradeoff computations, the Gemini IMU may be eliminated from further consideration. Its advantage in accuracy is not sufficient to offset the greater weight, power, and volume required. Furthermore, replacement in case of failure involves an entire platform assembly.

The choice between the SGT and IRU is not as clear cut. The IRU is somewhat better than the SGT in terms of weight and power requirements, but its accuracy under dynamic condition ( $0.5^\circ/\text{hour}$ ) does not meet IRS design requirements. It, therefore, appears that under the conditions of the present state of the art, the single-axis concept is better suited to MORL requirements than the strap-down rate-measurement concept. For this reason, no change is recommended in the present basic configuration of the MORL IRS. The baseline SGT remains the best potential IRS mechanization at the present time.

#### D. 4 COMPUTATIONAL REQUIREMENTS

The following paragraphs discuss the computational requirements.

##### D. 4. 1 Single-Gimbal Triad

A separate digital differential analyzer is required to implement the SGT concept. This computer uses a direction cosines method to determine the orientation of the laboratory. The direction cosines can be converted directly to Euler angles. The basic elements of this computer are a direction cosines computer, an orbital angular velocity component computer, and a summer. The direction cosines computer employs an incremental method to generate a set of direction cosines from initial conditions and indicated attitude changes about a body axis. In the orbital mode, orbit rate must be resolved about body axes and, therefore, is multiplied by the direction cosines.

The main registers must have a capacity of at least 17 bits. However, the computation frequency need not exceed 100/sec. This low solution rate requirement allows the use of low-power integrated circuits. The well defined nature of the computation will permit the use of a simple memory scheme such as a core rope for program memory and storage of constants. A glass delay line is the optimum type of erasable memory for storage of variables in this application, and its serial output will simplify the arithmetic operations. A microprogram type of instruction list will also help simplify the arithmetic. The computer configuration will employ an instruction list in which a maximum of four words is required to implement an integrator.



The core rope permanent memory must have a capacity of 256 words and a cycle time of 200 kc. The delay line erasable memory must have a capacity of 128 words in 2 delay lines (64 words in each line) and operate at a speed of 6 mc. The arithmetic section should utilize low-power microelectronic circuitry and operate at a speed of 2 mc. A total of 80 microelectronic flip-flops can be used for incremental storage. Excluding input/output circuits, the required computer has the following characteristics:

Volume	126 cu in.
Weight	5 lb
Power	15 W
Estimated (MTBF) reliability	10,000 hours

#### D. 4. 2 Gemini IMU

The Gemini IMU has only minimal computation requirements. The stable member remains fixed in inertial or orbital space and the orientation of the laboratory is defined completely by the gimbal angles at any instant. A small analog computer may be provided to convert from gimbal angles to Euler angles. All other incidental computation functions, such as addition of inner and outer roll angles, are performed in the platform electronic package, with the control and output functions. The Gemini vehicle includes a separate digital computer for guidance and navigation. Since these functions are performed in the MORL by the DPC, there is no need for a separate full-scale computer in a mechanization using the IMU.

#### D. 4. 3 Strap-Down Inertial Reference Unit

The computer implementation for the strap-down IRU is similar to that for the SGT. The major exception is that an integration stage is required prior to the direction cosines computation, in order to convert from rates to angles. An analog-to-digital pulse generator, with pulse rate proportional to input signal, can provide this capability. The computation frequency should not exceed 100/sec and the register size should be at least 17 bits. Size, weight, and power figures are essentially similar to those for the SGT computer.

## D. 5 PROJECTED IMPROVEMENTS

Projected improvements are presented in the sections below.

### D. 5. 1 Single Gimbal Triad

The single gimbal triad (SGT) system (References D-1, D-2 and D-3) is subject to improvements in accuracy and reliability. The most important single improvement is the substitution of a high accuracy (30 arc-sec) digital output encoder for the present 5 arc-minute device. This substitution is within the present state of the art if an electronic analog-to-digital converter is employed. The capacity of the digital differential analyzer used as the inertial reference system (IRS) computer is also sufficient to meet the potentially higher computation rate. The necessary slight increase in system weight and power and the decrease in reliability are considered to be justified by the upgraded stability and control system (SCS) accuracy requirements. It is likely that within 5 years an incremental digital encoder will be built providing a direct optical digital output with a resolution of 30 arc-sec. Such an encoder will provide a worthwhile improvement to the present single-axis system, particularly where short-term precise attitude holding is required.

This mechanization gives improved accuracy figures as follows:

1. Encoder resolution-- $0.01^{\circ}$ /hr.
2. Overall accuracy-- $0.09^{\circ}$ /hr.

### D. 5. 2 Gemini inertial Measurement Unit

The primary disadvantages of the inertial measurement unit (IMU) (Reference D-4) are its weight, power, and difficulty of maintenance. It is unlikely that any of these factors could be significantly improved without entirely changing the configuration of the platform. While it is not impossible that a low-power, lightweight, high-accuracy gimbale platform might be developed in the next few years, the law of diminishing technological returns seems to be overtaking the development of the fully gimbale platform. Therefore, the development effort will probably be better spent on other forms of inertial reference systems with greater potential payoff.

### D. 5. 3 Strapdown Inertial Reference Unit

There are several possible ways in which the strapdown inertial reference unit (IRU) (References D-5, D-6 and D-7) might be modified to improve its accuracy, (1) the placing of the entire unit in a temperature-control oven so that the fluid viscosity, and hence torquer linearity, can be precisely controlled and (2) using pulse-rebalancing circuitry to eliminate the direct dependence on rate measurement and thus bypassing the pickoff null uncertainty error. Either or both of these methods promise to reduce the error below the required  $0.3^{\circ}/\text{hr}$ , but they do not indicate any foreseeable reduction below  $0.1^{\circ}/\text{hr}$ . The use of an oven would virtually nullify any initial advantage the IRU might have in weight and power. Even with improvements considered, the IRU appears less potentially useful than the SGT as an inertial reference.

### D. 5. 4 Potential Future Mechanizations

An inertial reference system sensor which shows considerable promise, even though it is only in the experimental prototype stage, is the electrostatic gyro (ESG). This employs a spinning sphere supported by electric fields for attitude reference. One (or perhaps two for spin axis coverage and redundancy) device provides complete all-attitude reference with an extremely low drift rate ( $<0.01^{\circ}/\text{hr}$ ), long running times ( $>1$  year), and virtually no wear. Problems remain to be solved in their development, particularly in the area of readout. The ESG would seem to be most valuable in a long-term inertially fixed application, such as a manned planetary fly-by.

## D. 6 REFERENCES

References for Appendix D are as follows:

- D-1 MORL Technical Note on MORL Attitude Reference System Selection. E-P Document EP-TN-35, 24 August 1965.
- D-2 MORL Phase IIa Final Report, Volume XV.
- D-3 MOL ACTS/SCE Technical Proposal, Part 1, Contract Definition. EP Control No. 7572, 15 October 1965 (Secret).

- D-4 Gemini IMU and AGE, Volumes 1 and 2, Honeywell Aeronautical Division. R-ED 24194, 15 September 1964 (Volume 2 - Confidential).
- D-5 Letter from D. H. Keyes, Sperry Inertial Division. File No. 4700, 31 August 1965.
- D-6 SYG-100 Gyro Specification CA-60-0007B, April 1961 (reported to be under revision, but new specification has not yet been published).
- D-7 Jack M. Simon. Inertial Reference Unit for Lunar Orbiter. Sperry Eng. Rev., Vol. 18, No. 1, Spring 1965.